THE EFFECT OF VIBRATION AND TEMPERATURE ON THE LATERAL PRESSURE OF CONCRETE ON FORMWORK

by

AMJID RAUF QURESHI

Submitted in partial fulfillment

of the requirement for the degree

of

Master of Applied Sciences

School of Graduate Studies

Department of Civil Engineering

University of Ottawa

August, 1978

ABSTRACT

The objective of this investigation was to determine the variation of lateral pressure of fresh placed concrete with power of vibrator, immersed depth of vibrator, duration of vibration and concrete temperature, keeping concrete strength, slump, rate of pour and form dimensions constant. The lateral concrete pressure envelopes and maximum design pressure were also compared with those recommended by ACI Committee 347 and CIRIA.

Experimental tests were conducted by pouring concrete from a ready-mix concrete truck into a 15 feet deep rigid steel formwork.

Cambridge cells were used to measure the normal and shear pressures at five locations over the height of the form structure. Strain gauges installed over the webs of the cells were connected to the strain indicator to measure the strain induced by concrete pressure.

By analysis of the experimental results, following conclusions were obtained:

The actual pressure envelope is characterized by a linear relationship of pressure with depth tending to hydrostatic up to a certain maximum value and then followed by a parabolic curve reaching a maximum and eventually decreasing. For design purposes the lateral pressure distribution of freshly poured vibrated concrete can be represented by a bilinear curve - hydrostatic up to maximum and then constant at maximum value.

The shear force acting parallel to the height of the formwork, is inversely related to the normal force acting on the face of the form.

Vibration and its parameters have a very significant effect on the magnitude of the lateral pressure exerted by fresh concrete. An increase in the power of vibrator from 1 H.P. to 2.5 H.P. increased the pressure of concrete equivalent to 2 to 5 feet of concrete head in different tests. An increase in the duration of vibration increases the lateral pressure of concrete but this factor is effective only up to a certain limit after which any further increase in the duration of vibration results into either a constant value of maximum pressure or a drop in pressure. An increase in the depth of immersion of vibrator head increased the lateral pressure of concrete; the increase measured varied by an average of 1.28 ft of equivalent concrete head, due to an increase in the depth of immersion of vibrator head from 2 feet to 1 metre.

The temperature of the concrete has a significant effect on the lateral pressure of concrete. A major fall in temperature gives rise to a significant increase in lateral pressure exerted by the concrete.

The pressure formulae recommended by the American Concrete Institute in ACI 347-68, are over conservative in respect of high rates of pour.

The recommendations to determine the lateral pressure of concrete provided by CIRIA are influenced predominantly by the arching limit criteria and the recommended design pressures provided could be useful at moderate concrete temperature conditions but cannot be applied for concrete at low temperatures. CIRIA's stiffening criteria is conservative and provides pressures which are significantly high.

ACKNOWLEDGEMENTS

The author wishes to express his sincere appreciation and gratitude to the following persons and organizations for their contribution to this thesis:

Professor N. J. Gardner, not only for his supervision and guidance throughout the entire investigation but also as a source of encouragement as a friend.

Mr. William Watson for his continuous assistance as a technician, his contribution to the successful completion of this programme cannot be overlooked.

The National Research Council of Canada for their financial assistance by means of NRC Grant No. A5654.

Mrs. Wanda Storto for typing the thesis.

Miss Nicole Renaud for friendly encouragement at all times.

Mr. Tanvir Rizvi, graduate student of Mechanical Engineering, who helped during the pouring of concrete.

My wife, Farida, for being a continuous source of help and encouragement throughout this programme.

TABLE OF CONTENTS

LIST OF TABLES

LIST OF ILLUSTRATIONS

LIST OF ABBREVIATIONS AND SYMBOLS

A	Constant
d	Minimum dimension of the form in inches
e	Eccentricity
e^+	Load cell constant
e^-	Load cell constant
es	Load cell constant
E	Stiffness coefficient of form
F	The concrete area in a horizontal section
H_m	Head of concrete at maximum pressure
h_w	Pore water pressure expressed as head of water
h_s	The height to which the concrete has risen when it has taken the final set, counting from the vibrated depth of the concrete
h_1	The depth to which the effect of vibration penetrates
k	Constant
K	The coefficient giving the pore water as the function of the height of concrete
K_1	Relaxation factor of the form
N	Normal load
n^- n^+ ns	Load cell constants
P_m	The maximum pressure of concrete
P_∞	Residual form pressure
R	Rate of pour in feet per hour
S'	The ratio of residual form stiffness to initial form stiffness
S	Shear load

s^+ s^- ss	Load constants
T	Temperature of concrete in degrees Fahrenheit
T'	Ratio of hardening time to relaxation time
t	The time in hours from the commencement of the placing of concrete
t_{max}	Stiffening time of concrete (hours)
t_s t_H	Setting time of concrete
U	The circumference
V	Rate of pour (ft/hour)
V^+	Output strain from + normal circuit
V^-	Output strain from - normal circuit
V_x	Output strain from the shear circuit
γ	Unit weight of the concrete mix
γ_b	Unit weight of water
X	Active lateral pressure coefficient
X_1	The coefficient, function of the stiffness of the concrete
ϕ	The angle of internal friction of concrete
ϕ_1	Angle of internal friction between the form and the concrete

CHAPTER 1

INTRODUCTION

Concrete due to its low cost, high structural strength, inertness to chemical attack, high fire resistance and ease with which massive elements of complex shapes can be formed has become the major structural material used in Civil Engineering. In order to make the best use of concrete in engineering, considering structural, architectural and economic aspects, the various mechanical and chemical properties of concrete have been under investigation for many years. But one of the properties of concrete which has been particularly perplexing is its physical behaviour between the time of mixing and the time the cement paste has attained its final set. During this time the physical properties of the concrete change from a plastic condition to a solid state. If the concrete in its plastic state is poured into a container or form, it will flow to the shape of the form. The cost of formwork has been estimated to vary from thirty to sixty percent of the total cost of concrete work in a construction. Forms are basically the tools and dies of concrete construction, they mould the concrete to the desired size and shape and control its position and alignment. But formwork is more than a mould, it is a temporary structure that supports its own weight and that of the freshly placed concrete as well as construction live loads including materials, equipment and workmen. Hence the form builder must be concerned with more than simply making forms the right size, his objective must be three fold; to build substantially

so that the formwork is capable of supporting all dead and live loads without collapse or danger to workmen and to the concrete structure, to design and build forms accurately so that the desired size, shape, position and finish of the cast concrete is attained, and to build efficiently, saving time and money for the contractor and owner alike.

In order to achieve the above objectives in the design of formwork it is essential to have as complete a knowledge as possible of the properties and physical behaviour of concrete as a material, between the time of mixing and the time that it has obtained its final form. The lateral pressure exerted by concrete in its liquid or plastic state is the property which controls formwork design for vertical faces.

When concrete is first mixed, it has properties lying between those of a liquid and those of solid substance. With the passage of time, concrete loses its plasticity and changes into a solid. The ability to change from a semiliquid to a solid state appears to be the result of setting of the cement which is considered to begin some 30 minutes after addition of water but this seems to be an arbitrary estimation. However slowly the process of setting may begin, it must commence as soon as the cement comes into contact with water. This phenomenum results in the development of shear strength of the concrete which is a function of time and is contributed to by the angle of internal friction, cohesion and interlocking between the particles. The magnitude of the internal friction is higher in a dry concrete than in wet, and it increases with the loss of water from a concrete mass.

ACI Committee 622 in its report on Pressures on Formwork (5)

surmised that the lateral pressure of freshly mixed concrete on formwork is at least a function of the following:

1. Depth of placement
2. Rate of pour of concrete
3. Temperature of the concrete mix
4. Ambient temperature
5. Method of compacting the concrete
6. Weight of concrete
7. Consistency of concrete
8. Maximum aggregate size
9. Smoothness and permeability of forms
10. Cross section of forms
11. Placing procedures
12. Porewater pressure
13. Type of cement

Many of the above variables are interrelated and it should be very difficult and time consuming to identify their individual effects on the lateral pressure of concrete and their participation in the design formulae.

Previous research, generally field tests on actual construction sites, lead the investigators to conclude that the lateral pressure of concrete on vertical form faces is hydrostatic to a certain depth from the pouring surface, and after a certain depth it deviates from the hydrostatic line, reaches a maximum and thereafter shows a measurable reduction in spite of increase in concrete head. The depth of the region, which behaves as a fluid, and the maximum pressure achieved is

believed to be dependent on the above stated parameters. Figure 1.1 presented by Ritchie (16) shows typical envelopes of lateral pressure of concrete.

To understand more fully the phenomenum involved it is necessary to consider the pouring sequence in detail. Consider a wall form 5 metres in depth to be filled with concrete in lifts of 1 metre each and to be vibrated with an internal vibrator immersed to a depth of 1 metre; Figure 1.2 shows in detail the sequence of pouring, vibrating, raising the vibrator, pouring the next lift, etc.

Figure 1.2a shows the first metre of concrete placed and the vibrator immersed over the whole depth of the concrete. The resulting lateral pressure is hydrostatic as the vibrator completely fluidizes the concrete removing all shear strength and wall friction. In the second stage illustrated in Figure 1.2b the second metre of concrete is placed and the vibrator immersed into the top 1 metre mass of concrete, and the lateral pressure continues to be hydrostatic.

Figure 1.2c shows the third metre of concrete placed and only the top 1 metre of the concrete vibrated. The resulting lateral pressure is hydrostatic in the top section of the form, but it is observed to slightly deviate from the hydrostatic line at the bottom.

Figure 1.2d illustrates the fourth metre of concrete placed, and the vibrator immersed into the top 1 metre of the concrete mass. The lateral pressure is hydrostatic to a certain depth, when it starts deviating from the hydrostatic time and after achieving a maximum pressure, shows a prominent reduction in pressure. This phenomenum, observed in

Figures 1.2c and 1.2d can be attributed to the friction between the surface of the form and the concrete and the development of shearing strength in concrete.

Figure 1.2e shows the fifth metre of concrete poured, with the vibrator immersed to the top 1 metre. The lateral pressure deviates from the hydrostatic line and after achieving a maximum value shows a significant drop in pressure, this unexpected drop in pressure is due to the shrinkage in concrete.

Generally, the lateral pressure envelope is idealized as a bi-linear curve initially hydrostatic and thereafter constant at the maximum value. The magnitude of the maximum pressure is dependent upon the depth of concrete fluidized, the gain in shear strength and wall friction on the concrete below the vibrated layer.

The depth of fluidized concrete is dependent upon the immersed depth of the vibrator, power of the vibrator, duration of vibration, width of section and depth of influence of the vibrator which is dependent upon the gain of shear strength and wall friction in the concrete below the head of the vibrator. Rate of pour (time) and temperature are important to the extent that they control the gain of shear strength of the concrete.

Shear strength is a function of head of concrete, time (rate of pour), temperature, mix proportions, mix consistency, additives used and the rigidity of the formwork. The more flexible the formwork, the more the concrete can strain laterally and develop shear strength. Hence the considerations controlling lateral pressure given by ACI can be regrouped to reflect these two ideas.

Shear Strength

1. Depth of placement
2. Time (rate of pour) from the start of pour
3. Temperature of concrete mix and ambient temperature
4. Mix proportions and maximum aggregate size
5. Mix consistency
6. Type of cement
7. Smoothness and permeability of form
8. Porewater pressure

Fluidized Depth of Concrete

9. Power of vibrator
10. Immersed depth of vibrator
11. Duration of vibration
12. Depth of influence of vibration
13. Cross section of the form
14. Shear strength of concrete

CHAPTER 2

THEORETICAL BACKGROUND AND HISTORICAL REVIEW

2.1 One of the first reports, concerned with the lateral pressure of fresh concrete, was published in 1894 by McCullough as quoted by Leung (10). Since 1894 many investigators from various countries reported their observations on this particular topic in the technical press. In 1952 Rodin collected together and critically reviewed the then published experimental data on the lateral pressure of fresh concrete against vertical forms, and discussed the various factors that affect this lateral pressure (17).

In this section only the conclusions and recommendations of Rodin and the investigations carried out subsequently will be discussed as being relevant and covering all the necessary information available to-date.

2.2 Rodin (17), in 1952, presented a review of the published experimental data on the lateral pressure of concrete against forms, discussed the various factors that effect the lateral pressure and gave a rational explanation of the physical phenomena causing the type of pressure found in practice. Rodin deduced that the factors directly influencing the lateral pressure of concrete on formwork were as follows:

1. Rate of filling the forms
2. Method of placing the concrete, whether by hand or mechanical vibration
3. Consistency and proportions of the mix
4. Temperature of the concrete

5. Rate of setting of the concrete

6. Size and shape of the form.

Rodin, after study of the available data, concluded that the following physical factors determine the general shape of the pressure distribution against the form:

a) The degree of the arching action of the aggregate.

b) The rate of hardening of the cement mortar, and the setting shrinkage of the cement.

c) The relative rigidity of the formwork.

d) The method of placing the concrete.

The greater the degree of the above factors, the more the pressure distribution will tend to deviate from the equivalent hydrostatic pressure of a fluid having the same density as the concrete.

Rodin observed that the principal factors and concrete characteristics affecting the values of maximum pressure P_m and the head of concrete H_m at maximum pressure are:

a) Rate of Filling the Forms: As the rate of pour increases both P_m and H_m increase at a decreasing rate, indicating that at low rates of pour the hardening of the cement has a more important effect than the arching action and conversely at high rates of pour. The time required to reach P_m ranges from about 2 hours for rates of pour of 2 to 3 feet per hour to less than 30 minutes for rates of pour of more than 20 feet per hour. Figures 2.1, 2.2 and 2.3 give the relations between the rate of pour and the maximum recorded pressure, the head of concrete at maximum pressure, and the time required to reach the maximum pressure; these results are

based on experimental data deduced from tests conducted on 1:2:4 concrete at a temperature of 70°F.

The following general equations were considered satisfactory by Rodin for designing forms for a 1:2:4 mix, at a temperature of about 70°F.

$$P_m = 110^* H_m \text{ lb per square foot, for hand placed concrete} \quad 2.1$$

$$= 150^* H_m \text{ lb per square foot, for internally vibrated concrete} \quad 2.2$$

$$H_m = 3.6\ R^{1/3} \text{ feet,} \quad 2.3$$

where R denotes rate of pour in feet per hour.

Where external vibrators are used the full depth of concrete is in agitation and appears to act as a fluid, so that the forms should be designed for the full hydrostatic pressure of a liquid having the same density as the concrete.

However, where internal vibrators are used, it is normal practice to insert the vibrator into only the top 2 feet or so of the concrete, and as the height of the pour increases, it seems reasonable to assume that only the mass of concrete in the upper few feet will be affected by the vibration sufficiently to produce a full fluid pressure. Below this depth, it might be expected that the concrete will behave in a manner similar to hand placed concrete.

Thus it is considered satisfactory to assume a behaviour similar to that of hand placed concrete, in that the concrete pressure increases to a maximum value at a head given by equation 2.3, but

---

*unit weight of concrete is 150 lbs/ft^3 in Imperial units. Vibration is only considered to the extent that the effective density is increased from 100 lbs/ft^3 to 150 lbs/ft^3.

assuming a full hydrostatic pressure to this depth. This is given by equation 2.2 and shown in Figure 2.1.

b) Proportions of Concrete Mix: The richer the mix the greater is the value of maximum lateral pressure of concrete, possibly because of the increasing lubricating action of the cement and hence a decreasing arching action. This is summarized in the results plotted in Figure 2.3b.

c) Consistency of the Concrete: It is expected that, for a particular mix, the higher the water/cement ratio, or slump, the smaller would be the deviation of the pressure from a hydrostatic distribution, resulting from the increased fluidity of the concrete. The results available are plotted in Figure 2.3c.

d) Temperature of the Concrete: The pressure seems to rise significantly with a decrease in temperature. The limited data available in this respect is illustrated in Figure 2.3d.

e) Size and Shape of the Form: It is assumed that the smaller the width of the form, the greater would be the arching action, which will reduce the lateral pressure. No correction curve was presented for this factor.

Rodin suggested use of the pressure diagram shown in Figure 2.4, which provides maximum pressure, depth of fluid region of concrete and the resultant reduced pressure. Figures 2.3b, 2.3c and 2.3d suggest the percentage corrections to be made for type of mix, slump and temperature; but the accuracy of these results is in doubt.

2.3. R. Schjodt (18), using the concepts of soil mechanics, developed mathematical relations for the calculation of the pressure of concrete on forms. The factors considered in these derivations are the setting time, consistency and density of concrete; the smoothness, permeability and cross-section of the form; rate of pour and the depths to which the vibration penetrates.

Schjodt considered the fresh concrete, when compacted by vibration, to behave as a liquid and the pressure curve always to begin tangential to the line of hydrostatic pressure. As soon as the concrete is left alone, it developes cohesion and friction. With time this cohesion in the concrete will increase but here this phenomenum has been assumed of theoretical importance and of little practical significance.

Schjodt stated that the angle of internal friction will have a relatively small value to begin with, but will increase during setting to a maximum value of 90°. This assumption is obviously not correct.

Schjodt in his study of the pressure of concrete gave considerable importance to the porewater pressure, which is part of the total pressure against the form, but this is difficult to estimate due to leakage from the form and adsorption of water into the cement gel.

Schjodt developed equations for two different sets of assumptions.

2.3.1 Pressure Without Friction Between the Concrete and the Forms

The lateral pressure of concrete, below the depth of the effect of vibration, was derived using earth pressure theories and assuming rapid internal drainage,

$$P = [\gamma(h_1 + h) - \gamma_o h_w]\lambda_1 + \gamma_o h_w$$

$$= [(\gamma - \gamma_o K)\lambda_1 + \gamma_o K](h_1 + h) \qquad 2.4$$

where $h_w = K(h_1+h)$ is the porewater pressure, and K is a coefficient giving the porewater pressure as a function of the height of concrete.

γ is the unit weight of the mix, γ_o unit weight of water and h_1 the depth to which the effect of vibration penetrates, h is the distance from this level to the point where the pressure is to be calculated.

The coefficient λ_1 is a function of the stiffness of the concrete and varies with time. Here in order to take into account the setting, λ_1 is written as

$$\lambda_1 = \tan^2(45-\phi/2)(1 - \frac{h}{h_s}) = \lambda(1 - \frac{h}{h_s}) \qquad 2.5$$

where $\lambda = \tan^2(45-\phi/2)$ is the active lateral pressure coefficient for a cohesionless mass and h_s is the height to which the concrete has risen when it has taken the final set, counting from the depth h_1.

ϕ is the angle of internal friction of the concrete after it is left unvibrated.

Assuming slow internal drainage, equation 2.4 can be written as

$$P = (\gamma - \gamma_o)(h_1 + h)\lambda_1 + \gamma_o h_w \qquad 2.6$$

If the concrete rises at the speed V in the forms, then

$$h_s = Vt_s \qquad 2.7$$

where t_s is the setting time. Equation 2.4 can be written as

$$P = [(\gamma - \gamma_o K)\ \lambda\ (1 - \frac{h}{h_s}) + \gamma_o K](h_1 + h) \qquad 2.8$$

The maximum value of the pressure is given as

$$P_m = [\frac{\gamma\lambda}{2}(1+\frac{h_1}{h_s}) + \frac{\gamma_o K}{2}(1-\lambda-\lambda\ \frac{h_1}{h_s})][h_1 + \frac{h_s}{2}(1 - \frac{h_1}{h_s} + \frac{K}{\lambda}\ \frac{\gamma_o}{\gamma-\gamma_o K}] \qquad 2.9$$

the depth of this pressure from the surface is given by the relation

$$H_m = \frac{h_s}{2}\ [(1 - \frac{h_1}{h_s}) + \frac{K}{\lambda}\ \frac{\gamma_o}{\gamma-\gamma_o K}] \qquad 2.10$$

If it is assumed that $h_1 = K = 0$ and $\lambda = 1$

then

$$P_m = \frac{1}{4}\ \gamma h_s \qquad 2.11$$

Schjodt in his use of the lateral pressure coefficients assumed the concrete mass to fail which is far from reality, and not applicable.

2.3.2 Pressure with Exterior Friction

In narrow walls and in columns especially when the forms have the rough surface of ordinary form boards, the friction of the concrete against the forms has a significant influence and cannot be neglected.

In order to find an expression for the pressure in this case, the equilibrium of a horizontal section of the concrete below h_1, shown in Figures 2.5 and 2.6 must be considered.

$$dP_v F = \gamma_1\ F\ dh - P_1\ U\ dh\ \tan\phi_1^* \qquad 2.12$$

where P_1 is a horizontal pressure, not counting the porewater pressure

$$\gamma_1 = \gamma - \gamma_o K$$

where γ is the unit weight of mix, γ_o of water and K is a coefficient giving the porewater pressure as a function of the height of concrete.

F is the concrete area in a horizontal section and U is the circumference.

ϕ_1 is the angle of friction between the concrete and the formwork.

It should be noted that the angle of wall friction actually developed is indeterminate and less than the limiting value.

$\frac{F}{U}$ can be represented by R.

then $$\frac{dP_v}{d_h} = \gamma_1 - \frac{\tan\phi_1 P_1}{R} \qquad 2.13$$

and $\frac{P_1}{P_v}$ = ratio between horizontal and vertical pressure = $\lambda(1-h/h_s)$ 2.14

Equation 2.13 is written as

$$\frac{dP_v}{d_h} = \gamma_1 - \frac{a}{h_s}(1 - \frac{h}{h_s})P_v \qquad 2.15$$

With $a = \lambda\tan\phi_1 \; h_s/R$.

From equation 2.15, using $P_v = \gamma_1 h_1$ for h = 0 the constant can be determined

$$P_v = \gamma_1(Ah_1 + kh_s) \qquad 2.16$$

Here

$$A = e^{-a\frac{h}{h_s}(1 - \frac{h}{2h_s})}$$

$$k = e^{a/2(1 - \frac{h}{h_s})^2} \sqrt{\frac{2}{a}} \int_{\sqrt{\frac{a}{2}}(1 - \frac{h}{h_s})}^{\sqrt{\frac{a}{2}}} e^{-h^2} \, dh$$

The numerical values of A and K are plotted in Figure 2.7 and Figure 2.8, respectively. The pressure against the forms is calculated from equations 2.14 and 2.16, and the porewater pressure added

$$P = P_v\lambda(1 - \frac{h}{h_s}) + \gamma_o K(h_1 + h)$$

$$= \gamma_1(Ah_1 + Kh_s)(1 - \frac{h}{h_s}) + \gamma_o k(h_1 + h) \qquad 2.17$$

If ϕ_1 is small, or if the wall is thick so that R is great, "a" will have a small value, then A $\approx$ 1 and K $\approx \frac{h}{h_s}$ and equation 2.17 will be identical to equation 2.8.

2.4 ACI Committee 622 (Redesignated Committee 347) (8) was organized in 1955 to improve the safety and quality of formwork for concrete construction. With the basic goal of developing specifications for the design and construction of formwork, the Committee reviewed existing test reports and design formulae developed since the nineteenth century.

The Committee after studying all the variables affecting the lateral pressure of concrete concluded that the following variables affect the lateral pressure of concrete after placement in forms:

1. Rate of placement
2. Consistency of concrete
3. Weight of concrete
4. Maximum aggregate size
5. Temperature of concrete mix
6. Ambient temperature

7. Smoothness and permeability of form
8. Cross section of forms
9. Effect of consolidation by vibration
10. Placing procedures
11. Porewater pressure
12. Type of cement
13. Depth of placement.

The following general relation was produced by ACI Committee 622 for form design (8), taking into account the variables of temperature of the concrete and rate of pour when compacted by internal vibration

$$P_m = C_1(1 + \frac{C_2 R}{T}) \qquad 2.18$$

where C_1 is a function of the unit weight of mix and C_2 is some function of the consistency of the concrete. P_m is the maximum lateral pressure in psf, R is the rate of pour in feet per hour, and T is the temperature of the concrete in degrees Fahrenheit.

Assuming the unit weight of concrete mix as 150 lbs/ft^3, the Committee proposed the following formula for columns

$$P_m = 150 + \frac{9000\ R}{T} \qquad 2.19$$

maximum 3000 psf or 150 h, whichever is less.

For walls the following relations were recommended

a) With rate of placement controlled and less than 7 ft/hr

$$P_m = 150 + \frac{9000\ R}{T} \quad \text{psf} \qquad 2.20$$

with a maximum of 2000 psf or 150 h whichever is less.

b) With rate of placement greater than 7 ft/hr

$$P_m = 150 + \frac{43,400}{T} + \frac{2800\ R}{T} \quad \text{psf} \qquad 2.21$$

[150 h or 2000 psf which ever is less].

Where h represents the height of wall.

Table 2.1 gives the maximum lateral pressure of concrete for design of wall forms based on ACI Committee 347 pressure formulae 2.20 and 2.21.

Table 2.2 gives the maximum lateral pressure of concrete for design of column forms based on ACI Committee 347 pressure formula 2.19.

2.5 Ritchie (16), experimentally investigated the effects of rate of pour, mode of compaction, workability of the concrete and the size of the form, on the shape of the pressure envelope and the maximum pressure exerted on the formwork.

2.5.1 Rate of Pour

Four rates of pour were used, namely 4, 10, 20 and 70 ft per hour; the results are given in Figures 2.9 and 2.10 for both 1:3 and 1:6 mixes compacted by internal vibration. Both mixes show a rapid initial increase in pressure with rate of pour which then levels off considerably at higher rates. It was noticed that there was a wide difference between the results for the 1:6 mix and the 1:3 mix.

2.5.2 Method of Compaction

Due to the marked difference in behaviour recorded between

TABLE 2.1 Maximum Lateral Pressure of Concrete on Wall Forms Recommended by ACI Committee

Rate of Placement R, ft per hr	p, maximum lateral pressure psf, for temperature indicated					
	90°F	80°F	70°F	60°F	50°F	40°F
1	250	262	278	300	330	375
2	350	375	407	450	510	600
3	450	488	536	600	690	825
4	550	600	664	750	870	1050
5	650	712	793	900	1050	1275
6	750	825	921	1050	1230	1500
7	850	938	1050	1200	1410	1725
8	881	973	1090	1246	1466	1795
9	912	1008	1130	1293	1522	1865
10	943	1043	1170	1340	1578	1935

TABLE 2.2 Maximum Lateral Pressure of Concrete on Column Forms Recommended by ACI Committee 347.

Rate of Placement R, ft per hr	p, maximum lateral pressure, psf, for temperature indicated					
	90°F	80°F	70°F	60°F	50°F	40°F
1	250	262	278	300	330	375
2	350	375	407	450	510	600
3	450	488	536	600	690	825
4	550	600	664	750	870	1050
5	650	712	793	900	1050	1275
6	750	825	921	1050	1230	1500
7	850	938	1050	1200	1410	1725
8	950	1050	1178	1350	1590	1950
9	1050	1163	1307	1500	1770	2175
10	1150	1275	1436	1650	1950	2400
11	1250	1388	1564	1800	2130	2625
12	1350	1500	1693	1950	2310	2850
13	1450	1613	1822	2100	2490	3000
14	1550	1725	1950	2250	2670	
16	1750	1950	2207	2550	3000	
18	1950	2175	2464	2850		
20	2150	2400	2721	3000		
22	2350	2625	2979			
24	2550	2850	3000			
26	2750	3000	3000	psf maximum governs		
28	2950					
30	3000					

the 1:3 and 1:6 mixes, both mixes were studied to determine the relative effects of compaction by hand and by mechanical vibration. The results are shown in Figures 2.11 and 2.12. In both cases the maximum pressure developed was greater with vibrated compaction, but the average percentage increase for the two mixes was quite different. Although the mixes had nominally the same workability, the lean (1:6) mix was more influenced by the effects of vibration. The pressure developed in this case increased by an average of 56 percent compared with only 10 percent for the rich (1:3) mix. The corresponding increase in pressure predicted by Rodin for a 1:2:4 mix was 36 percent.

It was observed that the head of concrete at maximum pressure tended to increase as the pressure itself was increased with vibration. Ritchie noted that with both the 1:3 and 1:6 mixes, when compacted by hand, the batches with low workability gave slightly higher pressures than those with high workability: This he considered to be due to the wedging action of the aggregate particles, when they were compacted by hand ramming, as opposed to the floating action produced by mechanical vibration.

2.5.3 Formwork

To determine the effect of size of the formwork on the maximum lateral pressure of concrete, the maximum pressures were recorded with column sizes of 6 in. x 6 in. and 10 in. x 10 in. Concrete placed in the 10 in. x 10 in. formwork gave an increase of 26 percent in lateral pressure as compared to the 6 in. x 6 in. form. The comparison of different column sizes is given in Figure 2.13. Ritchie commented that the results

obtained with formwork of 24 in. x 96 in. cross-section, with heavy vibration, agreed almost exactly with Rodin's theoretical estimate for P_m and H_m. The maximum pressure developed was 268 percent greater than that for the original column of 6 in. x 6 in. section.

2.5.4 Properties of the Concrete Mix

a) Richness of the Mix

The comparison between 1:3 and 1:6 mixes is shown in Figure 2.14. It was observed that the richer mix gave the higher pressure. The percentage increase in pressure was 91 percent at 10 ft per hour and 38 percent at 20 ft per hr or an average correction factor of 165 percent for the richer mix. This corresponded to Rodin's 136 percent increase in pressure for a 1:1:2 mix over the basic 1:2:4 mix.

b) Workability

The lateral pressure of concrete was observed to increase with workability as shown in Figures 2.15a and 2.15b. However, there was a significant difference between the 1:3 and 1:6 mixes as illustrated in Figures 2.11, 2.12 and 2.15a and 2.15b.

2.6 The Civil Engineering Research Association (Now called CIRIA - Construction Industry Research and Information Association) (9) sponsored a large scale field investigation on the lateral pressure of concrete on formwork by making over 200 pressure measurements under actual industrial conditions in England during 1961-1962. The results were published as a research report in 1965.

The range of conditions covered by this series of tests was considerable. Concrete temperatures were observed as low as 38° to over

90°F, rates of placing varied from 1 ft/hour to 120 ft/hour, sections varied in minimum dimensions from 5 inch to 8 ft, heights of pour were normally not less than 10 ft and a few were in excess of 20 ft. Internal vibration was invariably used but external vibration was sometimes employed in addition. Maximum sizes of aggregate varied up to 1-1/2 inch with slumps from 0 to 6 inch.

The authors concluded from a preliminary investigation that fresh concrete behaves almost as a liquid under the mobilizing influence of vibration, the pressure generated being simply the product of density and head. Deviation of the pressure curve from the equivalent hydrostatic condition occurs in consequence of two factors - stiffening of the concrete and arching effects.

2.6.1 Stiffening of concrete was defined as the progressive increase in resistance of the concrete to mobilization, which is partly due to chemical changes in the cement matrix but is also dependent upon the degree of mechanical interlocking between aggregate particles. As stiffening developes, the concrete becomes capable of supporting additional surcharge without increase in lateral pressure; this phenomenon was assumed to be related to the rate of increase of shear strength of the fresh concrete.

2.6.2 Arching effects - Kinnear *et el* considered that in all sections, the vertical load at any horizontal section is reduced by frictional forces developed between the concrete and the form faces. These frictional forces assume particular importance in narrow sections where the surcharge volume is comparatively small. This effect has been termed

arching and is dependent on the minimum dimensions of the section, the profile and slope of the form surface, and the variation of the coefficient of friction between the concrete and the form faces. It was also concluded that the arching limit increased with higher rate of placing, and could be represented by the equation

$$P = 300 + 50d + 20R \qquad 2.22$$

where d is the minimum dimension of form in inches.

2.6.3 CIRIA after preliminary study of the test results, concluded that five influencing variables were of particular importance and classified the test results according to the magnitude of these variables. The subdivisions adopted were:

1. Concrete Temperature - °F

A	B	C	D	E	F	G
<40	40-50	50-60	60-70	70-80	80-90	>90

2. Rate of Placement - R ft/hour

A	B	C	D	E	F	G	H
1-2	2-3	3-5	5-8	8-12	12-20	20-30	>30

3. Minimum Dimension - d inches

A	B	C	D	E
<6	6-12	12-18	18-24	>24

4. Workabiltiy

A	B	C
Stiff	Normal	Highly Workable

The above classification of workability is further explained in terms of slump.

Workability Ranges

	Stiff	Normal	Highly Workable
Slump (inches)	0-1	1-2-1/2	2-1/2-5

5. Vibration

A	B	C
Low	Intermittent	Continuous

This classification did not give a very clear division hence an appropriate division was made in terms of continuity of vibration expressed as a percentage of total placing time

Low	Intermittent	Continuous
10-40%	40-70%	70-100%

Each of the above results were then coded for rapid identification with a five letter symbol representing each of the above divisions, e.g., a result with the Index CDACB represented a test when the concrete temperature lay between 50 and 60°F, placing continued at a rate of 5-8 ft/hour in a wall up to 6 inches wide using a highly workable concrete vibrated intermittently.

2.6.4 Stiffening Time of Concrete

The stiffening time t_{max}, may be defined (7) as the time at which maximum pressure occurs. It must be stated here that this definition of time is more realistic than the more usual set times as defined in ASTM C191-70. This time should be dependent on the concrete temperature and on the workability of the concrete. The derived relationship between the stiffening time and temperature of the concrete is given in Figure 2.16.

2.6.5 The Shape of the Pressure Curve

CIRIA gave the following relation for the pressure curve

$$P = \frac{\Delta R t}{1 + C\left(\frac{t}{t_{max}}\right)^4} \qquad 2.23$$

where P = pressure lb/ft^2

Δ = density of the concrete (lb/ft^3)

R = rate of placing (ft/hour)

t = time from commencement of placing (hours)

t_{max} = stiffening time of the concrete (hours), Figure 2.16

C = factor depending upon the workability of the concrete and the continuity of vibration

Empirical values of C are given in Figure 2.17 and were derived directly from the experimental results. A correction to the above equation was introduced to account for the withdrawal of the source of vibration which normally occurs with very high rates of placing. The correction 12(8-R) has the effect of adding small pressures at $R < 8$ and subtracting comparatively large pressures at $R > 8$. The final equation is

$$P = \frac{\Delta R t}{1 + C\left(\frac{t}{t_{max}}\right)^4} + 12(8-R) \qquad 2.24$$

CIRIA recommended an additional pressure of 200 psf to allow for impact surcharge due to pouring of concrete from heights.

2.6.6 Pressure Design Chart

CIRIA developed a chart from the test results to provide a guide to determine the design pressure for formworks, this is presented in

Figure 2.18. The radial lines represent rates of placing R from 1 ft/hr to 50 ft/hr, while the full spiral lines represent different temperatures of concrete from 40°F to 90°F. The broken spiral lines, d, are arching limits for minimum section dimensions from 6 in. to 18 in. whereafter arching effects are considered to be inappropriate.

The diagram would be used by selecting the appropriate rate of pour and concrete temperature and then measuring the pressure radially, from point 0 in accordance with scale P, to the point at which the lines representing the above criteria intersect. The basic pressure thus derived is then modified by multiplying by a factor F obtained from Figure 2.19 to compensate for concretes of different workabilities and for different continuities of vibration. The arching limit for the appropriate section is then checked on the same radial "rate of placing" line and the lesser value used to determine the design pressure. An addition of 200 lb/ft^2 is made after the application of factor F, to take account of pressure due to impact.

The pressure design chart is bounded by two arbitrary limits, a maximum pressure of 3000 lb/ft^2 and a minimum temperature of 40°F.

2.7 Olsen (13) in his Ph.D. thesis, presented a design method based on the ACI and CIRIA approaches, modified by introducing the concept of shear strength of the fresh concrete.

The shear strength of fresh concrete was determined by use of a triaxial testing arrangement. The triaxial tests were conducted at different concrete set times, defined as time after addition of water to the mix and a shear strength-set time relationship was established. Only

one concrete mix 1:1.5:1.5 with a water cement ratio of 0.40 and a test temperature of 77°F was used so that the factor of shear strength could be isolated and its effects on concrete pressure established.

Under these conditions, the lateral pressures obtained by this method were compared with the pressures that were computed using the methods recommended by ACI and CIRIA.

Olsen then made the following conclusions:

1. Triaxial tests may be used to determine the lateral pressure on vertical formwork by wet concrete.
2. The shear strength parameters of concrete are a linear function of set time.
3. Coulomb's rupture theory does apply to concrete before it sets.
4. The shear strength of fresh concrete can be related to the lateral pressure of concrete on formwork provided the associated boundary conditions are considered.
5. Both the ACI and CIRIA methods for determining the concrete pressures give similar results. However, in some cases they are both overly conservative.

2.8 Ritchie (15), in a study sponsored by CIRIA, investigated the effect of stiffening of concrete on the lateral pressure of concrete on vertical formwork.

A detailed study was conducted to establish a relationship between types of cement, types of aggregates and the workability of the concrete mix. It was established that slump tests, vebe tests and by means of flow table, stiffening of concrete can be determined, but the

slump test becomes inoperative when a zero slump has been obtained. Ritchie concluded that the compaction of concrete mixes by mechanical means increases the shear strength over those compacted by hand; this effect is more noticeable with decrease in the ratio of cement to aggregate. It was also concluded after experimental investigation that the ACI calculated pressures are excessively conservative, probably because of the non-recognition of the effects of mix characteristics, and intensity of vibration. Ritchie also observed that the CIRIA design chart provided the closest agreement between predicted and recorded pressures, although the increase in pressure forecast by the chart due to increase in rate of pour was not obtained experimentally. A greater difference in the pressures predicted and observed occurred with concretes of low cement content. Also the correction factor 'F' by which the basic pressures from the CIRIA design chart are multiplied, was observed to cover too wide a range, predicting greater reductions and increases from a standard condition than were actually achieved.

Ritchie formulated a new concept of the mechanisms intrinsic in the pressure of concrete on formwork, by considering a slug of freshly mixed concrete initially placed in the formwork, to consist of a heterogeneous conglomerate of discrete batches of aggregate particles bound together in a cement matrix. Each of these batches is interlinked by this matrix and enclose large air voids. With vibration this semi-continuous mass is rendered homogeneous, with a majority of the air being expelled and the aggregate particles being kept in suspension by dispersive pressure. When the mix is in such a condition it acts as fluid with a density of around 150 lbs/ft^3 and exhibits a hydrostatic

pressure on the form in proportion to its depth. With the withdrawal of the source of vibration the concretes structural viscosity is immediately increased, although the yield strength of the cement paste matrix may be removed, diminished or augmented depending upon the duration of shear. The form pressure which the mix exhibits as it congeals will reduce rapidly from the totally fluid to that necessary to maintain equilibrium, since a resistance to dilatancy of the cement paste together with the regained viscosity, and cohesion will contain a large proportion of the shearing stresses induced by the mix self weight. With the imposition of a further slug of concrete which is also rendered fluid by vibration, the shearing stresses induced in the lower slug will be such that the dilated resistance to deformation and cohesion are easily overcome and the mix will tend to deform plastically, such that the pressure produced at all levels will appear to be hydrostatic in 1:1 ratio. During this process the aggregate particles in the matrix will tend to approach one another since because the yield strength of the cement paste has been removed it becomes incapable of suspending these particles. The particles will gravitate although this will depend on the dispersive pressure between any two particles caused by transmitted vibration and also hydrodynamic lag effects. Eventually, with the superimposition of further slugs of concrete and transmitted vibration, a particulate system will form, with sizes ranging from unhydrated cement particles to the largest aggregate size with such a system pressure may still be transmitted in a lateral direction through pore-fluid of the cement paste matrix. As the shearing stresses induced by the head are transferred to the skeleton structure a compression of the volume occupied by the

particles will occur, resulting in the expulsion of the interstitial cement paste and water and thus the transference of vertical pressure to the form walls.

When, however, a maximum density of the particulate system occurs, any further shearing stresses induced by the head will cause a dilation of the structure and thus a slight increase in the volume which it occupies. This will cause the pore fluid to be drawn into the interstitial spaces formed, and hence will result in a reduction of the pressure transmitted in the lateral and vertical directions. Thus, the concrete pressure reaches a maximum and then exhibits the phenomenon of no pressure increase with further head. A distinct drop off in pressure is experienced with time as thixotropic regain is established and the chemical bonds restrain any tendency to plastic deformation.

During his investigation, Ritchie also discovered the following:

1) The effect of increasing the workability of concrete as measured by the slump test does not necessarily produce an increase in the lateral pressures generated on formwork.

2) An increase in the continuity of vibration applied to any one mix at any level of workability does not appear to necessarily produce an increase in the maximum pressure. It would appear that for the form used and the type of vibration applied, a critical continuity exists whereby a reduction, or increase, in this value gives a reduction in the maximum lateral pressure. The degree of this reduction, however, would appear to be dependent on the combined effect of mix characteristics, workability, the continuity of vibration applied and the rate of placing.

3) The degree of pressure reduction is not related directly to the degree of workability as measured by the slump test at zero time, the history of vibration, mix cement to aggregate ratio, or rate of concrete placement.

4) It was suggested that the degree of pressure reduction under any circumstances is dependent on the degree of mix mobility, matrix fluidity obtained at the time of occurrence of maximum pressure, and the setting action of cement producing an increase in the cohesion of the mass, i.e., its isotropic tensile strength.

2.9 Adam (1) conducted tests to study the effect of certain variables on the lateral pressure of concrete by using a steel wall formwork 3 metres high (9.75 ft), 2.5 metres (8.13 ft) wide and of variable thickness. He considered the type of cement, size of aggregates, additives, slump of the mix, rate of pour and vibration to be the factors affecting the concrete pressure significantly.

During his study, Adam measured concrete pressure using a device which consisted of a metallic membrane attached to the vertical face of the formwork supported by oil, which transmitted the concrete pressure from the membrane to a monometer.

Adam conducted tests with various types of cement, and additives. Concrete pressure was determined experimentally varying the rate of pour from 0.33 m/hr (1 ft/hr) to 8 m/hr (26 ft/hr), wall thickness 12 cm (5 in.) to 40 cm (15 in.) and temperature from 0°C to 25°C. During the tests slump, porewater pressure and the influence of vibration were measured.

Adam concluded that the depth of influence of vibration is a significant factor affecting the concrete pressure though he did not take into consideration the power of the vibration or the duration of vibration. Adam also commented that the slump and thickness did not have a very significant effect on the lateral pressure and the effect of the rate of pour was less than suggested by previous investigators.

Adam concluded the following factors to have a significant influence on the lateral pressure of concrete.

1. Temperature: As the temperature decreases, the pressure increases, but this phenomenon is appreciable only in case of high rates of pour and in case of rates of pour as low as 1 m/hr its effect is negligible.

2. Rate of Pour: It was concluded that the increase in rate of pour of concrete gives rise to an increase in pressure, as illustrated in Figure 2.20, but this effect is less than predicted by Rodin, ACI Committee 622 and Schjodt.

3. Type of Cement: It was found that the type of cement has a significant effect on the pressure of concrete.

4. Size of Aggregate: Adam concluded that the size of the aggregate is a factor significantly affecting the concrete pressure.

5. Thickness of Form: Adam concluded that an increase in form thickness increases the concrete pressure only for a moderate rate of pour (2 to 3 m/hr) and does not have any influence on pressure for rate of pour less than 1 m/hr or greater than 4 m/hr.

6. Additives: Tests were also conducted with various types of cement and additives and these variables were concluded to have a major effect on concrete pressure.

Adam proposed prediction equations relating concrete pressure to rate of pour and temperature of the concrete mix which are illustrated in Figure 2.21 and summarized in Table 2.3.

2.10 Levitsky (11) attempted to approach the problem analytically by hypothesizing that the shape of the pressure curve was the result of a simultaneous hardening and shrinkage of the concrete mix following placement, and in addition a relaxation of the formwork.

Levitsky considered pouring a vertical wall between form surfaces some arbitrary distance apart, as depicted in Figure 2.22; the wall extending to infinity, horizontally and resting upon an infinitely rigid body. The form surfaces were modelled to exhibit a large initial stiffness under impulsive loading, limited creep under constant pressure, and a relaxation of pressure with constant displacement. The coefficients of such a model are associated with the physical parameters of the formwork according to the following definitions, also illustrated in Figure 2.23.

(1) $E_1 + E_2$ = initial stiffness coefficient

(2) E_1 = residual stiffness coefficient

(3) n = viscous coefficient

(4) $n/E_2 = t_R$ = relaxation time constant of the formwork.

Assuming R to be the rate of pour in feet per hour, t_H the settling time for the concrete mix, z_H representing the depth of liquid region of concrete and z the vertical coordinate of the system, the maximum form pressure, occurring at the hardening surface of the concrete, is given by the relation

$$P_m = \rho R t_H \qquad 2.25$$

TABLE 2.3 Maximum Lateral Pressure of Concrete in Tons Per Square Metre (Adam)

Temperature	P_{max} t/m^2	(V) Rate of Pour (m/h)	
		V < 2 m/h	V > 2 m/h
	< 5°C	2 + 1.25 V	4.1 + 0.2 V
	15°C	2 + V	3.6 + 0.2 V
	≥25°C	2 + 0.85 V	3.3 + 0.2 V

The residual value of the form pressure P_∞ is represented by

$$P_\infty = P_m (1 - k) \qquad 2.26$$

where k is called the relaxation factor and is given as

$$K = \frac{1-S'}{S'T'} [1 - \exp(-S'T')] \qquad 2.27$$

$T' = \frac{t_H}{t_R}$ = ratio of hardening time to relaxation time

and

$S' = \frac{E_1}{E_1 + E_2}$ = ratio of residual form stiffness to initial form stiffness given in Figure 2.24.

In the final form the pressures for hydrostatic region and beneath the hardening interface were given as the following:

$$P = \text{density x depth} = \rho z, \quad 0 < z < Rt_H \qquad 2.28$$

$$P = \text{pressure below the hydrostatic limit} = P_\infty + (P_m - P_\infty) \exp\left(\frac{z_H - z}{Rt_R}\right), \quad Rt_H \leq z \leq \infty \qquad 2.29$$

Levitsky's theoretical approach, to determine the lateral pressure of concrete, reproduces the characteristic shape of the pressure curve but the variation of the form pressure distribution with rate of pour does not correspond to the experimental data; it is observed that this method gives a linear variation of lateral pressure with pouring rate.

Levitsky did not take into consideration the development of shear strength and stiffening of concrete, shrinkage, vibration, arching and porewater pressure, but is more or less based on the structural aspects of the form.

2.11 Summary

Owing to the large number of different variables affecting the lateral pressure of concrete and the different empirical approaches adopted by different investigators to solve the problem, it is important to summarize the different factors responsible for the general pattern of the pressure distribution of concrete on the form and their effects on the maximum pressure.

2.11.1 Shape of Pressure Diagram of Forms

From the hypothetical and experimental reasonings given by different investigators, at this stage, it can be concluded that the shape of the pressure curve achieved is due to the following factors

(a) Arching, which is a phenomenon representing the friction between concrete and the face of the form and the internal shear strength mobilized due to the deflection of any part of the form. This factor has been considered to be important by Rodin, Schojdt, Kinnear and Ritchie.

(b) Shear Strength of Concrete. Shear strength in a particulate material is due to the development of cohesion and internal friction. It is obvious that the shear strength of concrete increases with time, probably the major change being the development of cohesion (interlocking crystal growth). Rodin, Ritchie, Schjodt's and Olsen agreed to this phenomenon. Rodin concluded that shrinkage and bleeding of concrete tends to accelerate the stiffening time of concrete and speed the development of its shear strength.

2.11.2 Influence of Physical Factors on the Lateral Pressure of Concrete

In addition to the factors stated above the following physical factors influence the development of maximum pressure of concrete.

(a) Rate of Placement of Concrete

As the rate of pouring of concrete increases the maximum pressure also increases. The significance of this factor has been taken into consideration in Rodin's equations 2.1, 2.2 and 2.3. This factor has also been observed to have a major affect on concrete pressure by ACI Committee 347, Ritchie (16), Kinnear (9) and Adam (1).

(b) Propertion of Concrete Mix

Rodin and Ritchie observed that the richer concrete mix exhibits higher pressure. Rodin attributed this phenomenum to the lubricating action of the cement which reduces the frictional properties of the mass and hence the arching action.

(c) Size of Aggregate

Adam (1) and ACI (8) concluded that the size of the aggregate is a factor significantly affecting the concrete pressure.

(d) Consistency of the Concrete

The higher the slump for a particular mix the lesser would be the deviation of the pressure from a hydrostatic distribution, and the higher the lateral pressure. This was concluded by Rodin and Ritchie and indirectly by CIRIA.

(e) Temperature of the Concrete Mix

A decrease in temperature increases the concrete pressure significantly. This affect has been observed by Rodin, Ritchie, Kinnear and Adam.

Rodin's formulae for maximum pressure of concrete provide

pressures at 70°F to which a correction factor has to be applied to obtain pressure for a given temperature of concrete mix, the relation of temperature and correction factor is given in Figure 2.4d.

Kinnear (9) considered the effect of temperature on the pressure of concrete in his derivation of the relation (Eq. 2.26) giving lateral pressure of concrete by assuming that the setting time of concrete is affected by temperature.

Ritchie (16) and Adam (1) also observed this effect during their investigations.

(f) Size and Shape of the Form

It is generally considered that the smaller the width of the form, the greater would be the arching action which would reduce the concrete pressure.

(g) Method of Compaction

Rodin concluded that the concrete compacted by vibration will exhibit higher pressures than that compacted by hand. Rodin also observed that using external vibrators results in hydrostatic concrete pressure over the total depth of the form.

Ritchie (16) observed that the pressure developed during the compaction of lean mixes by mechanical vibration was 56 percent greater than that exhibited during hand placing, whereas the influences of vibration on a rich mix (1:3) gave a 10 percent difference of pressure due to lubrication.

CIRIA (9) considered continuity of vibration to be a significant factor influencing the concrete pressure and adopted a constant of vibration in its relation for pressure.

2.11.3 Comparison of Results

The pressures which would be predicted by the methods recommended by Rodin, CIRIA, ACI and Adam at temperatures of 70°F, 50°F and 35°F, at a rate of pour of 20 ft/hr are compared and illustrated in Figures 2.25a, 2.25b and 2.25c.

It is noticed that Rodin's approach towards the calculations of lateral pressure takes into consideration the effects of temperature changes which are quite significant, whereas the effect of vibration is considered only to the extent of the method of compaction with no specific attention to the parameter of vibration.

The method recommended by CIRIA takes into consideration the effects of rate of pour, temperature, continuity of vibration and width of the form but the pressures achieved are highly influenced by the arching criteria which only takes into consideration the rate of pour of concrete and width of the form.

The ACI Committee 622 (347) recommendations do not show significant effects due to small changes in temperatures and usually provides higher values for the lateral pressure.

Adam considered the variation in temperature and rate of pour to have significant effects on the lateral pressure of concrete; however, his conclusions from the experimental results showed the temperature effects to be significant only over a major temperature variation as illustrated in Table 2.3.

In order to compare the methods of determining lateral pressures of concrete, the pressures calculated by the methods recommended by Rodin, ACI Committee, CIRIA and Adams are tabulated in Table 2.4 for various rates of pour, temperature, slump and mix proportions.

TABLE 2.4 Maximum Pressure of Concrete in Pounds Per Square Foot

	Rate of Pour			R = 5 ft/hr			R = 10 ft/hr			R = 20 ft/hr		
	Temp of Concrete			40°F	50°F	70°F	40°F	50°F	70°F	40°F	50°F	70°F
	d in	Conc Mix	Slump									
Rodin		1:2:4	2"	1151	984	757	1450	1240	954	1827	1563	1202
			4"	1263	1080	831	1591	1361	1047	2005	1715	1319
			8"	1543	1320	1015	1945	1664	1280	2451	2096	1612
		1:3:6	2"	978	836	644	1233	1054	811	1553	1329	1022
			4"	1074	918	706	1352	1157	890	1704	1458	1121
			8"	1312	780	863	1653	1414	1088	2083	1782	1370
ACI				1275	1050	793	2400	1950	1436	3000	3000	2721
CIRIA-Stiffening Criteria	12"		2"	561	558	507	1099	1091	991	2101	2086	1886
			4"	598	597	588	1100	1099	1080	2105	2102	2065
			8"	*	*	*	*	*	*	*	*	*
Arching Criteria	12"		2"	1000	1000	1000	1100	1100	1100	1300	1300	1300
			4"	1000	1000	1000	1100	1100	1100	1300	1300	1300
			8"	1000	1000	1000	1100	1100	1100	1300	1300	1300
Stiffening Criteria	18"		2"	561	558	507	1099	1091	991	2101	2086	1886
			4"	598	598	588	1100	1099	1080	2105	2102	2065
			8"	*	*	*	*	*	*	*	*	*
Arching Criteria	18"		2"	1300	1300	1300	1400	1400	1400	1600	1600	1600
			4"	1300	1300	1300	1400	1400	1400	1600	1600	1600
			8"	1300	1300	1300	1400	1400	1400	1600	1600	1600
Max Design Pressure**	12"		2"	761	758	707	1299	1291	1191	1500	1500	1500
			4"	798	797	788	1300	1299	1280	1500	1500	1500
			8"	1200	1200	1200	1300	1300	1300	1500	1500	1500
Max Design Pressure	18"		2"	761	758	707	1299	1291	1191	1500	1500	1500
			4"	798	797	788	1300	1299	1280	1500	1500	1500
			8"	1200	1200	1200	1300	1300	1300	1500	1500	1500
Adam				804	725	725	967	864	864	1093	990	990

*Under given conditions this criteria is not predominant, hence not considered.

**Max design pressure = minimum pressure value obtained from stiffening and arching criteria - 200 psi (impact pressure).

CHAPTER 3

OBJECT OF THE PRESENT STUDY

The lateral pressure of concrete is a function of numerous parameters. Tests to determine the lateral pressure of freshly-placed concrete have been conducted by many researchers, but the results varied too much to provide reliable data. This has been attributed to the different conditions under which the experiments were carried out, and also to the multitude of factors that influence the fresh concrete.

The original intention of this study was to experimentally determine a conservative envelope of lateral pressure with the parameters of slump and concrete strength kept constant and varying the width of the form, the temperature of the concrete and rate of pour. The first pour of this series of tests was a repeat of a pour in a previous series of tests to calibrate and reproduce the results obtained previously and to measure lateral pressure of concrete by using Cambridge cells; the Principles of Cambridge cell will be discussed in detail in Chapter 4. Unfortunately, the results in no way correspond with the previous results and the reason for this discrepancy had to be determined.

After studying the details of the present and previous experiments and much discussion it was realized that a different vibrator had been used, the depth to which the vibrator was immersed could have been different and that the duration of vibration could have differed. At this point it was realized that it would be unrealistic to determine a pressure envelope until the dependency of lateral pressure on vibration had been clarified. Hence the objectives were redefined as determining

the variation of lateral pressure with power of vibration, immersed depth of vibrator, duration of vibration and temperature keeping concrete strength, slump, rate of pour and form dimensions constant.

CHAPTER 4

EXPERIMENTAL APPARATUS

4.1 General

To determine the lateral pressure of concrete on formwork and to study the parameters responsible for the variations in concrete pressure and the extent of their influence, different investigators used many different types of equipment. However, the lack of correlation between results of the different investigators can be explained partly as due to the scarcity of knowledge and control of the parameters influencing the behaviour of the concrete, and partly due to the equipment used for measuring the lateral pressures.

It has been observed by several investigators that any outward movement or deflection of the form causes a tremendous reduction in lateral pressure, thus the current experimental investigation used rigid steel formwork to minimize this effect and hence maximize the lateral pressure.

4.2 Description of Formwork

The formwork used is a steel open ended box erected in the basement of the structural laboratory of the University of Ottawa. The basement floor is 12 feet below the main strong floor of the laboratory and hence 3 feet of the form projects above the ground floor. This location enables concrete to be poured directly from the mixing truck into the form. An overall view of the form is shown in Figure 4-1a.

The formwork has dimensions of 15 feet in height, 3 feet in width and thickness variable up to 22 inches. The movable 3 feet wide back face of the formwork has 5 holes, each 5 inches in diameter, to locate the pressure measuring devices.

The formwork is a rigid structure made from structural steel and details of the fabrication are illustrated in Figure 4-1b and given in Table 4.1. The major parts of the form are:

1. The movable back face
2. The two side faces
3. The front face
4. The supporting collars.

The movable back face is 0.5 inch thick steel plate stiffened by two vertical I-section beams and stiffeners; these beams in turn support 3 cross-beams to provide further stiffening and support a vertical I-section beam along the mid-width, which is used to carry the pressure cells, to prevent any movement of the movable face during concrete pouring. The supporting collars, made of box sections are also used to support the hydraulic jacks necessary to avoid any unforeseen movement in the back face of the form. The side faces are held tight against the front and back faces by beams bolted at three locations over the height of the structure.

4.3 Pressure Measuring Device and Principles

4.3.1 To measure the lateral pressure of concrete over the years many different types of instruments have been used. Roby (14) measured

TABLE 4.1 Details of Rigid Steel Formwork
(Refer to Fig. 4-1b)

Index No.	Description
1	Front face (2-15" channel sections and 1'6" channel sections).
2,3	Side faces, 12" channel section each, bolted to '5'.
4	4x4 WF Beam, welded to back of 'front face'.
5	4x4 WF Beam, hinged to '4', holding the 'side face' in vertical position.
6	Movable back face.
7	6x6 WF Beams, various lengths.
8	6x6 WF Beams, all the 5 load cells are mounted to it.
9	Pressure measuring device - load cell
10	6x6 Box section, welded to the back of front face, forming part of the supporting collar.
11	6x6 Box section, joining the movable part of the supporting collar, can be moved to the desired position 'a', 'b', 'c' or 'd' according to the desired form thickness.
12	Jack, trade mark 'ENARPAC-RC-102', 10 tons capacity and 2-1/8" stroke.
13	Supporting threaded rods.
14	Pull out threaded rods.
15	6" channel section, part of the supporting collar.
16	Threaded rod, holding the side faces from opening up while concreting, rod has to pass through each side face of each side at position of 'a', 'b', 'c' or 'd' according to form thickness.
a	Position for 6" thickness of the form.
b	Position for 9" thickness of the form.
c	Position for 12" thickness of the form.
d	Position for 18" thickness of the form.

the concrete pressure by the deflection of a 7/16 inch steel plate, 6 inches wide, extending the full width of the form and resting on knife edges 28 inches apart. The steel plate was located near the bottom of the form; by means of a pivoted bar, connected to a lever to give a ratio of 10:1, the deflection of the centre of the plate was read on a scale graduated in 1/64 inch, and by using a magnifying glass it was possible to read to within 1/256 inch. This corresponded to a plate deflection of 0.004 inch. The thickness of the timber sheathing above and below the steel plate was designed to give the same deflection under load as the steel plate.

Shunk (19) inserted a 9-1/4 inch diameter cylinder, fitted with a freely moving piston, into the wood formwork, and by means of a weighted lever arm determined the load required just to prevent the piston from moving under the applied concrete pressure.

McDaniel and Carver (12) used a pressure gauge consisting of a small flexible German-Silver diaphragm acting upon a reservoir containing mercury. The reservoir was connected to a glass tube, and the pressure was indicated by the position of the mercury in the tube.

Macklin (12a) calculated the pressure of concrete against formwork by measuring the deflection of the wood sheathing relative to the supporting studs by means of a dial type micrometer mounted on a bridge arrangement.

The pressure measuring device used by the California Division of Highways (13) consisted of a metal disk, to one side of which a sheet-rubber diaphragm was clamped in a manner similar to that of a drum head.

The shallow space between the rubber diaphragm and the disk was filled with liquid, which operated an ordinary pressure gauge mounted on the back of the disk. The cells, 6 and 12 inches in diameter, were inserted into the form wall so that the rubber diaphragm was flush with the inside surface of the wall.

David, Jensen and Neeland (3) during the restoration of the upstream surface of the Barker Dam with prepakt concrete attached strain meters to the 1 inch diameter steel bars which anchored the precast face slabs to the face of the old dam. The stresses in the anchor bar were measured and the pressures against the slab form, during the process of filling with aggregate and the later process of grouting, were back calculated. Carlson electric resistance meters were welded to the anchor bar to measure the loads in the anchor bar.

Smith, Slater, Goldbeck and Teller (17) used Goldbeck-type pressure cells inserted in the forms with the diaphragms flush with the inside form surface. This type of cell requires a small movement of the diaphragm against the concrete to break the circuit.

Civil Engineering Research Association (9) CERA now CIRIA used a nominally no displacement device to measure the lateral pressure of concrete, which comprised of a cylinder and piston. Air pressure within the cylinder was used to balance the direct thrust from the concrete. Sensitive microswitches were used to indicate small movements of the piston and so enable balance to be effected.

Considerable conflict exists between the results of these previous researchers which has largely been attributed to differences in

measuring techniques. Great importance has recently been attached, therefore, to the type of apparatus used and its sensitivity.

All the problems inherent in the lateral pressures of fresh concrete also occur in the measurement of earth pressures. Over the past few years the measurement of earth pressures has advanced considerably and for this investigation it was decided to use a standard developed earth pressure cell.

When selecting the type of pressure cell to be used in this investigation, it was decided to adopt a device capable of measuring both the lateral pressure of concrete on the vertical faces of the form and the shear forces developed due to the friction effects at the same location, simultaneously.

4.3.2 Type of Cells

There are two basic types of pressure cells which have been utilized in the past for various pressure measurements. These are cells with a flexible surface or diaphragm in contact with the soil and cells with a rigid face plate. A detailed study on this subject has been conducted by Doohan (4).

4.3.3 Shear and Normal Force Measurement using Earth Pressure Cells

Most earth pressure cells are capable of measuring only the pressure normal to the face of the cell. Recently several load cells have been devised that can measure force both perpendicular and parallel to the face of the cell.

The Cambridge cell developed by Arthur and Roscoe (2), which can measure both normal and tangential pressures, was chosen for this study as it could be made and calibrated in-house and experience of use existed in the Ottawa area.

4.3.4 Cambridge Cell

Basically the cell is designed so that the face plate is supported by thin webs which are infinitely stiff in their own direction and infinitely flexible in the transverse direction, load being measured by strain gauges on the webs. By using webs in any required direction the load in that direction can be determined. The cell shown in Figure 4-2. A normal load causes strain in the normal webs and a shear load develops strain in the shear webs. Eccentricity is calculated from the proportion of the normal load carried by each normal web. Range and sensitivity of the cell is determined by the thickness of the webs and by the area of the top plate.

4.3.4.1 Modification to the Cambridge Cell

The original Cambridge cell transmitted the shear forces through a shear pillar by two shear webs. A total of 20 strain gauges were used to measure the various load components. The original Cambridge cell was modified to transmit the shear force through four shear webs and the number of strain gauges required reduced to sixteen. Doohan (4) used the modified Cambridge cells to measure the distribution of shear and normal forces on a footing. The purpose of modifying the cell was to ensure higher precision in measurements and minimize the chances of damage.

A comparison of the original and modified cells is shown in Figure 4-4.

In each cell sixteen strain gauges were used, eight for shear and eight for normal pressure measurements . The strain gauges were connected to the strain indicator through the balance unit, using a quarter bridge arrangement for both shear and normal circuits, each using two active gauges and two dummy gauges connected in series.

4.3.4.2 Principle of Operation

Cambridge cells can measure a shear force S, a normal force N, and the eccentricity of the normal force e, in the plane of the shear force. As the force N is applied at a distance e, from the centre of the cell, it can be replaced by a force N' = N at the centre and a moment N x e. The force N' is balanced by reactions of N'/4 in each of the normal webs. The moment N.e results in forces in each pair of normal webs, of equal magnitude but opposite sign and a force in the shear webs. Similarly, a shear force S can be replaced by a force S' in the shear webs and a moment caused by the fact that the actual force S acts slightly above the level of the shear webs. This moment is balanced by forces in each pair of normal webs (see Figure 4-3).

4.3.4.3 Choice of Cell Material and Circuit

Temperature variations influence the performance of resistance strain gauges, due to temperature variations in gauge resistance, which can be of the same magnitude as that caused by the strain. Generally, the relative change $\frac{\Delta R}{R}$ at a strain e and a temperature variation

$\Delta\theta = \theta - \theta_o$ can be written as

$$\frac{\Delta R}{R} = e\, k_o\, (1 + m\Delta\theta) + (\alpha + k\Delta a)\Delta\theta \qquad 4.1$$

In the first term of equation 4.1, k_o is the conventional gauge factor at room temperature, θ_o and m is its temperature coefficient. The second term comprises contributions from the thermal coefficient of resistivity α, and from the product $k\Delta a$, where $\Delta a = a_1 - a_2$ is the difference between the coefficients of thermal expansion of the test structure, a_1, and of the gauge wire, a_2. The temperature error of a bonded resistance strain gauge, therefore depends not only on the properties of the gauge material but also on those of the test structure. It is possible, by a suitable combination of materials, to obtain temperature compensation with respect to $\frac{\Delta R}{R}$, so that

$$\alpha + k(a_1 - a_2) = 0 \qquad 4.2$$

It has been observed that a combination of a strain gauge with aluminum substructures shows comparatively low effects due to change in temperature.

This thermal effect can further be reduced by pairing active gauges with dummy gauges or with matched dummies in a 1/4 bridge arrangement.

The cell was machined from a solid piece of aluminum alloy HS15W. Aluminum was used as it has a low modulus of elasticity and is easy to machine. A material with a low modulus of elasticity provides larger strains, which are easier to measure under given conditions than a material with a high modulus.

4.3.4.4 Choice of Web Dimensions

The dimensions of the webs govern the range and sensitivity of the load cell. It should be noted that the minimum web thickness would be about 0.015 inches (0.381 mm) since machining thinner than this would be difficult. The webs were made 0.50 inches long and 0.25 inches wide (12.7 mm x 6.35 mm).

4.3.4.4.1 Normal Web Thickness

The maximum normal load which could be expected would be hydrostatic pressure with a density of concrete of 153 lb/ft^3 and under a concrete head of fourteen feet.

$$P = \gamma H = 153 \times 14 = 2142 \text{ lbs/ft}^2$$

Hence a cell would be subjected to a maximum load of 2200 lbs/ft^2 in extreme conditions. If this pressure was evenly distributed over the cell face plate of 19.12 square inch area (5" diameter), the normal force per cell would be not more than 293 pounds. The cell was designed to take a total load of 400 pounds. Under no eccentric load each web would be required to take 25 percent of the total load, but since the load can be eccentric each pair of webs was designed to take 75 percent of the total load. Hence the thickness of the web can be calculated from:

$$t = \frac{150}{fA \times b} \quad \frac{\text{lbs}}{\text{lb/in}^2 \times \text{in}} \qquad 4.3$$

where fA = allowable strength of aluminum

= 20,000 psi

b = width of web

= 0.25 inch

$$t = \frac{150}{20{,}000 \times 0.25} = 0.030 \text{ inches}$$

To check the web against buckling, Euler's buckling formula was used assuming the web to be fixed at both ends.

$$P_{cr} = \frac{\pi^2 E b t^3}{3L^2} \text{ lbs} \qquad 4.4$$

where E = modulus of elasticity 10^7 psi

P_{cr} = critical buckling load

L = length of web

b = width of web

or

$$t^3 = \frac{3P_{cr}L^2}{\pi^2 E b} \qquad 4.5$$

$$= \frac{3 \times 150 \times (0.5)^2}{\pi^2 \times 10^7 \times 0.25} = 4.56 \times 10^{-6} \text{ inches}$$

$$t = 0.0166 \text{ inches}$$

Therefore a thickness of 0.030 inches was adopted for the normal webs.

4.3.4.4.2 Shear Web Thickness

The maximum shear force was expected not to exceed the maximum normal force, hence the shear webs were made to the same dimensions as the normal webs.

4.3.4.5 Gauging and Bridge Circuit

Each cell contained sixteen CEA-13-125UW-120 type strain gauges manufactured by Micro-Measurements and compensated for aluminum. The gauges used had a gauge factor of 2.12 ± 0.5% at 75°F and resistance of 120 ± 0.3% OHMS. The strain gauges were placed on both sides of the shear and normal webs and connected in series to eliminate bending effects. Great difficulty was encountered in fixing the gauges to the webs and then soldering leads to these gauges; only single strand small diameter wire was attached to each solder dot. M bond 610 was used to cement the gauges to the webs.

To use a quarter bridge arrangement two gauges were cemented to a piece of aluminum and connected in series to act as a temperature compensated dummy.

4.3.4.6 Pressure Cell Calibration

1. Static Load Calibration

The cells were calibrated by applying directly vertical and horizontal loads on the rigid face plates of the cells. The normal load was applied by means of a hanger and weights at the centre and at eccentricities of 5/8 of an inch on both sides of the centre of the plate, through a steel ball. Shear load was applied in the direction parallel to the plane of the face plate through a hanger and pulley.

Arthur and Roscoe (2) stated and it was observed experimentally that the load cells recorded the same load whether the load was applied at a point through a steel ball or uniformly over the whole face plate of the cell.

2. Water Calibration

The cells were also water calibrated after installing them in the form to check their operation and accuracy. The results are illustrated in Figure 4.32 as a plot between the measured strain and the water pressure.

4.3.4.7 Calibration Tests and Load Cell Constants

Arthur and Roscoe (2) introduced the method of calibration by assuming that the sum of the outputs of the normal bridge circuit is directly proportional to the normal load.

Another method of calibration used by Doohan (4) but initially developed by Bozozuk of the National Research Council of Canada assumes that the output resistances or voltage are linearly dependent on the three applied loads, i.e., the normal load, shear load, and the moment due to eccentricity of the normal load. This assumption gives a matrix of coefficients or load cell constants as follows:

$$\begin{matrix} V^+ \\ V^- \\ V_x \end{matrix} = \begin{matrix} n^+ & s^+ & e^+ \\ n^- & s^- & e^- \\ ns & ss & es \end{matrix} \begin{matrix} N \\ S \\ Ne \end{matrix} \qquad 4.6$$

or $V = AF$

or $F = A^{-1}V$

where V^+ = output strain from + normal circuit

V^- = output strain from - normal circuit

V_x = output strain from the shear circuit

N = normal load

S = shear load

Ne = moment, normal load x eccentricity

A = matrix of load cell constants

In order to determine the load cell constants a series of calibration tests were performed.

4.3.4.7.1 Calibration Tests

a) Fix S = 0, and e = 0, varying N from 0 to 400 pounds in 80 pound increments and then from 400 pounds to 0, the results are plotted on Figure 4-6, for load cell number 1.

b) Fix N = e = 0, and vary S from 0 to 400 lbs in 40 lb increments and then return to zero. Plot the results as in Figure 4-7 for load cell number 1.

c) Fix S = 0 and e = ±0.635 inches from the centre of the cell face plate; vary N from 0 to 200 pounds in 40 pound increments, plotting the results as shown in Figure 4-8 for cell number 1.

Hence from the relation 4-6 the following relationship can be obtained for moments having opposite signs.

$$V^+ = N(n^+) + S(s^+) + N_e(e^+) \qquad 4.7$$

$$\overline{V}^+ = N(n^+) + S(s^+) - N_e(e^+) \qquad 4.8$$

From the above two relations the value of e^+ can be obtained

$$V^+ - \overline{V}^+ = P_e(e^+) + Ne(e^-)$$

or

$$e^+ = \frac{V^+ - \overline{V}^+}{2N_e} = \frac{1}{2}\left(\frac{V^+}{N_e} - \frac{\overline{V}^+}{N_e}\right)$$

e^+ is evaluated from the plot between V^+ and N_e taking the moment N_e with positive and negative eccentricities.

The calibration curves of load cells 2, 3, 4, 5 and 6 are shown in Figures 4-10 to 4-31.

Load cell constants for each cell were determined as outlined above, and are substituted into equation 4.6 as follows:

Cell No. 1

V^+		-5.396	5.25	6.32	N
$V^=$	=	-5.104	-4.33	-5.90	S
V_x		0.11	15.0	0.21	Ne

Cell No. 2

V^+		-5.39	4.92	6.15	N
V^-	=	-5.54	-4.213	-6.75	S
V_x		-0.08	15.31	0.23	Ne

Cell No. 3

V^+		-5.0	4.375	6.358	N
V^-	=	-6.016	-4.375	-6.93	S
V_x		-0.11	15.78	-0.032	Ne

Cell No. 4

V^+		-5.14	4.375	6.39	N
V^-	=	-5.55	-4.61	-6.32	S
V_x		-0.028	14.61	0.296	Ne

Cell No. 5

V^+		-5.56	4.76	6.6 N
V^-	=	-5.78	-4.085	-6.6 S
V_x		0.145	14.22	0.3 Ne

Cell No. 6

V^+		-5.625	5.0	6.79 N
V^-	=	-5.7	-4.53	-6.84 S
V_x		0.055	15.94	0.26 Ne

4.4 Matrix Inversions

In section 4.3.4.7 the load cell constants were determined from the basic relation which can be written in the form

$$V = AF \qquad 4.9$$

where V is the strain achieved from the bridge circuits

A is the matrix of load cell constants

F are the forces acting on the load cell

In order to determine these forces F, equation 4.9 can be written in the form

$$F = A^{-1}V$$

where A^{-1} is the inverse of A

The inversions of the matrices of load cell constants determined in section 4.3.4.7 are as follows:

Cell No. 1

$$A^{-1} = 10^{-4} \begin{bmatrix} -919.80 & -985.03 & 28.99 \\ -5.66 & 20.57 & 674.61 \\ 802.075 & -862.712 & -527.43 \end{bmatrix}$$

Cell No. 2

$$A^{-1} = 10^{-4} \begin{bmatrix} -959.85 & -872.179 & 68.45 \\ -17.11 & -7.111 & 660.63 \\ 798.5 & -770.09 & -468.51 \end{bmatrix}$$

Cell No. 3

$$A^{-1} = 10^{-4} \begin{bmatrix} -950.79 & -872.41 & 21.73 \\ -4.947 & -7.464 & 633.02 \\ 828.51 & -680.94 & -418.50 \end{bmatrix}$$

Cell No. 4

$$A^{-1} = 10^{-4} \begin{bmatrix} -969.61 & -940.77 & -18.47 \\ -18.56 & +13.75 & 694.36 \\ 829.89 & -766.16 & -490.26 \end{bmatrix}$$

Cell No. 5

$$A^{-1} = 10^{-4} \begin{bmatrix} -882.27 & -880.35 & 42.43 \\ -7.40 & 25.00 & 712.89 \\ 777.24 & -759.66 & -478.40 \end{bmatrix}$$

Cell No. 6

$$A^{-1} = 10^{-4} \begin{bmatrix} -886.67 & -879.11 & 28.29 \\ -9.091 & 15.09 & 634.49 \\ 744.91 & -739.39 & -443.79 \end{bmatrix}$$

The three load components can be calculated from the output resistance from the following equation

$$\begin{matrix} N \\ S \\ Ne \end{matrix} = A^{-1} \begin{matrix} V^{+} \\ V^{-} \\ V_x \end{matrix}$$

where N = normal load in pounds

S = shear load in pounds

Ne = normal load times the eccentricity of the normal load

V^{+} = sum of the strain given by gauges 1 and 2 or strain output of the '+' normal circuit

V^{-} = sum of the strain given by gauges 5 and 6 or strain output of the '-' normal circuit

V_s = strain given by the shear circuit

For example the strains measured by Cell No. 3 at a load of 160 lbs at an eccentricity of 0.625 inches, are V^{+} = -1438 micro inches/inch, V^{-} = -268 micro inches/inch and V_x = -31 micro inches/inch. The three loads can be determined from the strains as follows

$$F = VA^{-1}$$

$$\begin{matrix} N \\ S \\ Ne \end{matrix} = 10^{-4} \begin{vmatrix} -950.79 & -872.41 & 21.73 \\ -\ 4.947 & -\ 7.864 & 633.02 \\ 828.51 & -680.94 & -418.50 \end{vmatrix} \begin{vmatrix} -1438 \\ -268 \\ -31 \end{vmatrix}$$

N = +136.7236 + 23.38059 - 0.06736 = 160 lbs

S = +0.711379 + 0.2000 - 1.96 = 1.05 lbs

Ne = -119.1397 + 18.249 + 1.29738 = 99.6 lbs or e = 0.6225 inch

These cells are assumed to give an error not more than 2 percent

4.5 Comparison of Dead Load Calibration with Water Calibration

To compare the water calibration and static load calibrations, the results obtained in both cases were compared by plotting pressure against strain in micro inches as illustrated in Figures 4.31 and 4.32. Cells 2, 3, 4 and 5 show a difference of about 10 percent whereas Cell 1 showed a higher discrepancy; this could be due to changing of gauges in different cells whenever they were damaged and partly due to the normal forces acting eccentric to the face of the cell, when the form is filled with water. The water calibration test was adopted as a standard for measurements as the water test could be performed before performing every test and after any gauge was repaired or replaced.

CHAPTER 5

EXPERIMENTAL PROCEDURE

5.1 General

As stated previously this investigation was concerned with the effect of vibration on the lateral pressure exerted by freshly poured concrete on vertical form faces.

Basically the investigation consisted of pouring concrete under 'controlled' conditions into an instrumented form 15 feet deep, 3 feet wide and 11 inches between the form faces and measuring the resulting lateral pressure. Lateral pressure was measured by five Cambridge cells mounted 1 foot, 3 feet, 5 feet, 7 feet and 9 feet, respectively, above the base of the form.

The form was located below grade in the basement of the structures laboratory at the University of Ottawa allowing concrete to be poured directly into the form from a ready-mix truck; the duration of vibration, immersed length and power of vibrator used were kept constant for any one test.

5.2 Water Calibration Test

In addition to the dead load calibration carried out and discussed in Chapter 4, a water test was run to check calibrate the cells for normal pressure. Calibration tests were carried out directly in the form by means of hydrostatic pressure; the hydrostatic pressure being supplied by water contained in a large polyethylene bag placed in the

form. The bag was gradually filled with water, strain gauge readings being recorded at every 2 feet intervals of the water level in the form. Thus the pressure/gauge reading relationship was obtained for the load cells.

The results of the water calibration of the load cells, shown in Figure 4-31, were used to obtain the lateral pressure through all the experimental tests.

A number of water calibration tests were carried out successfully to achieve the presented results. Many tests proved to be unsuccessful due to difficulties in preventing water leaking through the polyethylene bag, and hence wetting the gauges.

The water calibration was performed regularly to check the calibration and that the cells worked satisfactorily.

5.3 Description of Concrete

The concrete used for the experiments was type 1 normal weight mix concrete 1:2.4:3.3, ordered from a local ready-mix company by specifying the required 28 days compressive strength and the desired slump. The concrete was specified to have a compressive strength of 4000 psi and 2-1/2"-3" slump, with a maximum aggregate size of 3/4 inches, the grading curve is shown in Figure 5.1.

Concrete was poured directly into the form at the required rate as soon as the concrete truck arrived. Generally the pour was started half an hour after the addition of water to concrete.

In order to measure the concrete strength, three cylinders were moulded, and tested at 28 days after casting. Slump tests were made after completion of the pour.

5.4 Experimental Programme

5.4.1 Parameters

This study was carried out under conditions such that some of the parameters were varied, as required keeping the remainder normally constant.

The concrete mix, strength, the rate of pour of the concrete and the dimensions of the form were kept constant throughout the study.

The parameters varied were

a) Power of vibrator

b) Depth of vibrator immersed into concrete

c) Duration of vibration per unit volume of concrete placed

d) Concrete temperature and lab temperature.

5.4.2 Steel Reinforcement

To extract the hardened block of concrete from the form and to enable the block to be handled with safety a cage of reinforcement was cast in the concrete. The reinforcement consisted of four #6 longitudinal bars tied into a box with #2 bars at two feet spacings on the sides of the box and at the top and bottom of the front and back faces of the box. There was no reinforcement towards the front and back faces of the form.

To minimize friction between the form and the concrete, to prevent the concrete from bonding to the form and to protect the load cells from getting wet a polyethylene bag was used to line the inner surface of the form.

5.4.3 Test Procedure

The general procedure consisted of zeroing the strain readings of all the gauges of the five cells, and then fresh concrete was placed from the truck into the form at a speed of 20 ft/hr. The formwork was filled in eight stages, in 2 feet intervals for the first fourteen feet and then the last one foot. The concrete was vibrated at every stage using the required vibrator, for the specified duration and immersed to a particular depth. The temperature in the laboratory and that of the concrete mix was recorded; slump of concrete was measured at the commencement, middle and at the end of the pour. At every two feet intervals after the concrete had been vibrated the gauge readings, for both shear and normal pressures, were recorded.

Twenty-two tests were carried out in total. In order to study the behaviour of concrete under different parameters, while keeping the temperature constant, the initial set of tests were performed in a temperature range of 65° to 75°F. During the investigation the rate of pour was maintained constant at 20 ft/hr; vibrators of 1 HP and 2.5 HP were used. The duration of vibration was varied at 0.5 minutes, 2.5 minutes, 3.5 minutes and 5 minutes. The vibrator head was immersed to a depth of either 2 feet or 1 metre. The strain gauge readings were recorded at each lift of concrete to measure the variation of lateral pressure and shear force with concrete head.

Similar tests were repeated in the cooler temperatures of fall and early winter to study the influence of temperature on the behaviour of concrete.

The strain readings obtained from the normal gauges were converted into normal pressures in pounds per square foot units and plotted against the depth of concrete in the form, shown in Figures 6.1a, 6.2a to 6.17a.

To check the performance of each cell and study the pressures exerted by the concrete at each level, the pressures given by each cell under different heads of concrete were plotted against concrete head as shown in Figures 6.1b, 6.2b to 6.17b. The concrete was expected to exhibit the same pressure under the same head of concrete at all levels of the form, but it was observed from the plots that the internal consistency of the results varied.

The lateral pressures obtained experimentally were compared with the lateral pressures recommended by the ACI Committee 347 and CIRIA as shown in Figures 6.1 to 6.17.

The strain gauge readings obtained from the shear gauges were converted to pressures in pounds per square foot and plotted against head of concrete. To project a better understanding of the relation between lateral pressures and shear force acting parallel to the face of the form, lateral pressures and shear pressures were plotted against the head of concrete on the same graphs as illustrated in Figures 6.18 to 6.23.

5.5 Experimental Problems

During the experimental investigation a number of observations and difficulties which were minor in nature but of significant importance regarding the magnitude and accuracy of the results, were encountered. These are stated below to be available for reference.

1. While carrying out the water calibration tests, polyethylene sheating, supported around a wooden frame, was used as a water proofing membrane. It was found to be a difficult task to provide a water tight membrane.

2. The strain gauges used in the load cells were very sensitive to moisture. The seepage of water past the face plate of the load cell could not be prevented and though a water-proof coating had been applied to the gauges, water affected the wire connections and seeped between the webs and the strain gauges, damaging them.

During both the water calibration tests and the concrete tests extreme care had to be taken to prevent the polyethylene membrane from being damaged.

3. When installing the cells in the back face of the form it was necessary to ensure that the face plate of the cell was flush with the face of the form. If the cell was projecting out it would press against the polyethylene membrane, and the effective area of the face plate of the cell would be increased, giving an apparent higher lateral pressure. Also the vertical impact of the falling concrete would give a higher shear force.

4. During static calibration of the cells it was observed that with a concentric load each of the four normal circuits, did not give the same output strain. However, the sum of the four normal web strains always remained the same under a specific load.

5. The gauges used in the Cambridge cells were very delicate and the webs were too small to fix the gauges conveniently. Whenever any gauge was damaged the particular cell was regauged and the recalibrated to compare with the previous calibration.

6. Each cell consisted of 16 gauges, eight circuits, numerous connections and eight wires leading to the balance unit. Thus a total of 40 wires were run to the strain reading equipment on the ground floor. Extreme caution had to be observed while moving the back face of the form, tightening of the ties and bolts and working around the form to avoid breaking the wires.

7. Due to the sensitivity and delicacy of the cells, there always existed a possibility of damaging the cells while vibrating the concrete.

8. While pulling out the set concrete slab, force was exerted against the cells, and on occasions damaged the cell webs.

9. To stop the leakage of water into the cells, plastic bags were used to cover the cells.

CHAPTER 6

DISUCSSION OF EXPERIMENTAL RESULTS

6.1 General

The parameters varied during this investigation were the depth of immersion of the vibrator, duration of vibration, power of the vibrator and temperature of the concrete. The specifications of the various tests are summarized in Table 6.1. All tests were carried out with a rate of pour of 20 ft/hr with a specified slump of 2.5 inches and the concrete poured in lifts of 2 feet.

6.2 Lateral Pressure Envelope

The lateral pressure envelopes, plotted against elevation of the concrete in the form, shown in Figures 6.1a, 6.2a to 6.17a. The same information is plotted against head of concrete in Figures 6.1b to 6.17b.

It can easily be observed that the pressure envelope is initially linear with increase in head deviating from the line of linearity after the concrete has been poured to a certain depth in the form; the pressure reaching a maximum and then declining. This phenomenum is typical and has been reported by all investigators including Adam, Kinnear (CIRIA), Ritchie and Rodin.

The concrete pressures plotted against the head of concrete are shown in Figures 6.1b to 6.17b. It is readily apparent that although

TABLE 6.1 Details of Test Program

Test No	Date	Slump ins.	Rate of Pour ft/hr	Fig No	Concrete Temp °F	Power of H.P.	Duration of Vibration minutes	Depth of Vibrator Immersion ft	Max Pressure psf
1	26.08.77	2.5	20	6.1	71	1	0.5	2	740
2	28.07.77	2.5	20	6.2	74	1	2.5	2	800
3	31.08.77	2.5	20	6.3	71	1	3.5	2	990
4	04.08.77	2.5	20	6.4	78	1	5.0	2	725
5	19.08.77	2.5	20	6.5	71	1	0.5	3.25	940
6	09.08.77	2.5	20	6.6	75	1	2.5	3.25	950
7	02.09.77	3	20	6.7	72	1	3.5	3.25	960
8	12.08.77	2.75	20	6.8	68	1	5.0	3.25	975
9	06.07.77	2.5	20	6.9	73	2.5	0.5	2	1112
10	28.10.77	3	20	6.10	65	2.5	2.5	2	1300
11	13.10.77	2.5	20	6.11	62	2.5	0.5	3.25	1275
12	20.10.77	3	20	6.12	55	2.5	2.5	3.25	1715
13	22.12.77	2.5	20	6.13	48	1	0.5	3.25	1380
14	25.11.77	3	20	6.14	54	2.5	2.5	2	2050
15	07.12.77	3	20	6.15	47	2.5	0.5	3.25	1840
16	14.12.77	2.25	20	6.16	66	1	0.5	3.25	1000
17	22.03.78	2.5	20	6.17	57	1	0.5	3.25	944
18	21.07.77	2.5	20	6.23	76	1	0.5	2	615

the pressure envelopes are similar, the internal consistency of any single test is not as uniform as could be hoped.

All tests show a similar behaviour except tests 1, 2, 4, 6, 8 and 9 where the pressure on the lowest cell increases with head for the last few feet of concrete pour.

To study the effect of friction between the concrete and the surface of the formwork, and any effect due to vertical shrinkage of the concrete, shear pressure and normal pressure in pounds per square foot are plotted against the head of concrete in Figures 6.18 to 6.24 for tests 1, 2, 5, 6 and 8. The shear forces recorded do not give conclusive results but the plots to some extent illustrate the relation between normal pressures and shear forces; Figures 6.19, 6.20, 6.22, 6.23 and 6.24 show a significant relation between normal and shear forces. It is interesting to note that the linear part of the lateral pressure envelope corresponds to zero shear force, the rate of increase of lateral pressure decreasing as shear friction develops, but the relation between lateral pressures and shear friction can only be developed after detailed further investigation. The anomalous shear force recorded by Cell 1 in Figures 6.18 and 6.21 could only be attributed to internal residual impact due to pouring of concrete.

In the plots shown in Figures 6.4a, 6.6a, 6.7a, 6.8a and 6.10 it is observed that the pressures recorded at the 1 foot elevation of the form, in contradiction to the generally expected distribution, exceed those recorded at the 3 feet elevation, under large concrete heads. This phenomenum was also observed in the tests performed by Ritchie (15) but was not explained; the reason could be the accumulation of drained water

at the bottom of the form, thus exerting a pore water pressure in addition to the concrete pressure. This hypothesis which was initially introduced by Rodin (17) can be put forward only as a possible explanation with no definite proof.

It is observed for tests 6, 7, 8, 9, 11, 13, 14, 16 and 17 that under a concrete head varying between 7 feet and 11 feet the lateral pressure dropped, followed by an increase in pressure; and then finally showing a drop in pressure forming a general pattern for the lateral pressure envelope, this is illustrated in Figures 6.6b, 6.7b, 6.8b, 6.9b, 6.11b, 6.13b, 6.14b, 6.16b and 6.17b. This phenomenum can be explained as due to the ineffectiveness of the vibration at depths remote from the vibrator and the developed shear strength of the concrete. Thus at a certain instant the vertical concrete load is supported by the shear strength of the concrete, however any further increase in superimposed load would increase the vertical forces and this pressure would still be transmitted through the pore fluid of the concrete mix in a lateral direction, thus showing an increase in a lateral pressure. The drop in pressure at large concrete heads can be attributed to friction between the form and the concrete, shrinkage of the concrete and perhaps partially to the deflection of the form under lateral pressure.

6.3 The Effect of Internal Vibration on the Lateral Pressure of Concrete on Formwork

As shown in Table 6.1 tests were carried out to study the effects of various parameters of vibration on the lateral pressure of concrete. This effect was commented upon by both the ACI and CIRIA as

significant. The importance of this effect can also be understood from the experimental data reviewed by Rodin and initially conducted by the Bureau of Public Roads, according to which if concrete is externally vibrated throughout the depth of the form, the concrete would retain its fluidity even with a slump as low as 1-1/2 inches exhibiting hydrostatic pressure.

To analyse the effect of internal vibration with the effective parameters taken into consideration being power of the vibrator, continuity of vibration and the depth of immersion of the vibrator head, the pressure values achieved by the cells installed at 1 foot and 3 feet above the bottom of the formwork are plotted against the head of concrete in Figures 6.25 and 6.26, respectively. The maximum design pressures measured under the various conditions of vibration under 14 feet head of concrete are illustrated as bi-linear curves, with an initial line tangent to the measured pressure envelope at the origin and tangent to the maximum pressure, in Figures 6.27 and summarized in Table 6.2. All the initial tangents in the bi-linear curves shown in Figure 6.27 tend to the line of hydrostatic pressure. In discussion of the results concrete pressure is expressed in terms of head of hydrostatic concrete with a unit weight of 150 lbs/ft^3.

From these results it is evident that generally the cumulative effect of the three parameters of vibration taken into consideration increase the lateral pressure exerted by the concrete. The concrete pressure is observed to have increased from a maximum value of 740 psf achieved by a vibrator of 1 H.P., duration of vibration 30 seconds and vibrator head immersed to a depth of 2 feet at a concrete temperature of 71°F to a

maximum value of 1715 psf with a vibrator of 2.5 H.P., duration of vibration 2.5 minutes and vibrator head immersed 1 metre at a concrete temperature of 54°F, which is an increase equivalent to 6.37 ft head of concrete, it must be pointed out that in this increase of pressure the drop in temperature from 71°F to 54°F would also be a participant.

In order to analyse the effects of the different parameters of vibration more closely it is convenient to examine them separately.

a) The Effect of Power of Vibrator

During this investigation 1 H.P. and 2.5 H.P. vibrators were utilized. The effect of the power of the vibrator can be visualized from the plots shown in Figures 6.25, 6.26, 6.27 and 6.28 which include the bi-linear curves giving maximum concrete pressures; the maximum pressure values and the equivalent hydrostatic depths of concrete achieved are given in Table 6.2.

During test No. 1 conducted with the vibrator of 1 H.P., 30 seconds duration of vibration per 2' lift of concrete, vibrator head immersed 2 feet into the concrete and a concrete mix temperature of 71°F the maximum pressure measured was 740 psf or 4.85 feet of fluidized depth of concrete from the surface behaving hydrostatically. Test No. 9 carried out with the vibrator power increased to 2.5 H.P. and keeping the other parameters constant, shows the maximum pressure as 1112 psf or a fluidized depth of concrete of 7.26 feet. These tests indicate an increase in pressure equivalent to 2.43 feet of concrete head.

Test No. 2 and Test No. 10 were carried out with 1 H.P. and 2.5 H.P. vibrators, respectively, the concrete vibrated 2.5 minutes for every

TABLE 6.2 Analysis of Experimental Results

Test No	Ambient Temp °F	Date	Conc Temp °F	Power of Vibrator H.P.	Duration of Vibration min	Depth of Vibrator feet	Max Pressure (Pm) psf	Design Hydro-static Concrete Depth ft*	Percent Increase of Test No. 1
1	71	26.08.77	71	1	0.5	2	740	4.93	0
2	71	28.07.77	74	1	2.5	2	800	5.3	8.1
3	71	31.08.77	71	1	3.5	2	990	6.6	33.8
4	74	04.08.77	78	1	5.0	2	725	4.8	-2.0
5	71	19.08.77	71	1	0.5	3.25	940	6.30	27.0
6	73	09.08.77	75	1	2.5	3.25	950	6.27	28.4
7	71	02.09.77	72	1	3.5	3.25	960	6.30	29.7
8	67	12.08.77	68	1	5.0	3.25	1000	6.7	35
9	73	06.07.77	73	2.5	0.5	2.0	1112	7.41	50
10	61	28.10.77	65	2.5	2.5	2.0	1300	8.7	75.8
11	61	13.10.77	62	2.5	0.5	3.25	1275	8.5	72.3
12	59	20.10.77	54	2.5	2.5	3.25	1715	11.41	13.2
13	58	22.12.77	48	1	0.5	3.25	1380	9.20	86.5
14	54	25.11.77	54	2.5	2.5	2	2050	13.67	177
15	40	07.12.77	47	2.5	0.5	3.25	1840	12.30	149
16	37	14.12.77	66	1	0.5	3.25	1000	6.70	35.1
17	46	22.03.78	54	1	0.5	3.25	944	6.3	27.6
18	75	21.07.77	76	1	0.5	2	615	4.1	-16.9

*Hydrostatic depth = $\frac{\text{max. pressure}}{150}$ (ft)

2 feet increase in concrete depth, the vibrator head immersed 2 feet into concrete and the temperature of the concrete mixes recorded at 74°F and 61°F, respectively. The maximum pressures recorded were 800 psf in Test No. 1 and 1300 psf in Test No. 10 and the hydrostatic depths of concrete 5.33 feet and 8.67 feet, respectively, from the surface. This shows an increase of 500 psf in pressure which is equivalent to a concrete head of 3.33 feet. It is important to note that in Test No. 10 the temperature could not be maintained at 74°F and the increase in pressure, although mainly attributed to parameters of vibration, was partially due to the influence of temperature changes.

In Table 6.2 and Figure 6.28b, Test Nos. 5 and 11 are shown to exhibit pressures of 940 psf and 1275 psf, respectively, all variables kept constant except the vibrator power increased from 1 H.P. to 2.5 H.P. The increase in pressure was observed to be 335 psf, equivalent to 2.19 ft of concrete head and the fluidized depth of concrete, exhibiting linear pressure was increased by 2.15 ft from the surface.

A similar comparison can be made between Test Nos. 6 and 12 shown in Figure 6.29b which shows an increase of pressure from 950 psf to 1715 psf which is equivalent to 5.1 ft head of concrete and the fluidized depth of concrete increased by 4.95 ft. The increase in pressure by an equivalent concrete head of 5.1 ft can be explained as a contribution of both an increase in the power of the vibrator and the drop in temperature of the concrete mix.

Many previous investigators including Rodin, Kinnear (CIRIA) and Teller have stressed the importance of vibration in the development

of concrete pressure, but there does not exist any published data available which specifically comments upon the effect of the power of the vibrator. From the above discussion it is obvious that an increase in the power of the vibrator, used for compaction of the concrete, increases the depth of hydrostatic pressure and the maximum pressure significantly. Figure 6.34 illustrates the relation between the power of vibrator and the percent of hydrostatic pressure.

b) The Effect of Duration of Vibration

Experimental tests were conducted to determine the variation of lateral pressure of concrete on the form with varying durations of vibration and the results measured are given in Table 6.2. A comparison of the effect of the different levels of vibration duration on the concrete pressure envelopes is illustrated in Figures 6.25, 6.26, 6.27 and 6.29.

In Figures 6.25 and 6.26 the pressures measured 1 ft and 3 ft above the bottom of the formwork, under varying concrete heads and vibration parameters, are compared.

Figures 6.27 and 6.29 illustrate the comparison between the bilinear pressure curves obtained under varying durations of vibration. It is observed that the lowest duration of vibration exhibits the lowest pressure and the increase in vibration time tends to increase the concrete pressure.

Comparing Test Nos. 1, 2, 3 and 4 in Table 6.2 graphically illustrated in Figures 6.1, 6.2, 6.3, 6.4 and the results compared in Figures 6.27 and 6.29. It is obvious that with a 1 H.P. vibrator and the

head of the vibrator immersed 2 ft into the concrete, varying the duration of vibration from 0.5 minutes, 2.5 minutes, 3.5 and 5 minutes per 2' lift of concrete under a temperature range of 71°F to 78°F, shows a general trend of an increase in concrete pressure up to an optimum limit of 3.5 minutes vibration, thereafter a drop in pressure is observed. The increase in pressure was recorded from 740 psf with 0.5 minutes of vibration to 990 psf with 3.5 minutes of vibration, which is equivalent to 1.63 ft of concrete head, and the drop in pressure equivalent to 1.73 ft of concrete head was observed by increasing the vibration period from 3.5 minutes to 5 minutes. This significantly shows that up to a certain limit the duration of vibration is effective in destroying the shearing strength of the concrete.

It is of interest to note that the effect of the duration of vibration on pressure in the case of a 1 H.P. vibrator immersed 1 metre into the concrete is insignificant. The results of these Test Nos. 5, 6, 7 and 8 are illustrated in Figures 6.5, 6.6, 6.7, 6.8 and the results compared in Figures 6.25, 6.26, 6.27 and 6.29. In Table 6.2 the results of these tests are summarized.

Similar tests were conducted with the 2.5 H.P. vibrator and the results are summarized in Table 6.2 as Test Nos. 9, 10, 11 and 12. These tests are graphically represented in Figures 6.9, 6.10, 6.11 and 6.12 and the results compared in Figures 6.25, 6.26, 6.27 and 6.29. It is observed that with the 2.5 H.P. vibrator and the vibrator head immersed 2 ft the pressure increases by an equivalent concrete head of 1.2 ft by increasing the duration of vibration from 0.5 minutes to 2.5 minutes under a temperature range of 65°F and 73°F.

A pressure increase equivalent to 2.9 ft head of concrete is observed in Test Nos. 11 and 12 conducted with a vibrator of 2.5 H.P., and the vibrator head immersed to 1 metre into the concrete, when the duration of vibration is varied from 0.5 minutes to 2.5 minutes.

It must be pointed out that with an increase in the duration of vibration the depth of initial linearity of the lateral pressure envelope of the concrete is also increased, this is illustrated in Figures 6.25, 6.26, 6.27 and 6.29.

It can be summarized that the pressure increased up to an optimum level of duration of vibration and there is either a drop in pressure or no further increase in pressure with increase in vibration time. This phenomenum was also observed by Ritchie (15). Ritchie carried out tests on cement mortars and concrete, varying the continuity of vibration, and concluded that the maximum concrete pressure occurred at 25 percent continuity of vibration; an increase in the continuity of vibration beyond this limit resulted into reduced pressure.

c) The Effect of Depth of Immersion of Vibrator

The effect of the depth of immersion of the vibrator head into the concrete, on the concrete pressure is obvious from the results of Test Nos. 1 to 12 summarized in Table 6.2 and graphically represented in Figures 6.1 to 6.12. These results are compared in Figures 6.25, 6.26, 6.27 and 6.31. From Figures 6.31a and 6.31b it can be concluded that by increasing the depth of the vibrator head immersion there is a general trend of increase in concrete pressure, and depth of linearity of the pressure

envelope. It is observed, by comparing Test Nos. 1 and 5 that with a vibrator of 1 H.P. keeping the duration of vibration constant at 0.5 minutes for every 2 ft increase in head of concrete and varying the vibrator head immersion from 2 ft to 1 metre, the maximum concrete pressure increases from 740 psf to 940 psf, which is an increase equivalent to 1.31 ft of concrete head and the depth of linearity of the pressure envelope is increased by 1.4 ft.

Comparison of Test Nos. 2 and 6, performed with a 1 H.P. vibrator duration of vibration 2.5 minutes, temperature 74 to 75°F and the vibrator head immersion increased from 2 ft to 1 metre (3.25 ft) show an increase of concrete pressure equivalent to 0.98 ft of concrete head and the depth of linearity of the pressure envelope increased by 0.9 ft. This is illustrated in Figure 6.31.

By comparing Test Nos. 3 and 7, performed with a 1 H.P. vibrator, the duration of vibration maintained at 3.5 minutes, temperature of the concrete mix kept between 71°-72°F., and the depth of the vibrator head varied as in the previous tests, it is observed that there was no major difference in pressure.

Comparison of Test Nos. 4 and 8 show that with a vibrator of 1 H.P., temperature of mix at 78°F and 68°F, respectively, vibration duration 5 minutes and depth of vibrator head immersion increased from 2 ft to 1 metre shows a difference in pressure equivalent to 1.8 ft of concrete head. The unexpectedly high difference in pressure observed between Test Nos. 4 and 8 can be explained as due to the development of shear strength in Test No. 4 due to the high temperature of the concrete mix.

Similar tests carried out with the 2.5 H.P. vibrator, summarized in Table 6.2 and illustrated in Figure 6.31 show a definite increase in pressure by changing the depth of vibrator immersion from 2 ft to 1 metre. Comparing Test Nos. 9 and 11 shows a pressure increase equivalent to 1.1 ft of concrete head. When comparing Test Nos. 10 and 12 an increase in pressure equivalent to 2.7 ft of concrete head is observed. It must be noted that in this case part of the increase in pressure must be attributed to the 11°F drop in temperature of the concrete mixes, which could not be controlled due to severe weather conditions.

The above discussion evidently indicates that increase in the immersed depth of the vibrator head increases the influence of vibration and this effect is true for both 1 H.P. and 2.5 H.P. vibrators and is significant up to 2.5 minutes duration of vibration. Figure 6.35 illustrates the relation between depth of vibrator immersion and the pressure expressed in terms of percent of hydrostatic pressure.

6.4 Temperature Effects on the Lateral Pressure of Concrete on Formwork

In order to investigate the effect of temperature on the lateral pressure of concrete seven tests were performed in moderately cold and extremely cold weather; three of these tests were rejected. The pressures recorded are plotted against the elevation of the formwork in Figures 6.13a to 6.17a and the same information is plotted against the head of concrete in Figures 6.13b to 6.17b. The maximum pressures are summarized in Table 6.2.

Figures 6.25 to 6.27 illustrate comparison between the pressure envelopes achieved from different tests. In Figure 6.32 the maximum

pressures achieved from Test Nos. 5, 10, 11, 13, 14, 15, 16 and 17 are compared. Test Nos. 5 and 13 were performed with the 1 H.P. vibrator, 0.5 minutes duration of vibration, and vibrator head immersed 1 metre into the concrete during the process of internal vibration; the temperature of the concrete mix was recorded during the tests. It is observed in Figures 6.5, 6.13 and 6.32 that the maximum pressures achieved during these tests at concrete temperatures of 71°F and 48°F are 940 psf and 1380 psf, respectively, which is an increase of pressure equivalent to 2.9 ft of head of concrete.

Comparison of Test Nos. 10 and 14 illustrates an increase of pressure equivalent to 4.9 ft head of concrete by reducing the temperature from 65°F to 54°F, with a vibrator of 2.5 H.P., duration of vibration 2.5 minutes and the vibrator head immersed 2 ft into the concrete. These tests are illustrated in Figures 6.10, 6.14 and 6.32. Observing Figure 6.14b it is evident that the pressure recorded by Cell A, located 1 ft above the bottom of the formwork, between 11 ft and 15 ft head of concrete shows a deviation from the generally expected pattern of the pressure. This could be attributed to outward deflection of the rigid form at the top, resulting in an inward movement of the form at the base, thus subjecting the bottom cell to passive pressure.

Comparison of Test Nos. 11 and 15 show an increase in pressure equivalent to 3.7 ft of concrete head, by a reduction of the temperature of the concrete mix from 62°F to 47°F., with a 2.5 H.P. vibrator, immersed 1 metre into concrete and the concrete vibrated for 0.5 minutes.

To confirm this effect of temperature of the concrete mix on

the pressure of concrete, Test Nos. 16 and 17 were performed in cold weather with the concrete mix heated to 66°F and 54°F. These are shown in Table 6.2 and the results illustrated in Figures 6.16, 6.17 and 6.32, It is observed that these tests are comparable to Test No. 5 which had approximately the same concrete temperature.

From the comparison of the above results shown in Figure 6.32 it is evident that the temperature of the concrete is a significant factor influencing the pressure of concrete and the ambient temperature is important only to the extent of its effect on the temperature of the concrete mix.

From the above discussion, although based on insignificant experimental results, it can be concluded that the temperature of concrete mix is a very significant factor in the magnitude of concrete pressure. However, the importance of this factor is interrelated to the parameters of vibration.

6.5 Comparison of the Maximum Measured Pressures with the ACI and CIRIA Recommendations for the Lateral Pressure of Concrete

The results achieved from the current investigation are compared to the standard values of concrete pressure predicted by ACI Committee 347 and CIRIA and the comparisons are shown in Figures 6.1 to 6.17 and summarized in Table 6.3.

ACI 347-68 specifies the design pressures to be used be the least of the pressures given by the following

TABLE 6.3 Comparison of Concrete Pressures Recommended by CIRIA and ACI with Experimentally Achieved Pressures

Test No	Continuity of Vibration %	Rate of Pour ft/hr	Temp of Mix (°F)	Concrete Pressures (psf)				
				150 h	ACI	CIRIA Arching Criteria	CIRIA Stiffening Criteria	Experimental Results
1	8.3	20	71	2100	2685	1250	1975	740
2	42	20	74	2100	2582	1250	1937	800
3	58	20	71	2100	2685	1250	2033	990
4	83	20	78	2100	2458	1250	1939	725
5	8.3	20	71	2100	2685	1250	2288	940
6	42	20	75	2100	2550	1250	2012	950
7	58	20	72	2100	2650	1250	2287	960
8	83	20	68	2100	2797	1250	2083	975
9	8.3	20	73	2100	2616	1250	1936	1112
10	42	20	65	2100	2919	1250	2077	1300
11	8.3	20	62	2100	3053	1250	2090	1275
12	42	20	55	2100	2423	1250	2135	1715
13	8.3	20	48	2100	3900	1250	2141	1380
14	42	20	54	2100	3483	1250	2135	2050
15	8.3	20	47	2100	3980	1250	2141	1840
16	83	20	66	2100	2877	1250	2051	1000
17	8.3	20	57	2100	3308	1250	2117	944

$$P_m = 150 + 9000 \frac{R}{T}$$

$$P_m = 150\ h \qquad (6.1)$$

$$P_m = 3000 \text{ psf}$$

where P_m is the maximum design pressure (psf)

R is the rate of pour in ft/hr

T is the temperature of the mix in °F

h is the head of concrete in feet.

If concrete behaved hydrostatically, the maximum pressure predicted by ACI under 14 ft head of concrete would be 2100 psf.

The pressure values predicted by the ACI, for concrete poured at 20 ft/hr and temperatures ranging between 70°F and 80°F, when compared to the results of Test Nos. 1 to 7 in Table 6.3 conducted with a 1 H.P. vibrator, show that the measured maximum pressures fall far below those given by ACI 347-68; the pressure differences are noted to vary from 127 to 210 percent of the pressure measured experimentally.

Comparing Test No. 9, conducted with the 2.5 H.P. vibrator at 73°F, to ACI 347-68 it is observed to provide a 1112 psf pressure against the predicted pressure of 2100 psf.

Test No. 8, conducted at 68°F with a 1 H.P. vibrator, gave a pressure of 1000 psf against the predicted value of 2100 psf.

Comparison of Test Nos. 8, 10, 11 and 16 conducted under different parameters of vibration and the concrete mix temperature ranging between 60 and 70°F, it is observed that the maximum pressure achieved is 1300 psf with a vibrator of 2.5 H.P., duration of vibration 2.5 minutes and immersed

to a depth of 1 metre into the concrete, against a predicted pressure of 2100 psf.

Test Nos. 12, 13, 14, 15 and 17 conducted at low temperature ranging between 47°F and 54°F show a maximum pressure ranging between 944 psf and 2050 psf. From these tests it is obvious that the maximum pressures obtained show a tendency towards the hydrostatic pressure of concrete, and it is reasonable to assume hydrostatic design pressures under severe test conditions, taking into account both low concrete temperature and the most severe parameters of vibration.

The above discussion indicates that the pressures calculated using the hydrostatic pressure of concrete agrees well with those measured for temperatures below 60°F. However, the pressures calculated using Equation 6.1 are conservative, sometimes excessively so, in all cases.

The pressure values given by the pressure formula

$$P_m = 150 + 9000 \frac{R}{T} \qquad (6.1)$$

are highly influenced by the rate of pour of concrete and are unreasonably high for higher rates of pour.

CIRIA identifies two limiting criteria for the calculation of the pressure of fresh concrete against formwork; the criteria giving the lower pressure to be used. As a design aid CIRIA produced the chart shown in Figure 2.18 which plots both criterias on one set of coordinates.

Stiffening Criteria

$$P = \frac{150\ R\ t}{1 + C(t/t_{max})^4} + 12(8-R) \qquad (6.2)$$

Arching Criteria

$$P = 300 + 50\ d + 20\ R \qquad (6.3)$$

where P is the pressure in pounds per square foot

d is the minimum sectional dimension of the form

R is the rate of pour in ft/hr

Δ is the density of concrete (lb/ft^3)

t is the time from the commencement of placing (hours)

t_{max} is the stiffening time of the concrete (hours)

C is the factor depending on the workability of the concrete and the continuity of vibration.

CIRIA recommends use of the minimum pressure calculated from the Stiffening and Arching Criterias stated in Equations 6.2 and 6.3 respectively with an additional 200 psf surcharge to allow for impact for all structures. The calculations in Table 6.3 do not include the surcharge.

In the Stiffening Criteria the factors considered important by CIRIA are the temperature of the concrete mix, rate of pour, slump and continuity of vibration but factors not taken into account are the power of the vibrator and the depth of immersion of the vibrator head.

The maximum concrete pressures achieved experimentally are compared to the pressures predicted by the Stiffening Criteria in Table 6.3. For times less than t_{max} Equation 6.2 degrades to the hydrostatic condition which gives good agreement for concretes poured at low temperatures in Test Nos. 12, 14 and 15. In general, the Stiffening Criteria provides higher pressures which are in no way comparable to the experimentally achieved pressures.

The Arching Criteria considers the thickness of the form and the rate of pour as the only significant variables contributing to the concrete pressure. This criteria does not take into account the temperature of the mix or the parameters of vibration. The pressures achieved experimentally and calculated from the Arching Criteria are compared in Table 6.3. It is is observed that the Arching Criteria does not show any variation in pressure with change in temperature or the parameters of vibration. It is evident that the concrete pressures given by the Arching Criteria at concrete temperatures ranging above 68°F and rate of pour 20 ft/hr are close to the experimental results but this criteria is not conservative in the case of concrete poured at low temperatures. Consequently, any form structures designed according to this criteria, as recommended by CIRIA, for cold weather conditions could result in dangerous failures.

The design form pressures postulated by ACI 347-68 are consistently conservative, and sometimes excessively conservative, and can be used with confidence.

The design form pressures postulated by the CIRIA Arching Criteria are too low for low temperatures and hence should not be used. The CIRIA Stiffening Criteria degenerates to the hydrostatic criteria for times less than the stiffening times of the concrete. The stiffening times given in CERA Report No. 1 are too long for the concretes used in these tests.

CHAPTER 7

CONCLUSIONS AND RECOMMENDATIONS

In view of the results achieved by previous investigators and the detailed discussion made in Chapter 6, the following conclusions can be drawn:

1. For design purposes the lateral pressure distributions of freshly poured vibrated concrete can be represented by a bi-linear curve, i.e., the lateral pressure is equal to the hydrostatic pressure of concrete up to a maximum value and thereafter may be considered constant at this maximum value.

The actual pressure envelope is characterised by a linear relationship of pressure with depth tending to hydrostatic up to a certain maximum value and then followed by a parabolic curve. The deviation of pressure from the linear pressure line can be attributed to a number of causes which include stiffening and arching effects, friction between the form surface and concrete, settlement of the concrete, bleeding and water absorption by aggregates.

3. The vertical force acting parallel to the height of the formwork, which is comparable to the shear force, is inversely related to the normal force acting on the face of the form. This shear force can be attributed to the settlement or shrinkage of the concrete and friction between the concrete and the face of the formwork.

4. Vibration and its parameters have a very significant effect on

the lateral pressure of concrete and its magnitude is governed by this factor.

4.1 The power of the vibrator contributes significantly to the lateral pressure of concrete and pressure increase in different tests, equivalent from 2 ft to 5 ft of concrete head has been recorded by an increase in the power of vibration from 1 H.P. to 2.5 H.P. Although some of this increase in pressure can be attributed to the drop in temperature of the mix, however the major increase, undoubtedly, has been due to the variation in the power of the vibrator.

4.2 The duration of vibration, which has also been termed as "time of application of effort per unit volume placed" has been observed to be a significant factor influencing the lateral pressure of concrete. An increase in the duration of vibration increases the lateral pressure of concrete but this factor is effective only up to a certain limit after which any further increase in the duration of vibration results into either a constant value of maximum pressure or a drop in pressure. This optimum value of the duration of vibration exists between 3.5 minutes (58 percent) and 5 minutes (83 percent) per 2 ft lift of concrete level.

From this investigation it is concluded that the increase in the duration of vibration can increase the concrete pressure of the order equivalent to a concrete head of 3 ft.

4.3 An increase in the depth of immersion of the vibrator head will increase the lateral pressure of concrete, this increase in pressure was determined to vary between 9 to 14 percent of hydrostatic pressure or 1ft to 2.7 ft of equivalent concrete head, by an increase in the depth of

vibrator head immersion from 2 ft to 1 metre. This is illustrated in Figure 6.35. [It can also be concluded that a maximum of 11% increase in pressure can be obtained by increasing the depth of immersion of the vibrator by 1 ft.]

5. The temperature of the concrete has a significant effect on the lateral pressure of concrete. A major fall in temperature gives rise to a significant increase in lateral pressure exerted by the concrete. Extremely cold temperatures distinctly contribute to the development of hydrostatic pressure throughout the mass of concrete depending on the height of the formwork. An increase of pressure equivalent to 20-40 percent of the hydrostatic pressure can be expected by dropping the concrete temperature from warm circa (70°F) to very cold circa (45°F).

6. The pressure formulae recommended by the American Concrete Institute in the ACI 347-68, are over conservative in respect of high rates of pour.

For the head of concrete available in these tests the maximum pressures under low temperatures are comparable to the hydrostatic case recommended by ACI 347-68. However, the maximum pressures given by the limiting condition of ACI 347-68 are extremely conservative. A major problem in the ACI limiting criteria is that it is too sensitive to the rate of pour.

7. The recommendations to determine the lateral pressure of concrete provided by CIRIA are influenced predominantly by the arching limit

criteria and the recommended design pressures provided could be useful at moderate concrete temperature conditions but cannot be applied for concrete at low temperatures.

CIRIA's Stiffening Criteria is conservative and provides pressures which are significantly high for higher rates of pour. The stiffening time factor assumed by this criteria does not provide realistic values and the following expression, for $t = t_{max}$,

$$P = \frac{150 \times R \times t_{max}}{1 + C} + 12(8-R)$$

gives excessively lare pressures when compared to those obtained from expression 2.24.

The CIRIA Stiffening Criteria is directly related to rate of pour which is not justified when compared to the data of Rodin and Adam.

REFERENCES

1. Adam, M. "Poussee beton frais sur les coffrages", Annales de 1'Institute Technique du Batiment et des Travaux Publics, Mars-Avril 1965.
2. Arthur, J.R.F. and Roscoe, K.H. "An Earth Pressure Cell for the Measurement of Normal and Shear Stresses", Civil Engineering and Public Works Review, Vol. 56, No. 659, pp.765-770, 1961.
3. Davis, E.R., Jansen, C.E. and Neelands, T.W. "Restoration of Barker Dam". J. American Concrete Inst., Vol. 19, pp.633, April 1948, Proc. Vol. 44.
4. Doohan, J.P. "Earth Pressure Cells to Measure the Distribution of Shear and Normal Forces on a Footing", M.A.Sc. Thesis, University of Ottawa, 1975.
5. Elsberg, H. "Pressures on Formwork". Journal of the American Concrete Institute, V.30, No. 2, August 1958, Proceeding V.55.
6. Ho, P.T.J. "A Study of the Lateral Pressure of Fresh Concrete on Formwork", M.Eng. Thesis, University of Ottawa.
7. Hanna, T.H. "Foundation Instrumentation", Trans Tech Publication, 1973.
8. Hurd, M.K. "Formwork on Concrete", Special Publication No. 4, American Concrete Institute, Detroit, pp.73-82, Trans Tech Publication, 1973.
9. Kinnear, Sadgrove, Acharya, George, Turner and Sheperd, "Lateral Pressure of Concrete on Formwork", CERA Research Report 1 (RR 1) Published 1965.
10. Leung, M.C. "Lateral Pressure of Fresh Concrete on Formwork", M.Eng. Thesis, University of Ottawa.
11. Levitsky, M. "Form Pressure and Relaxation in Formwork", Journal of Eng. Mech. Division, ASCE, June 1975.

12. McDaniel, A.B. and Garver, N.B. "Pressure of Concrete on the Sides of Column Forms", Eng. News, Vol. 75, p.933, May 18 1916.

12a. Macklin, C.A. "Pressure on Formwork", Discussion on a Report by ACI Committee 622. DISC 55-10, Published in ACI Journal, V.30, No. 2. Aug. 1958.

13. Olsen, R.H. "Lateral Pressure of Concrete on Formwork", Ph.D. Thesis, Oklahoma State University, Okla., U.S.A., 1968.

14. Roby, H.G. "Pressure of Concrete on Forms", C W Engineering, Vol. 5, p.162, March 1935.

15. Ritchie,A,G,B "Effects of Early Stiffening of Concrete on Formwork Pressure", Report by Construction Industry Research and Information Association.

16. Ritchie, A.G.B. "The Pressures Developed by Concrete on Formwork", Civil Engineering and Public Works Review, Part I, Vol. 57, No. 672, July 1966, pp.885-888; Part II, Vol. 57, No. 673, August 1962, pp.1027-1030.

17. Rodin, S. "Pressure of Concrete on Formwork", Proc. Inst. of Civil Engineering (London), Vol. 1, No. 6, Paper No. 5863, Nov. 1952, pp.709-746.

18. Schjodt, R. "Calculation of Pressure of Concrete on Forms", American Society of Civil Engineers, Vol. 81, May 1955, pp.680-1 - 680-16.

19. Shunk, F.R. "Pressure of Concrete on Forms", Engineering News, Vol. 62, pp.288, September 1909.

20. Wynn, A.E. and Manning, G.P. "Design and Construction of Formwork for Concrete Structures", Published by The Cement and Concrete Association, London, England.

ILLUSTRATIONS

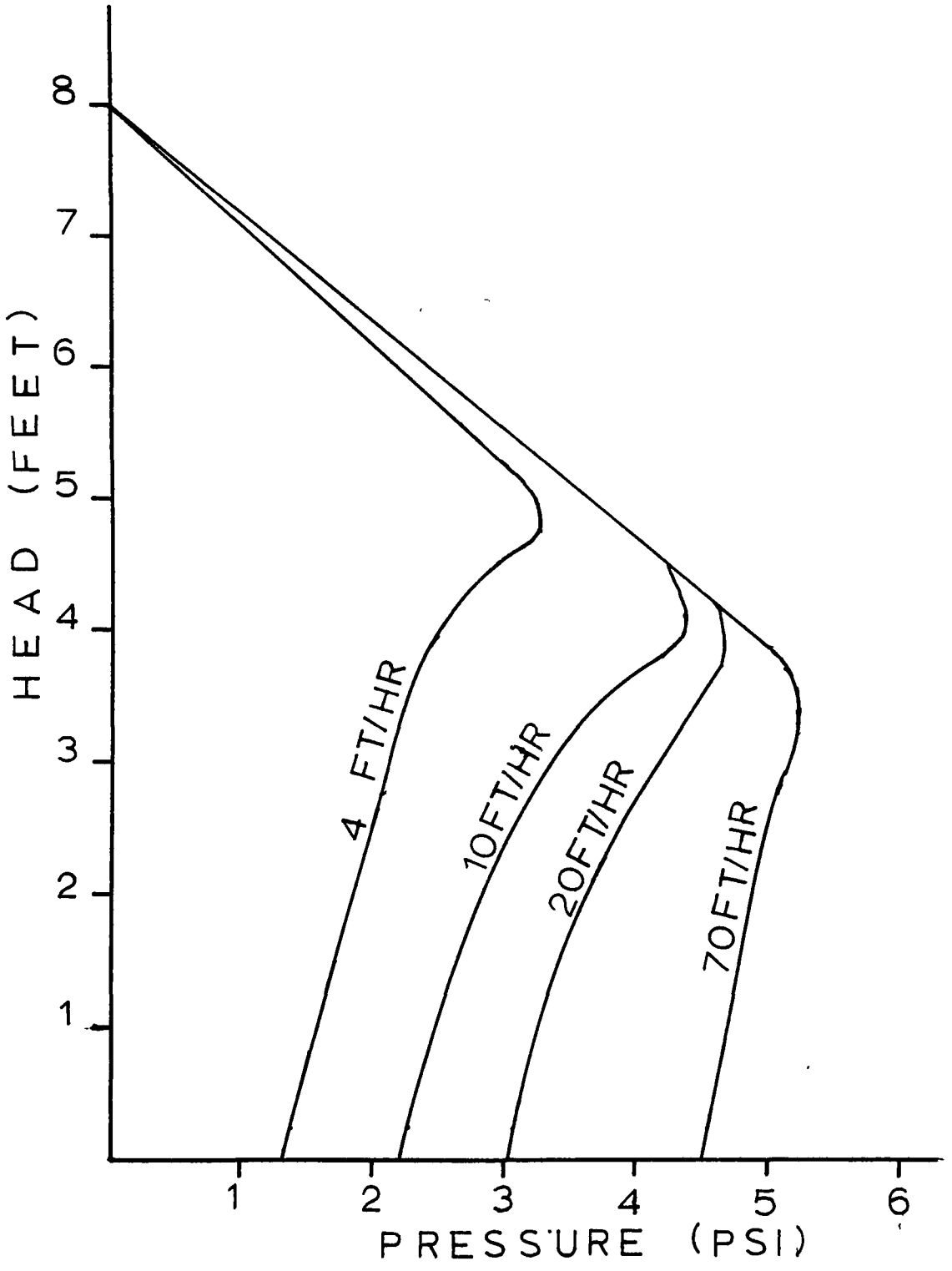

FIG.1.1 PRESSURES DEVELOPED AT VARIOUS RATES OF POUR
(1:3 MIX. HIGH WORKABILITY. VIBRATED)
(AFTER RITCHIE REF.16)

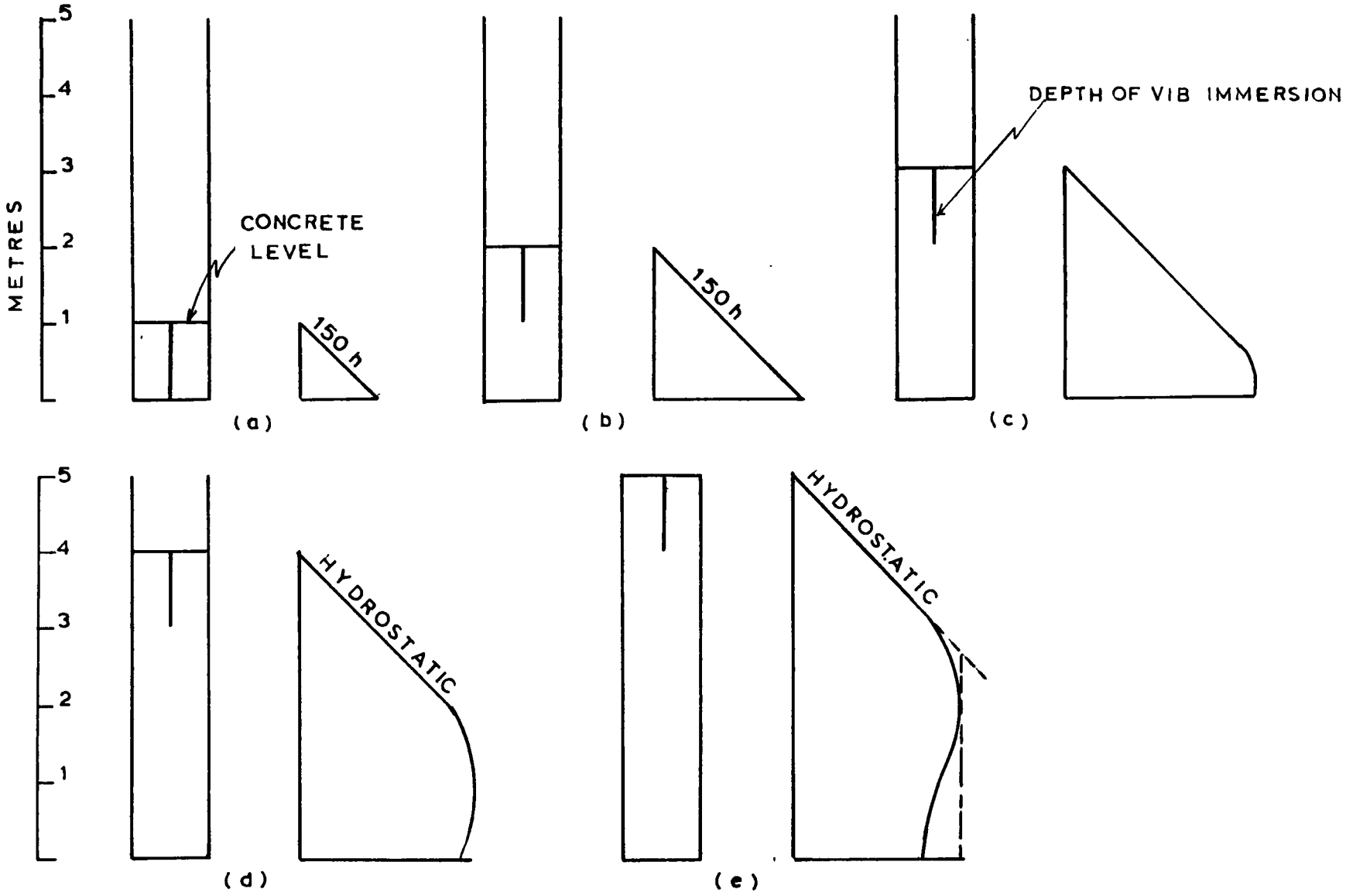

FIG.1·2 LATERAL CONCRETE PRESSURE ENVELOPE UNDER VARYING CONCRETE HEAD

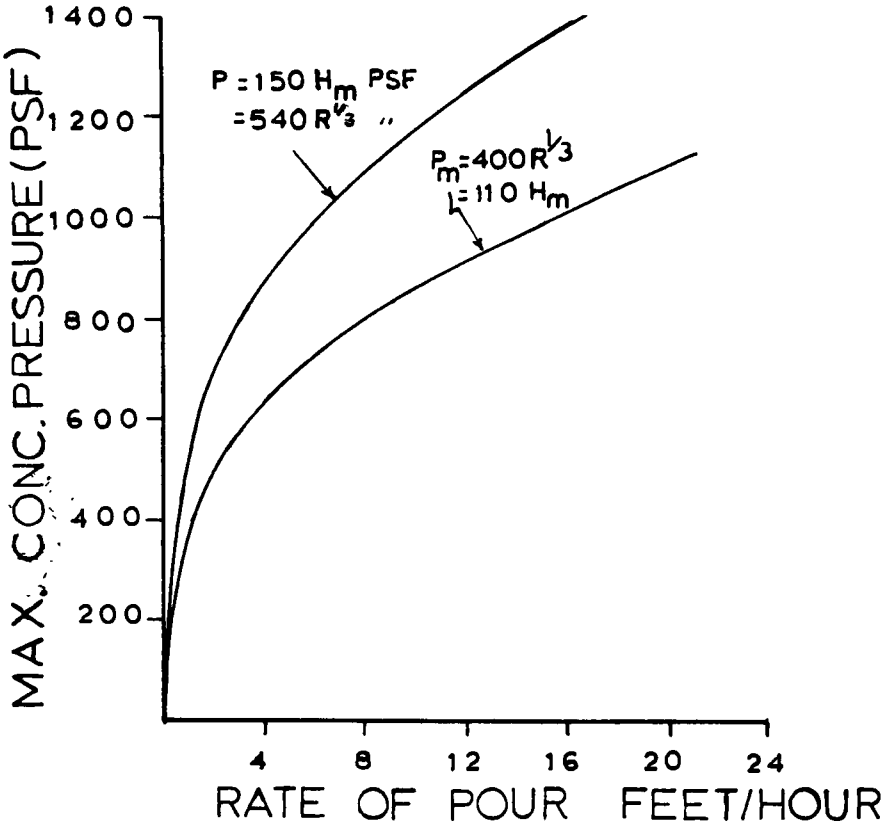

FIG. 2.1 RELATION BETWEEN MAXIMUM PRESSURE & RATE OF POUR

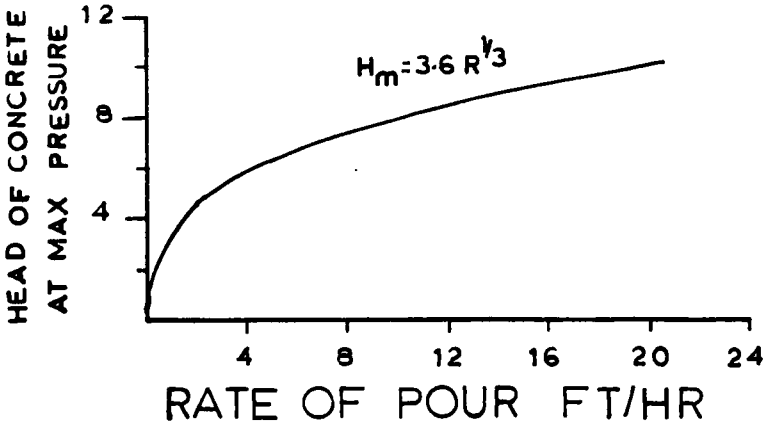

FIG. 2.2 HEAD OF CONCRETE AT MAXIMUM PRESSURE

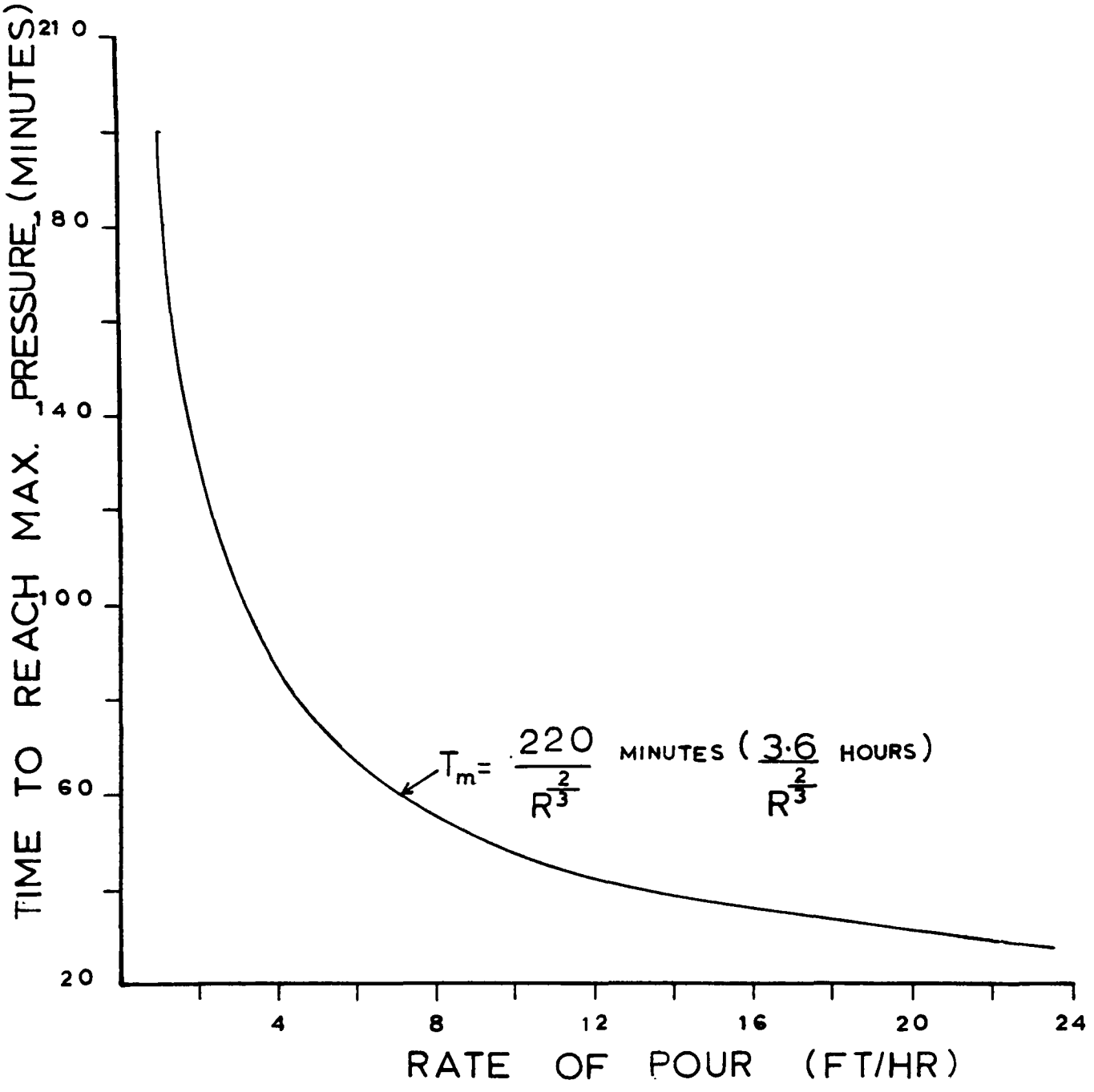

FIG.2-3a RELATION BETWEEN TIME TO REACH MAX.PRESSURE AND RATE OF POUR

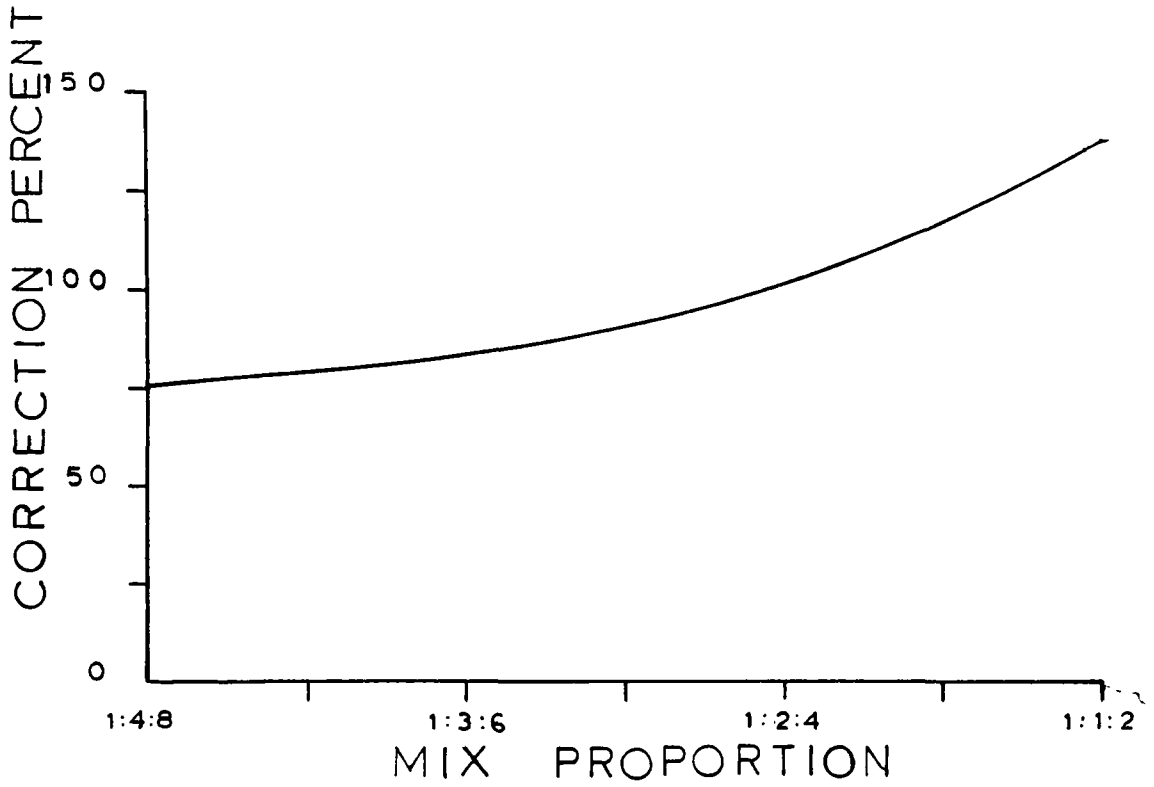

FIG.2·3b CORRECTION FOR DIFFERENT CONCRETE MIXES

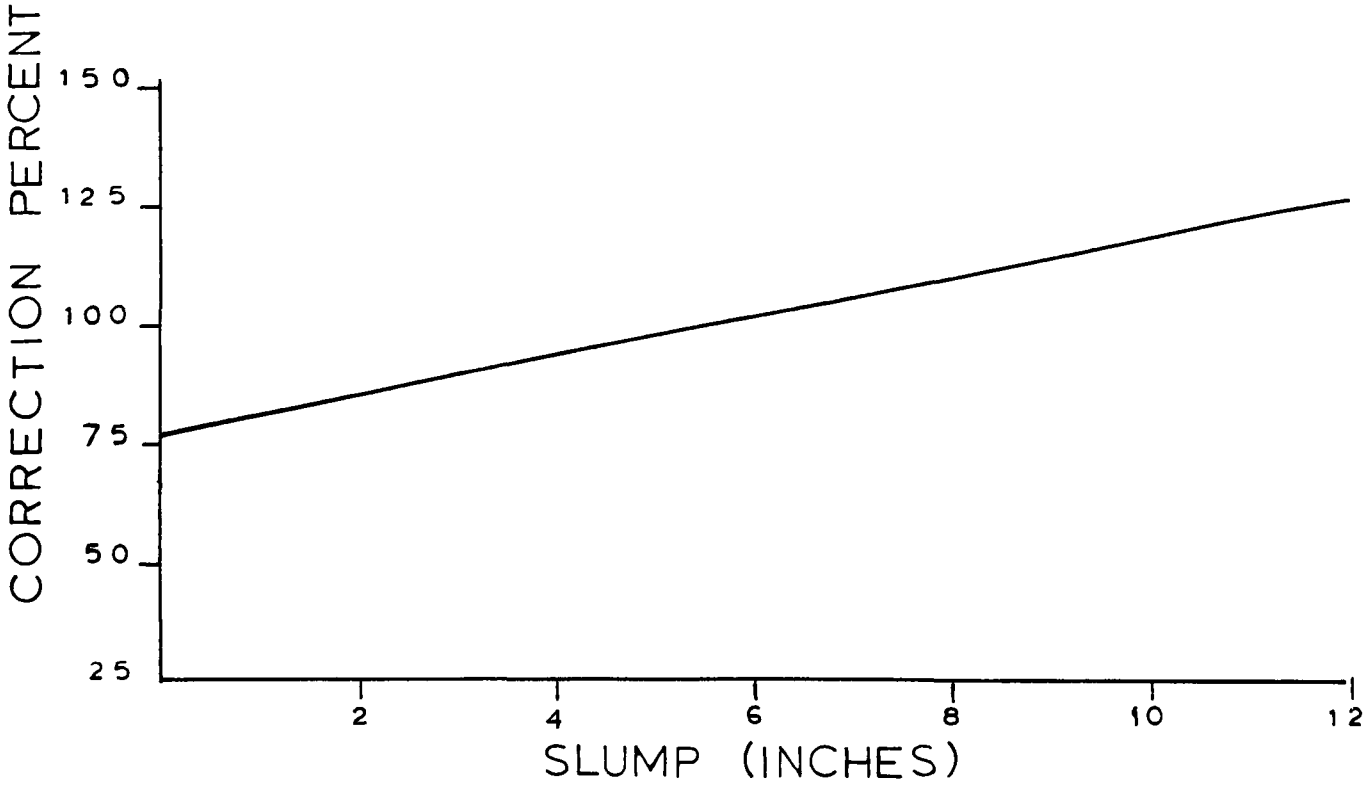

FIG.2·3C EFFECT OF SLUMP ON CONC. PRESSURE

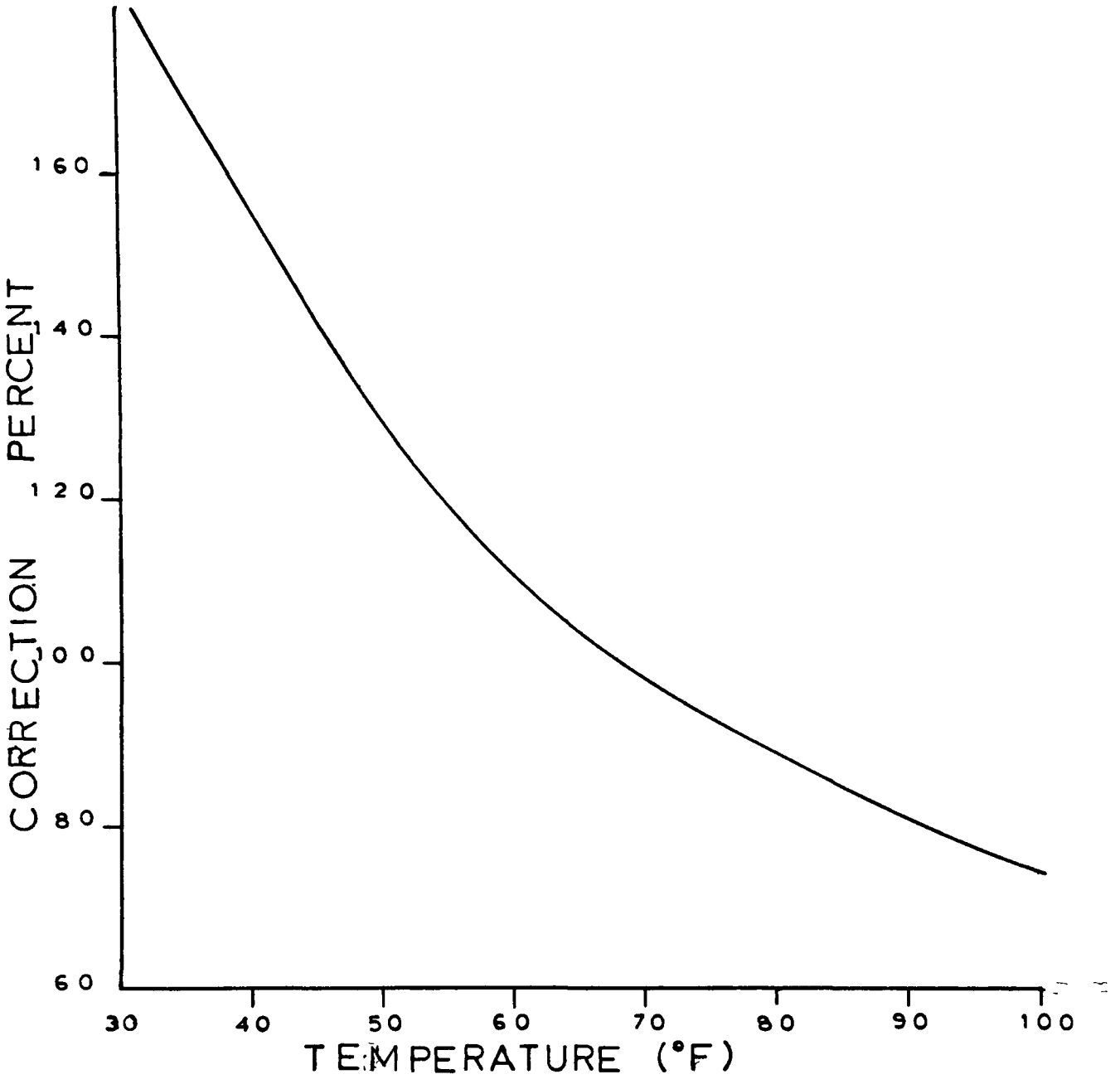

FIG.23d CORRECTION OF CONCRETE PRESSURE DUE TO VARIATION IN CONC. TEMPERATURE

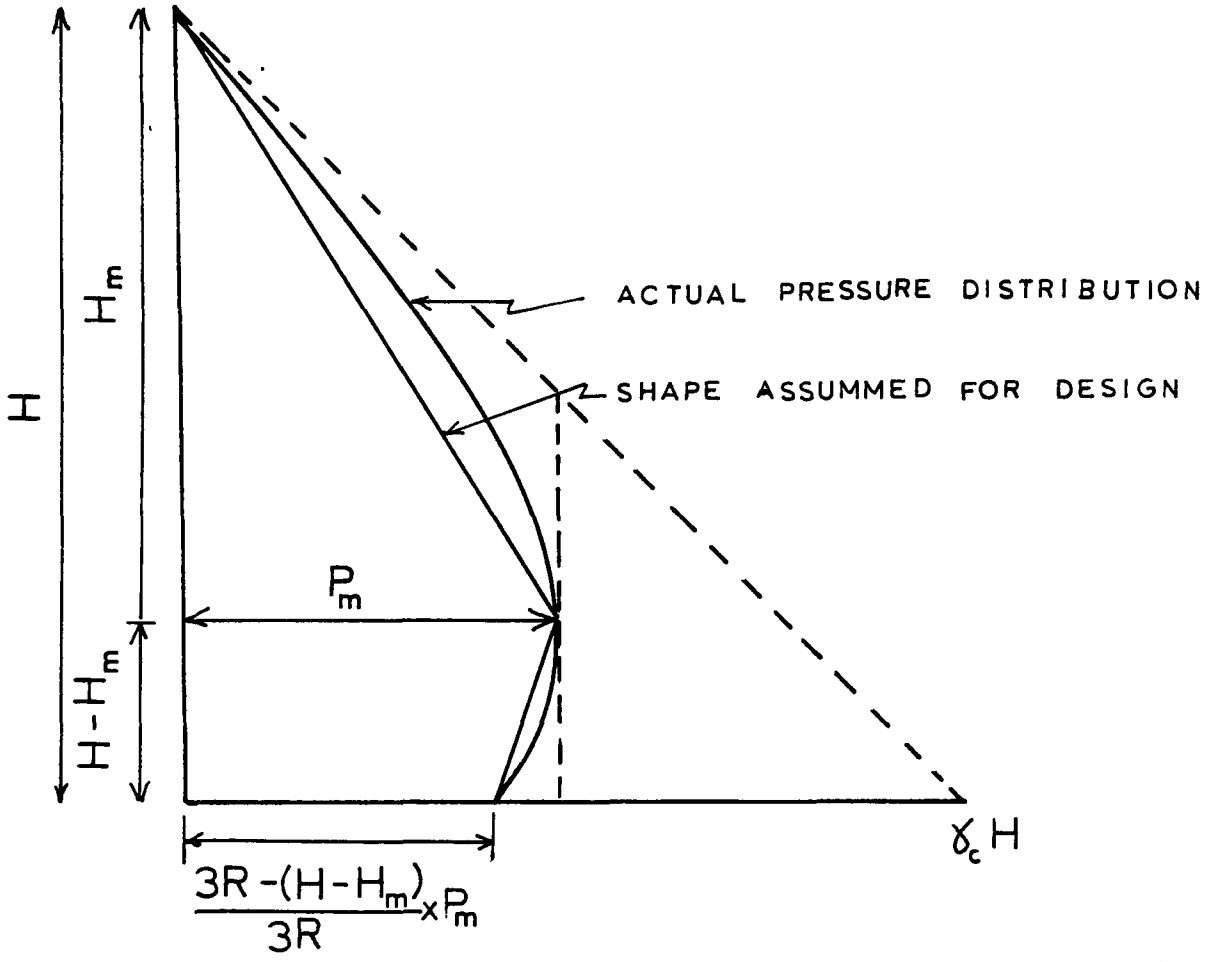

FIG. 2·4 SHAPE OF PRESSURE DIAGRAM FOR DESIGN OF FORMS
(AFTER RODIN REF.17)

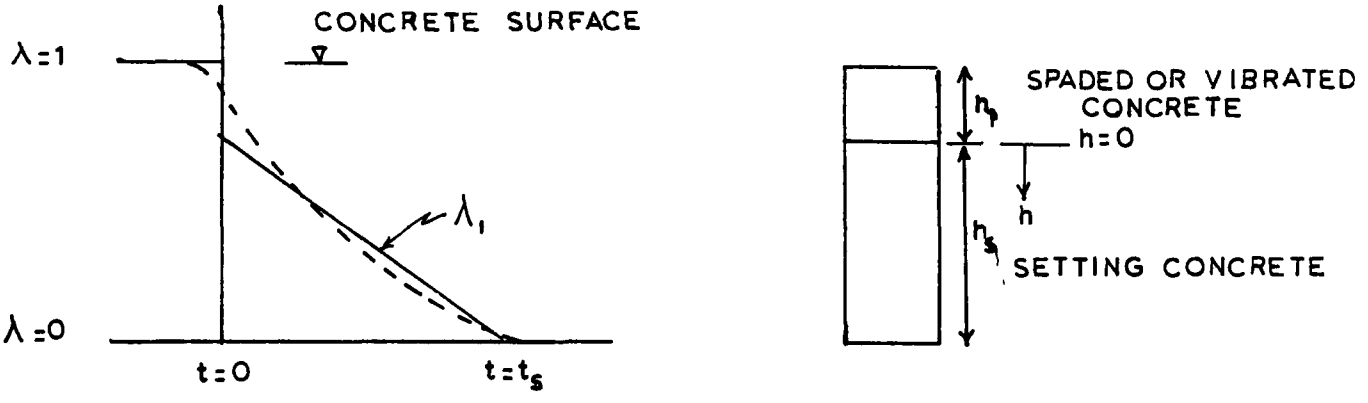

FIG. 2·5 VARIATION OF λ_1 WITH TIME
(AFTER SCHJODT REF.18)

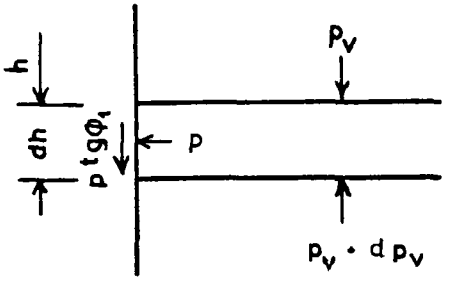

FIG. 2·6 INCREASE OF VERTICAL PRESSURE WITH DEPTH

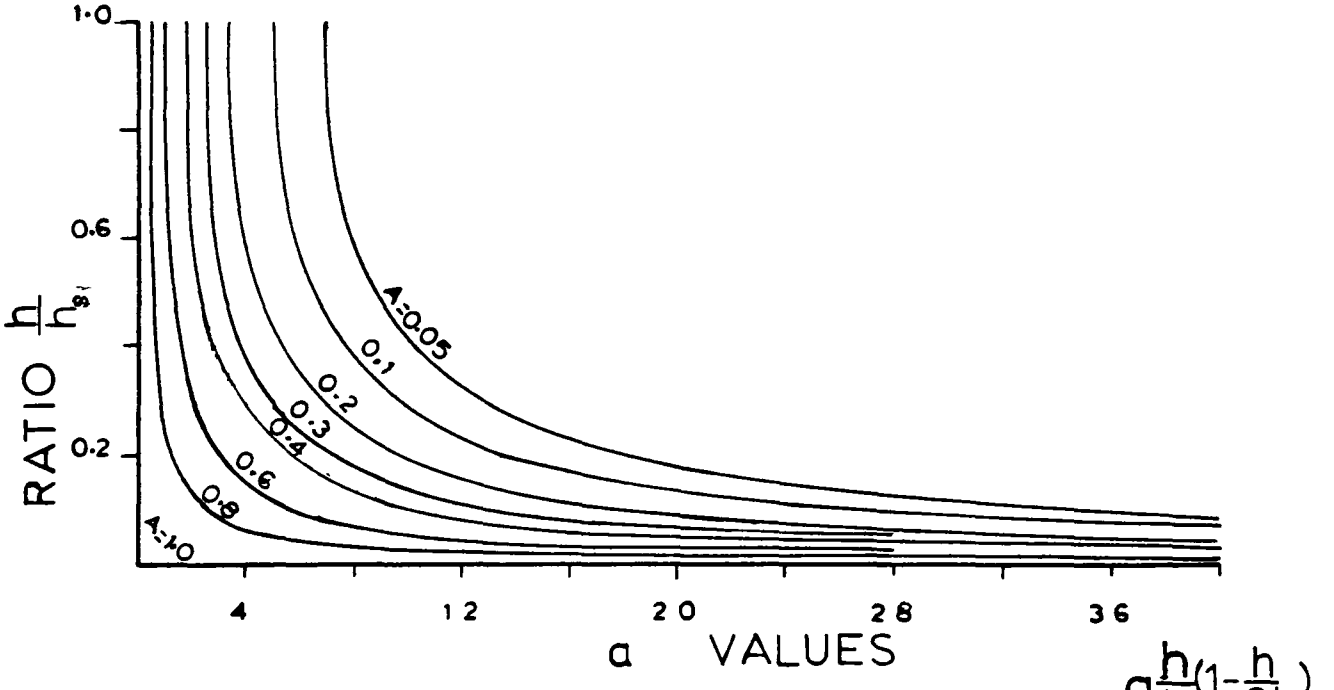

FIG. 2·7 DIAGRAM FOR $A = e^{-a\frac{h}{h_s}(1-\frac{h}{2h_s})}$

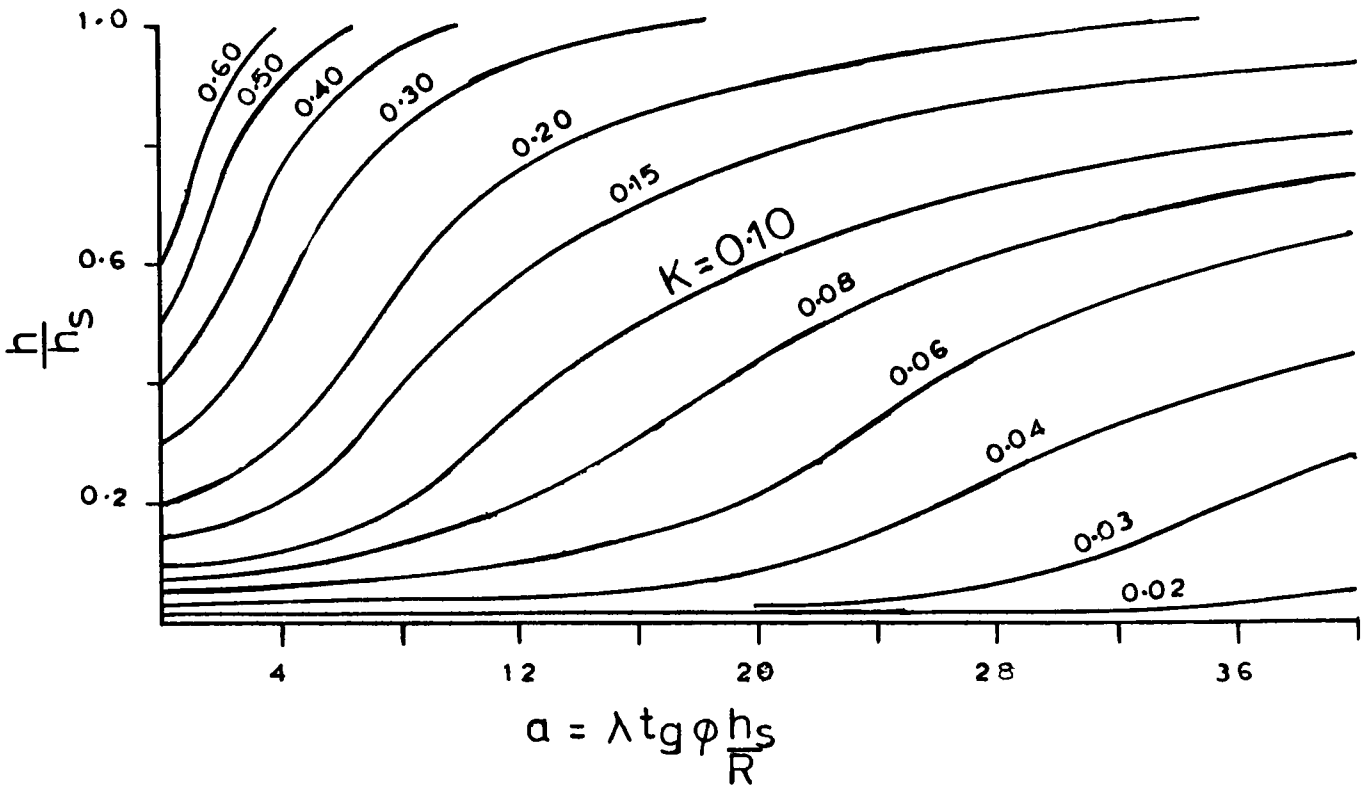

FIG.2·8 DIAGRAM FOR K

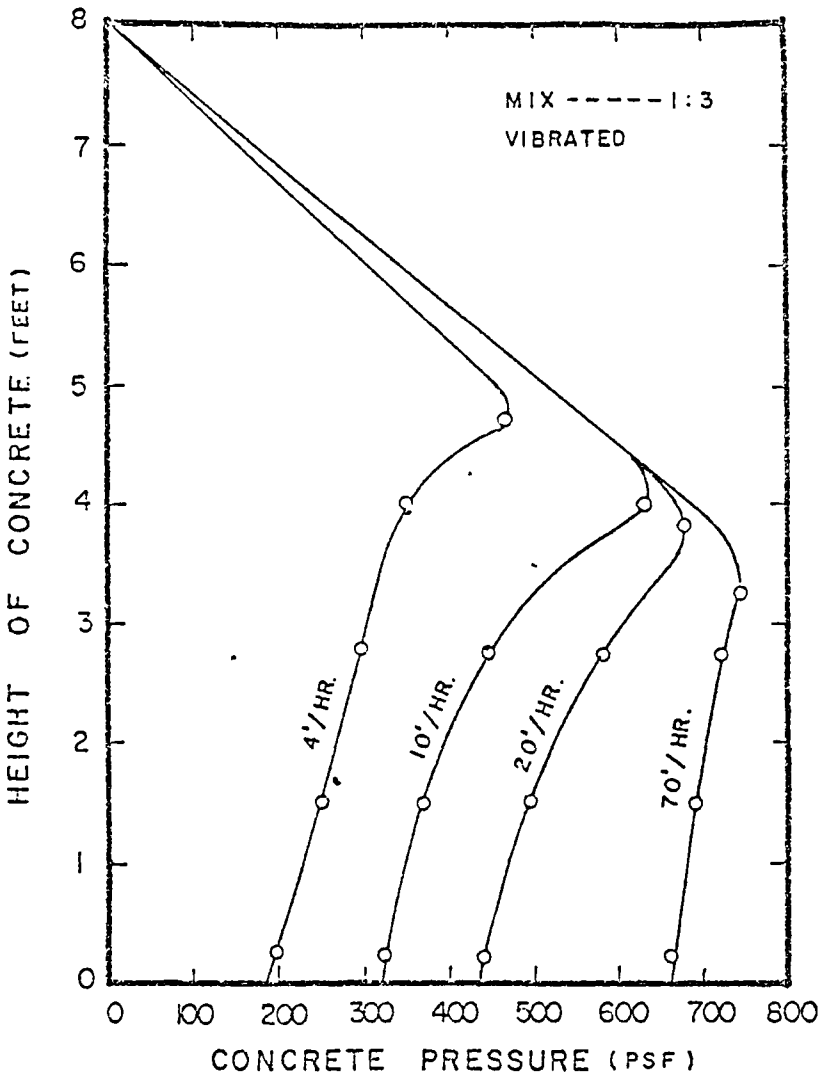

FIG.2·9 PRESSURE DEVELOPED AT VARIOUS RATE OF POUR (1:3 MIX)

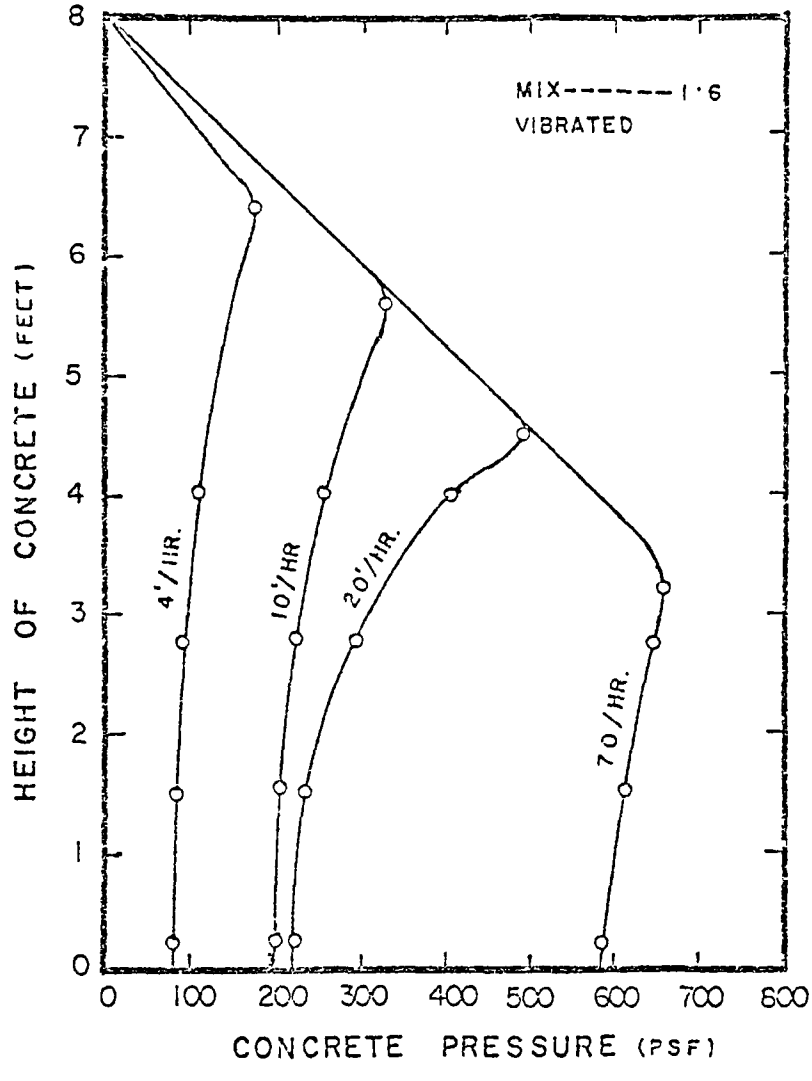

FIG 2·10 PRESSURE DEVELOPED AT VARIOUS RATES OF POUR (1:6MIX)

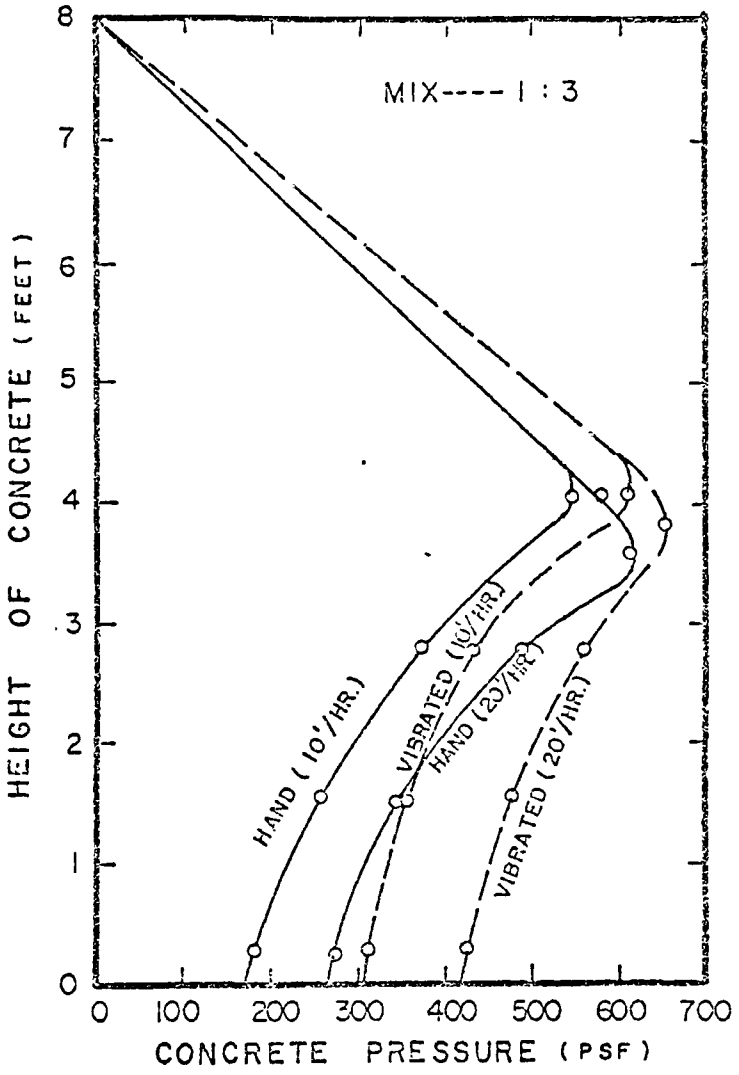

FIG. 2.11 COMPARISON OF PRESSURE DEVELOPED WITH HAND AND VIBRATED CONCRETE

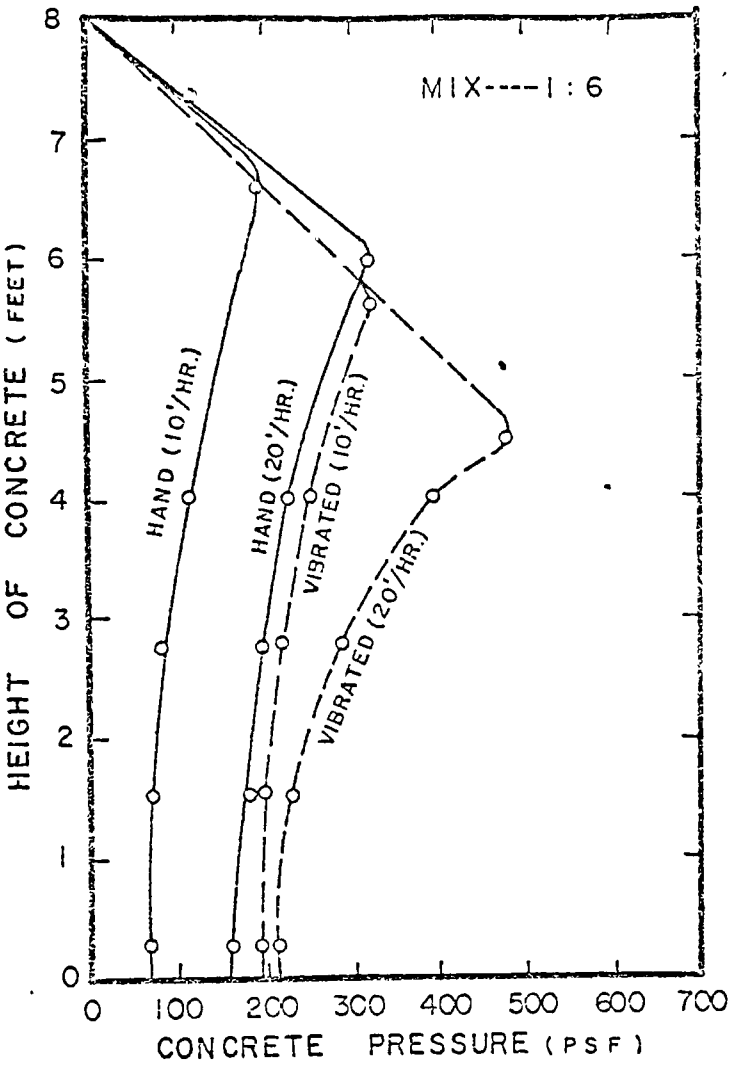

FIG 212 COMPARISON OF PRESSURE DEVELOPED WITH HAND AND VIBRATED CONCRETE (1:6 MIX)

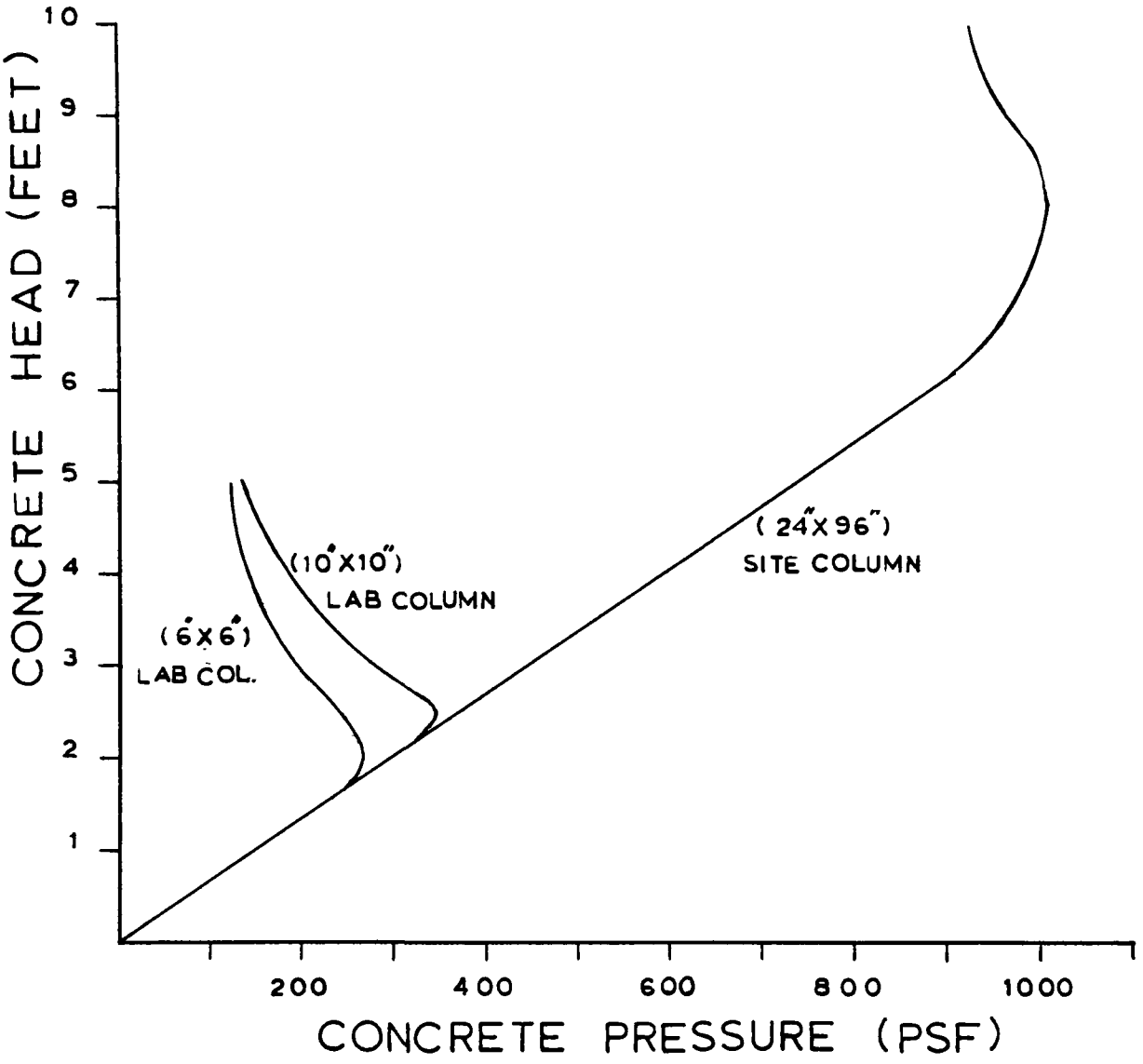

FIG. 2.13 VARIATION IN MAXIMUM PRESSURE DEVELOPED WITH SIZE OF FORMWORK

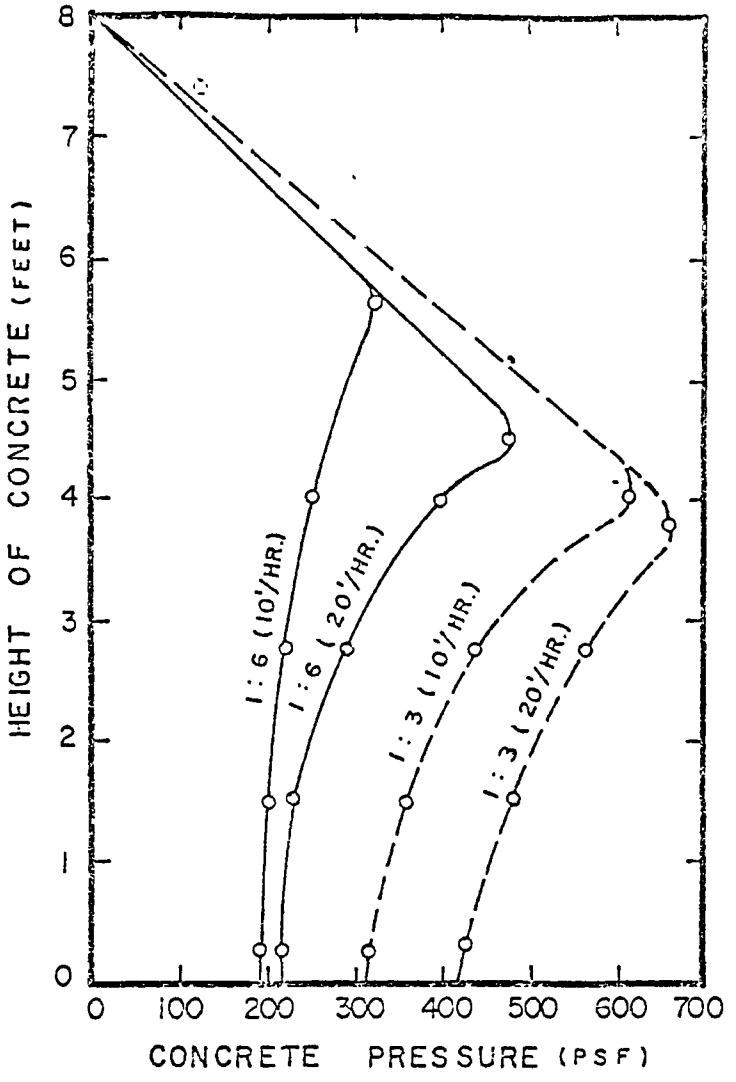

FIG. 2-14 EFFECT OF MIX ON CONCRETE PRESSURE

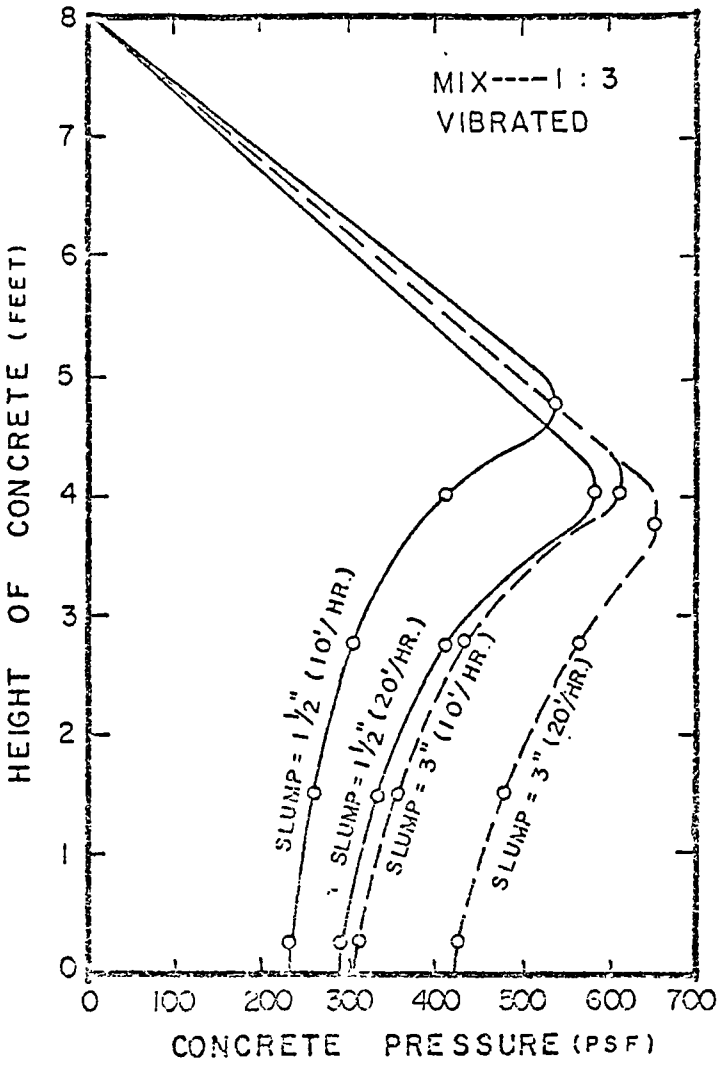

FIG.215a EFFECT OF CONSISTENCY ON CONCRETE PRESSURE (1:3MIX)

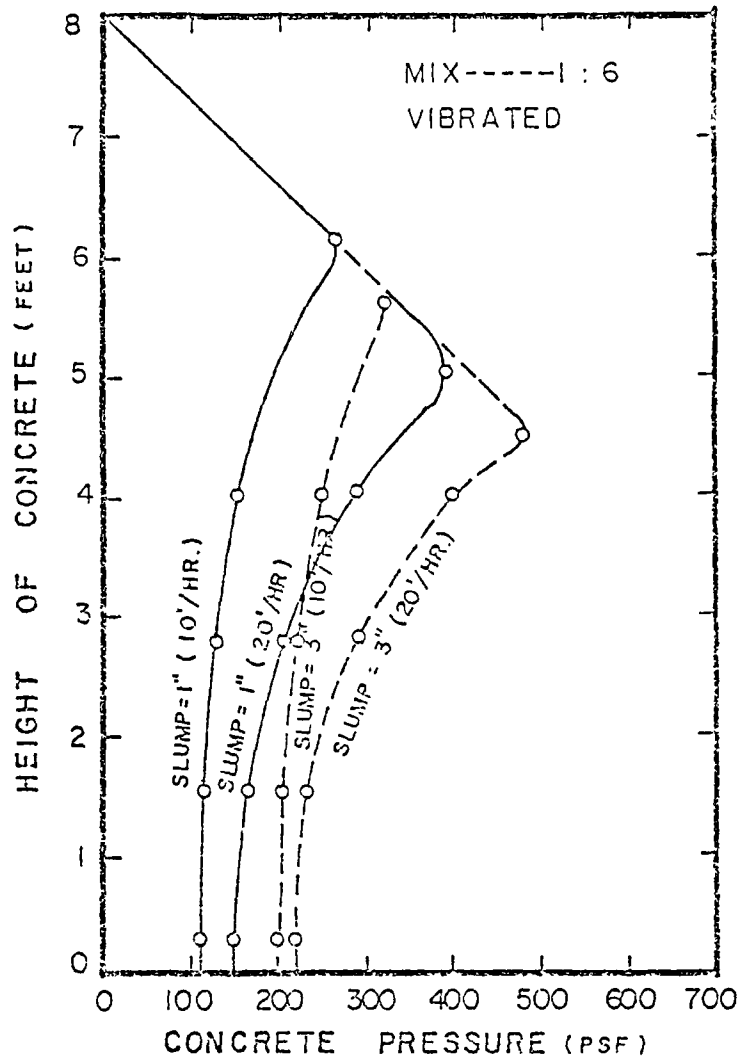

FIG.2·15b EFFECT OF CONSISTENCY ON CONCRETE PRESSURE (1:6MIX)

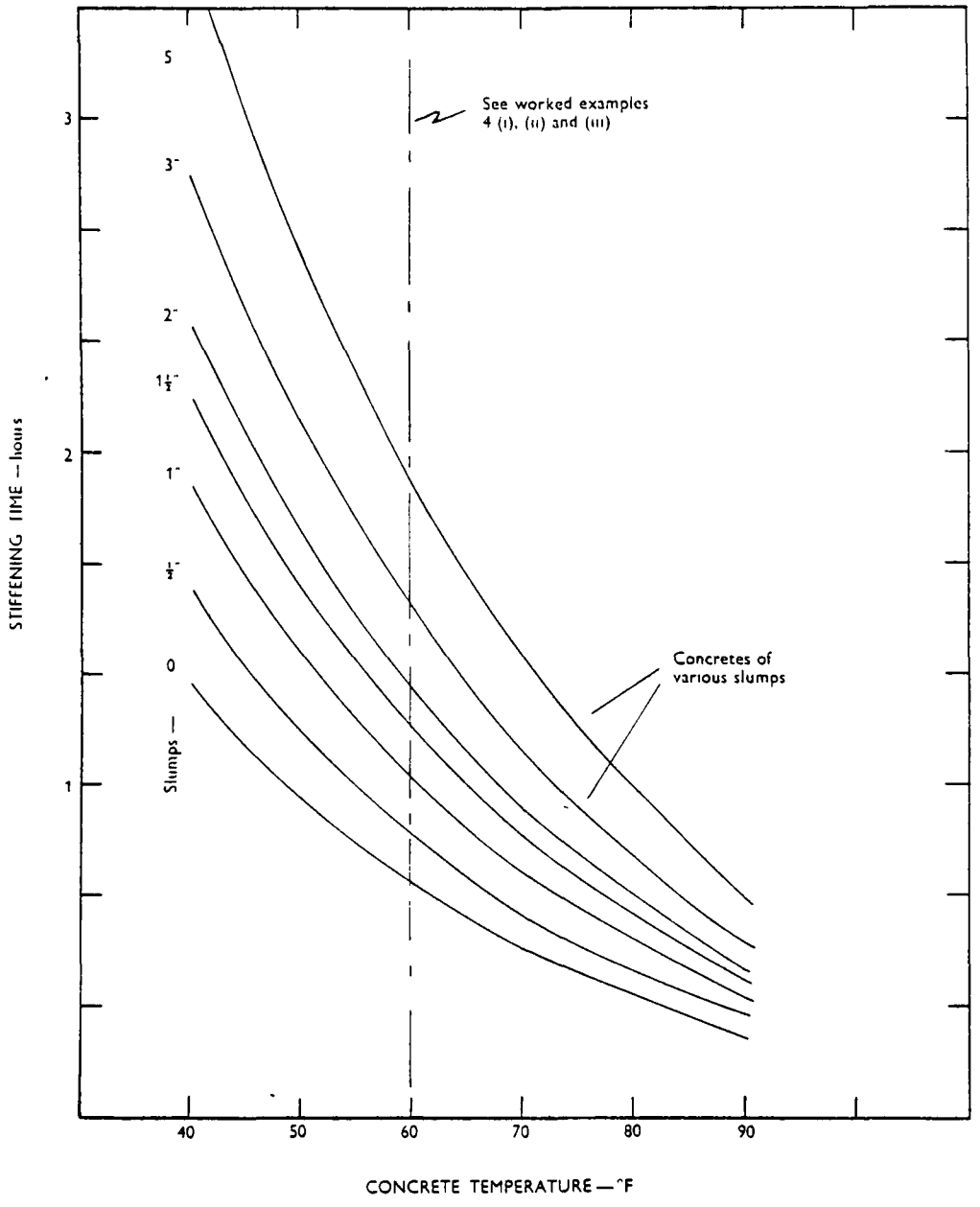

FIG. 2·16 RELATIONSHIP BETWEEN STIFFENING TIME AND THE TEMPERATURE OF CONCRETE (CERA)

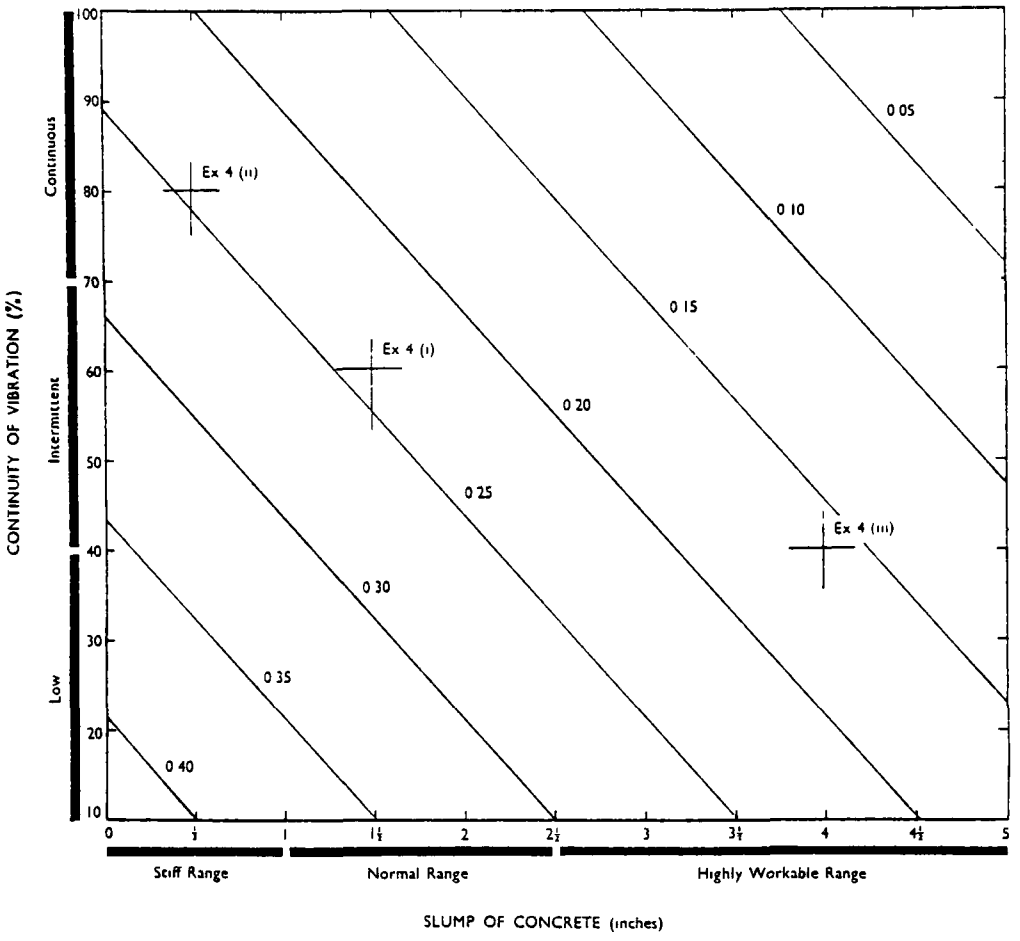

FIG.2·17 VALUES OF FACTOR C.
(CERA REF 9)

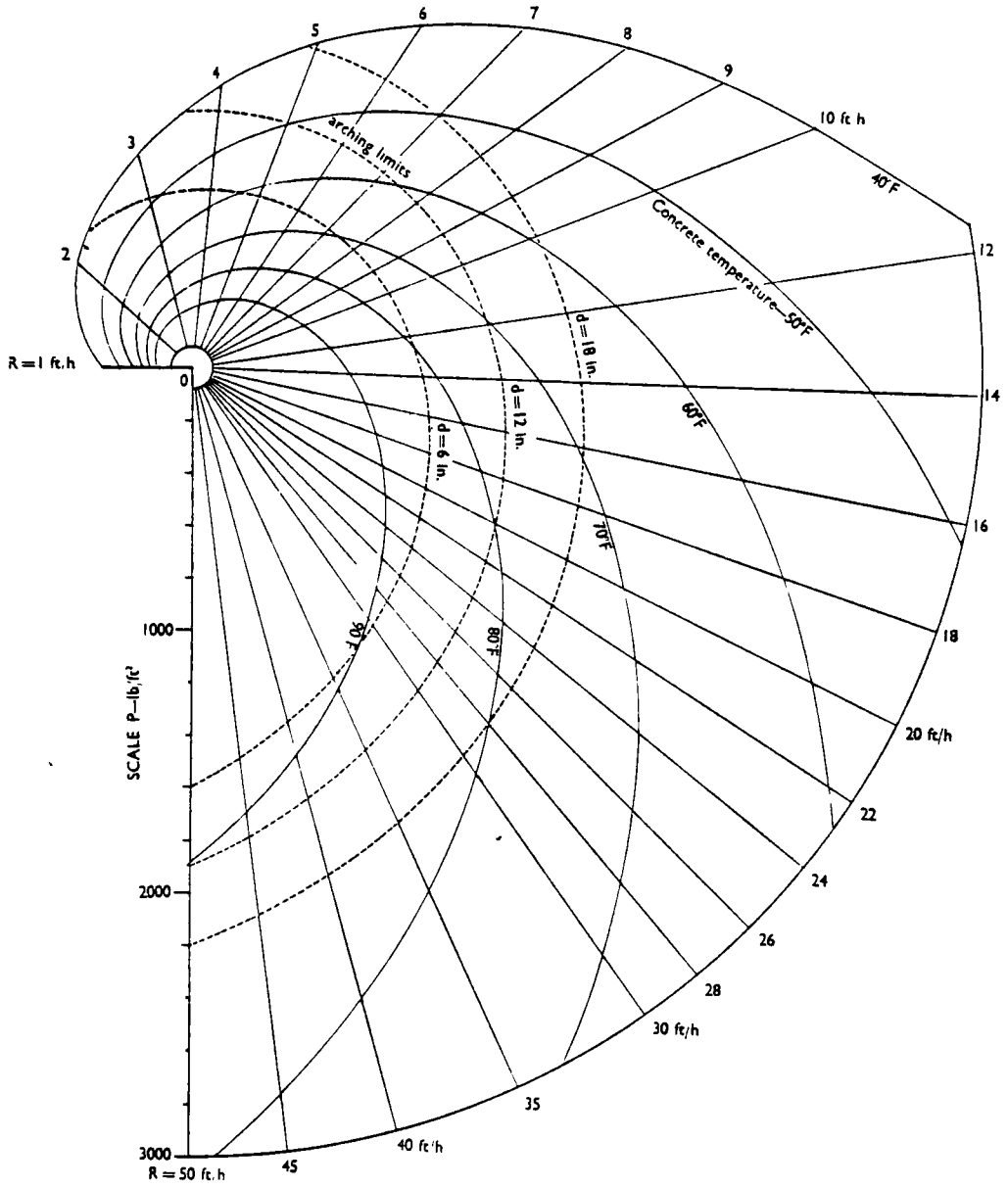

FIG.2·18 PRESSURE DESIGN CHART
(CERA REF. 9)

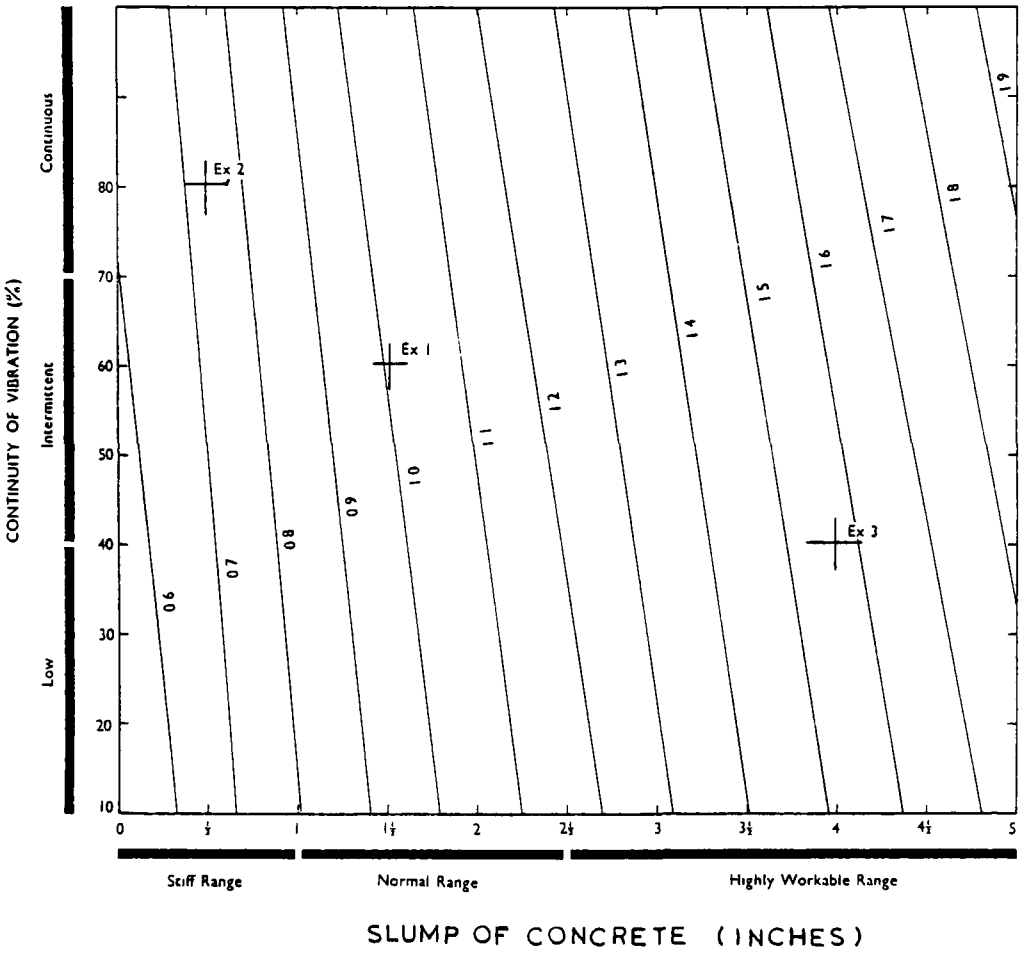

FIG 2.19 VALUES OF FACTOR F.
(CERA REF. 9)

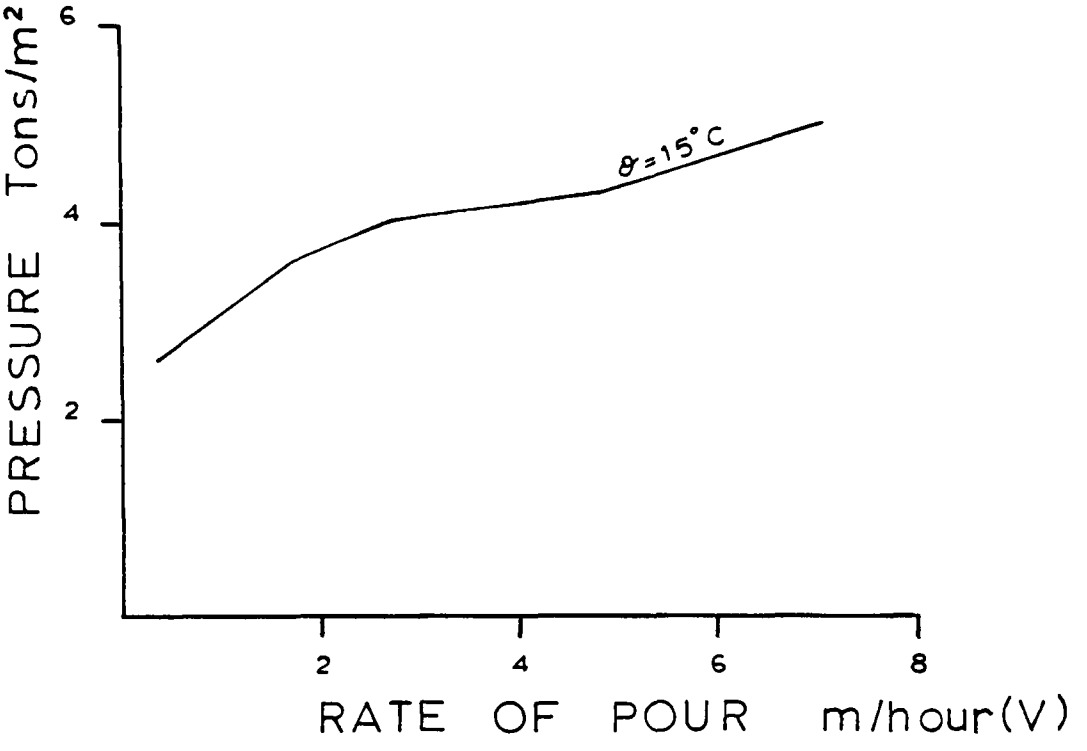

FIG. 2·20 RELATION BETWEEN PRESSURE AND RATE OF POUR

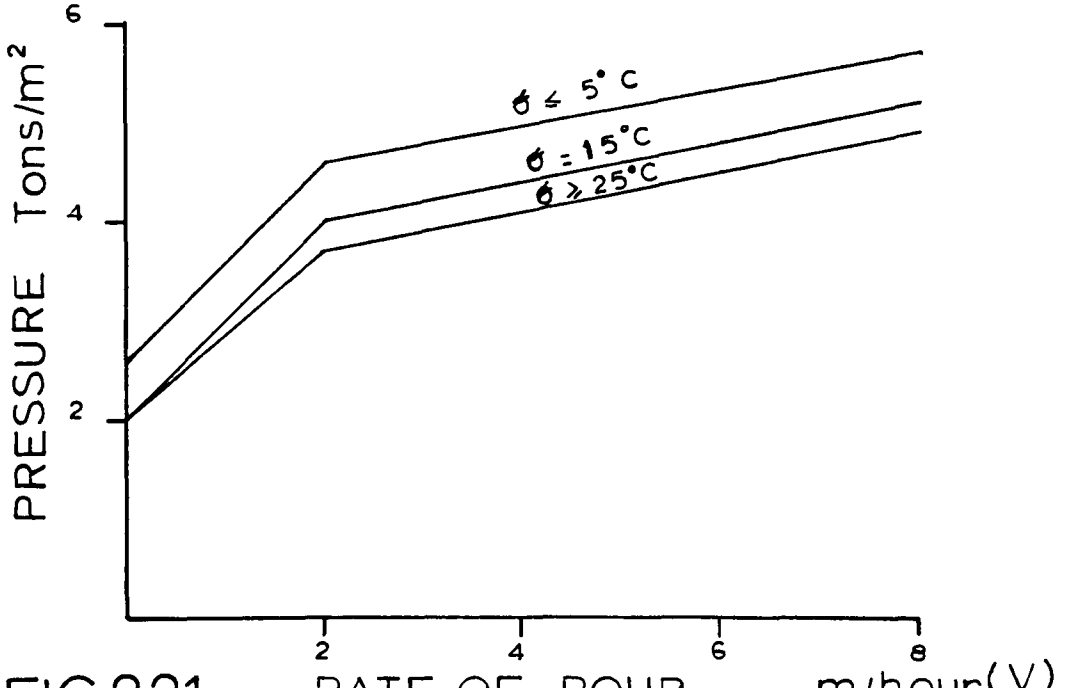

FIG. 2·21 RELATION BETWEEN RATE OF POUR, CONCRETE PRESSURE AND TEMPERATURE OF MIX.

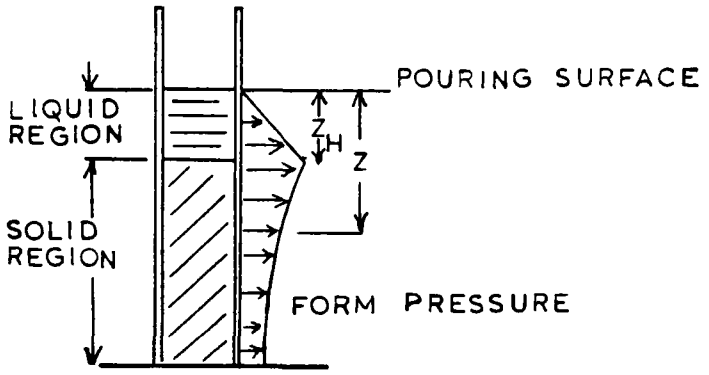

FIG. 2·22 CROSS SECTION GEOMETRY OF WALL AND QUALITATIVE DIAGRAM OF FORM PRESS. DISTRIBUTION

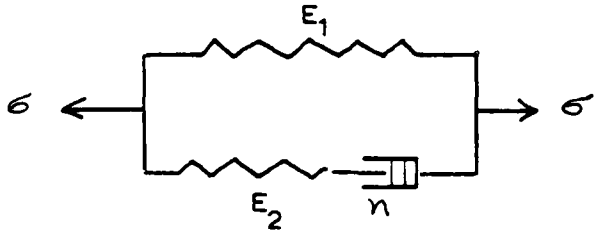

FIG. 2·23 DIAGRAM OF LINEAR STANDARD VISCO-ELASTIC SOLID AS MODEL FOR FORMSURFACE

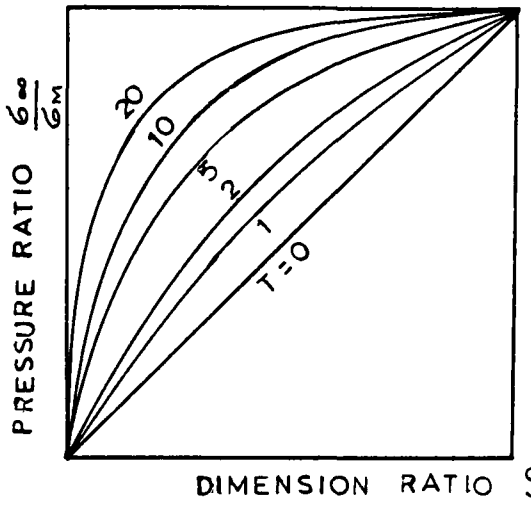

FIG. 2·24 VARIATION OF RESIDUAL TO MAXIMUM PRESS. RATIO WITH STIFFNESS RATIO S AND TIME RATIO T.

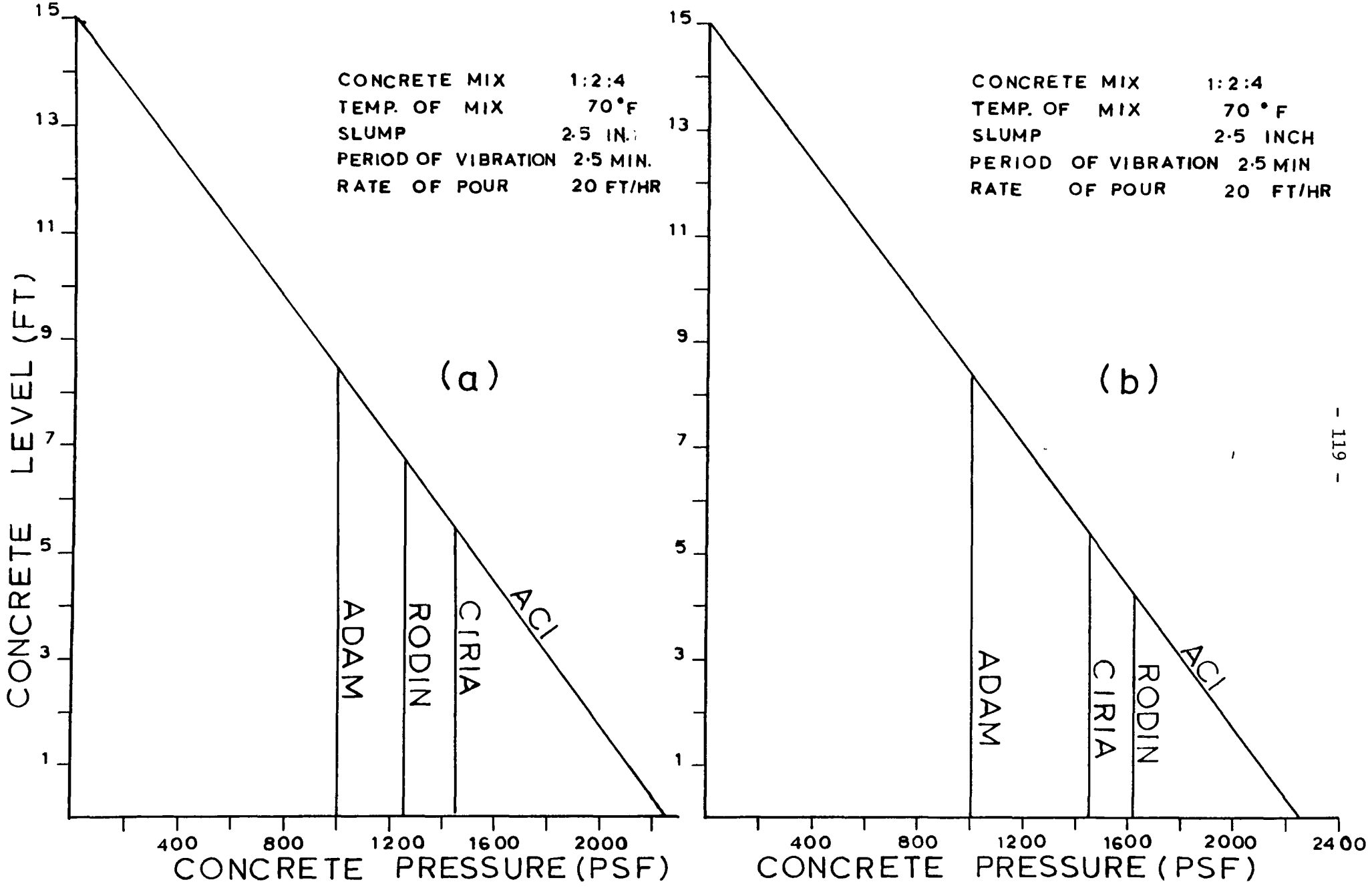

FIG.2·25 COMPARISON OF RECOMMENDED DESIGN PRESSURES

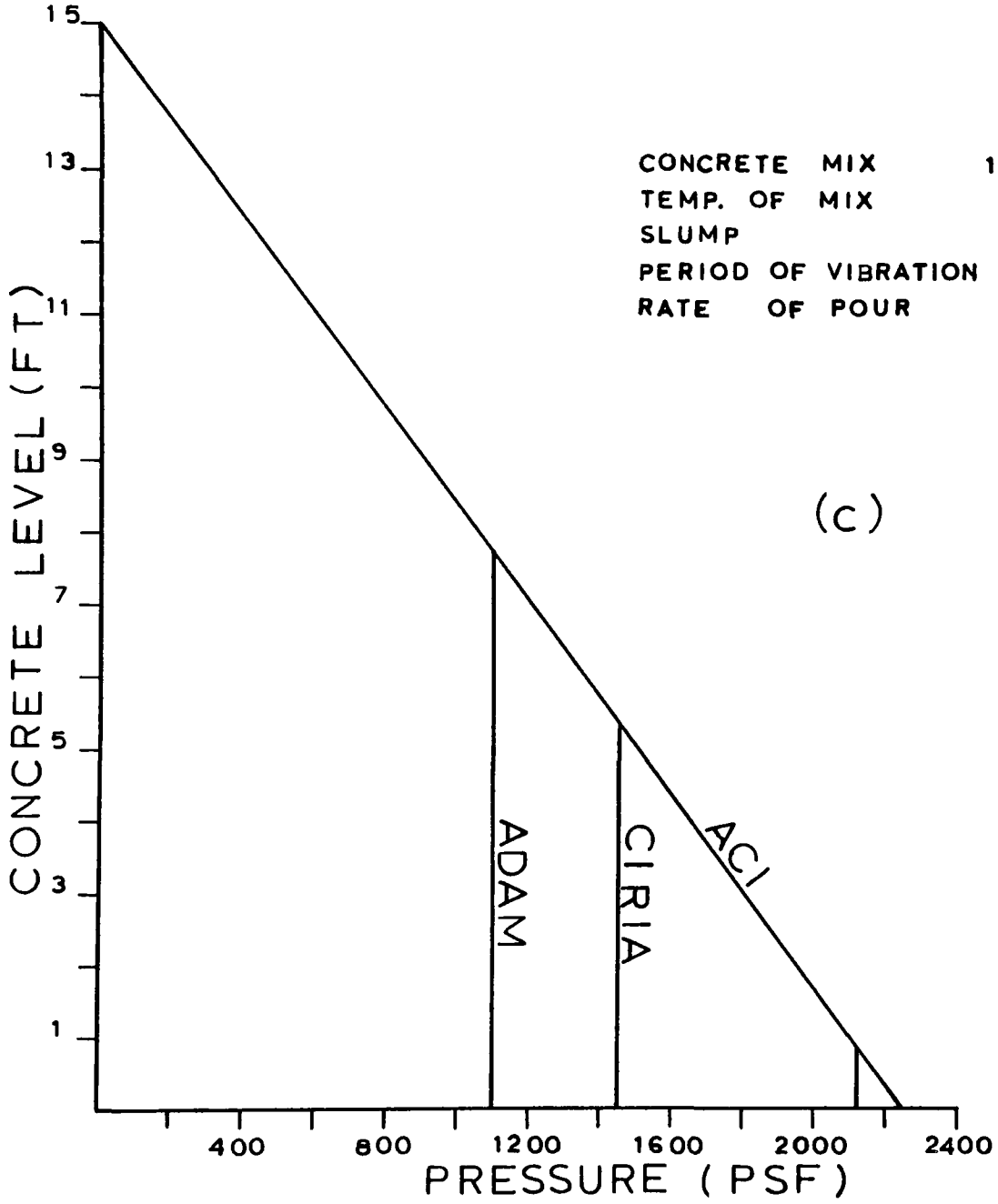

FIG.2·25 COMPARISON OF RECOMMENDED DESIGN PRESSURE

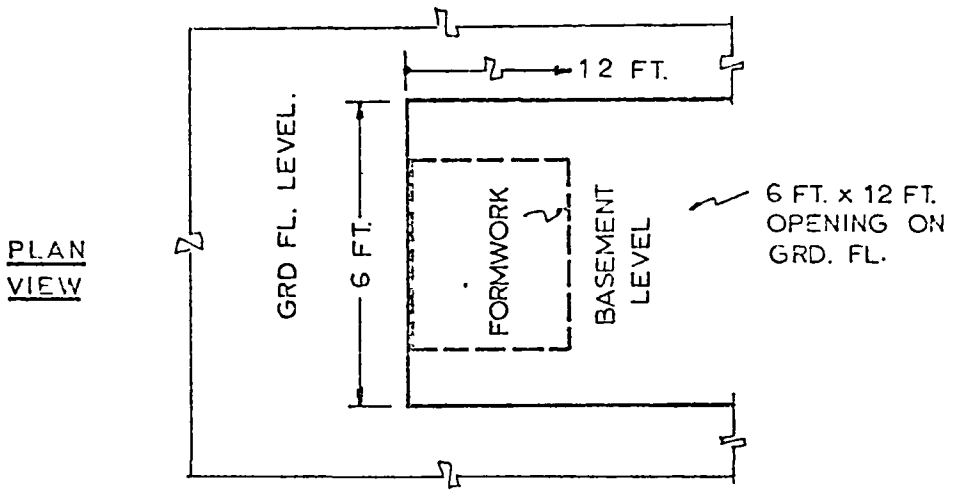

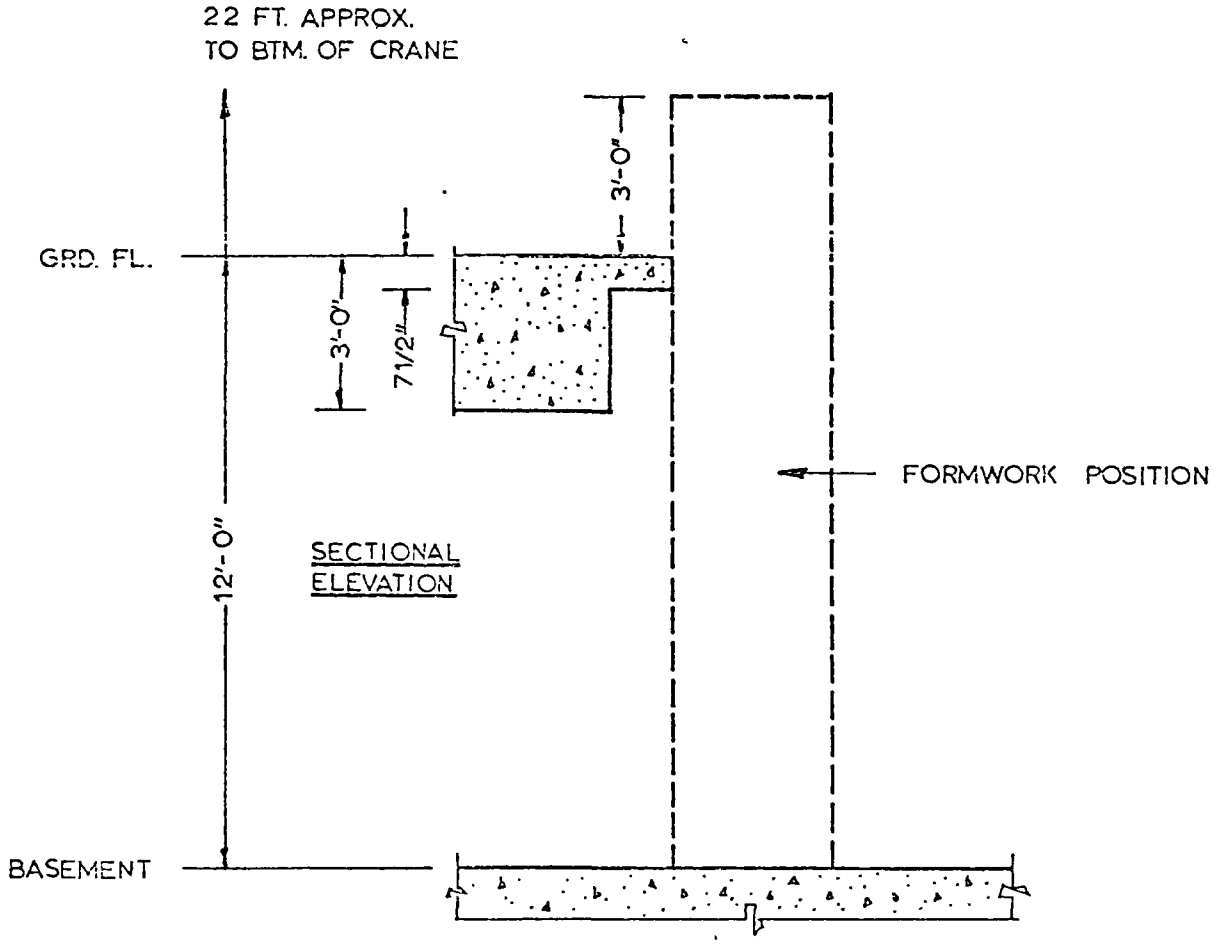

FIG 4.1a(i) FORMWORK POSITION IN STRUCTURAL LABORATORY.

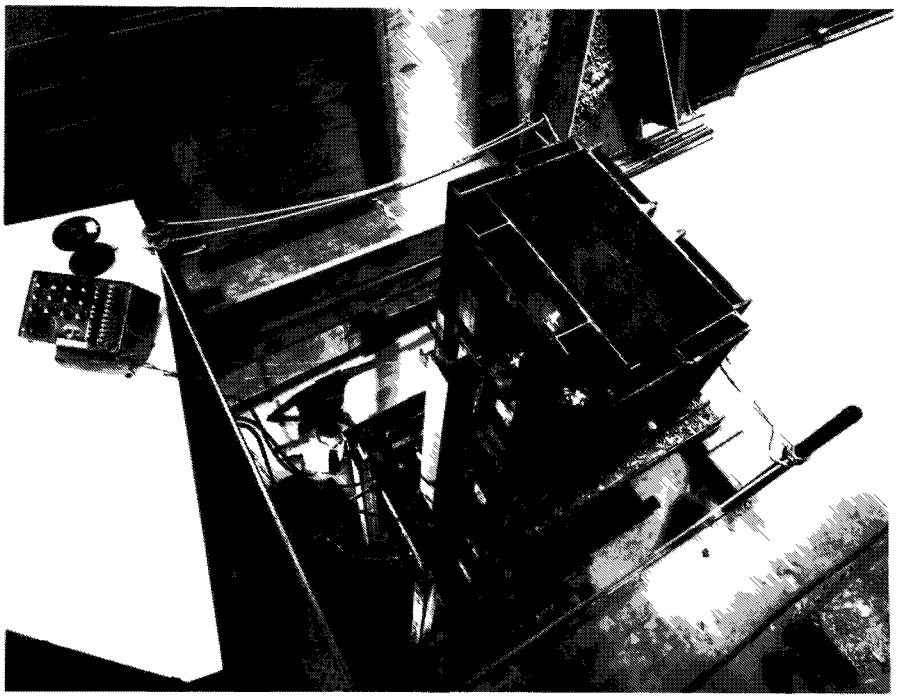

FIG 4.1a(ii) GENERAL VIEW OF FORMWORK FROM TOP

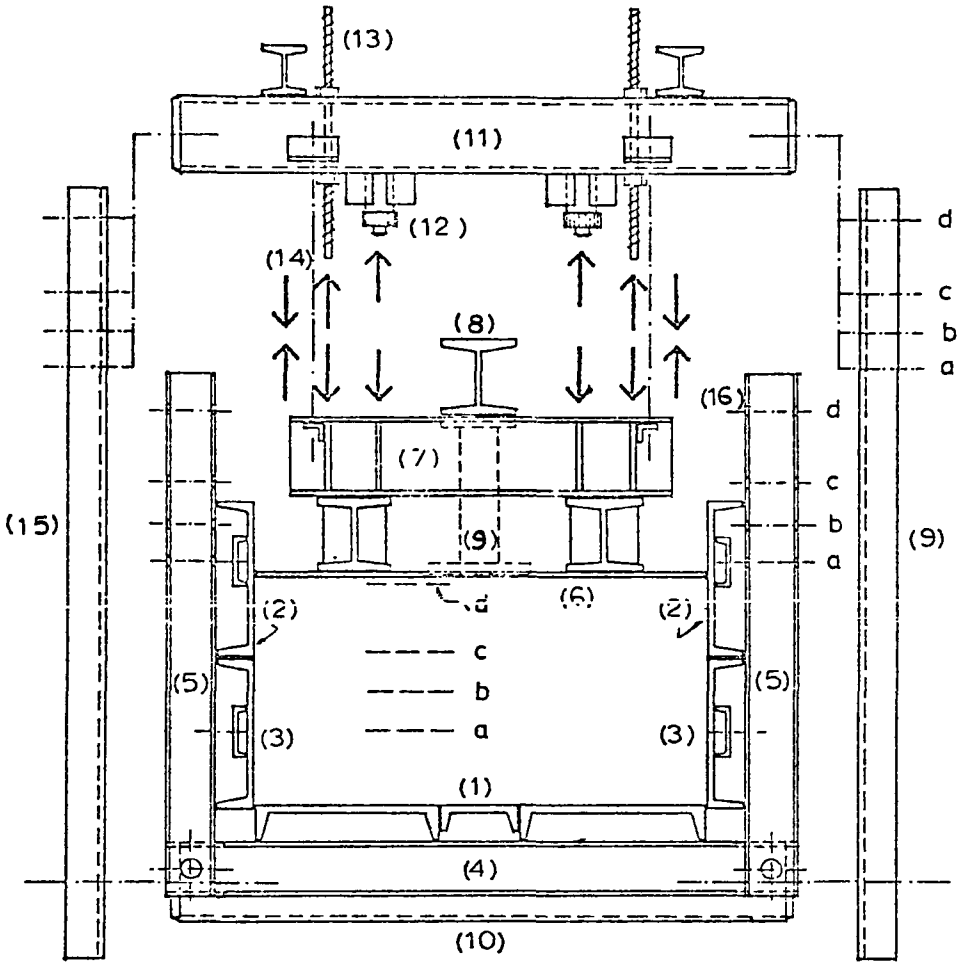

SCALE : 3/4 " = 1'-0"

FIG 4.1 b(i) GENERAL ASSEMBLY OF FORMWORK

TABLE 4.1 Details of Rigid Steel Formwork
(Refer to Fig. 4-1b)

Index No.	Description
1	Front face (2-15" channel sections and 1'6" channel sections).
2,3	Side faces, 12" channel section each, bolted to '5'.
4	4x4 WF Beam, welded to back of 'front face'.
5	4x4 WF Beam, hinged to '4', holding the 'side face' in vertical position.
6	Movable back face.
7	6x6 WF Beams, various lengths.
8	6x6 WF Beams, all the 5 load cells are mounted to it.
9	Pressure measuring device - load cell
10	6x6 Box section, welded to the back of front face, forming part of the supporting collar.
11	6x6 Box section, joining the movable part of the supporting collar, can be moved to the desired position 'a', 'b', 'c' or 'd' according to the desired form thickness.
12	Jack, trade mark 'ENARPAC-RC-102', 10 tons capacity and 2-1/8" stroke.
13	Supporting threaded rods.
14	Pull out threaded rods.
15	6" channel section, part of the supporting collar.
16	Threaded rod, holding the side faces from opening up while concreting, rod has to pass through each side face of each side at position of 'a', 'b', 'c' or 'd' according to form thickness.
a	Position for 6" thickness of the form.
b	Position for 9" thickness of the form.
c	Position for 12" thickness of the form.
d	Position for 18" thickness of the form.

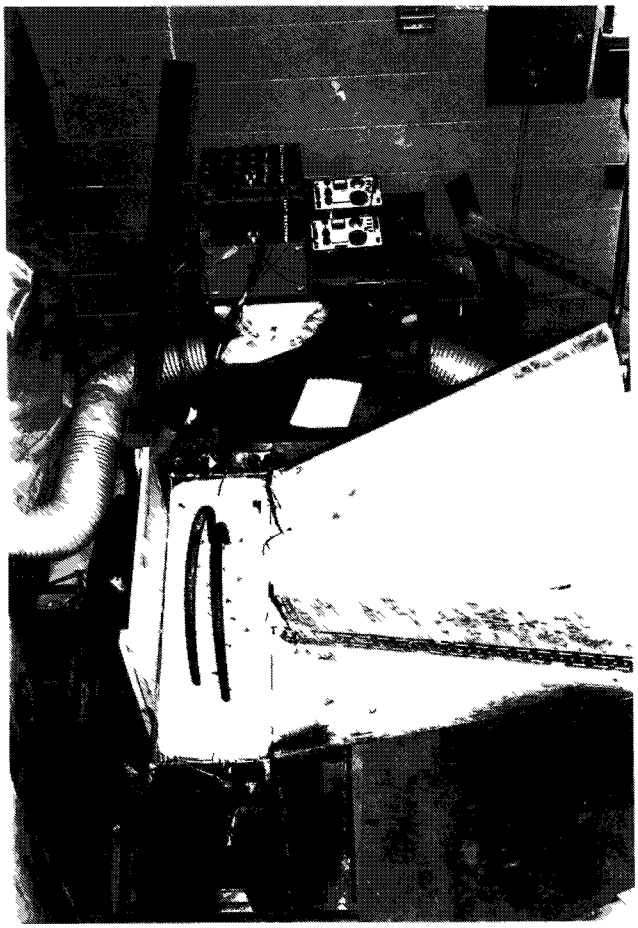

FIG 4.1 b(ii) GENERAL VIEW OF FORMWORK FROM TOP AFTER CONCRETE IS POURED

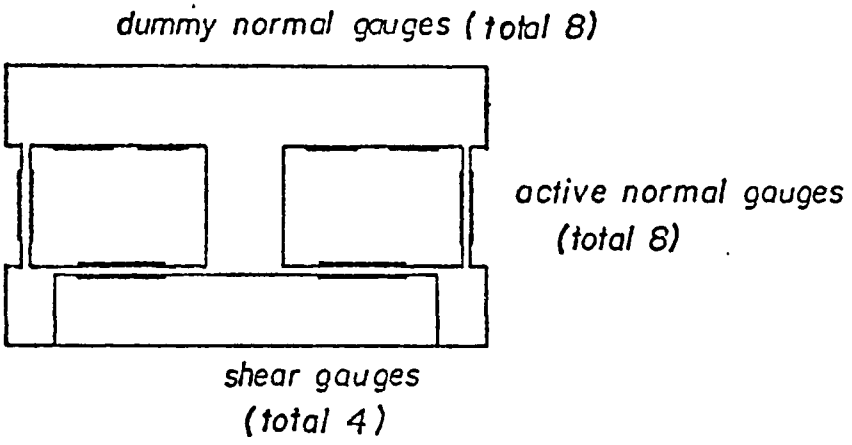

FIG.4-2 STRAIN GAUGES ON ORIGINAL CAMBRIDGE CELL

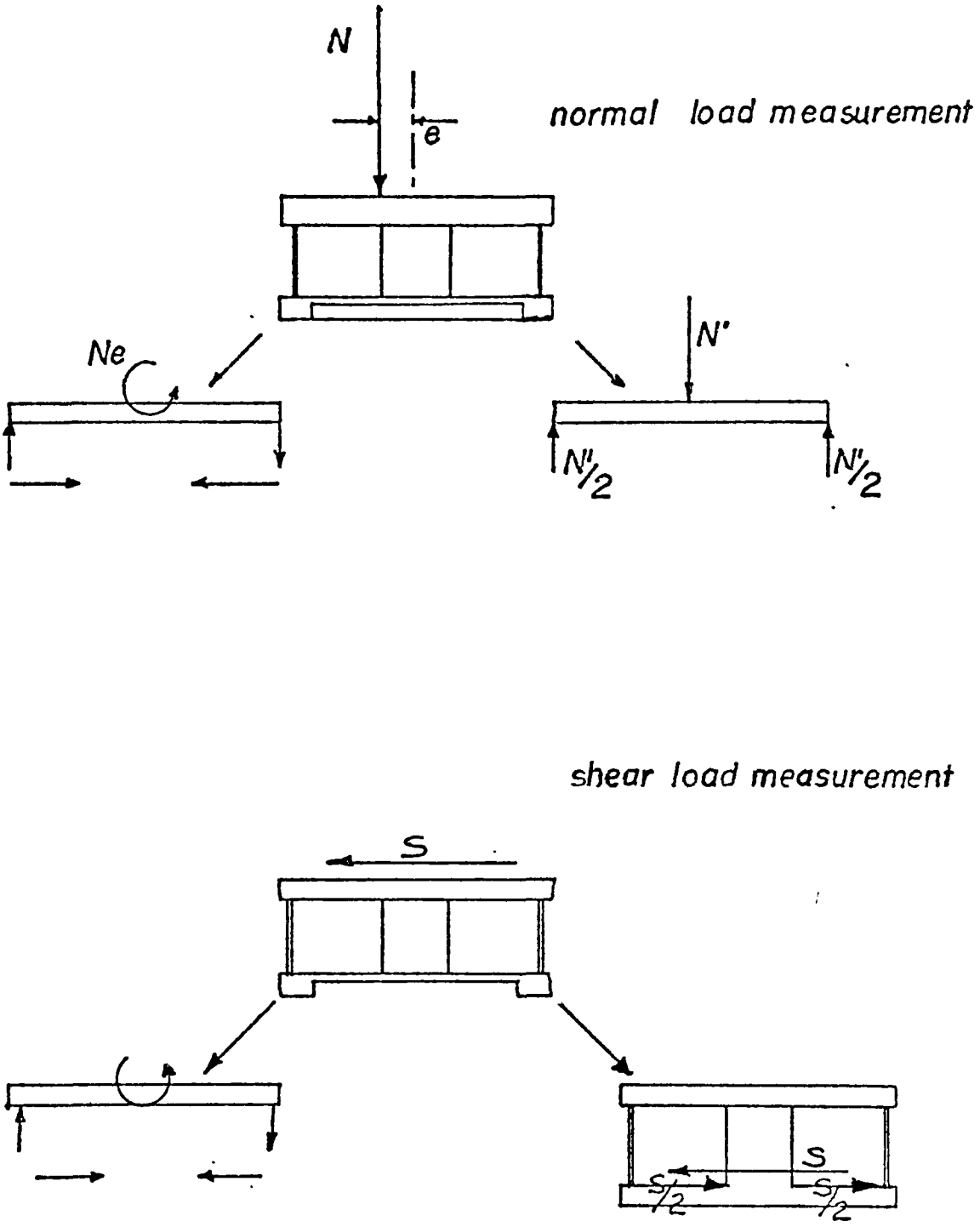

FIG. 4·3 STRAIN IN WEBS OF CAMBRIDGE CELL.

MODIFIED CAMBRIDGE CELL

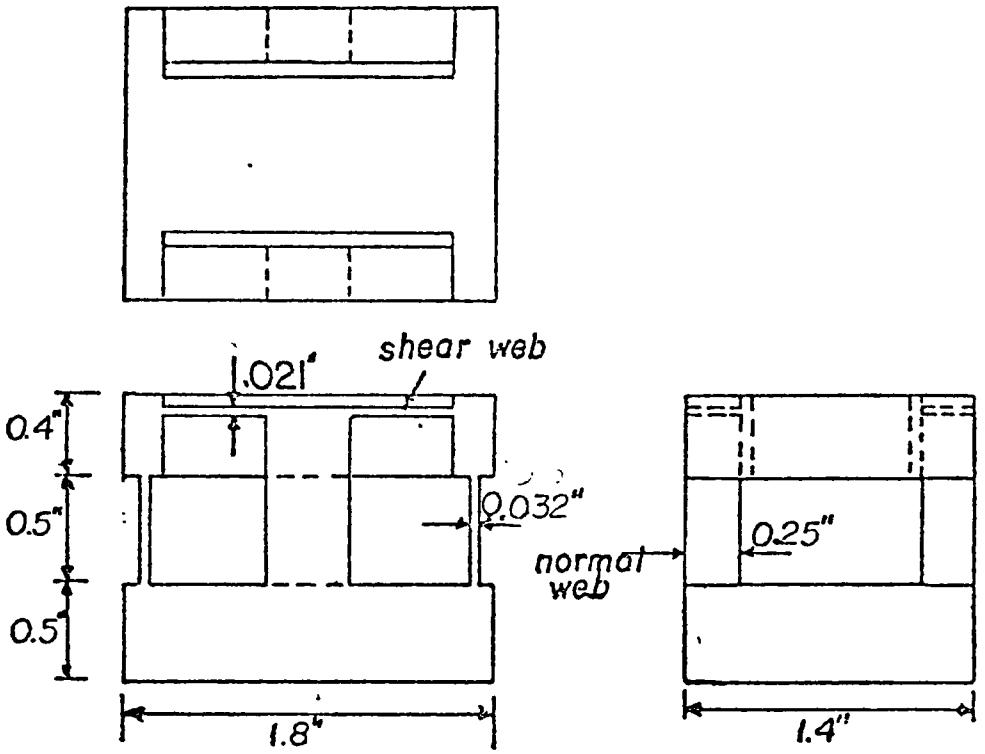

ORIGINAL CAMBRIDGE CELL

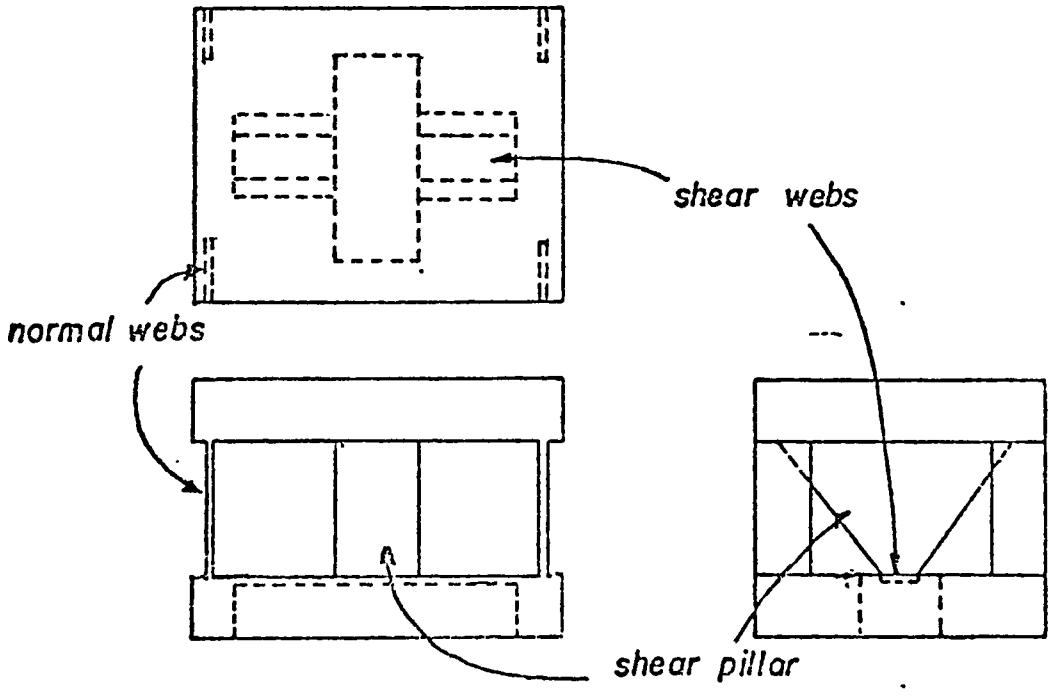

FIG.4·4 COMPARISON OF ORIGINAL AND MODIFIED CAMBRIDGE CELLS

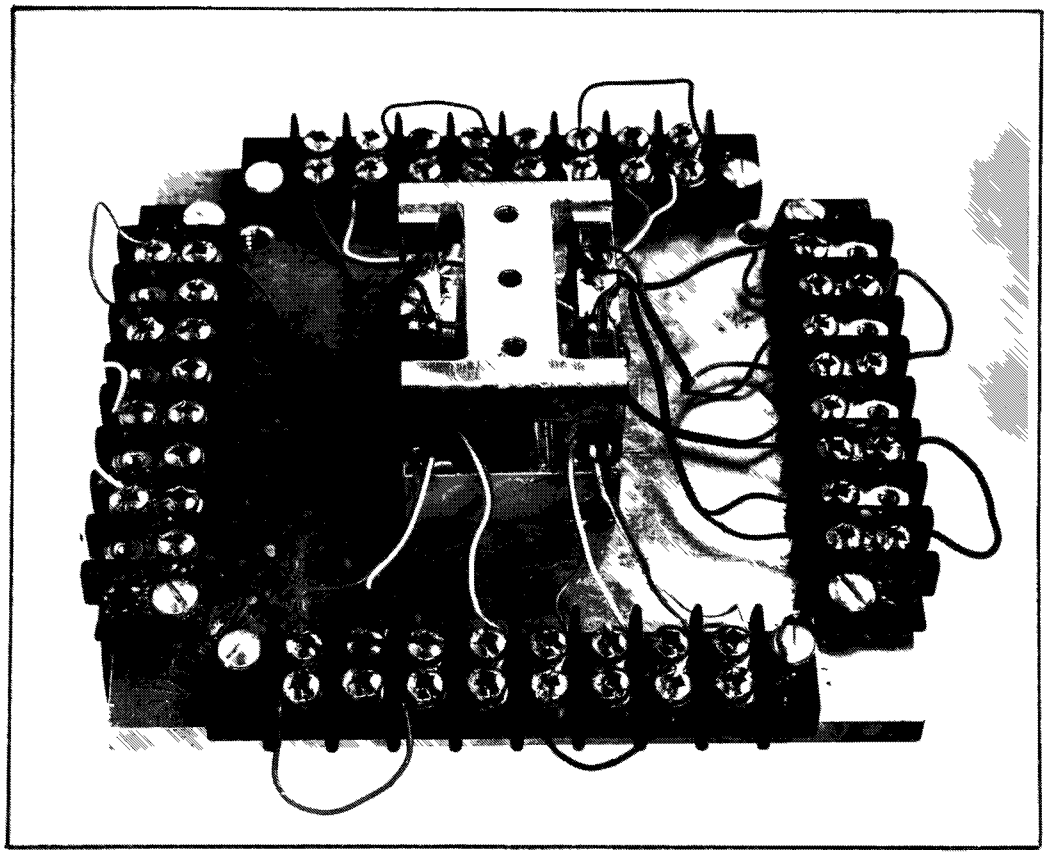

FIG.4·5a GENERAL VIEW OF CAMBRIDGE CELL WITHOUT FACEPLATE

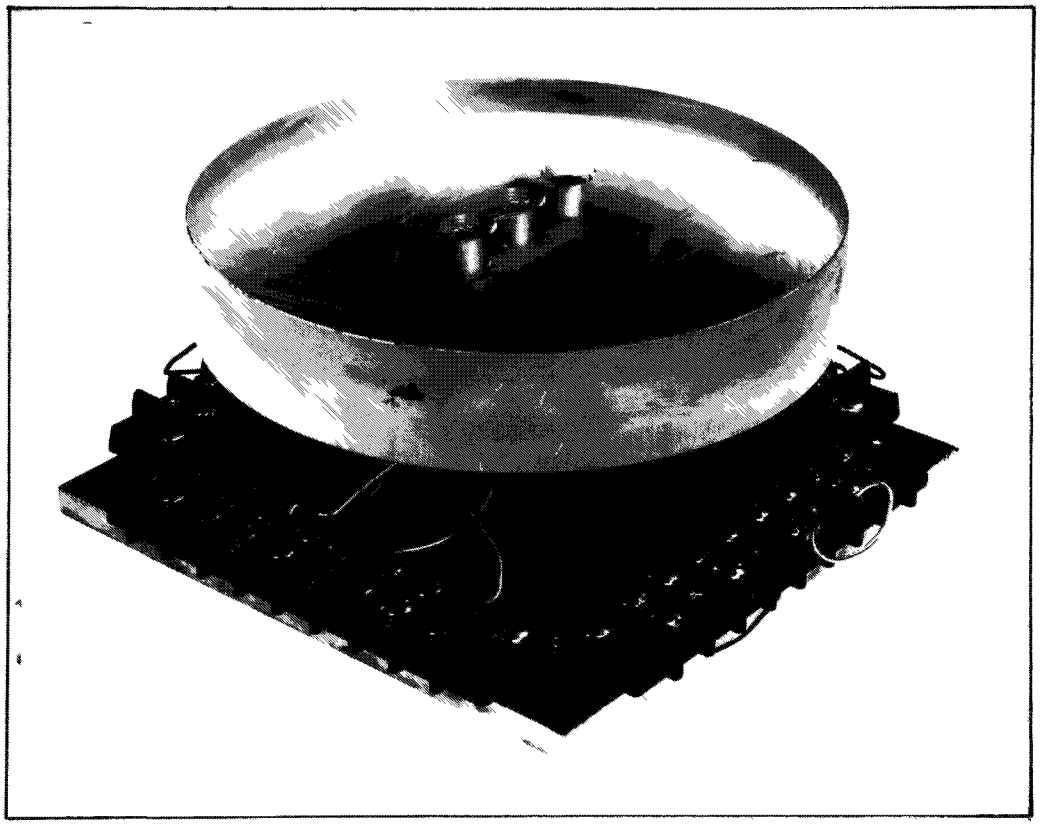

FIG. 4·5b GENERAL VIEW OF CAMBRIDGE CELL WITH FACEPLATE

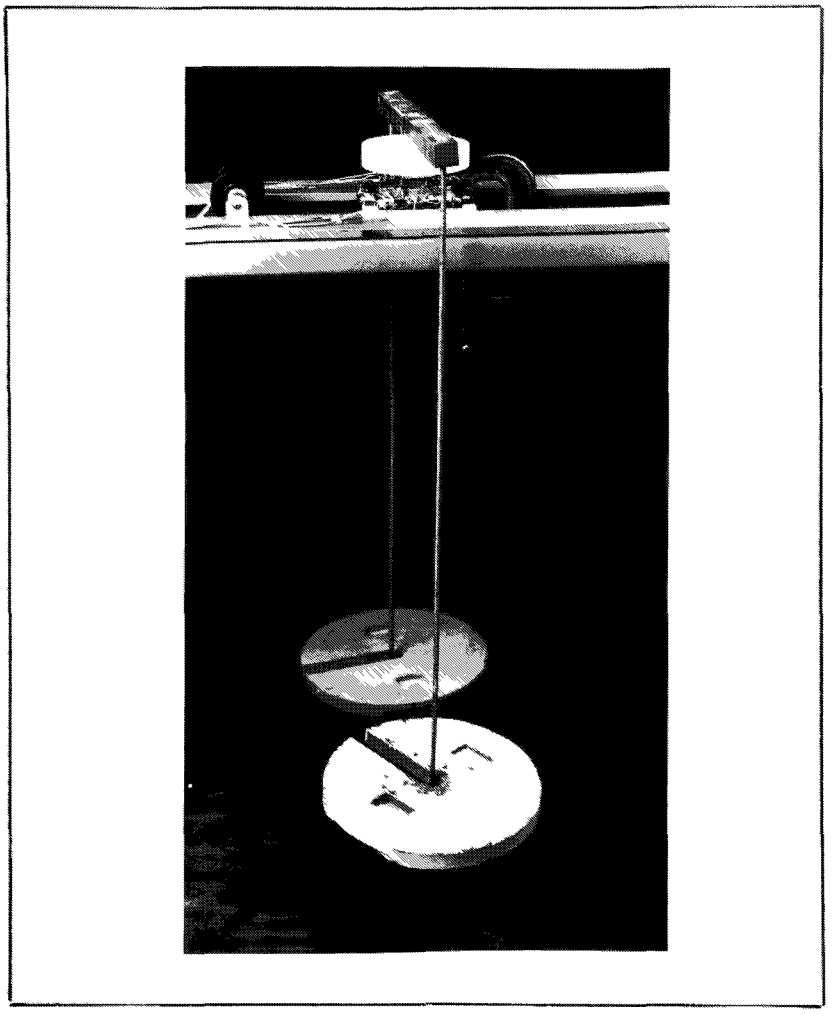

FIG.4·6 NORMAL STATIC LOAD CALIBRATION OF THE CELL

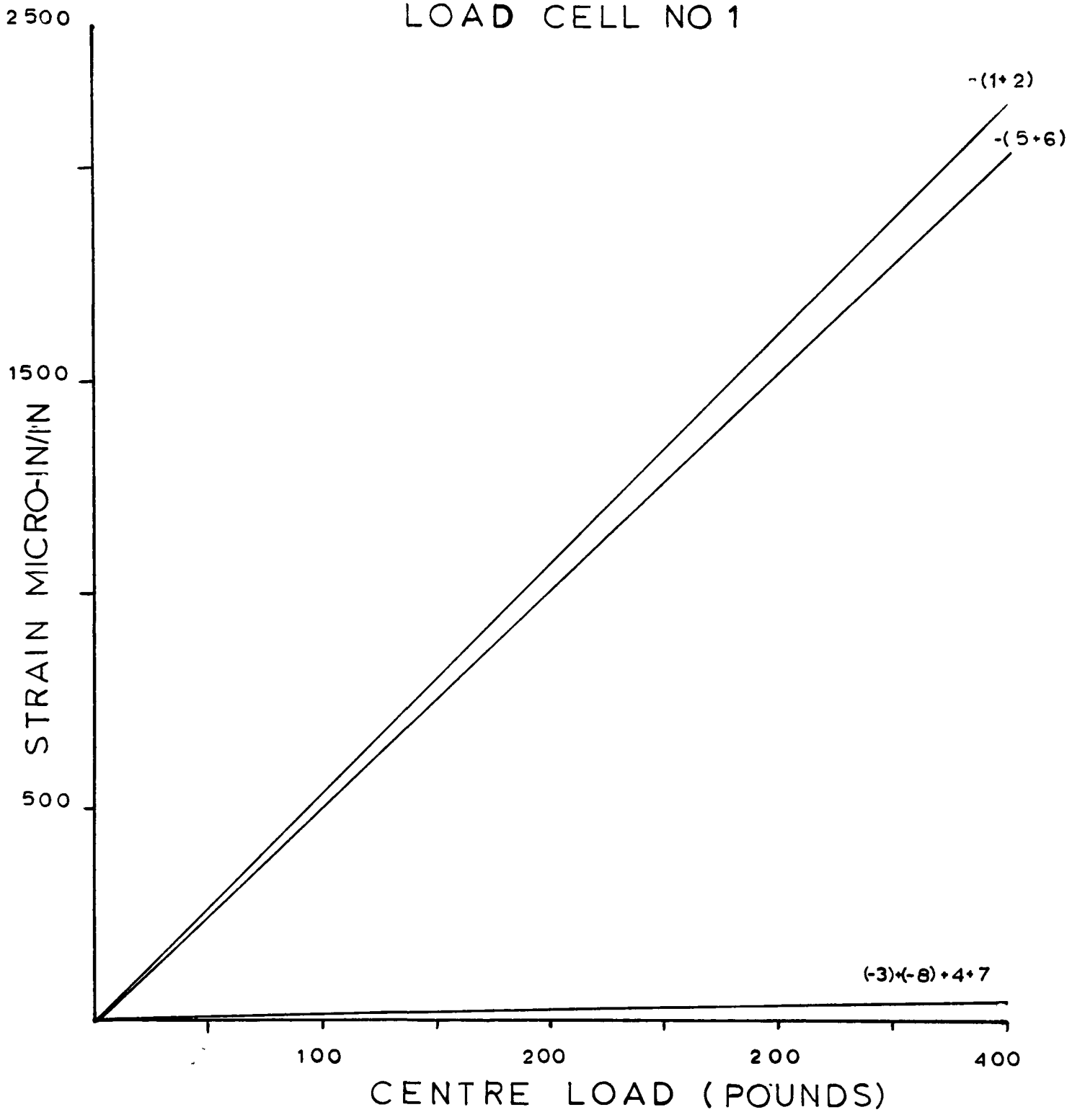

FIG. 4·7 CENTRE LOAD VS STRAIN

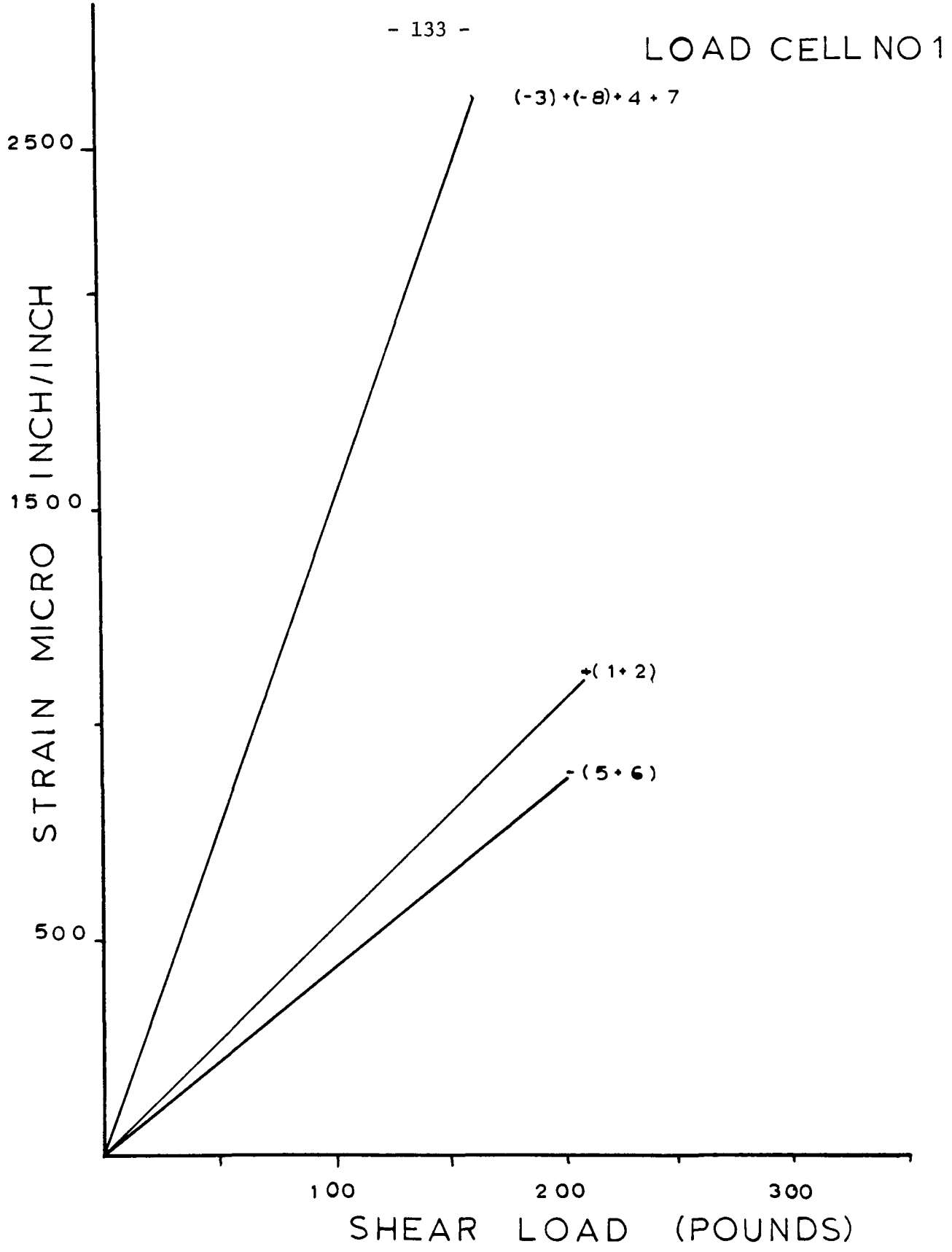

FIG. 4·8 SHEAR LOAD VS STRAIN

CELL NO 1

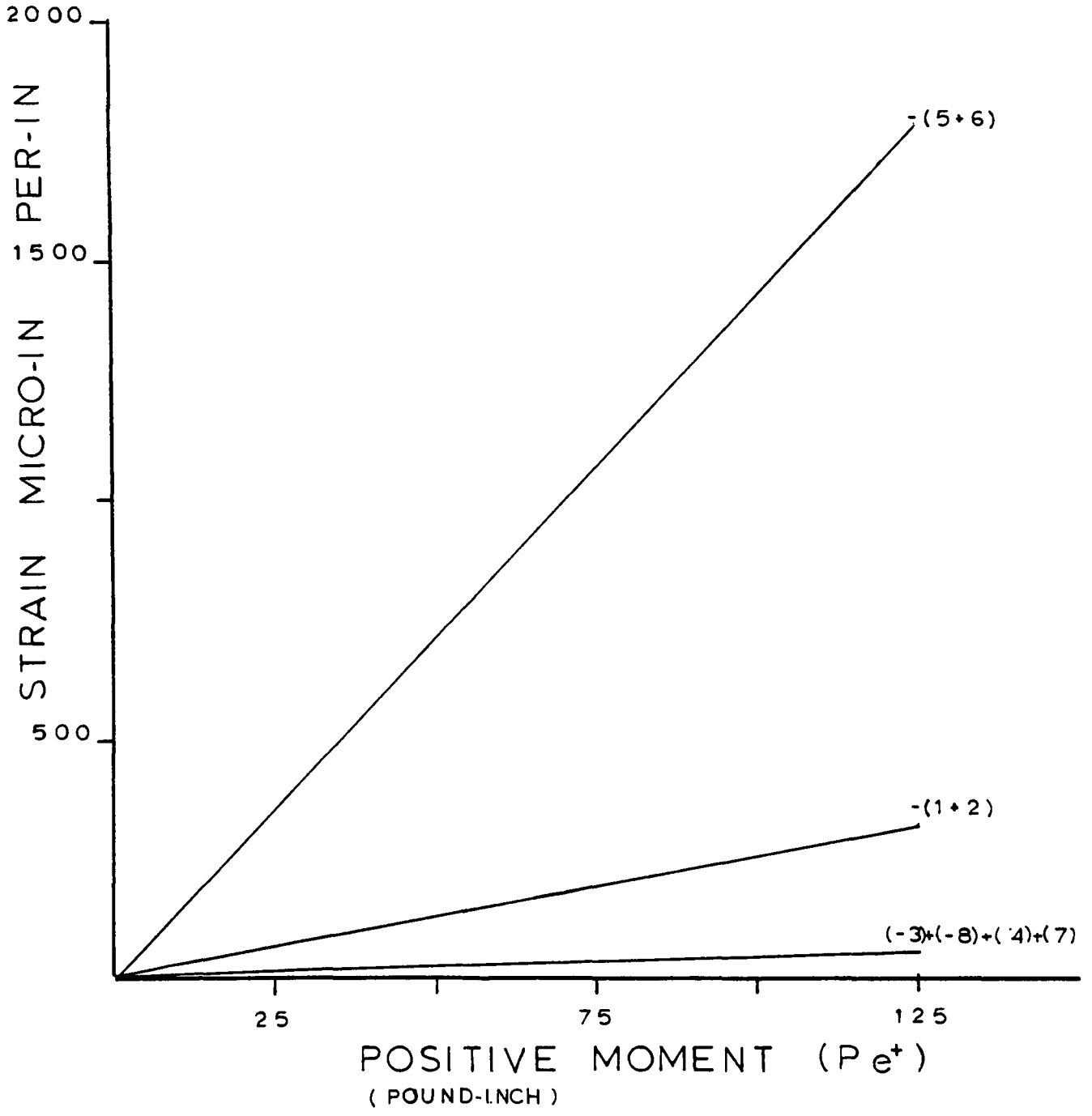

FIG 4.9 MOMENT VS STRAIN

CELL NO 1

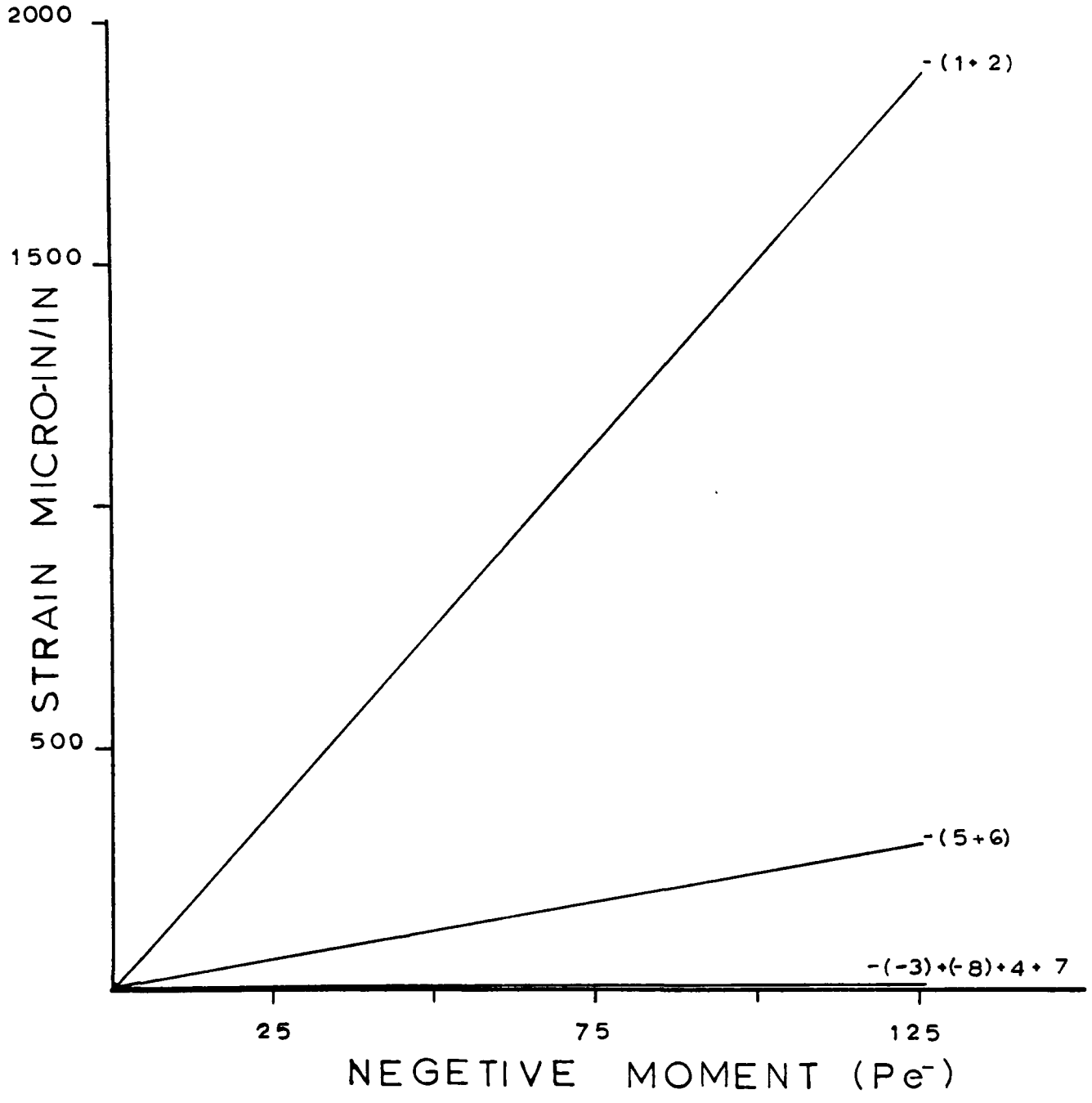

FIG. 4·10 MOMENT VS STRAIN

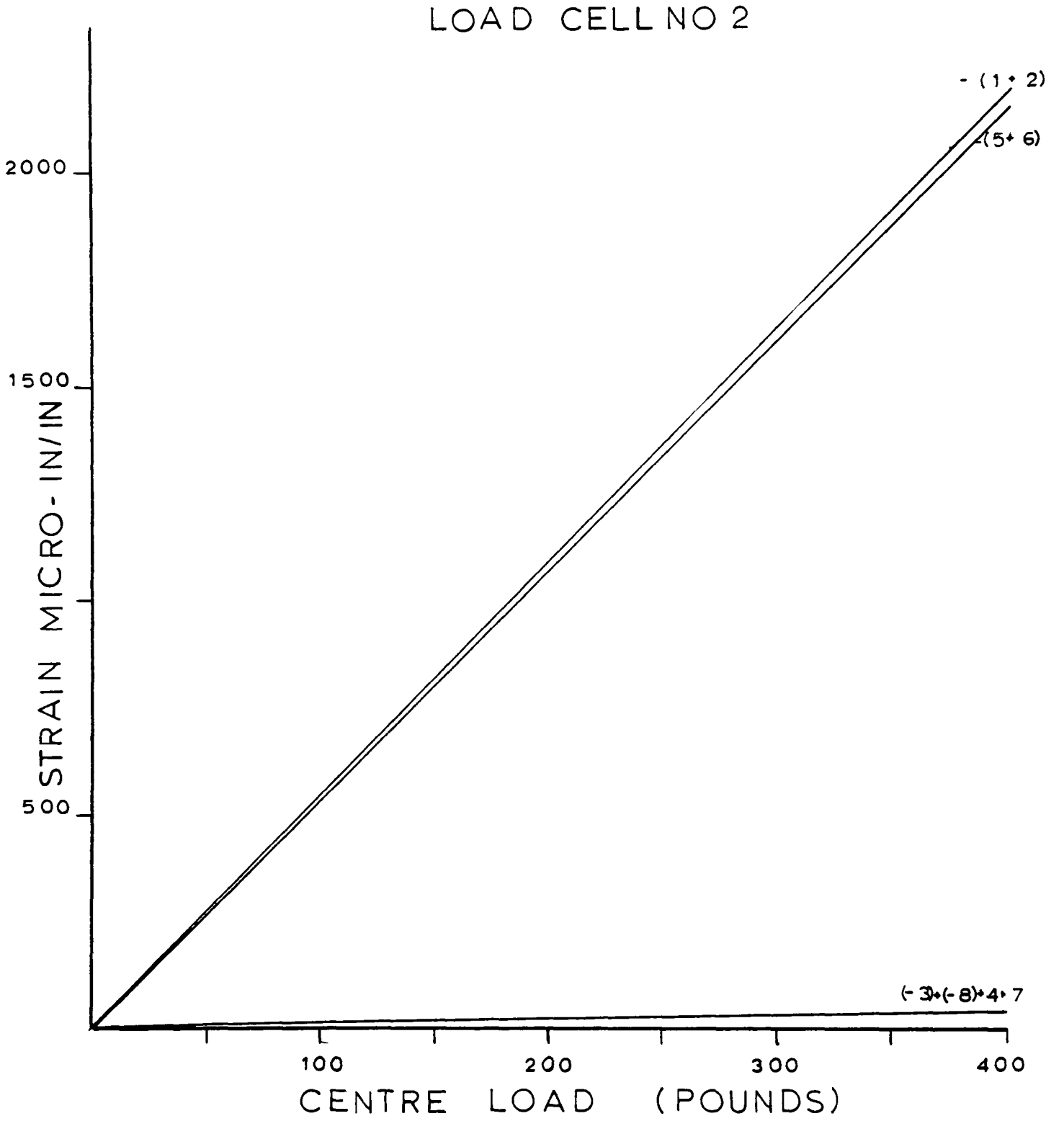

FIG 4.11 CENTRE LOAD VS STRAIN

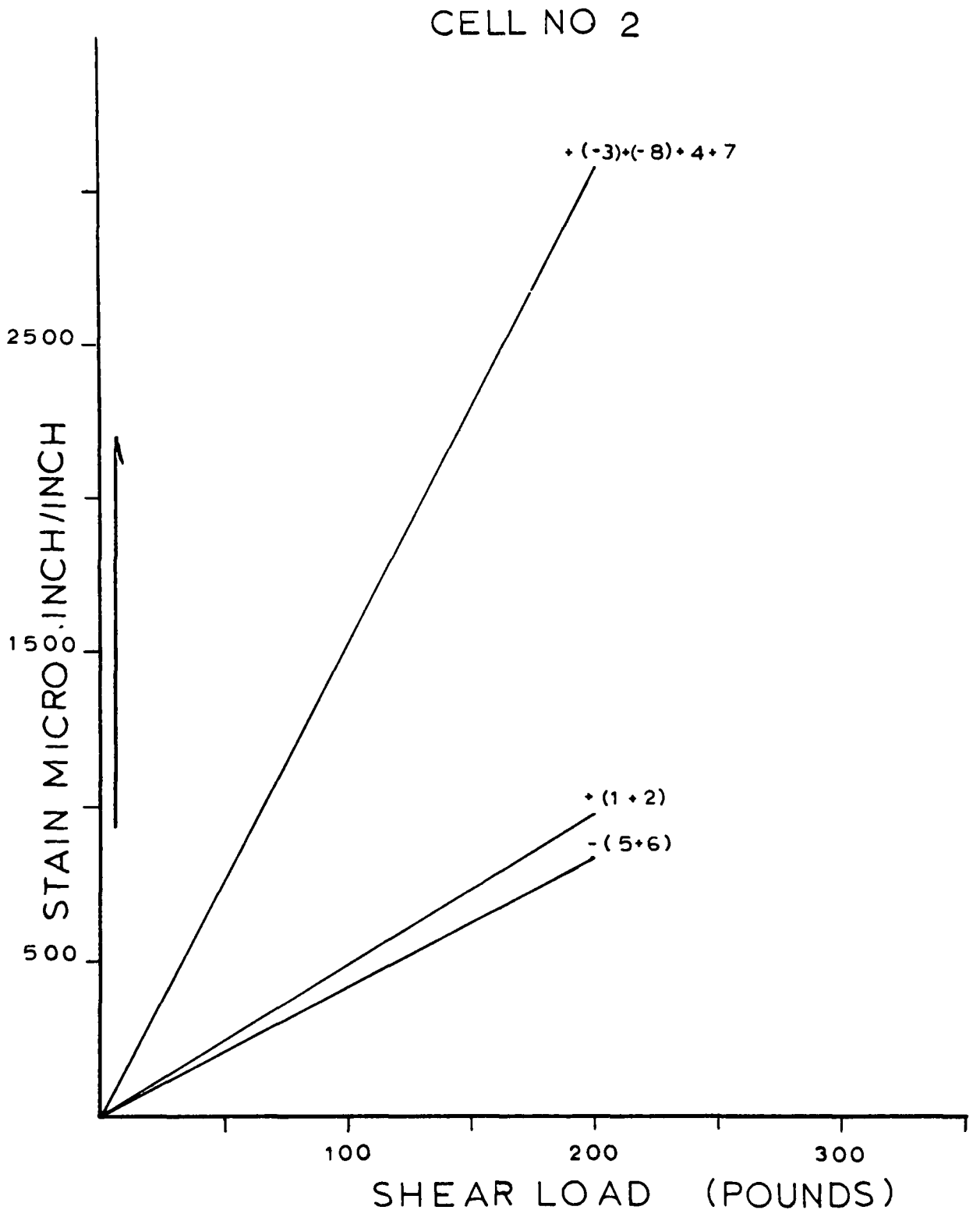

FIG.4.12 SHEAR LOAD VS STRAIN

CELL NO 2

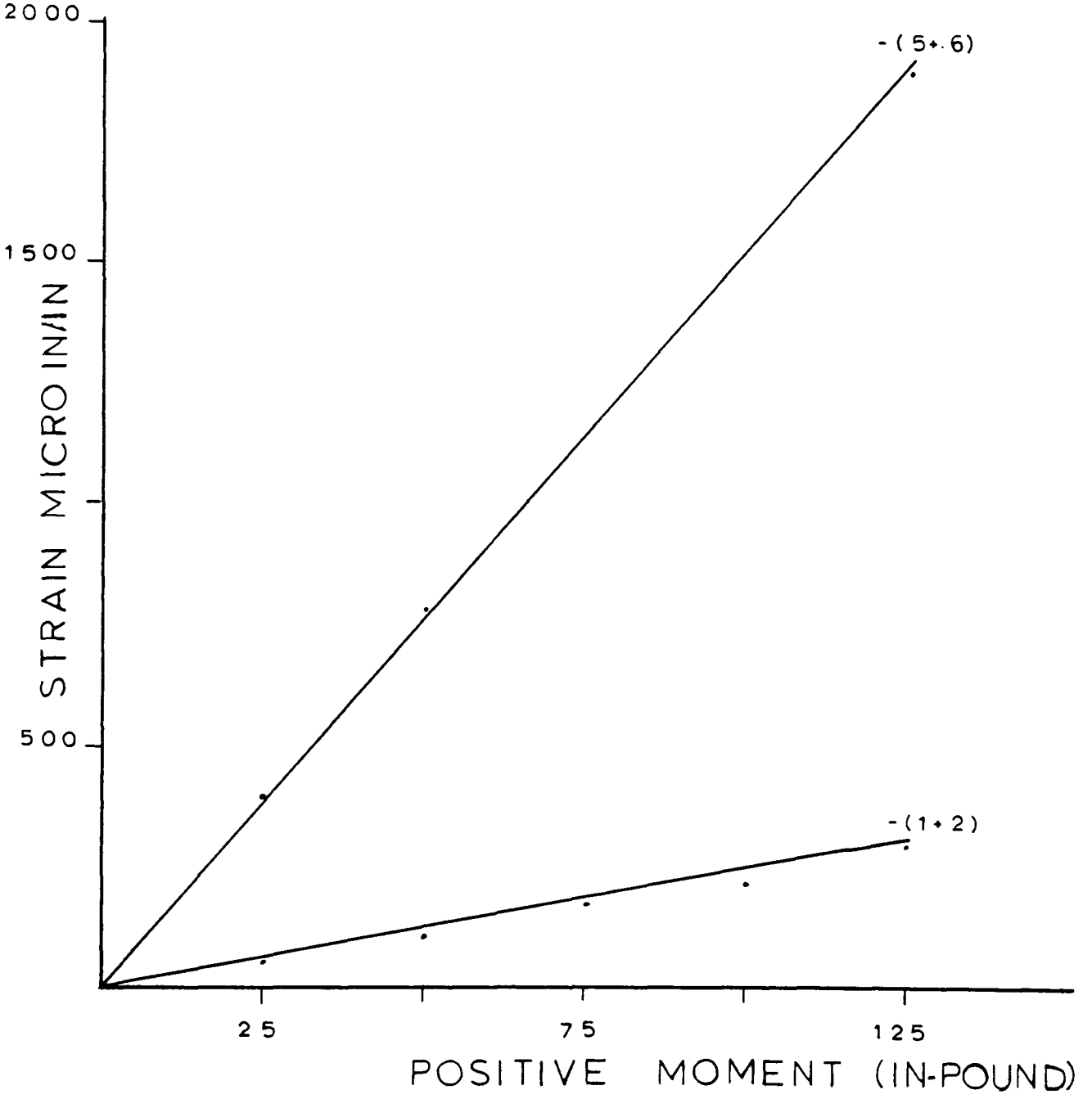

FIG 4.13 MOMENT VS STRAIN

CELL NO 2

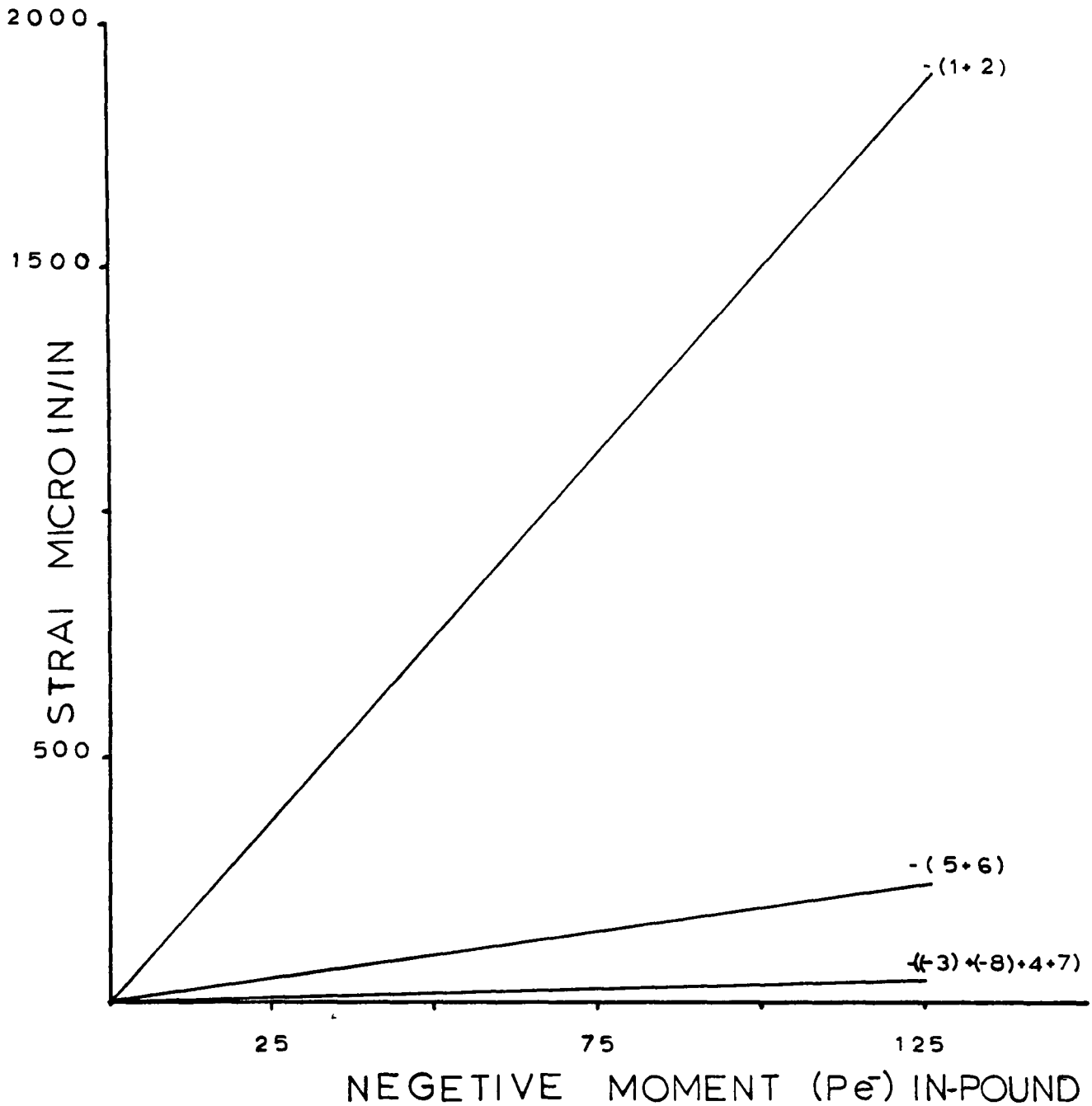

FIG 4.14 MOMENT VS STRAIN

CELL NO 3

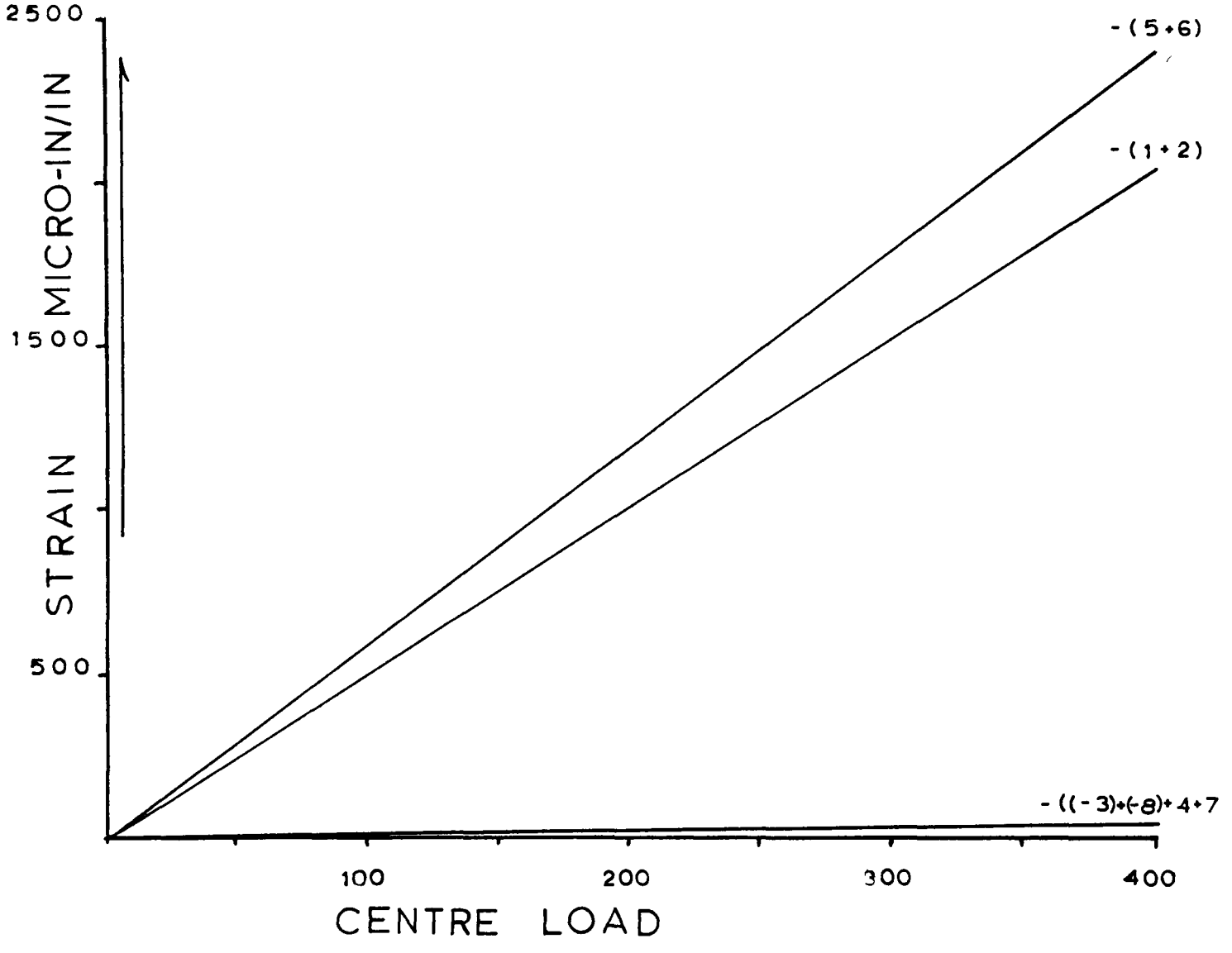

FIG. 4.15 CENTRAL LOAD VS STRAIN

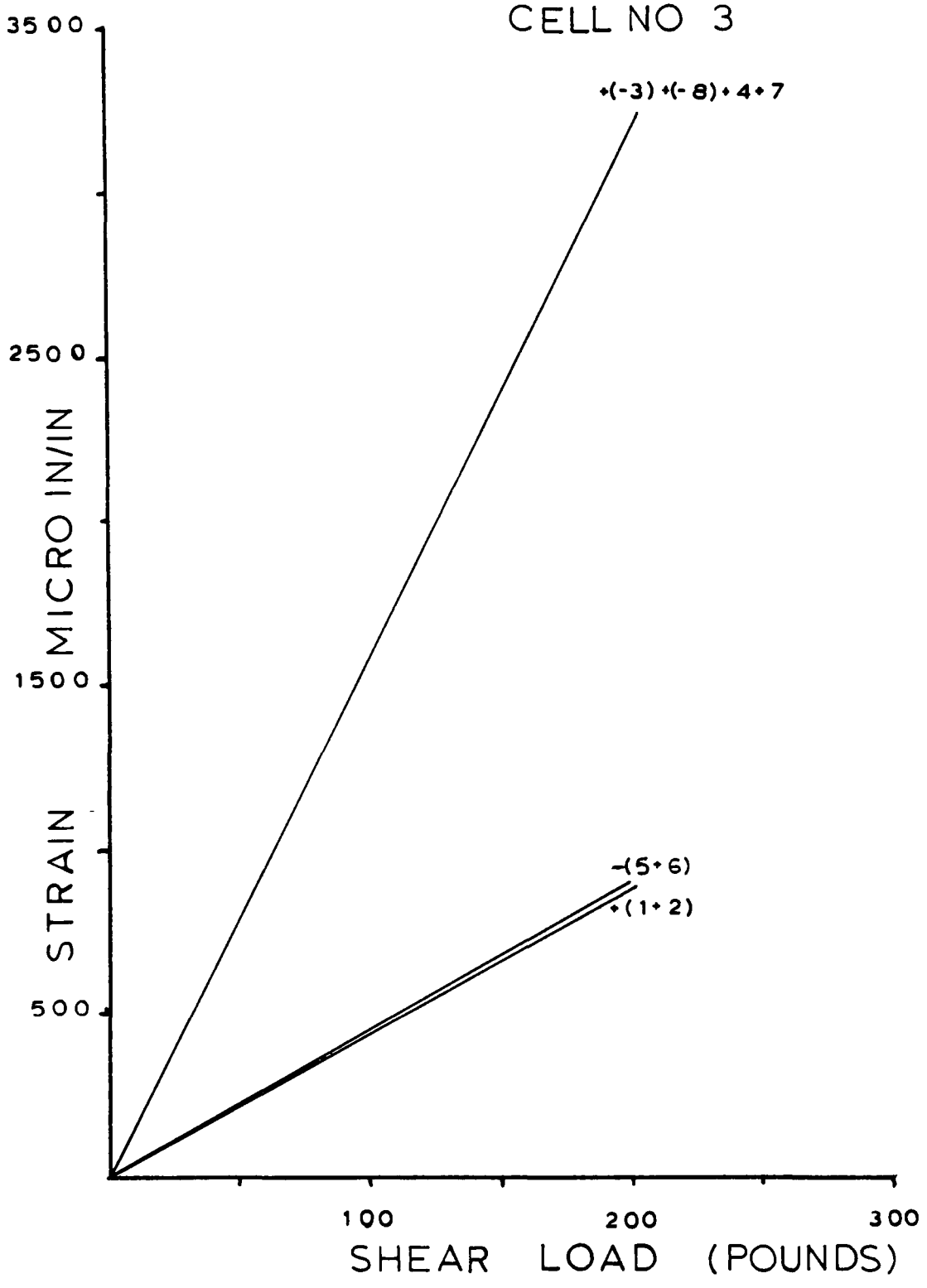

FIG.4.16 SHEAR LOAD VS STRAIN

CELL NO 3

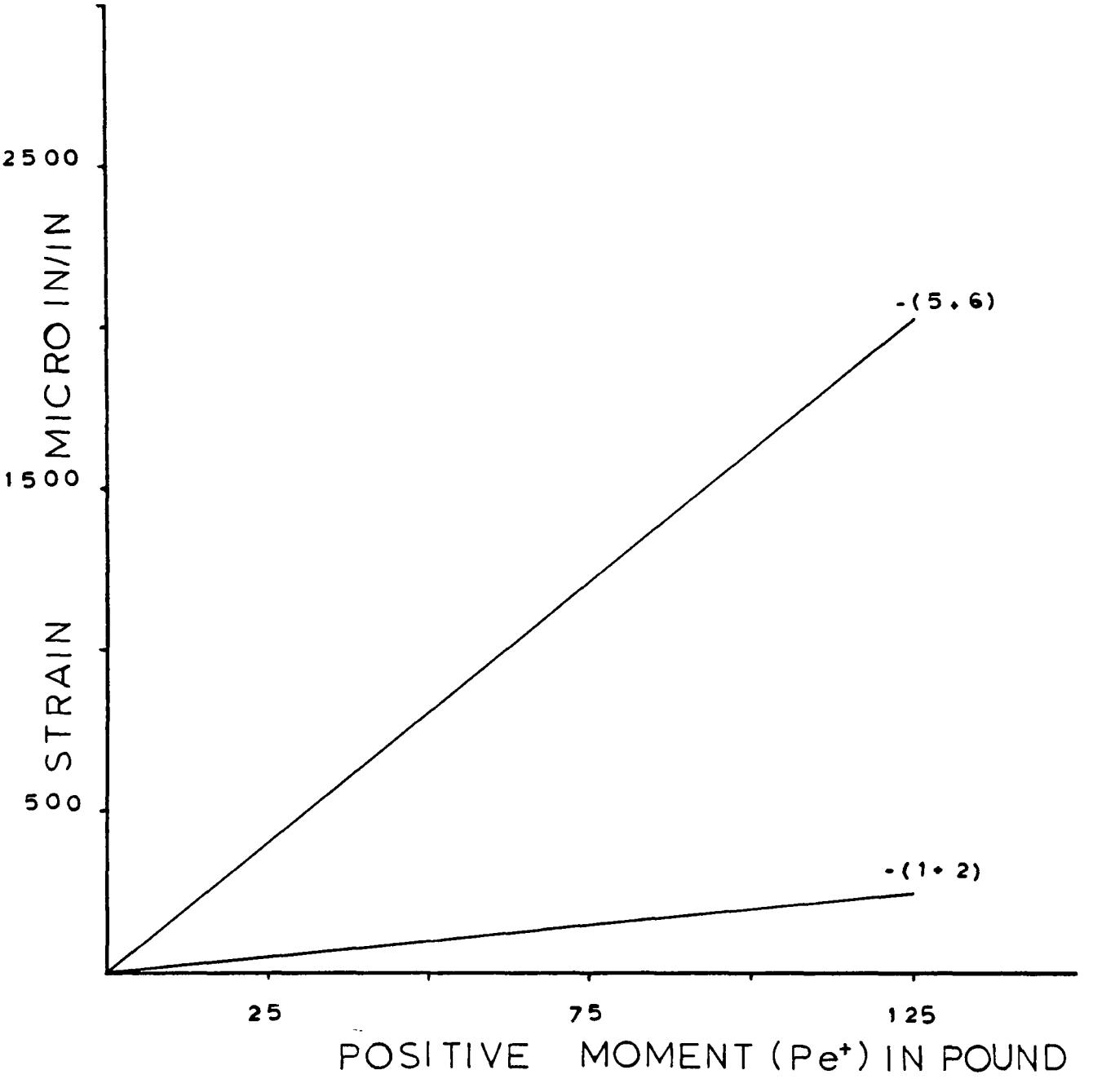

FIG. 4.17 MOMENT VS STRAIN

CELL NO 3

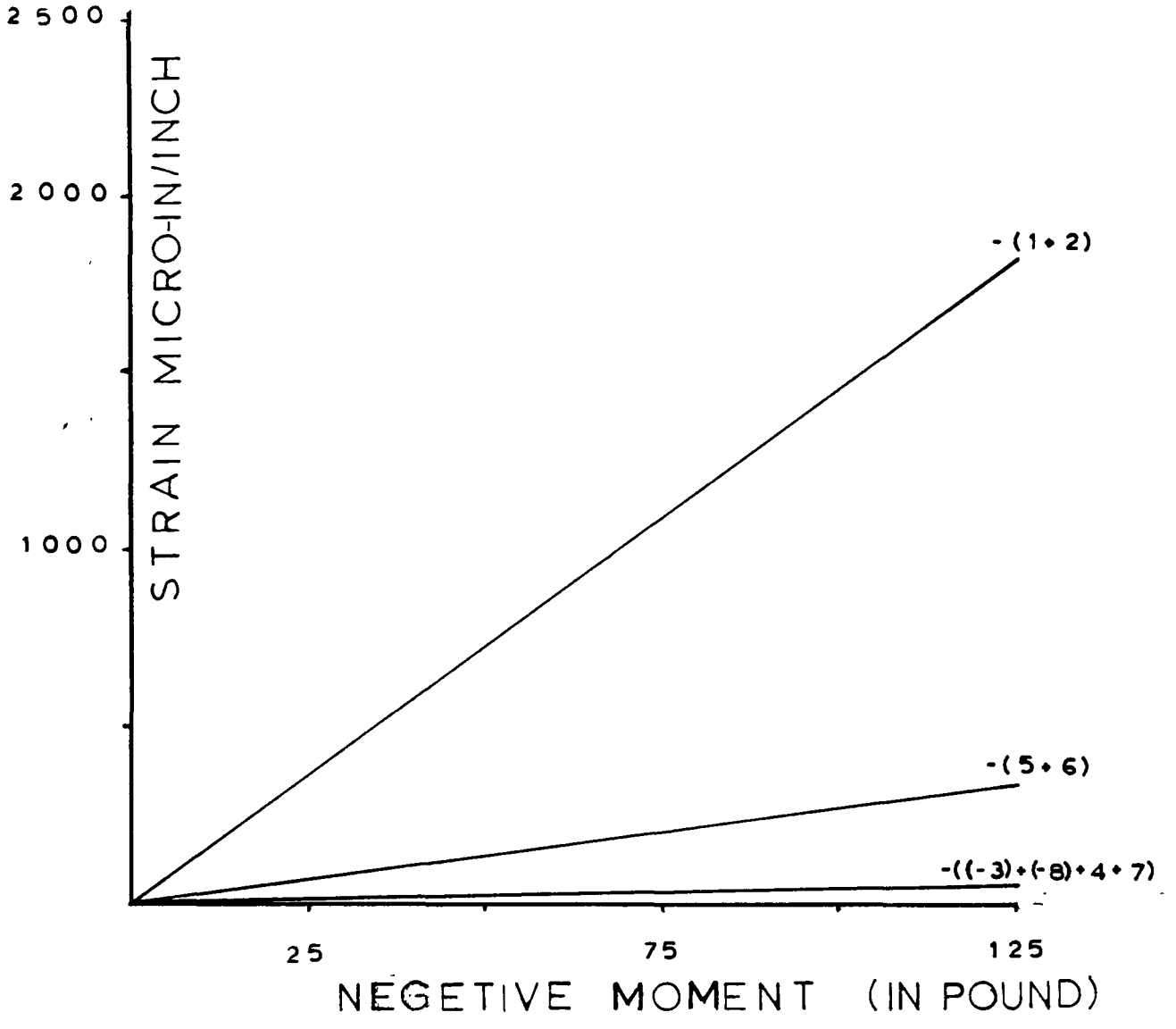

FIG.4.18 MOMENT VS STRAIN

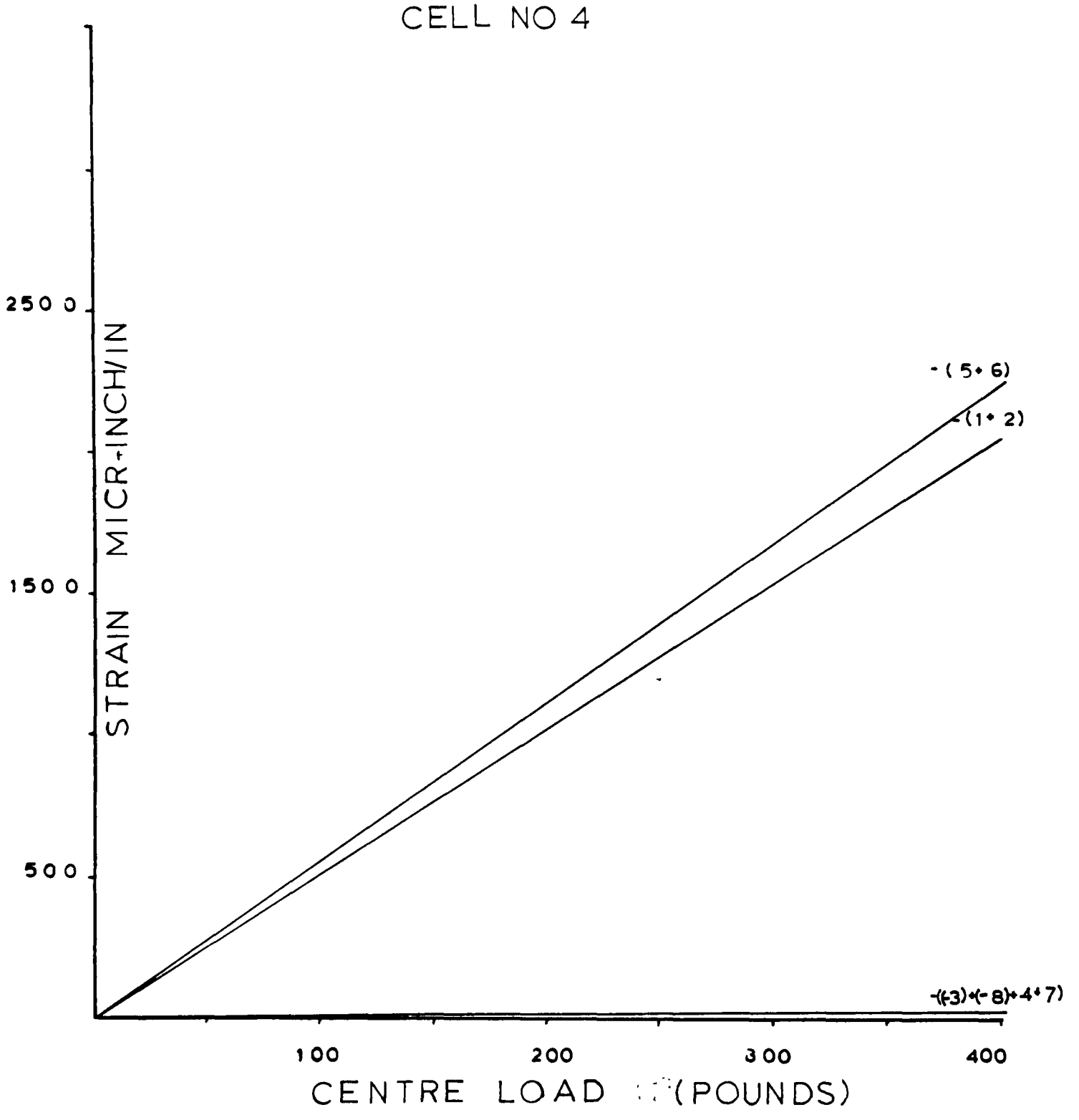

FIG 4.19 CENTRE LOAD VS STRAIN

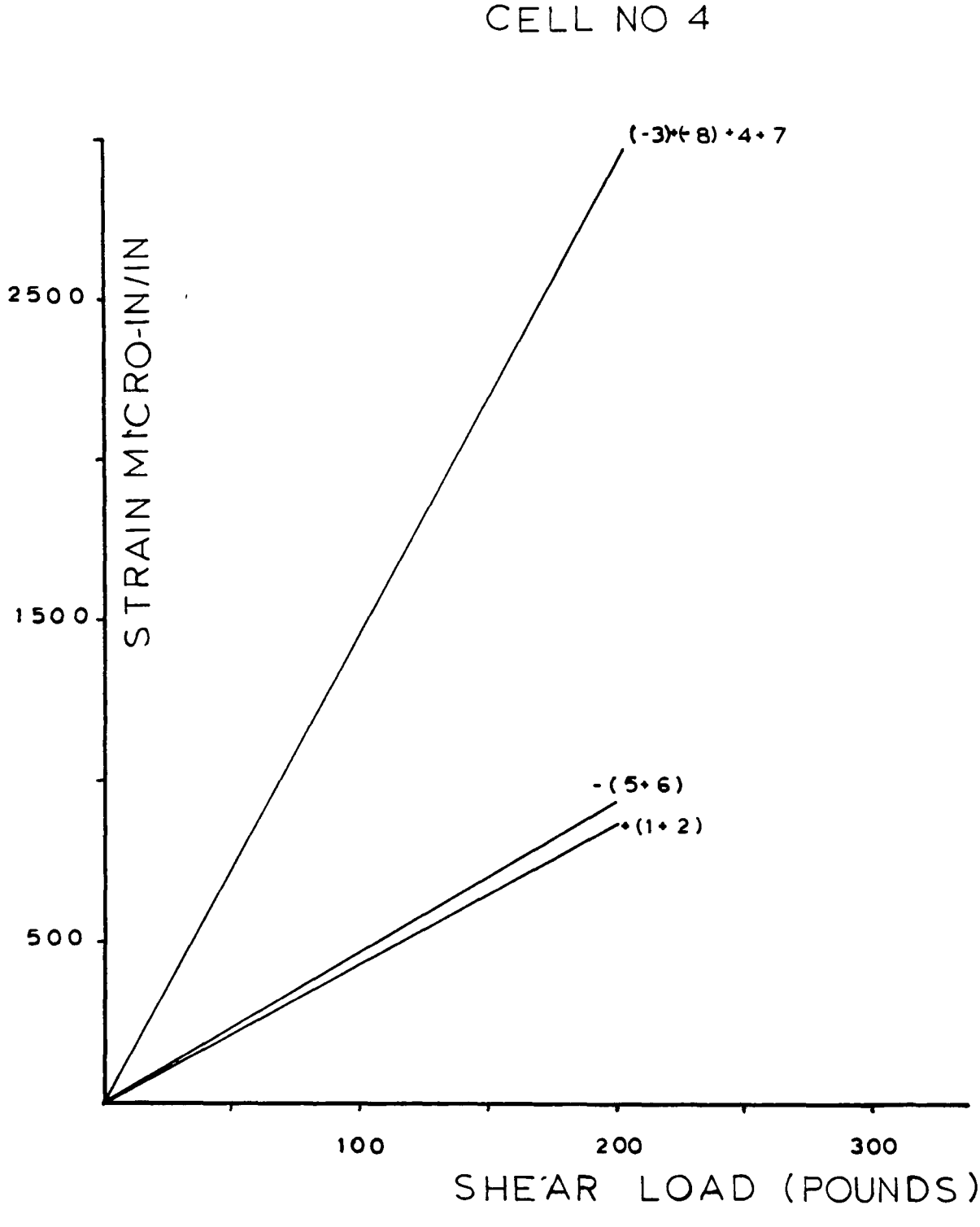

FIG 4.20 SHEAR LOAD VS STRAIN

CELL NO 4

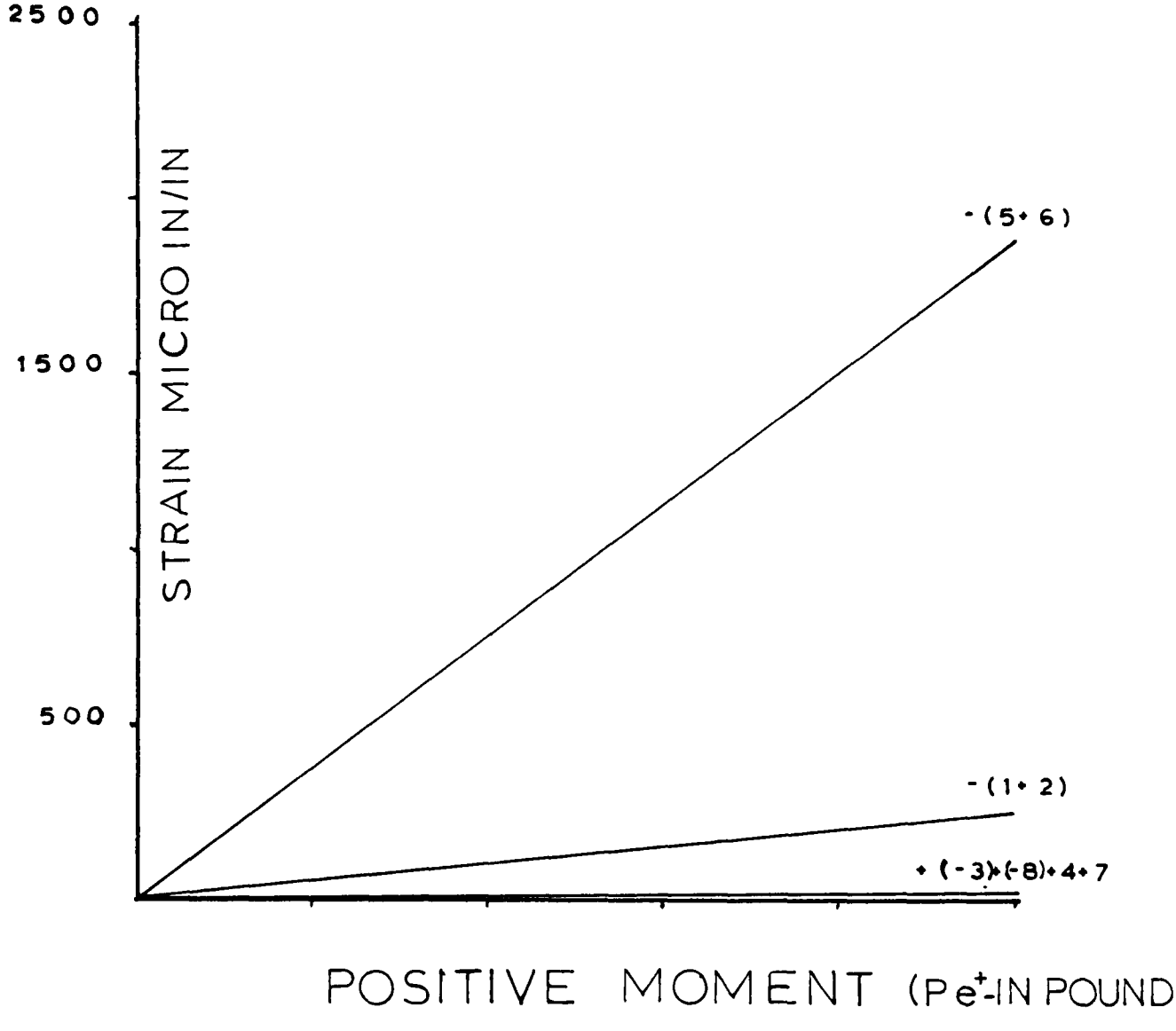

FIG.4.21 MOMENT VS STRAIN

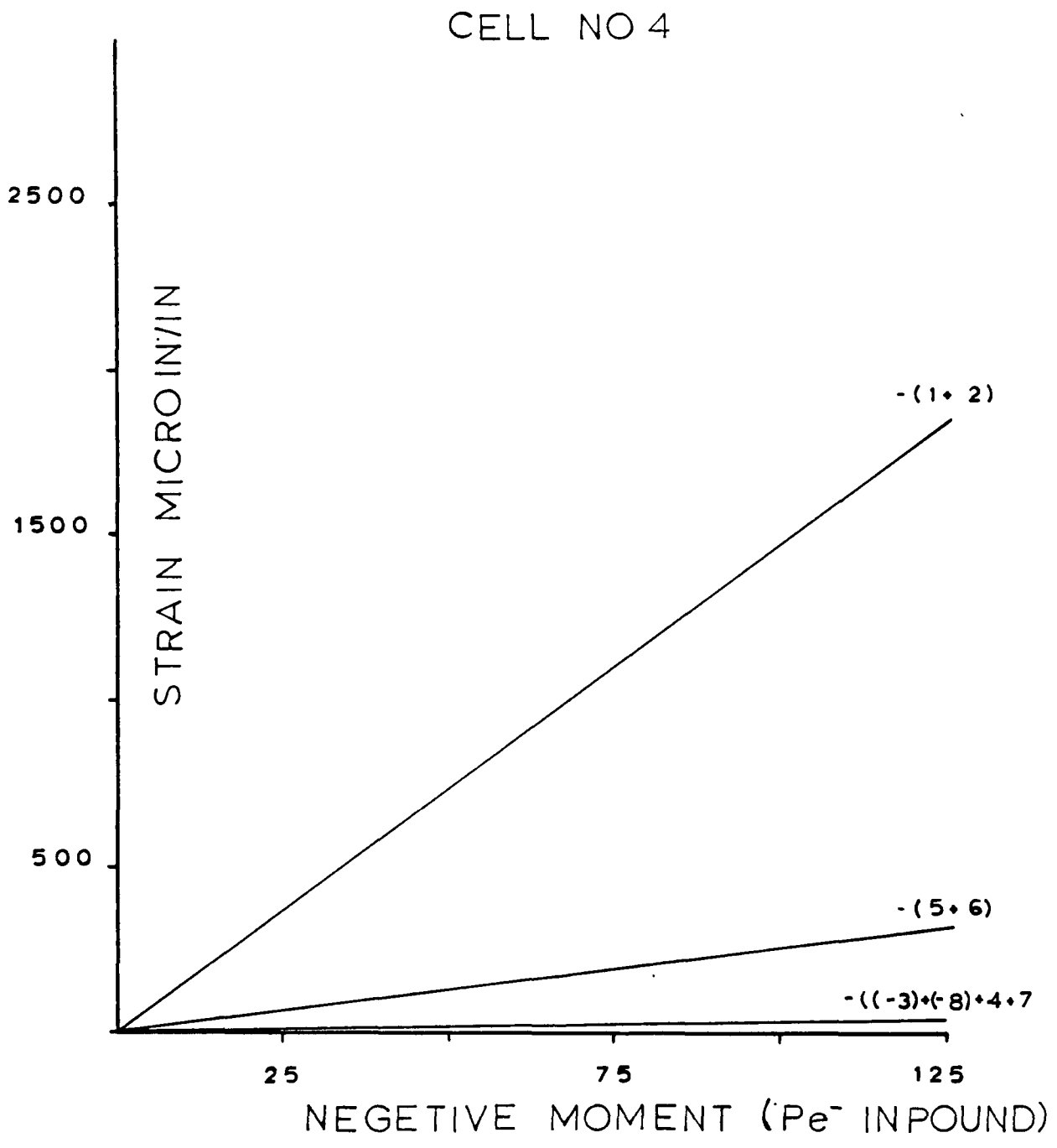

FIG.4.22 MOMENT VS STRAIN

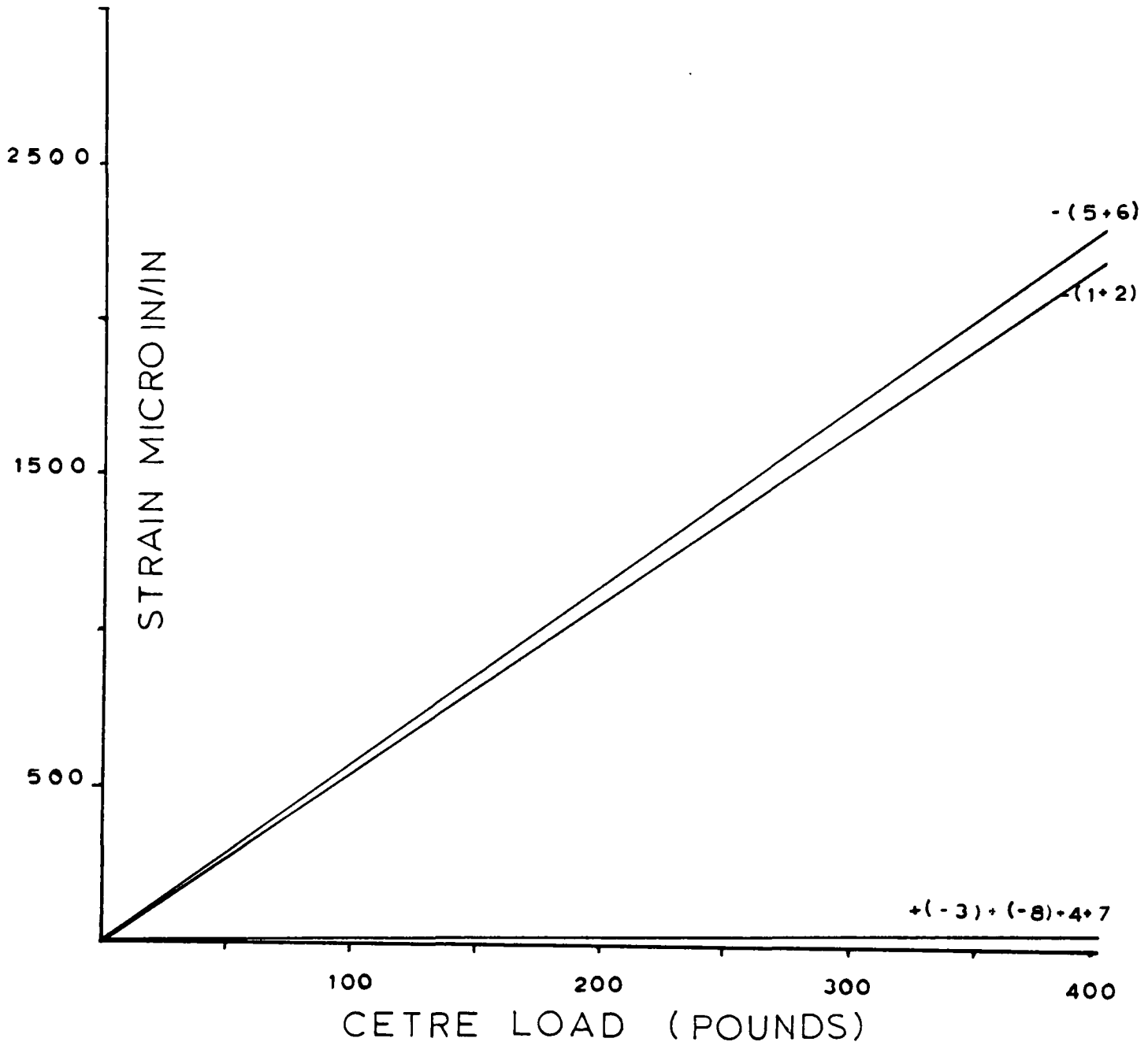

FIG.4.23 NORMAL LOAD VS STRAIN

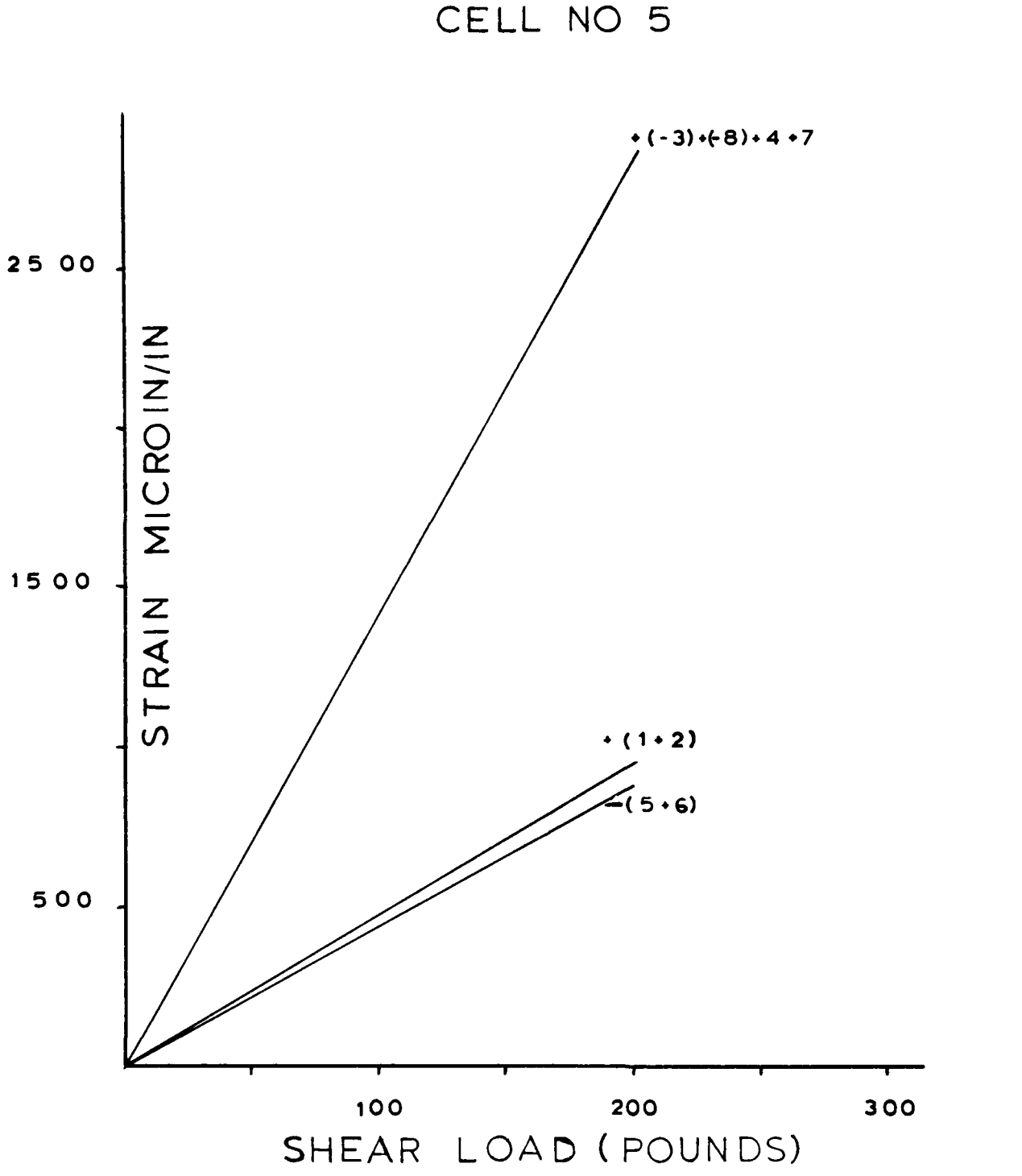

FIG. 4.24 SHEAR LOAD VS STRAIN

CELL NO 5

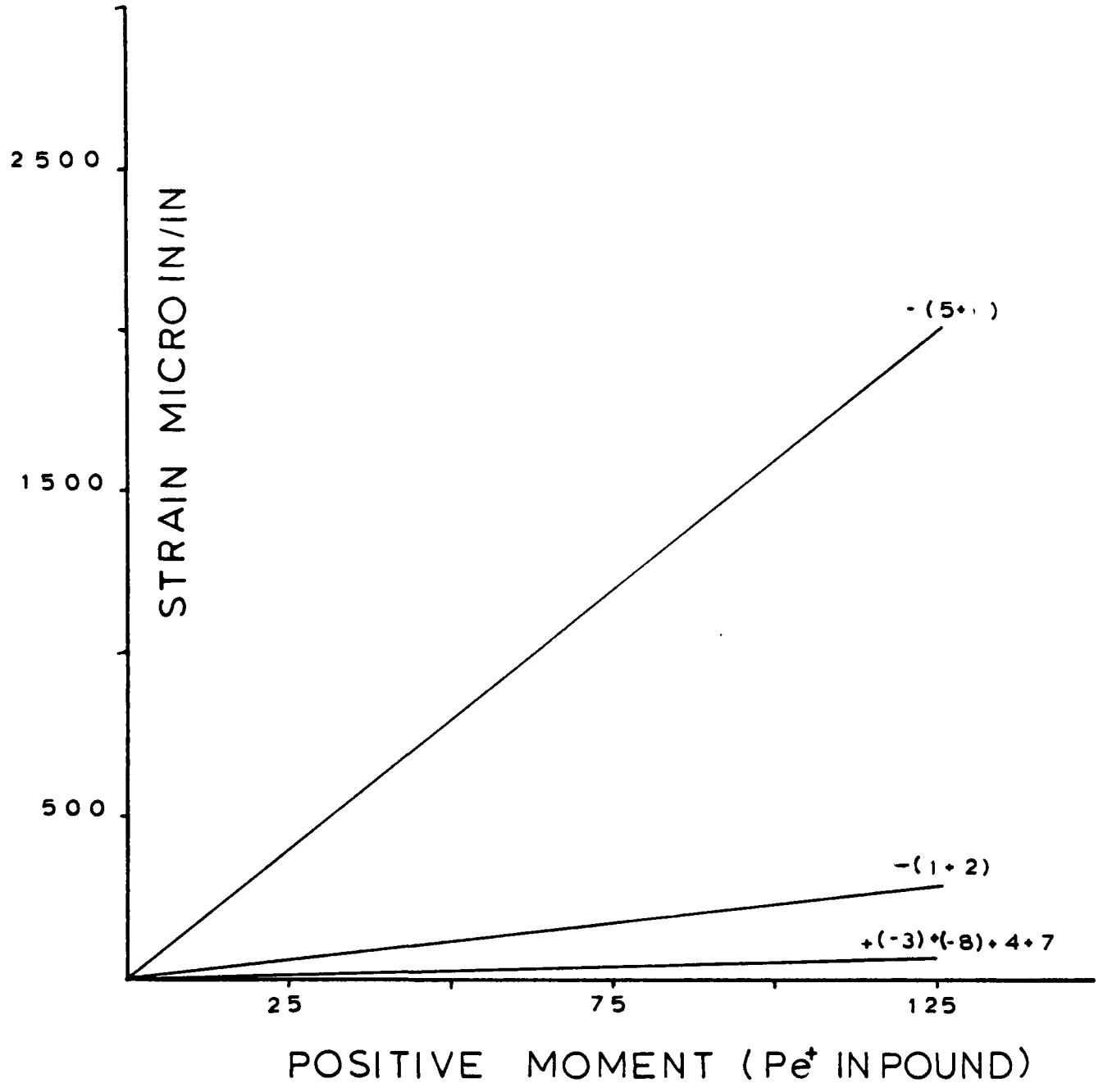

FIG 4.25 MOMENT VS STRAIN

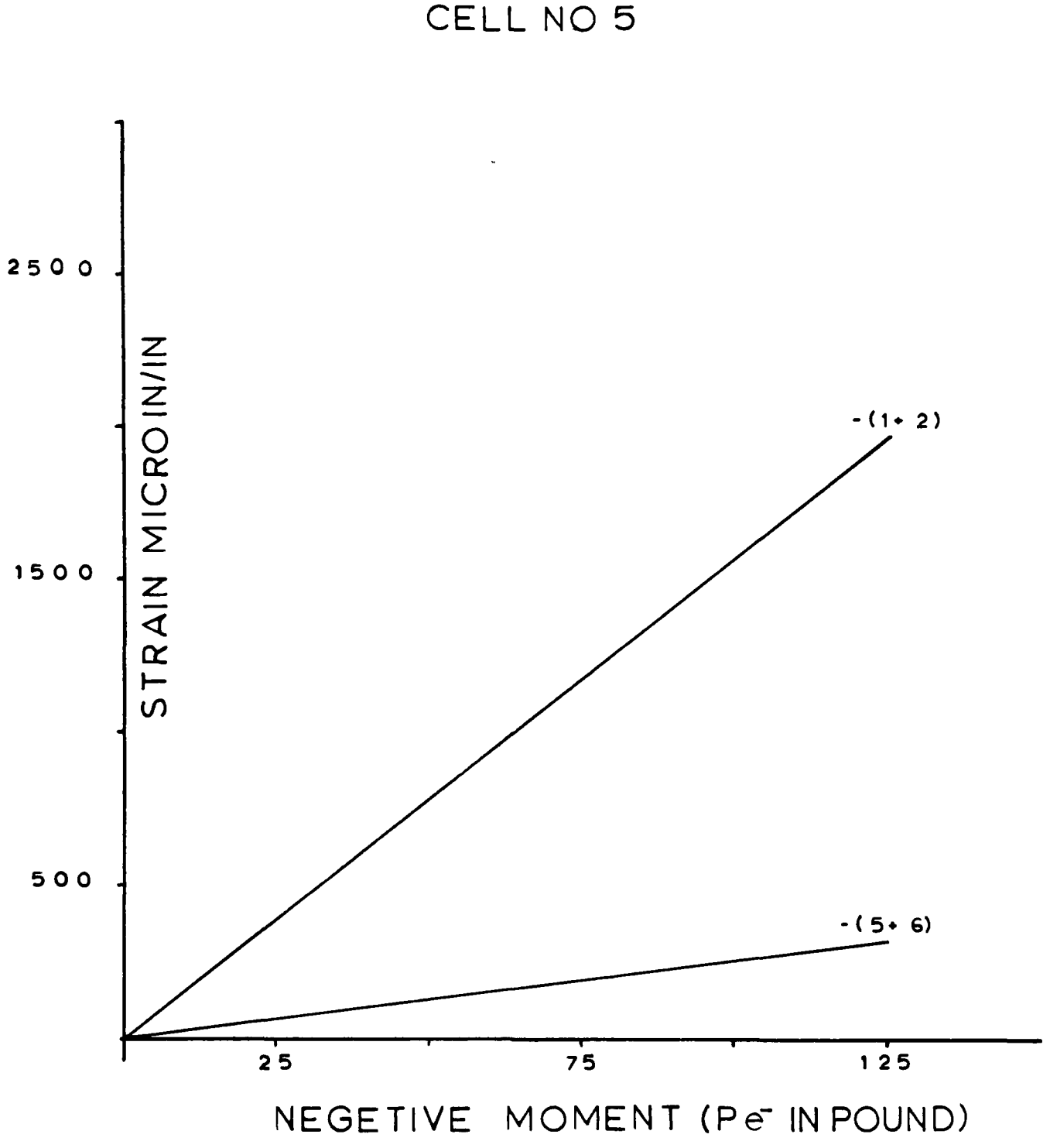

FIG. 4·26 MOMENT VS STRAIN

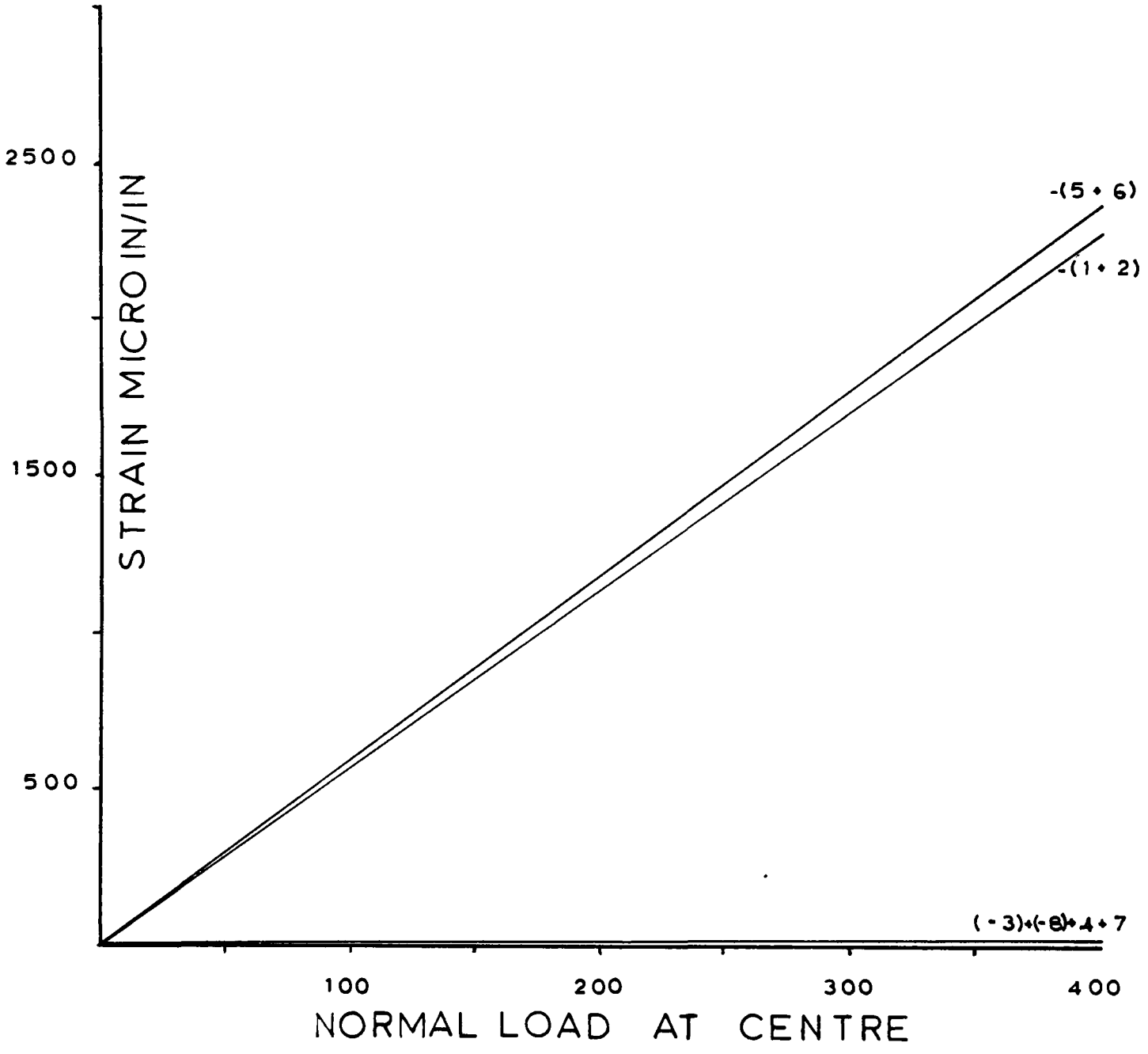

FIG.4.27 NORMAL LOAD VS STRAIN

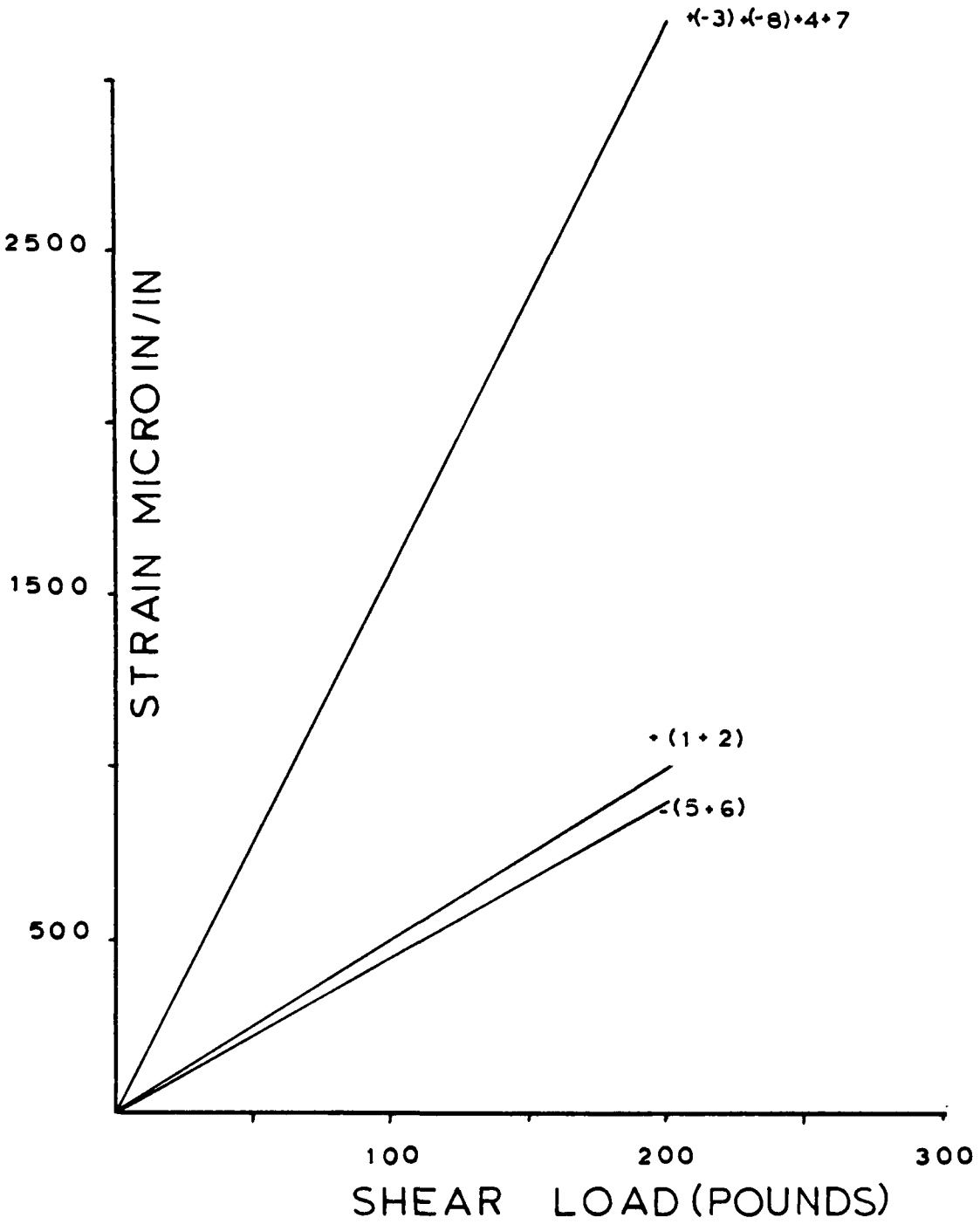

FIG.4.28 SHEAR LOAD VS STRAIN

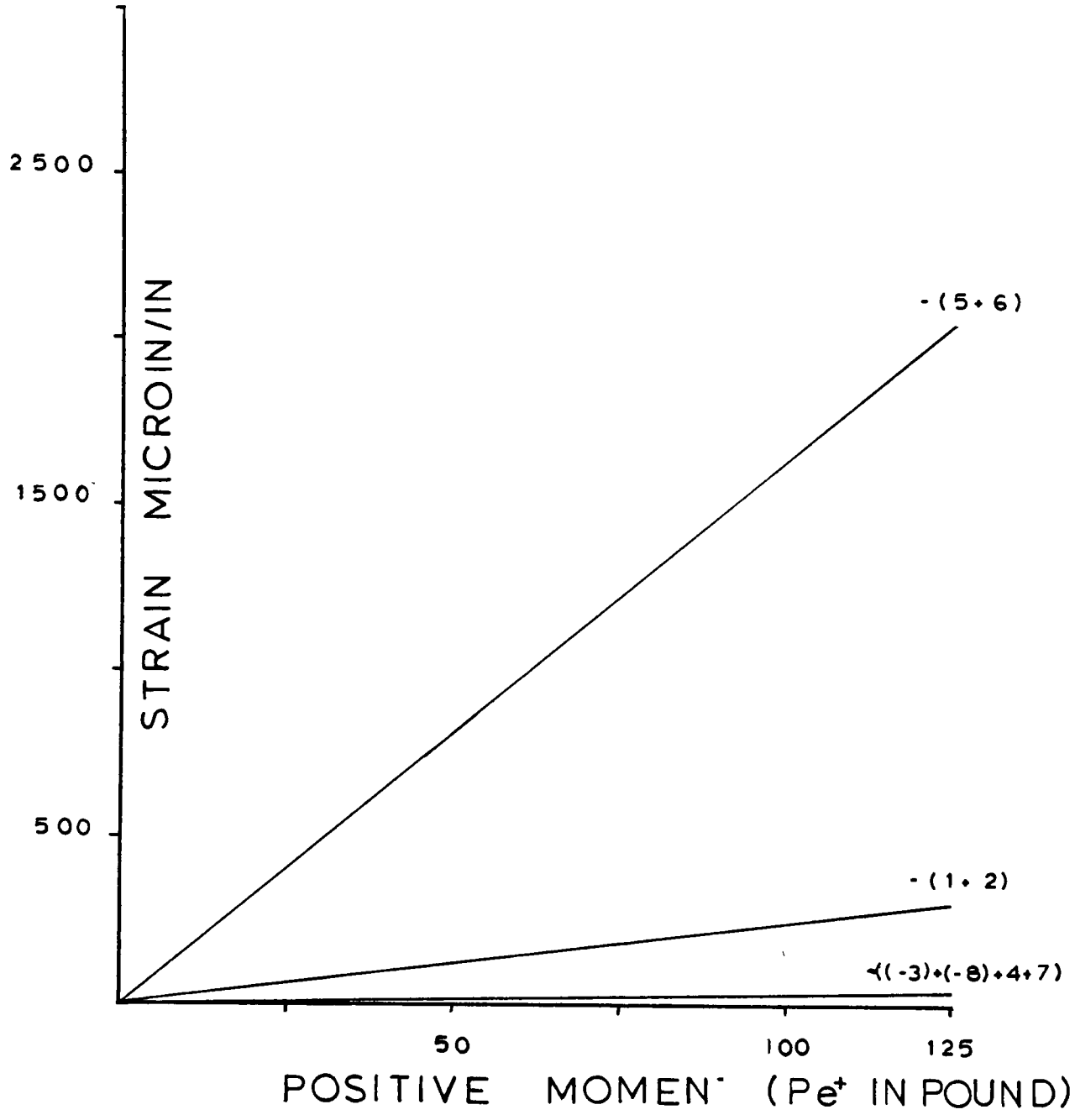

FIG.4.29 MOMENT VS STRAIN

CELL NO 6

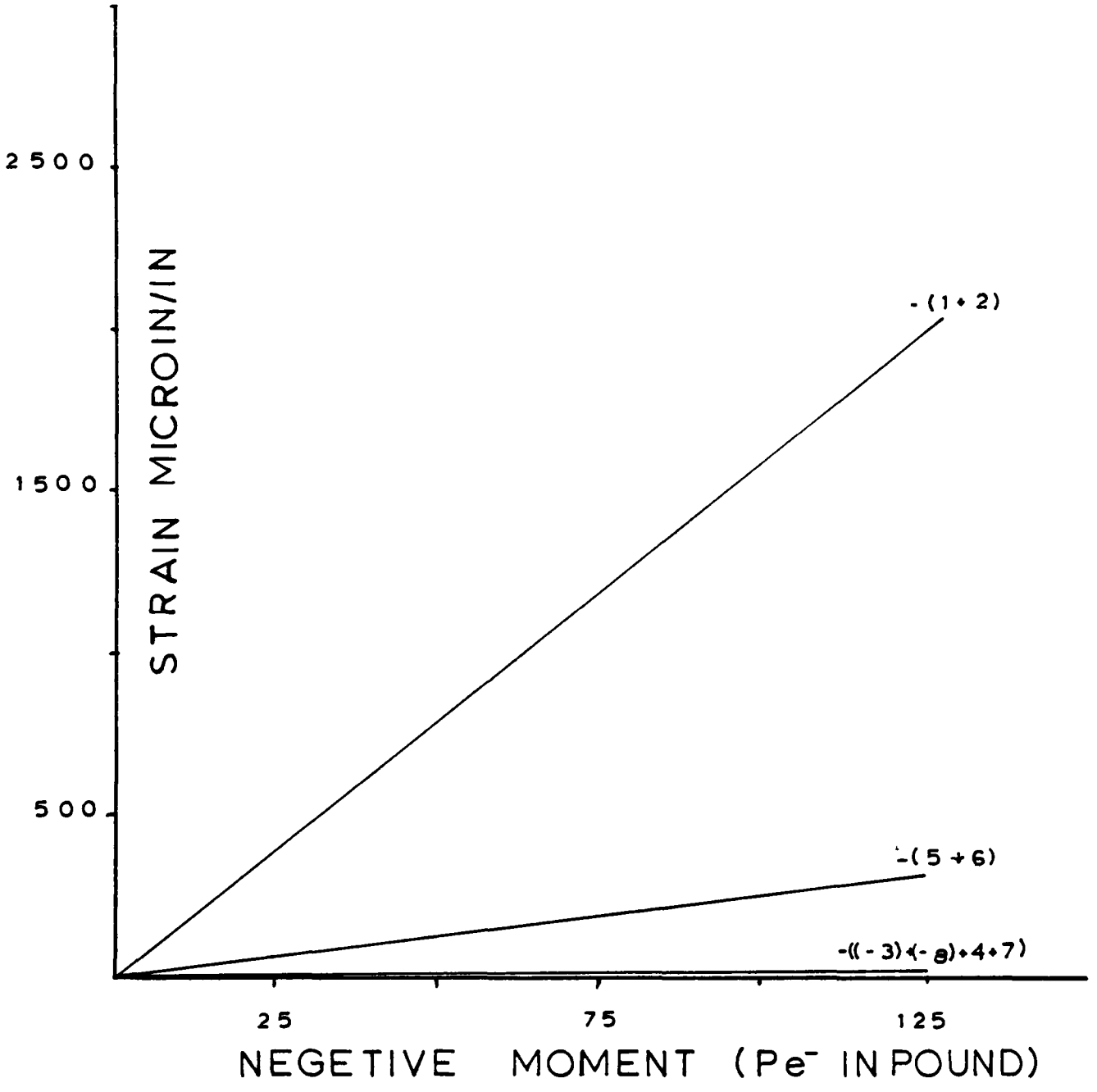

FIG.4.30 MOMENT VS STRAIN

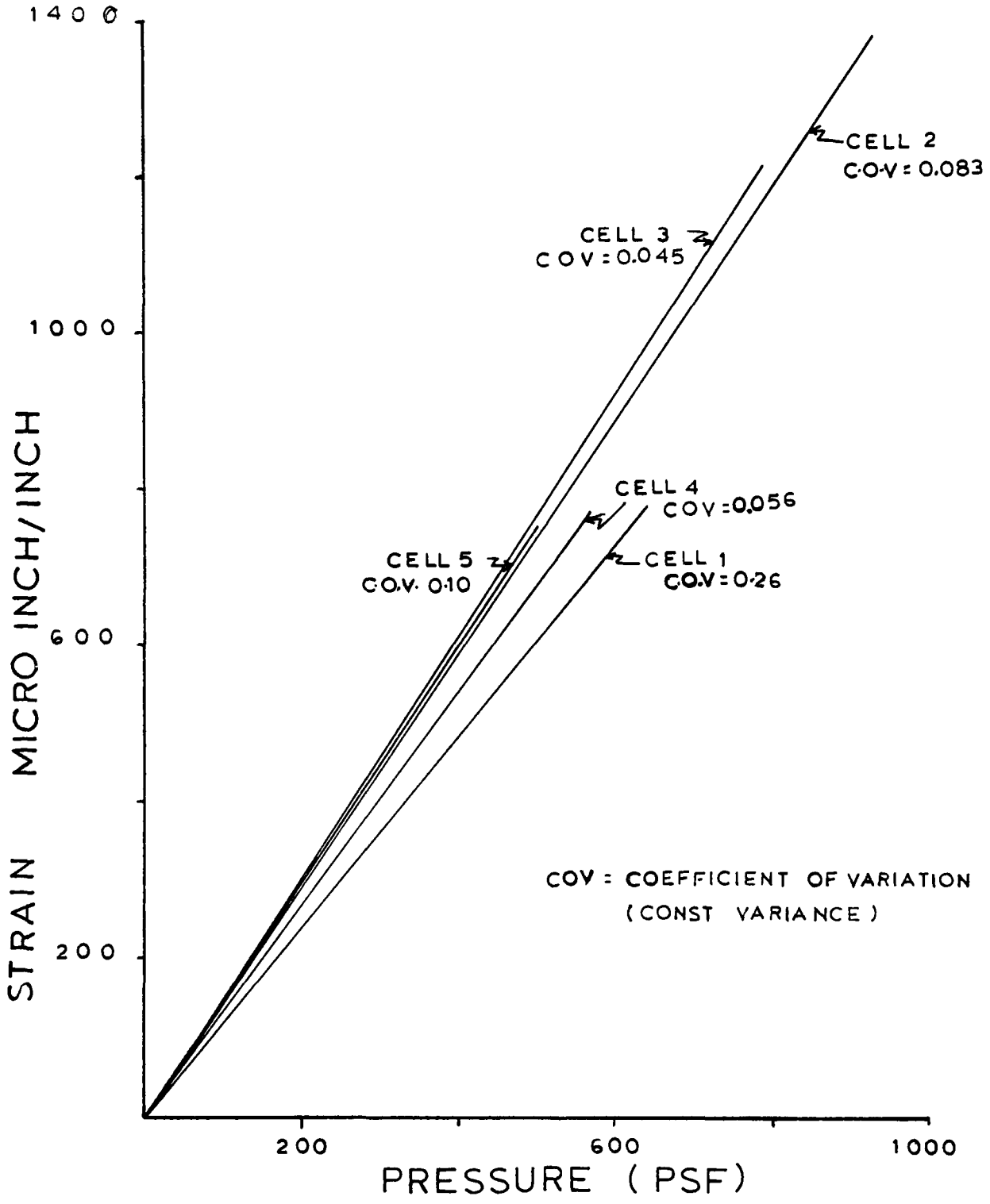

FIG. 4 31 WATER CALIBRATION OF LOAD CELLS (72°F)

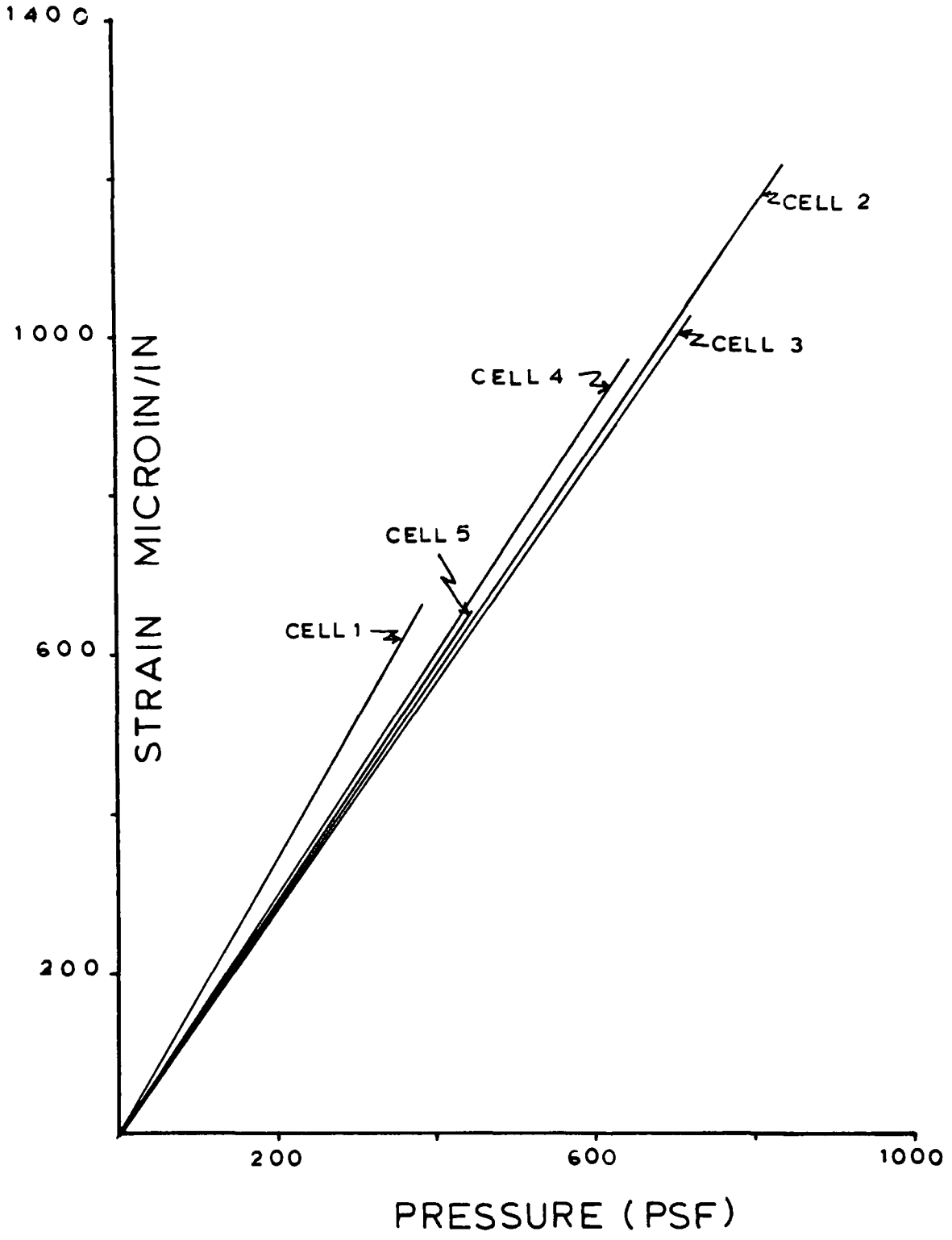

FIG. 4·32 CALIBRATION OF LOAD CELLS WITH STATIC LOAD CONSTANTS

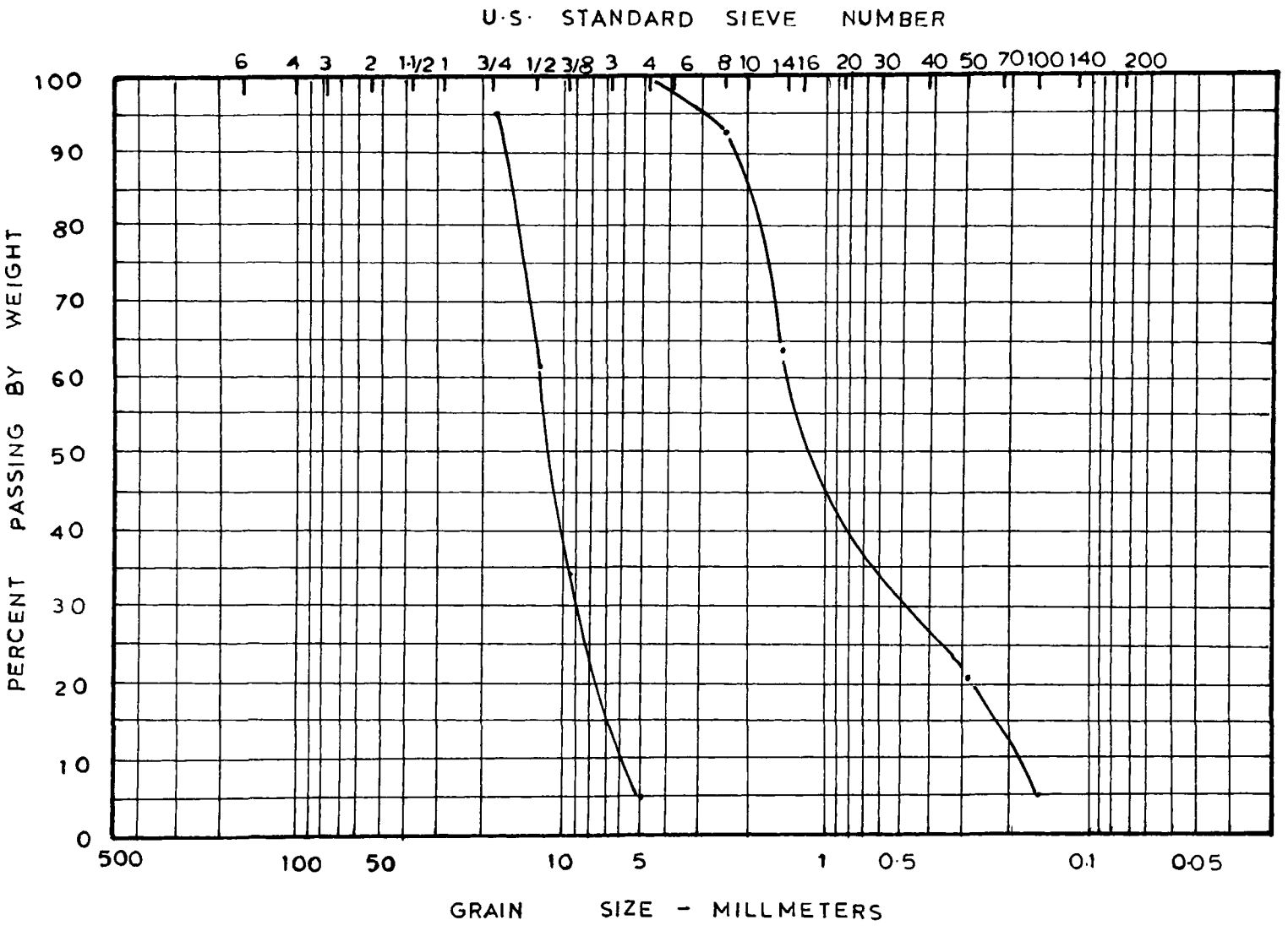

FIG: 5.1 GRADING CURVES OF AGGREGATE (MAX. COARSE AGG SIZE = 3/4")

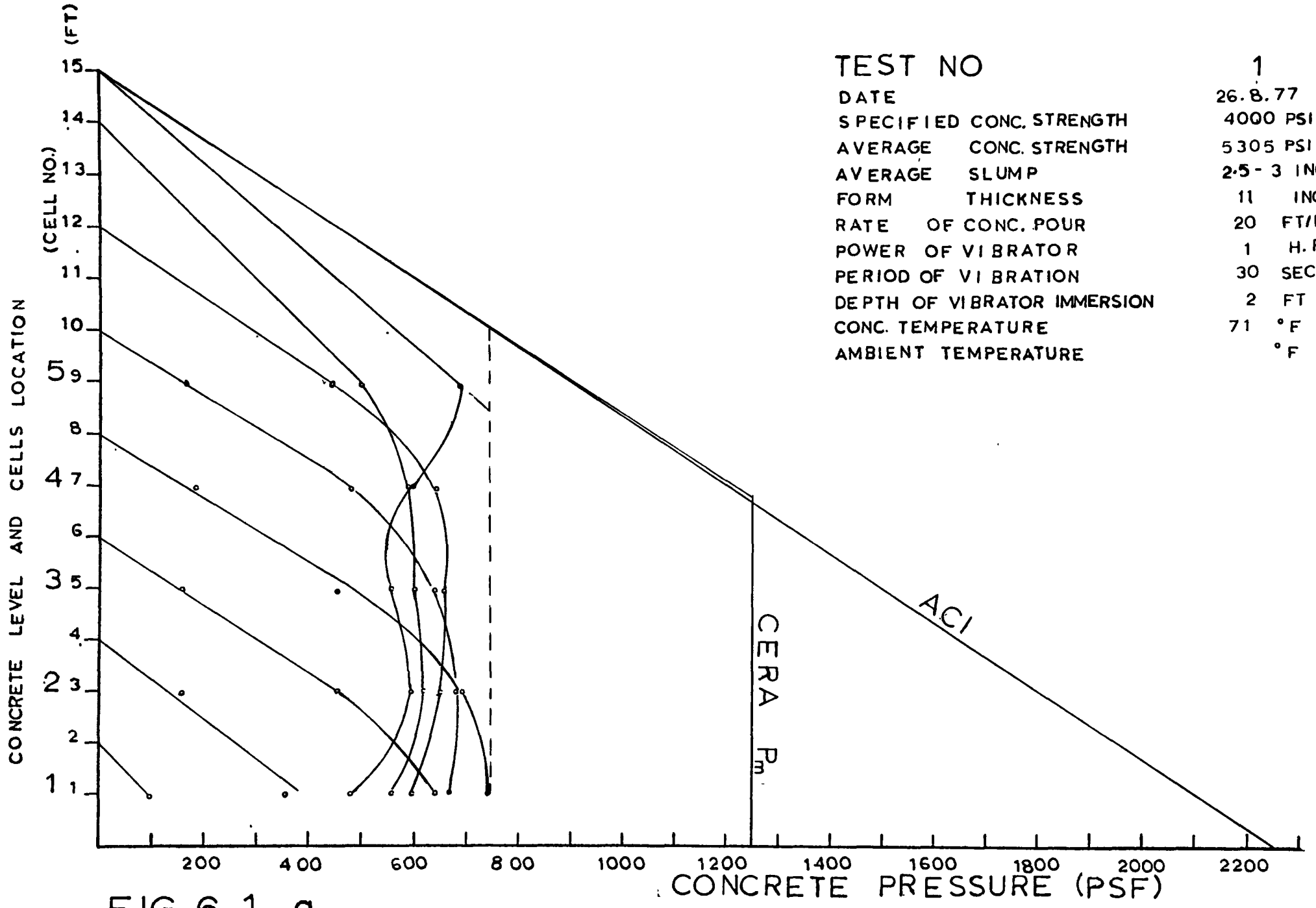

FIG. 6·1 a PRESSURE DEVELOPED AT VARIOUS CONC. LEVELS IN FORM

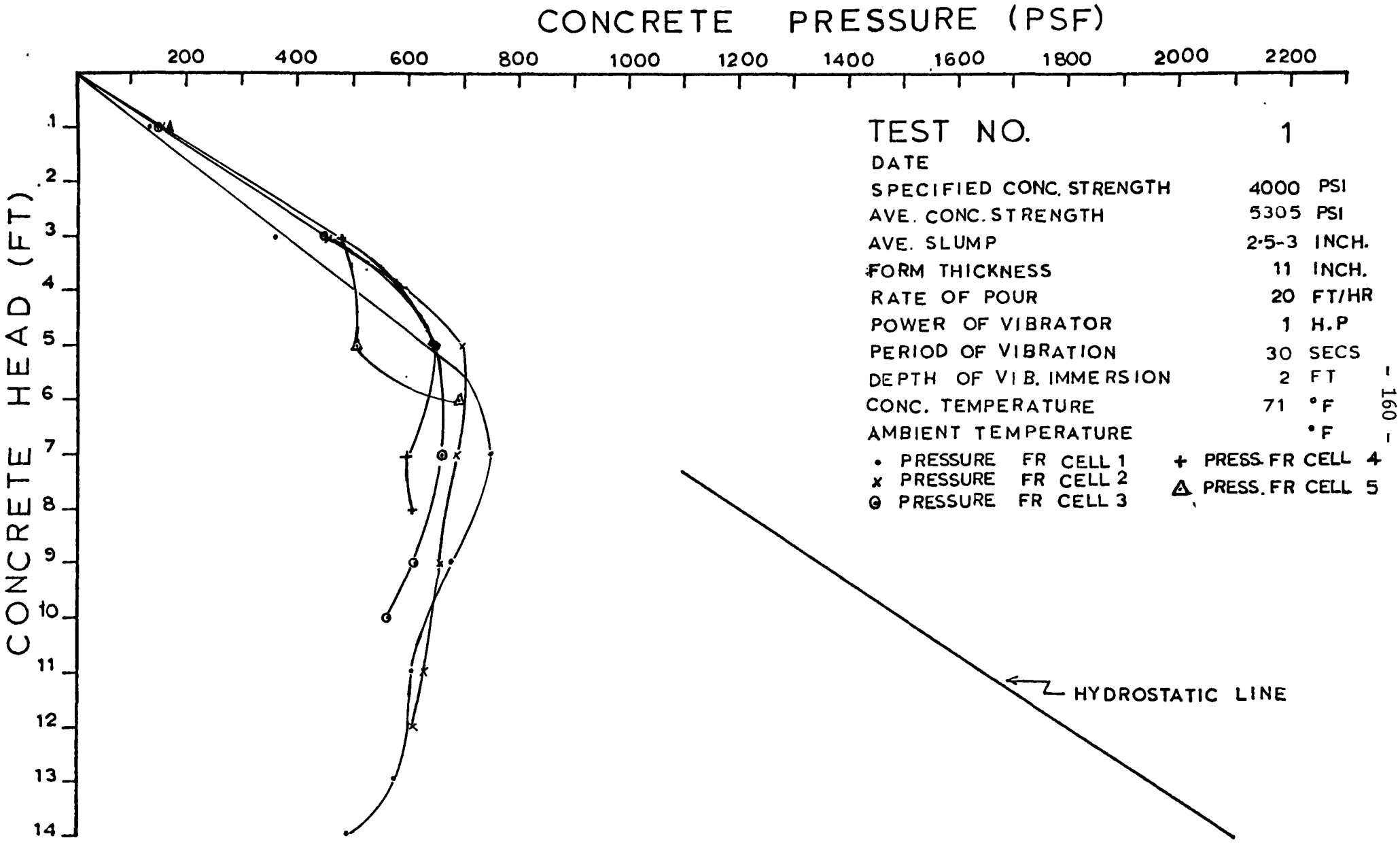

FIG. 6·1 b RELATION BETWEEN PRESSURE & CONC. HEAD

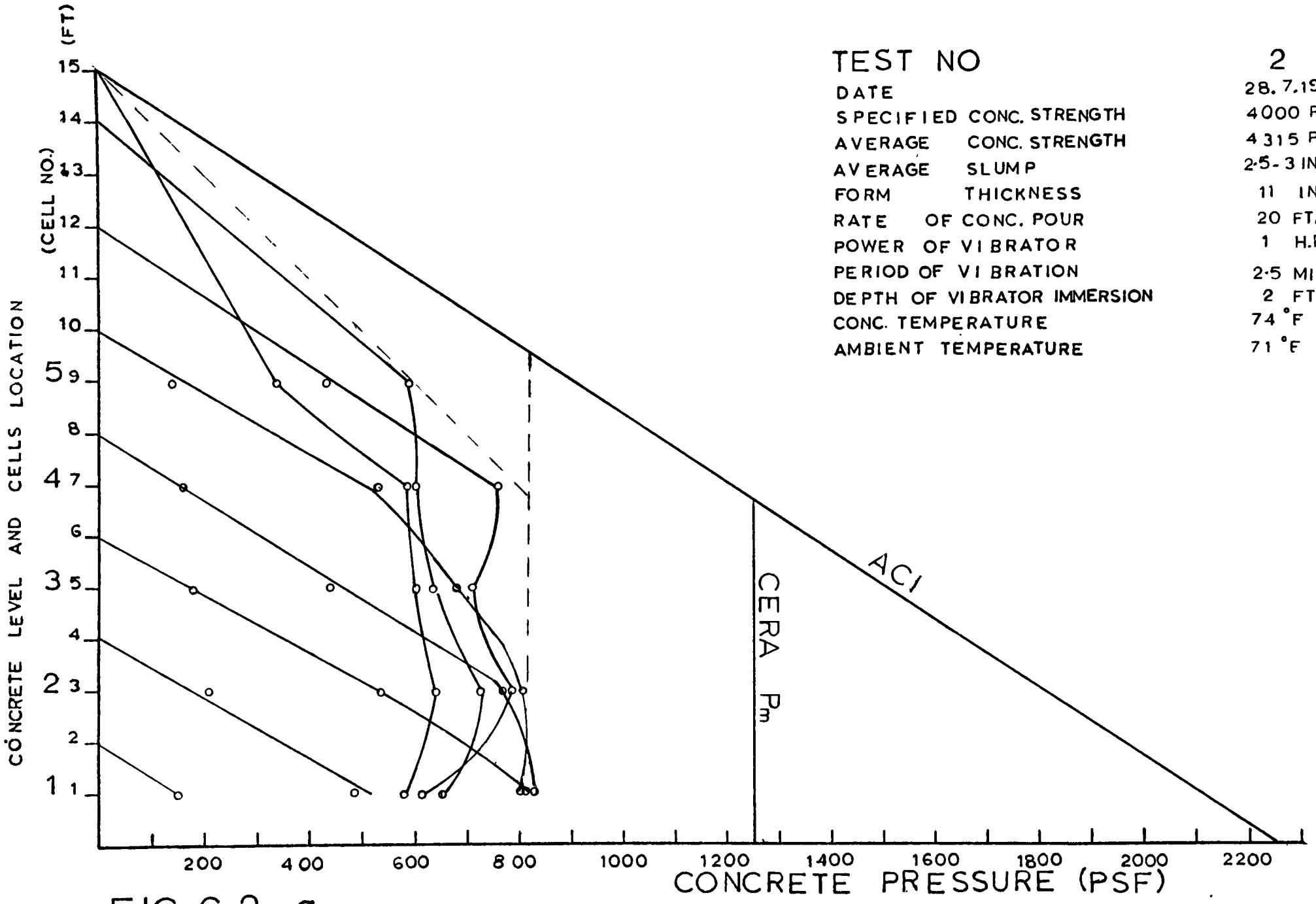

FIG. 6·2 a PRESSURE DEVELOPED AT VARIOUS CONC. LEVELS IN FORM

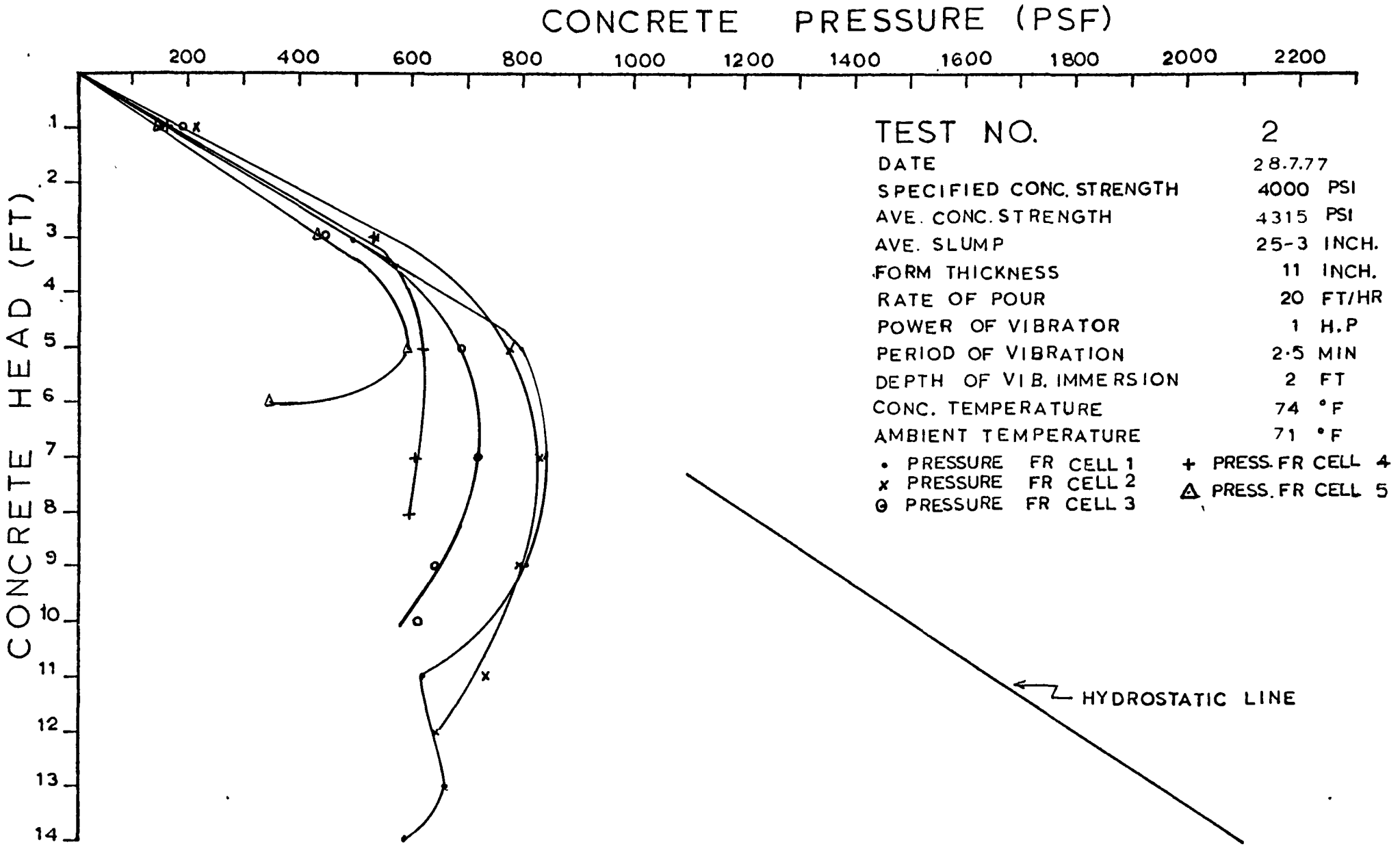

FIG. 6·2 b RELATION BETWEEN PRESSURE & CONC. HEAD

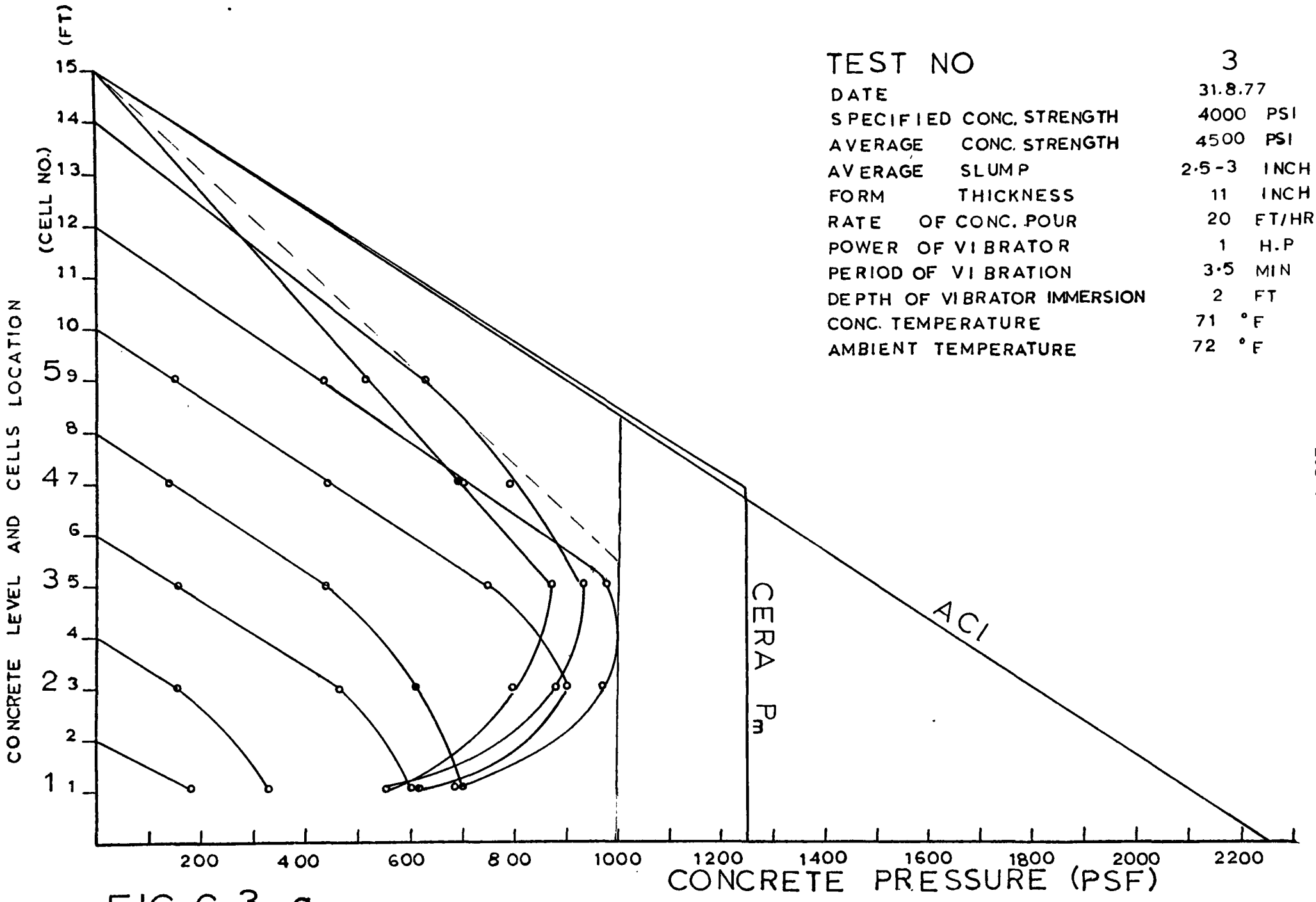

FIG. 6.3 a PRESSURE DEVELOPED AT VARIOUS CONC. LEVELS IN FORM

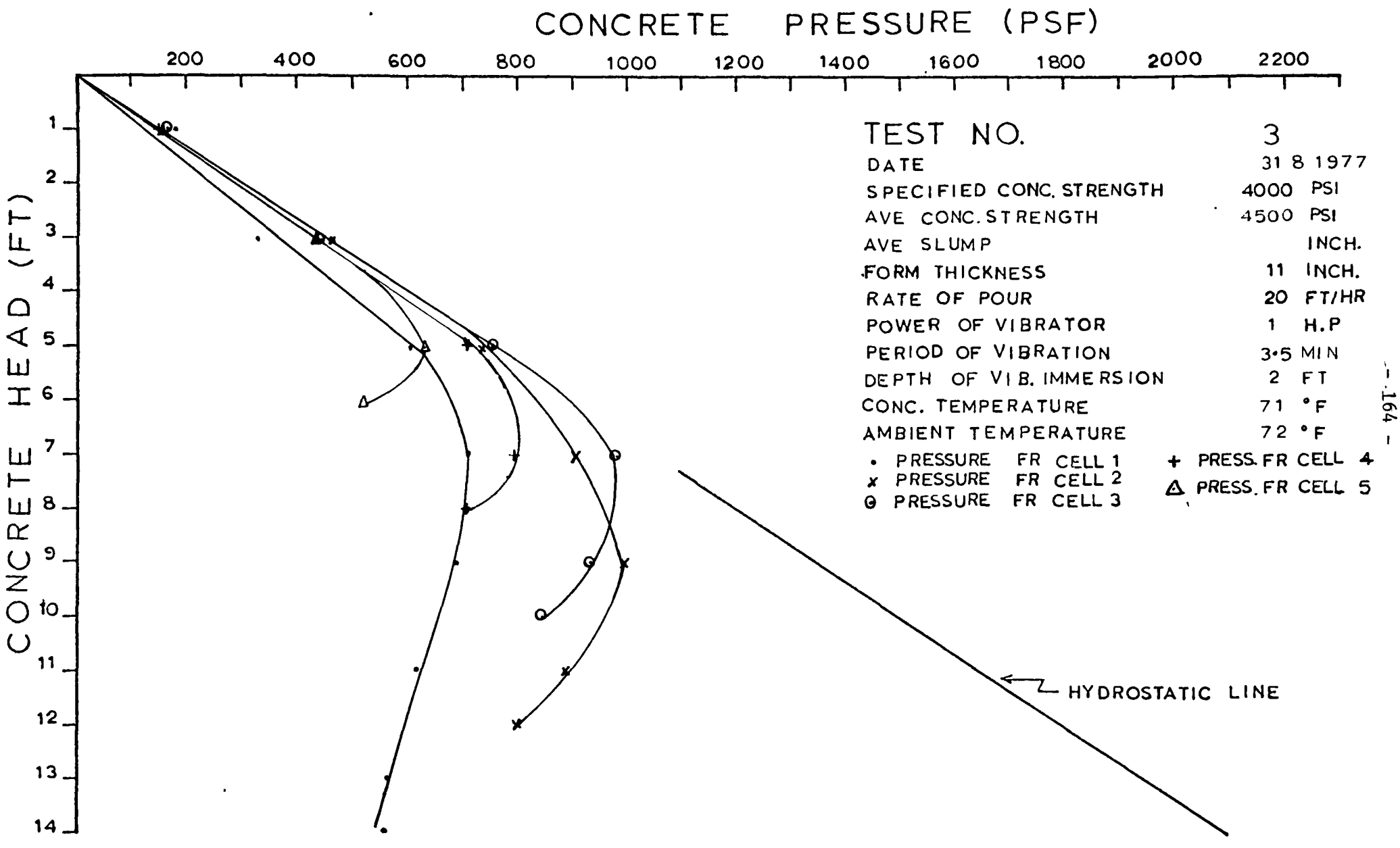

FIG. 6·3 b RELATION BETWEEN PRESSURE & CONC. HEAD

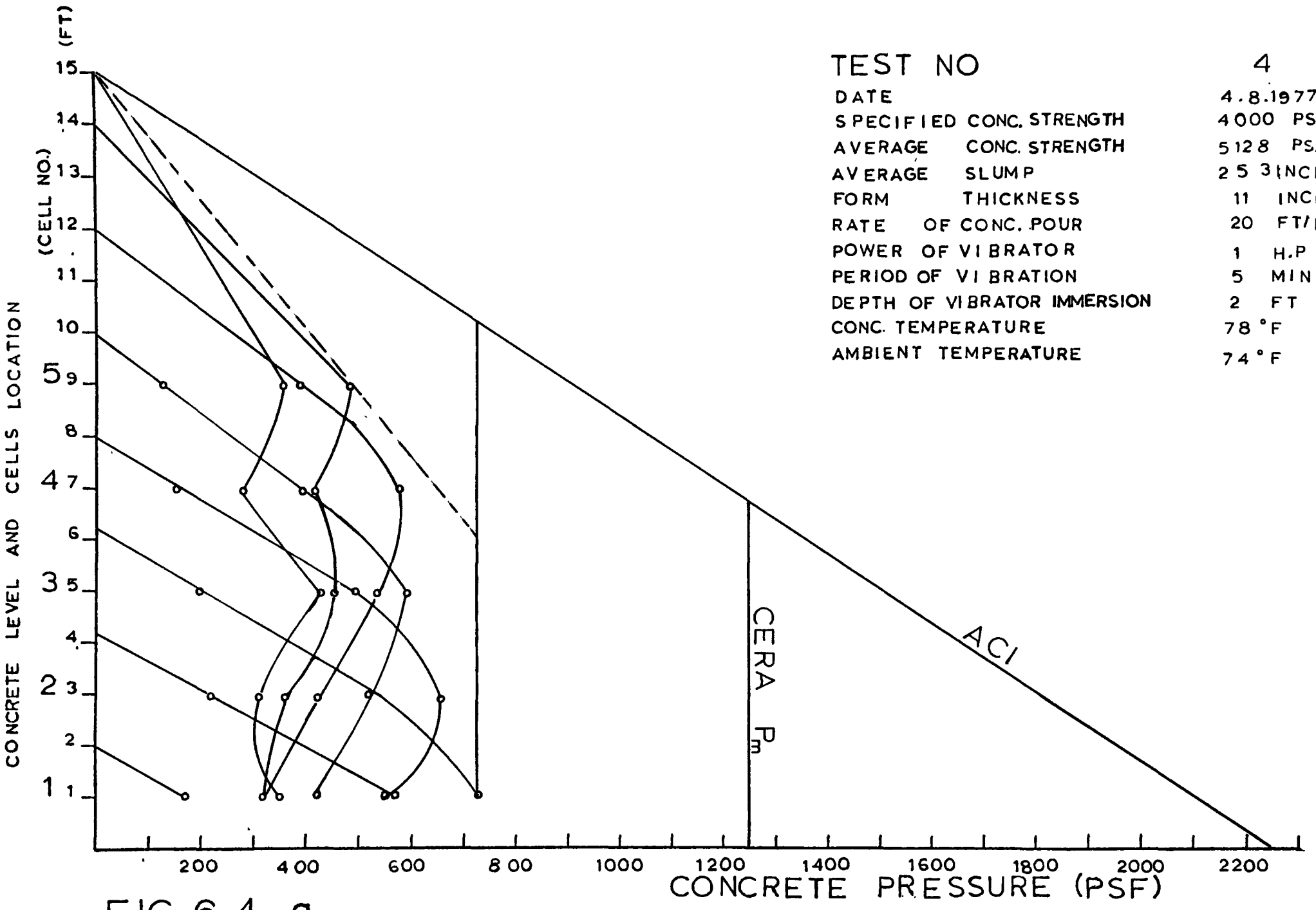

FIG. 6.4 a PRESSURE DEVELOPED AT VARIOUS CONC. LEVELS IN FORM

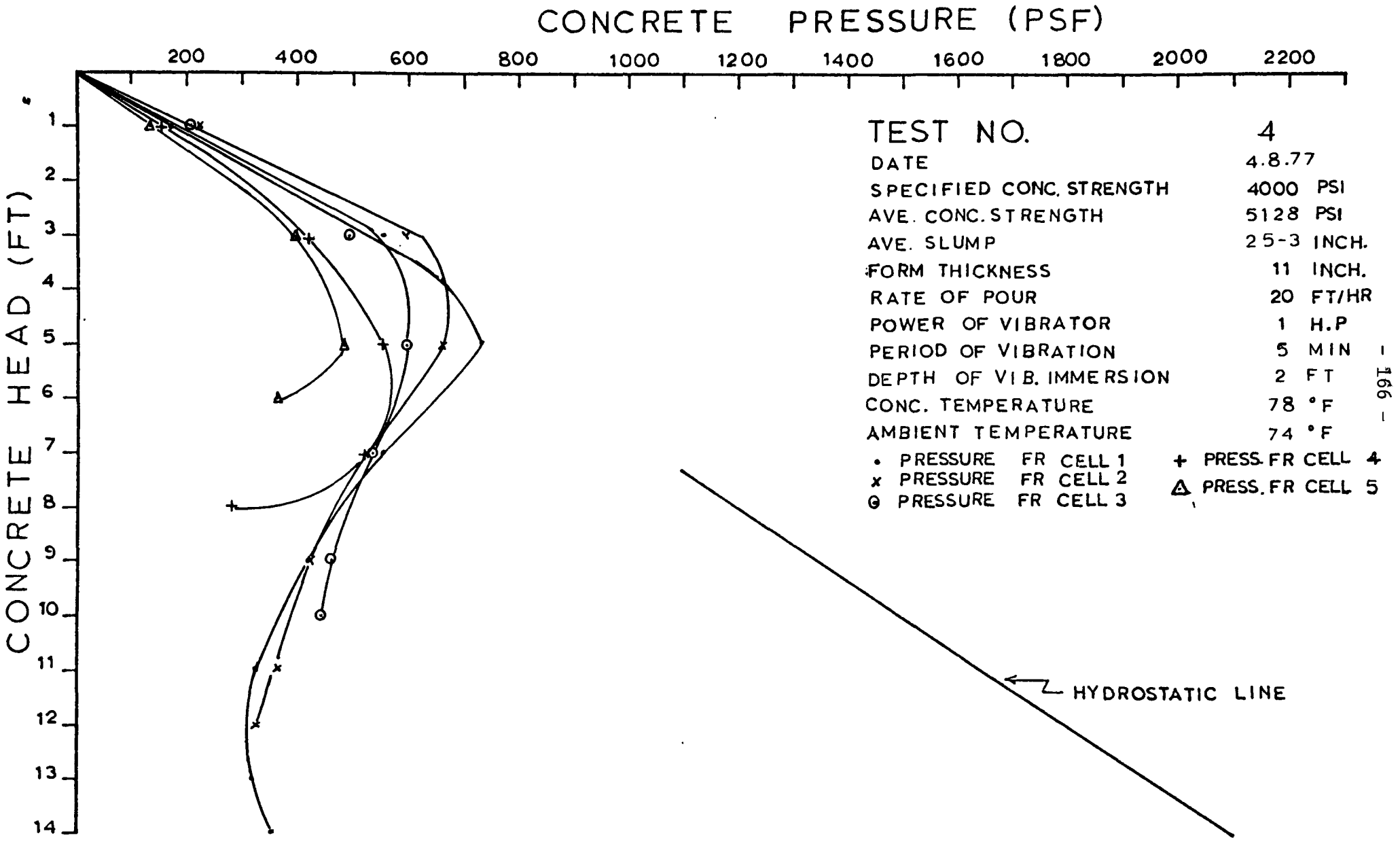

FIG. 6·4 b RELATION BETWEEN PRESSURE & CONC. HEAD

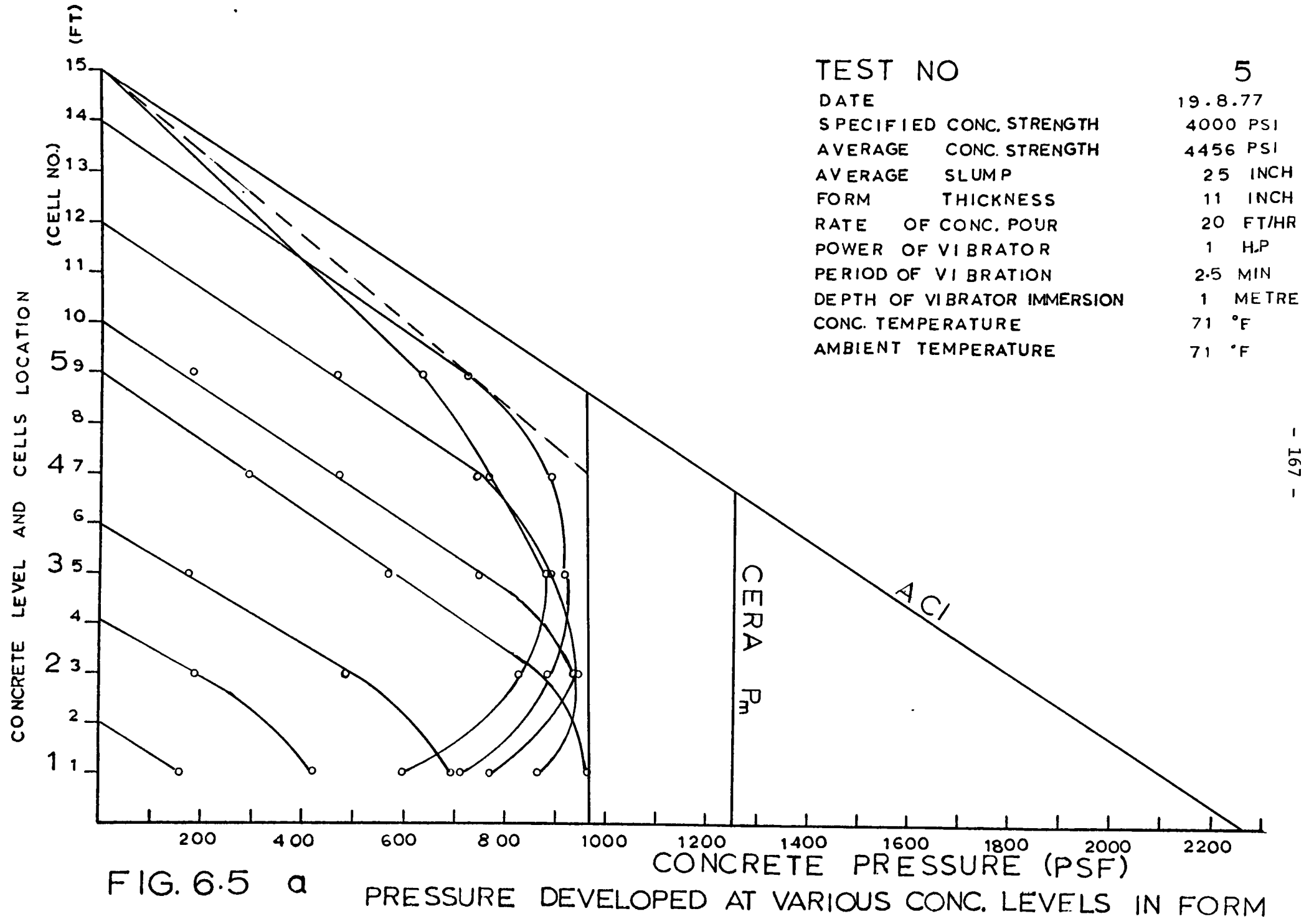

FIG. 6·5 a PRESSURE DEVELOPED AT VARIOUS CONC. LEVELS IN FORM

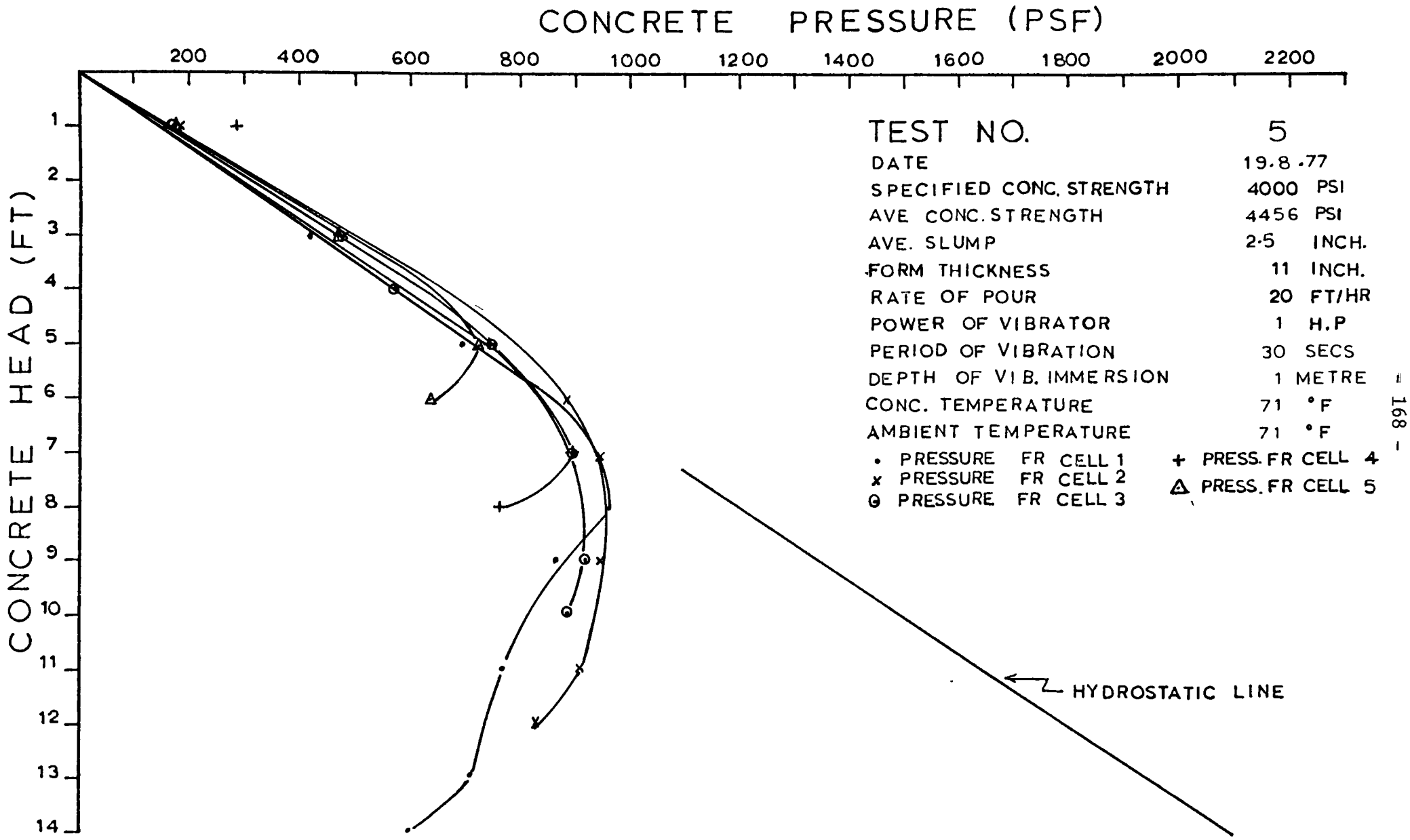

FIG. 6·5 b RELATION BETWEEN PRESSURE & CONC. HEAD

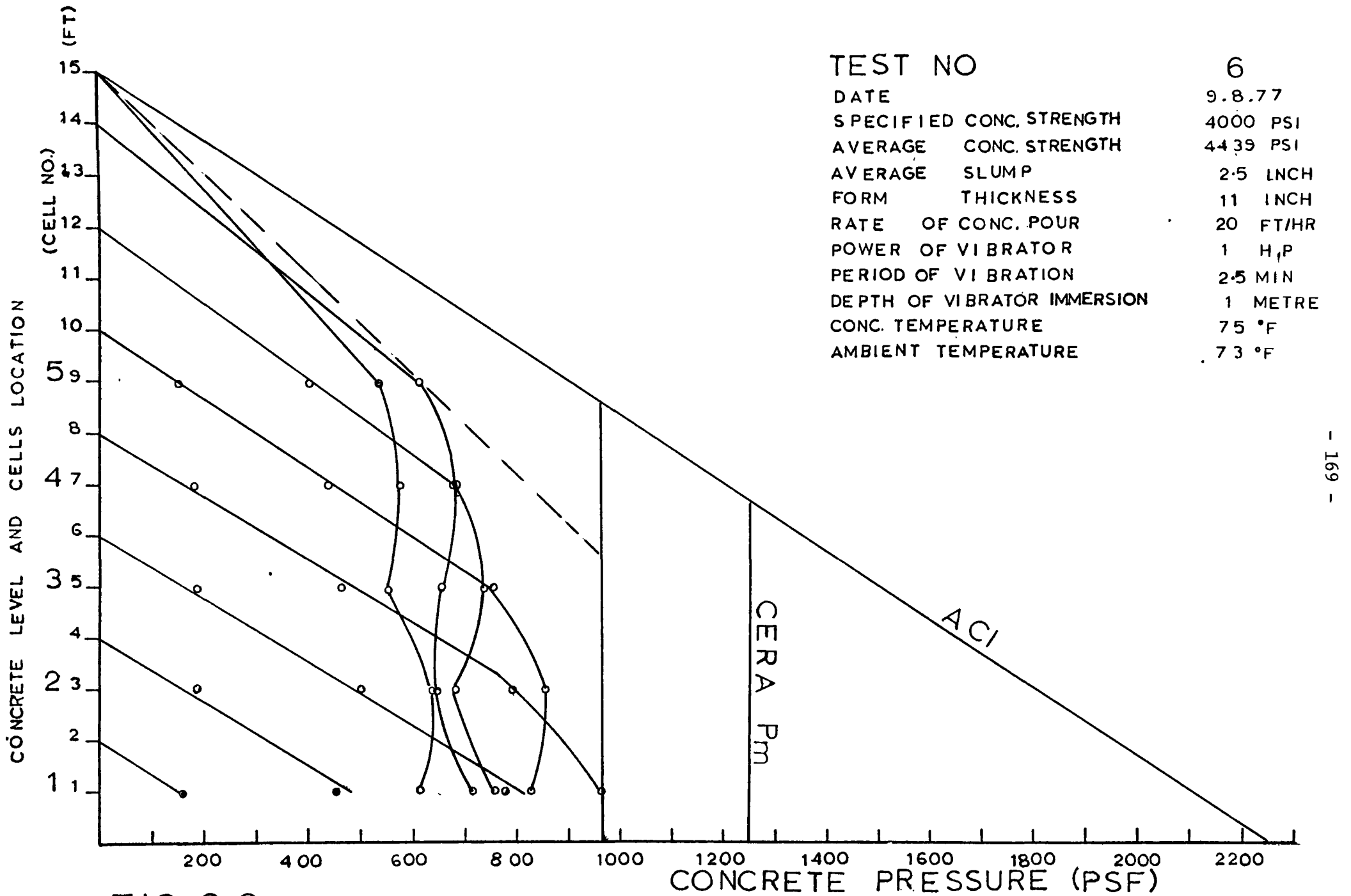

FIG. 6·6 a PRESSURE DEVELOPED AT VARIOUS CONC. LEVELS IN FORM

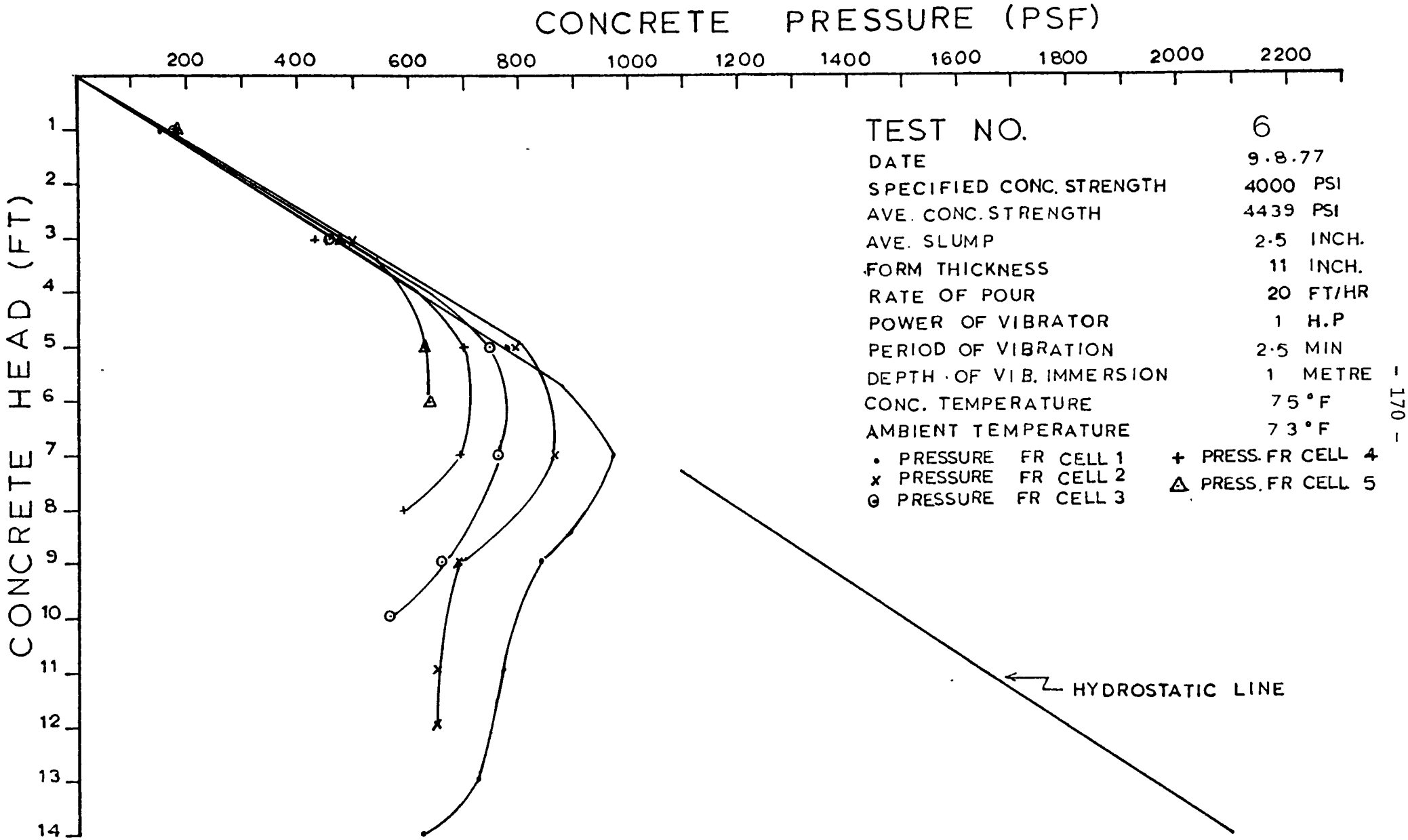

FIG. 6·6 b RELATION BETWEEN PRESSURE & CONC. HEAD

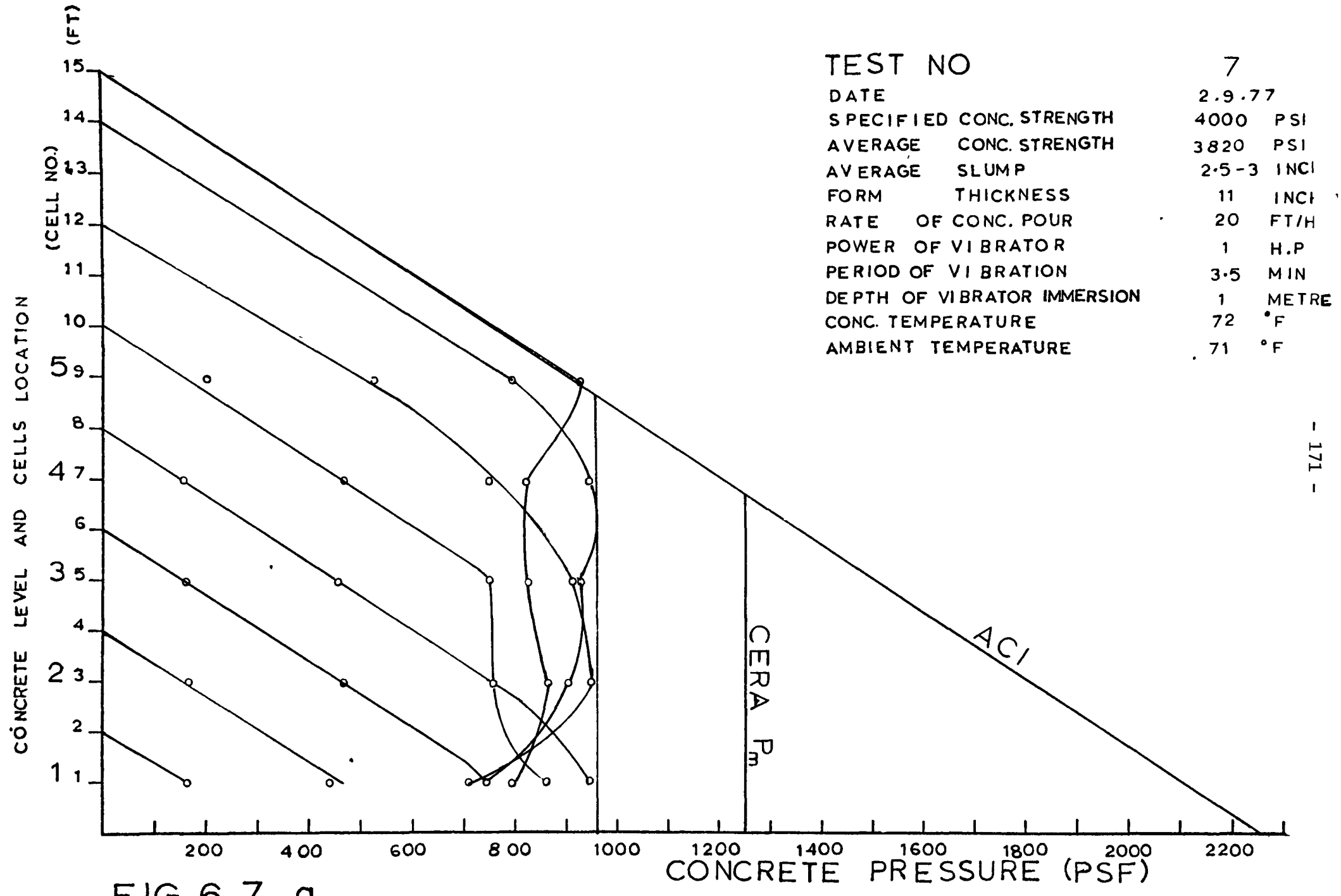

FIG. 6·7 a PRESSURE DEVELOPED AT VARIOUS CONC. LEVELS IN FORM

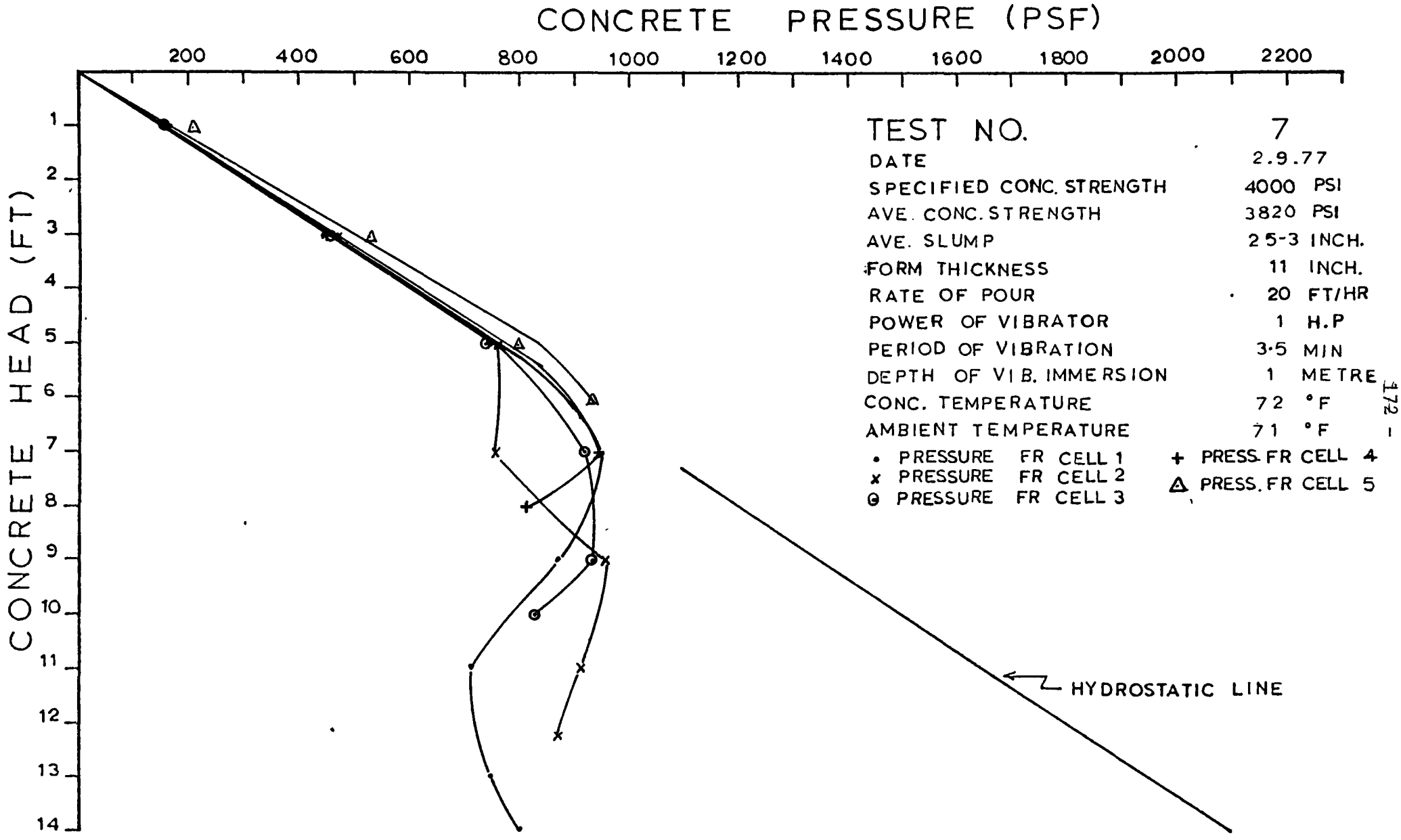

FIG. 6·7 b RELATION BETWEEN PRESSURE & CONC. HEAD

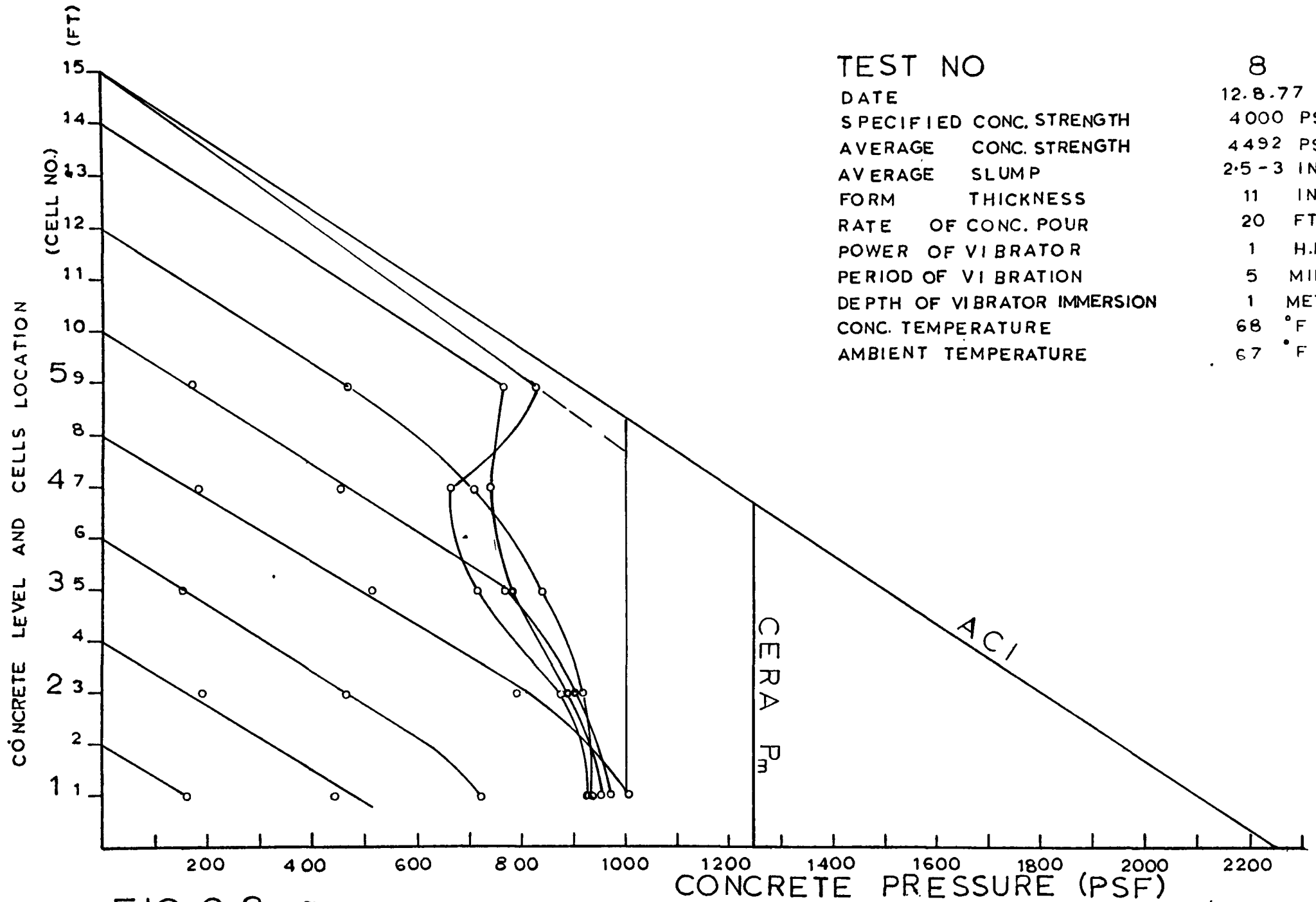

FIG. 6·8 a PRESSURE DEVELOPED AT VARIOUS CONC. LEVELS IN FORM

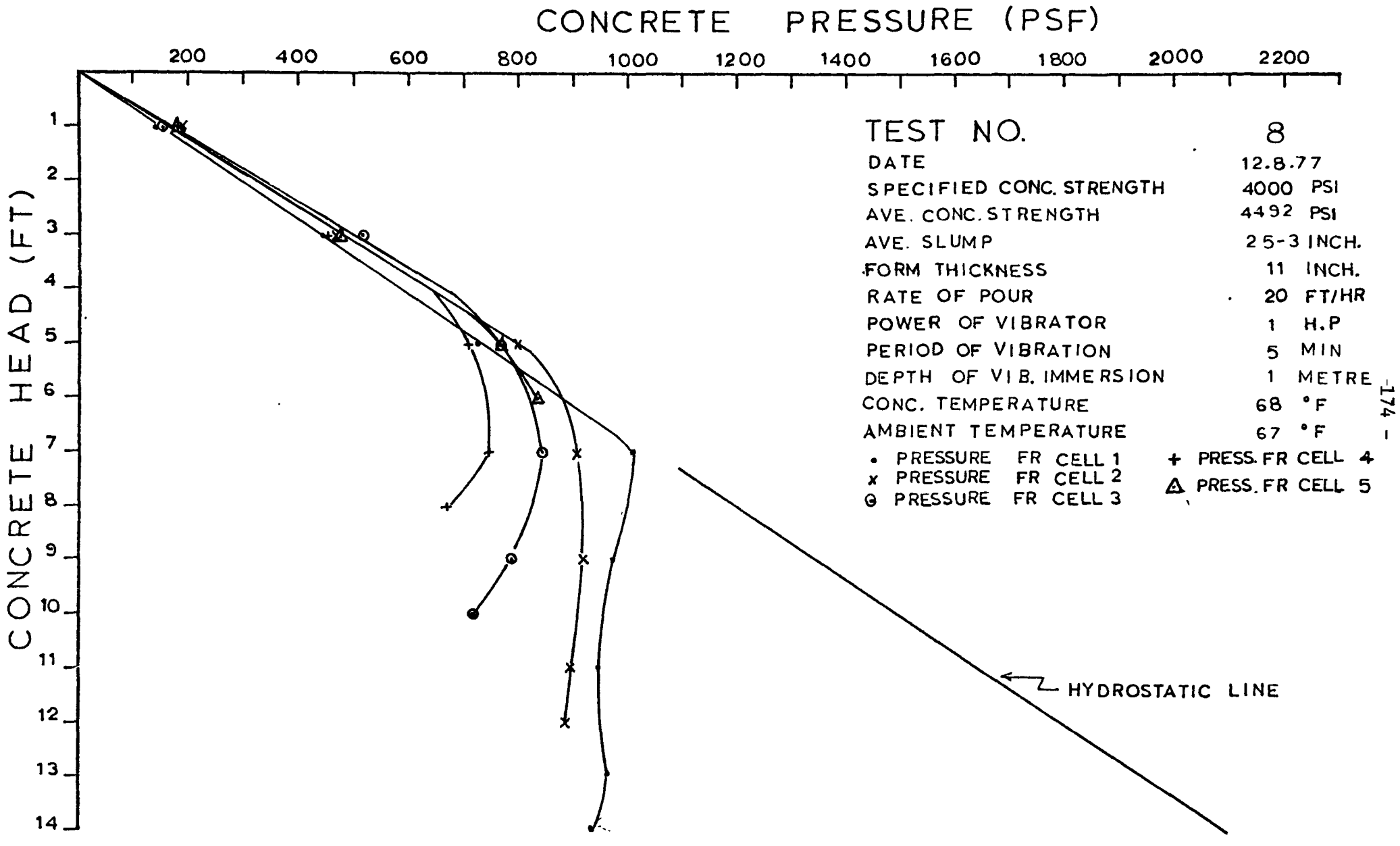

FIG. 6·8 b RELATION BETWEEN PRESSURE & CONC. HEAD

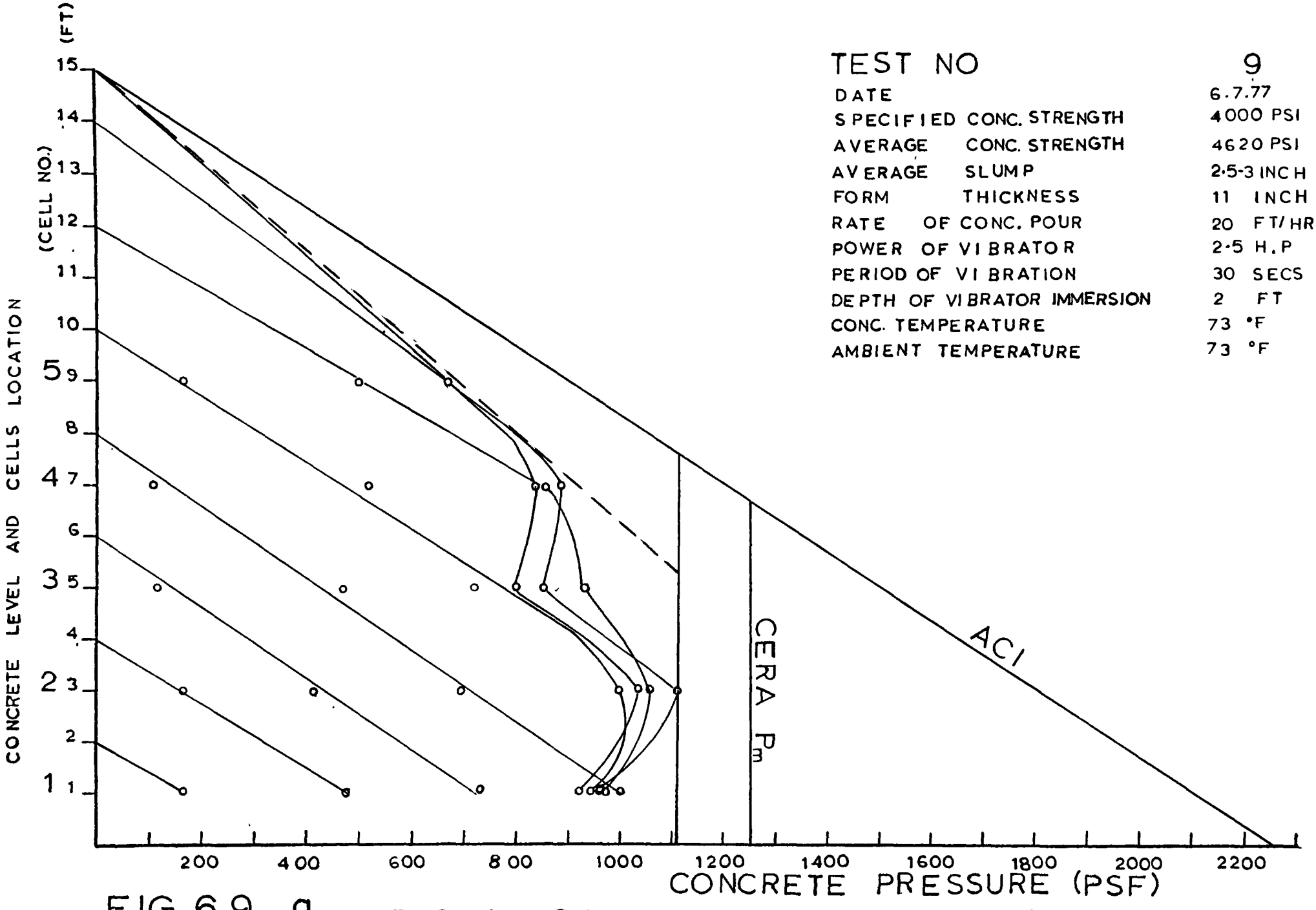

FIG. 6·9 a PRESSURE DEVELOPED AT VARIOUS CONC. LEVELS IN FORM

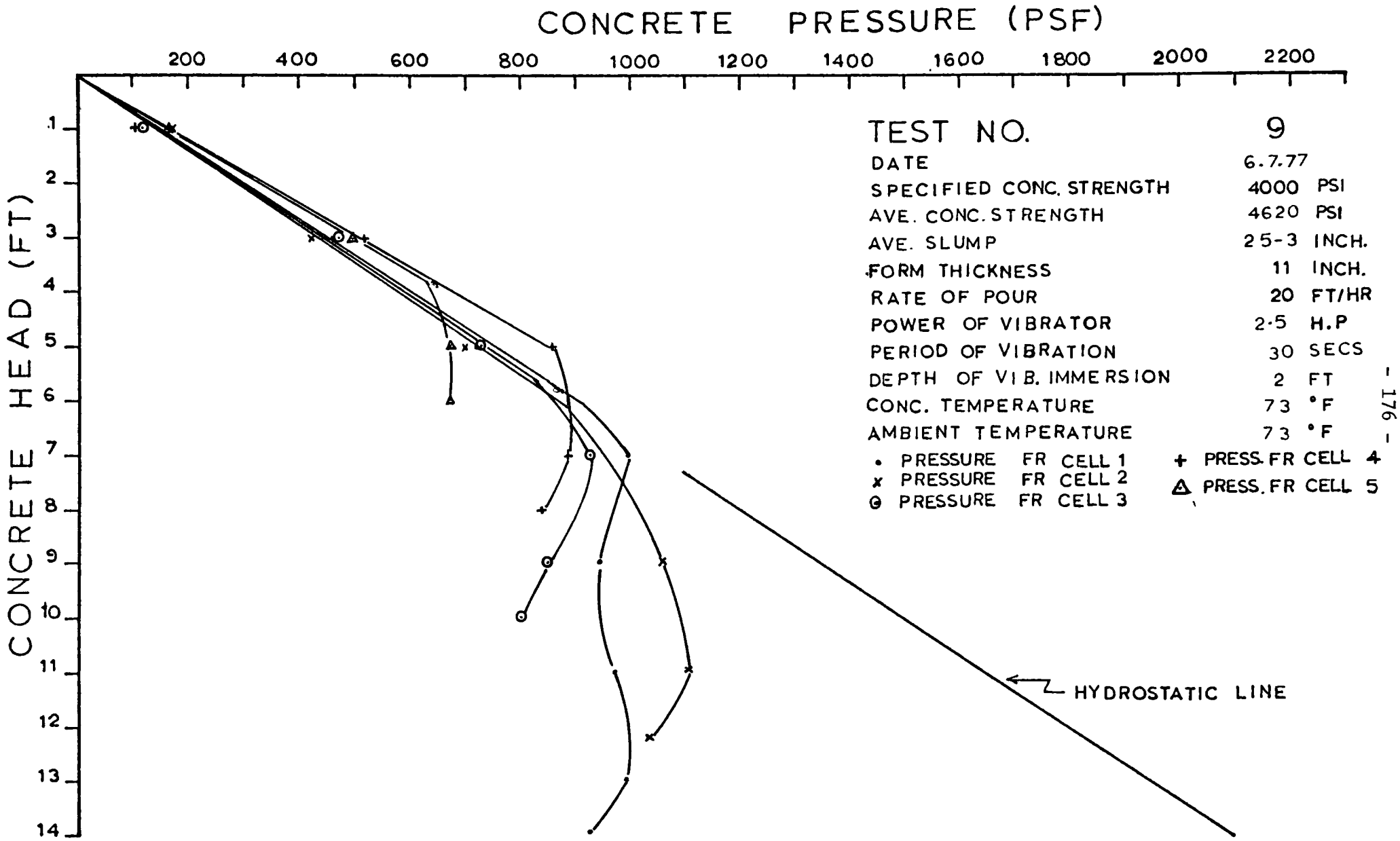

FIG. 6·9 b RELATION BETWEEN PRESSURE & CONC. HEAD

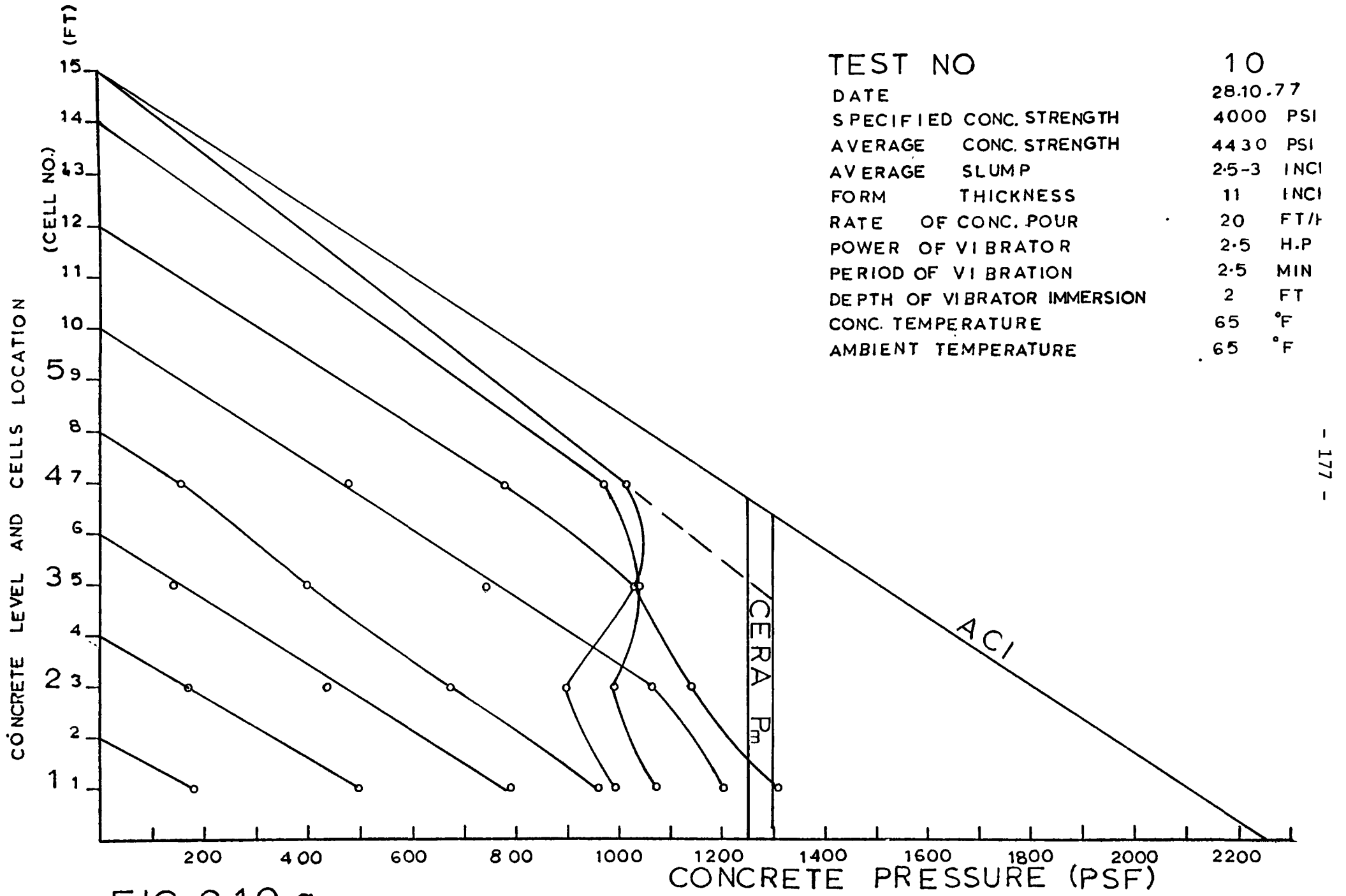

FIG. 6·10 a PRESSURE DEVELOPED AT VARIOUS CONC. LEVELS IN FORM

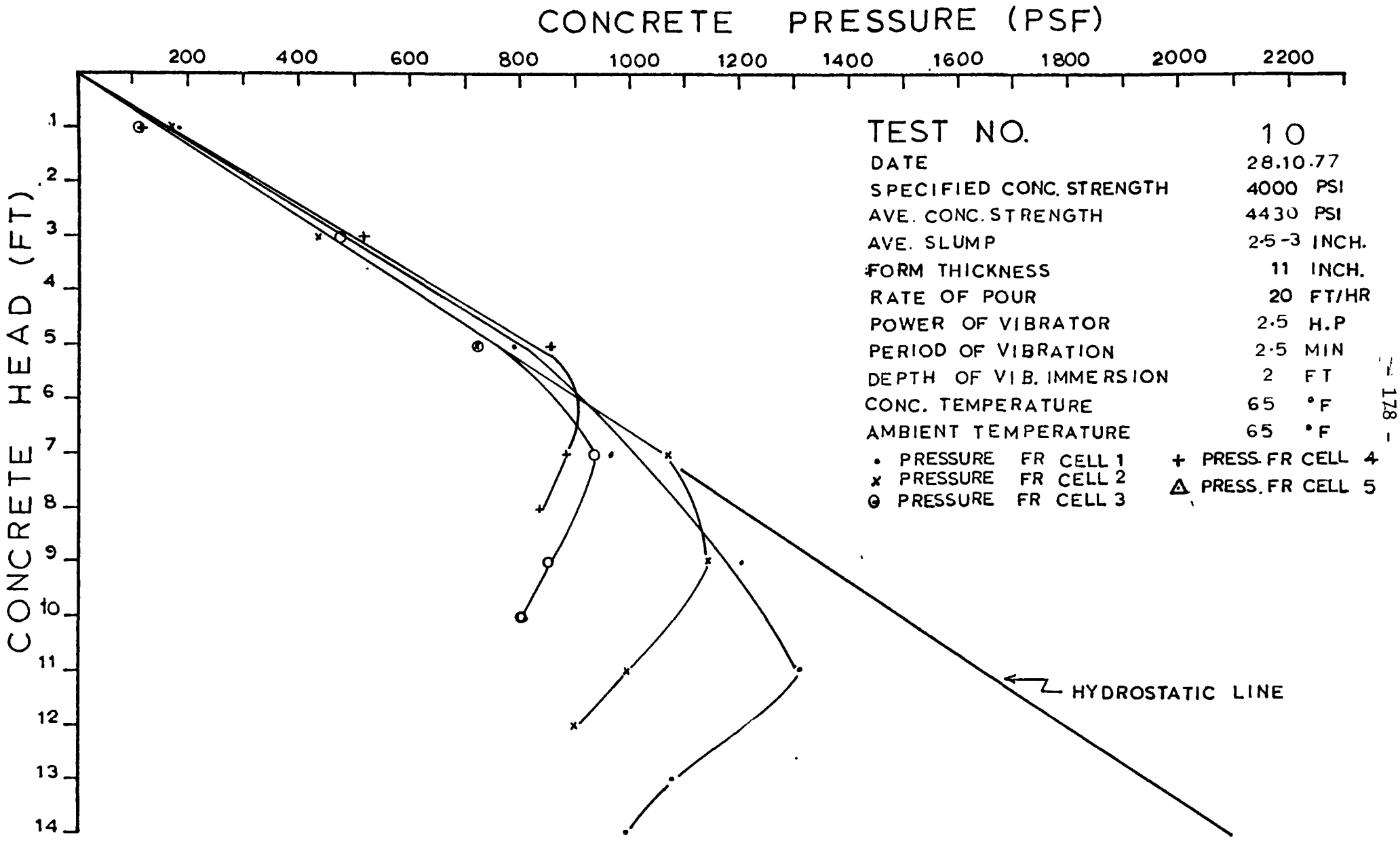

FIG. 6·10b RELATION BETWEEN PRESSURE & CONC. HEAD

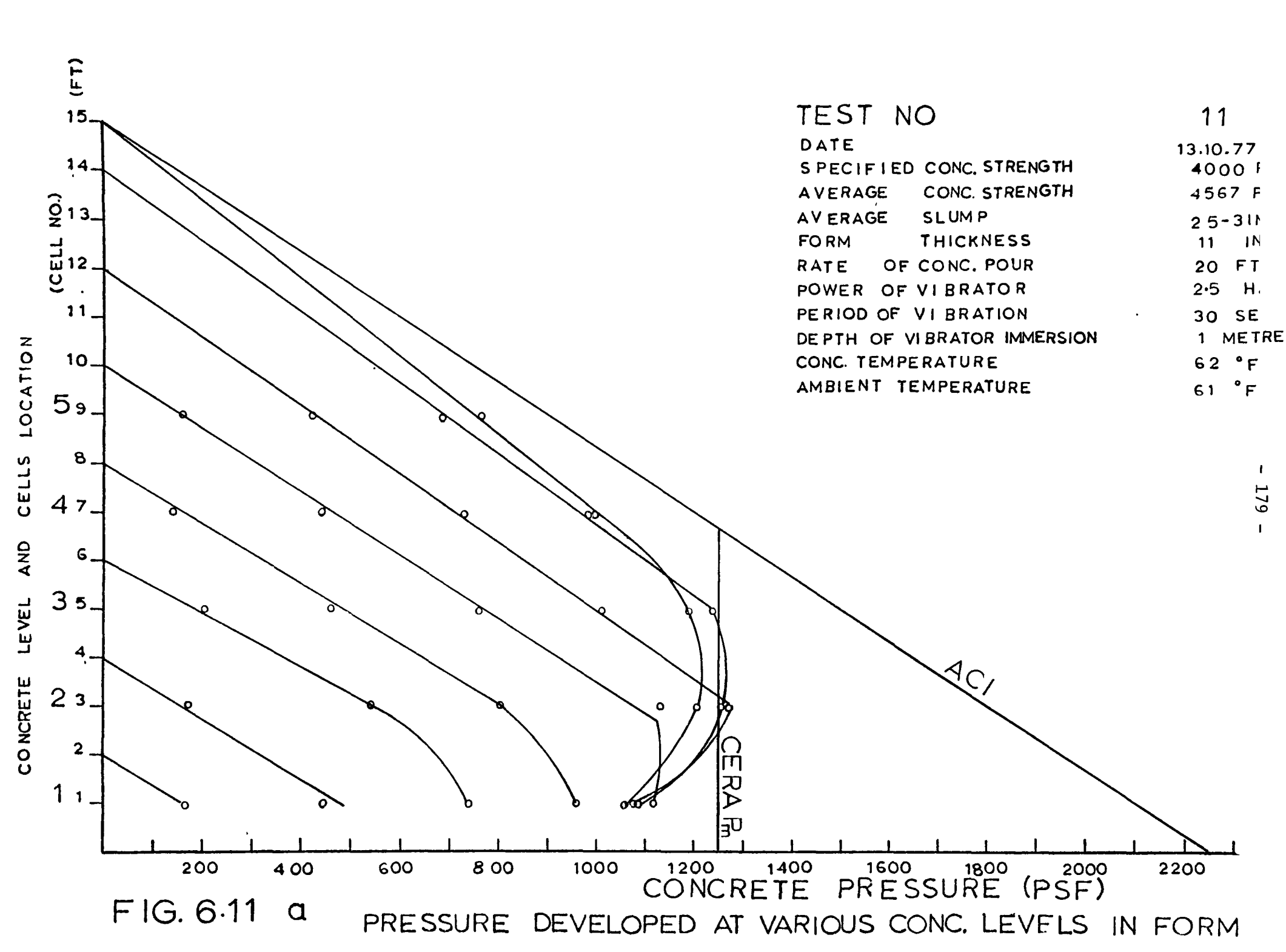

FIG. 6·11 a PRESSURE DEVELOPED AT VARIOUS CONC. LEVELS IN FORM

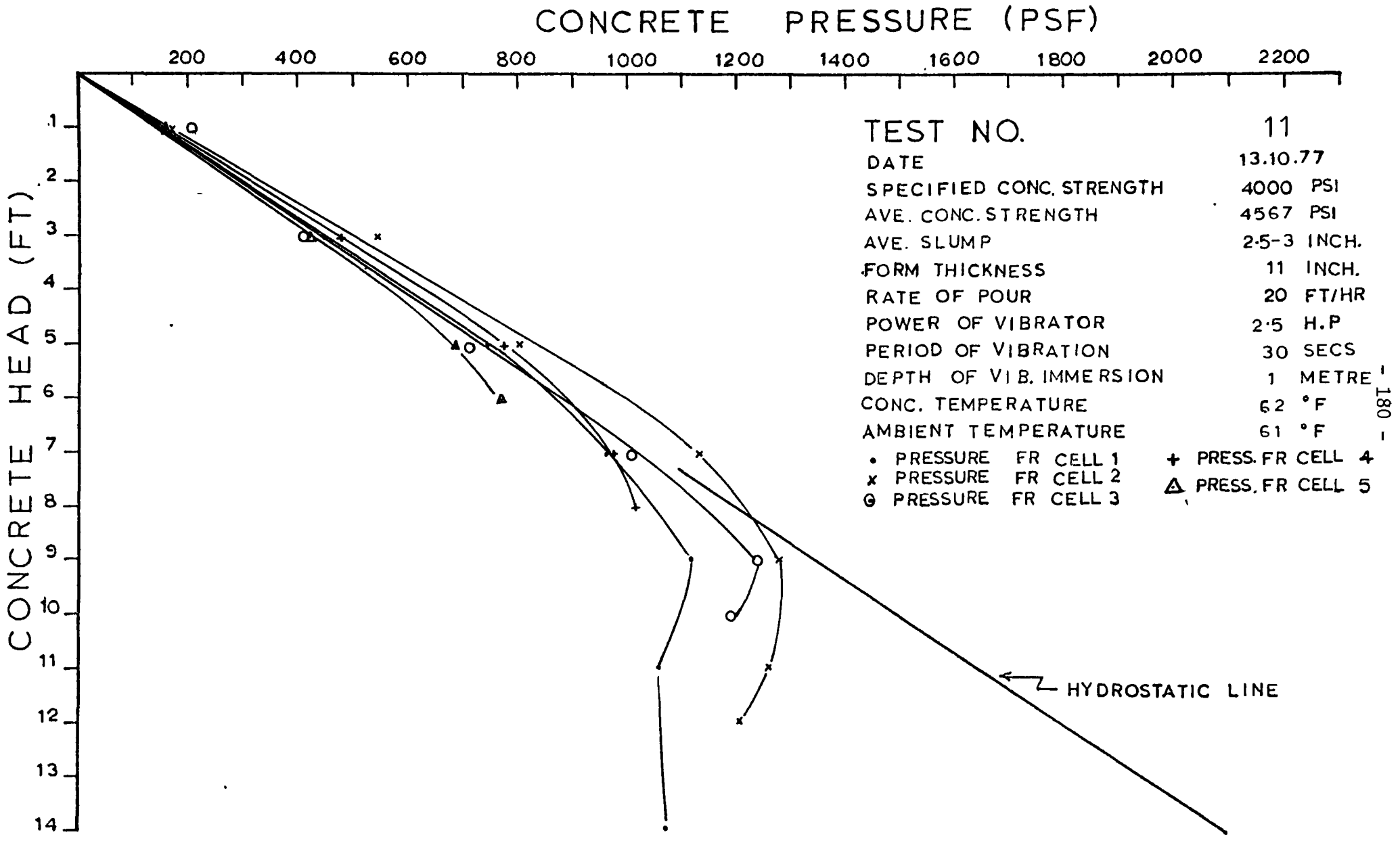

FIG. 6·11 b RELATION BETWEEN PRESSURE & CONC. HEAD

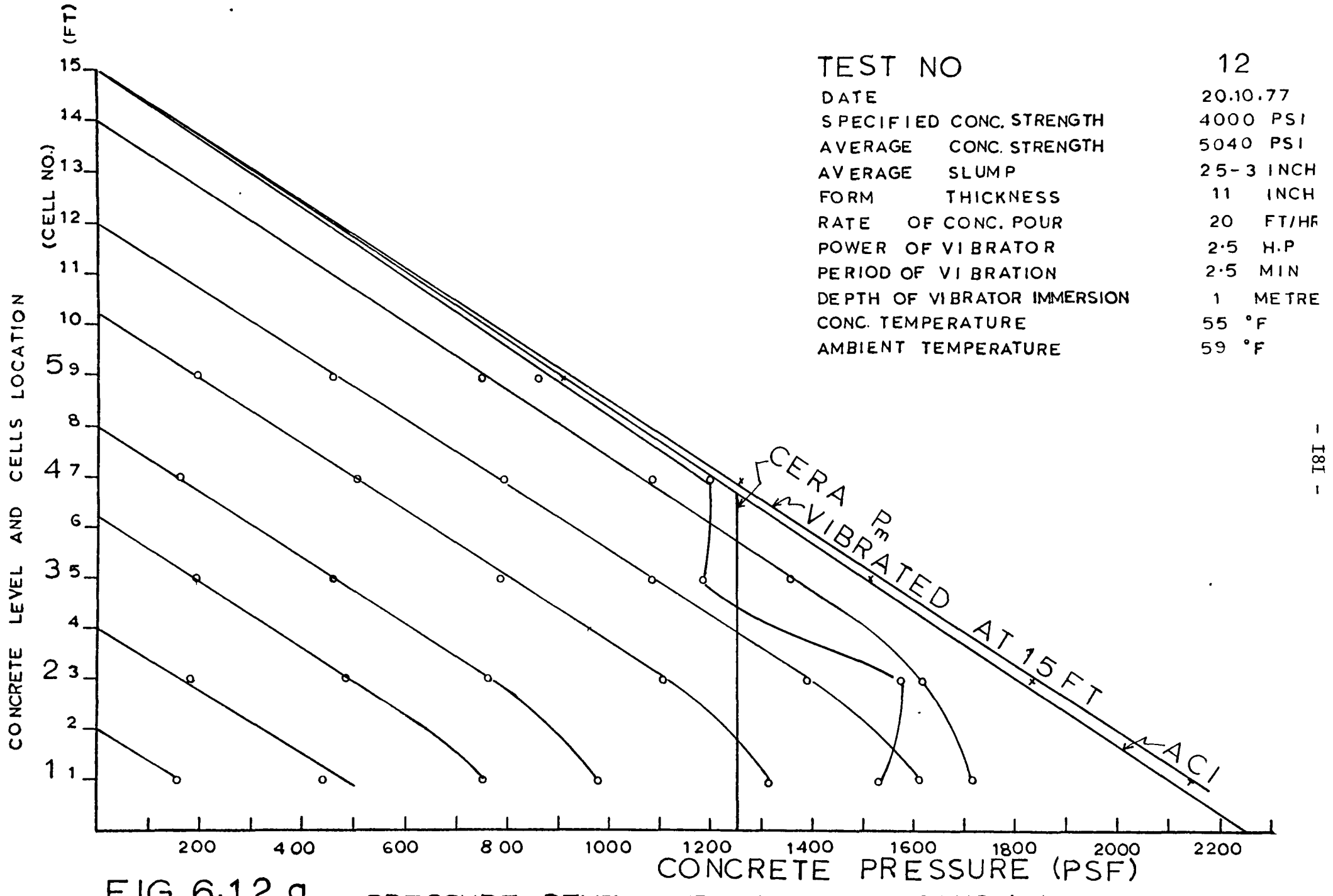

FIG. 6·12 a PRESSURE DEVELOPED AT VARIOUS CONC. LEVELS IN FORM

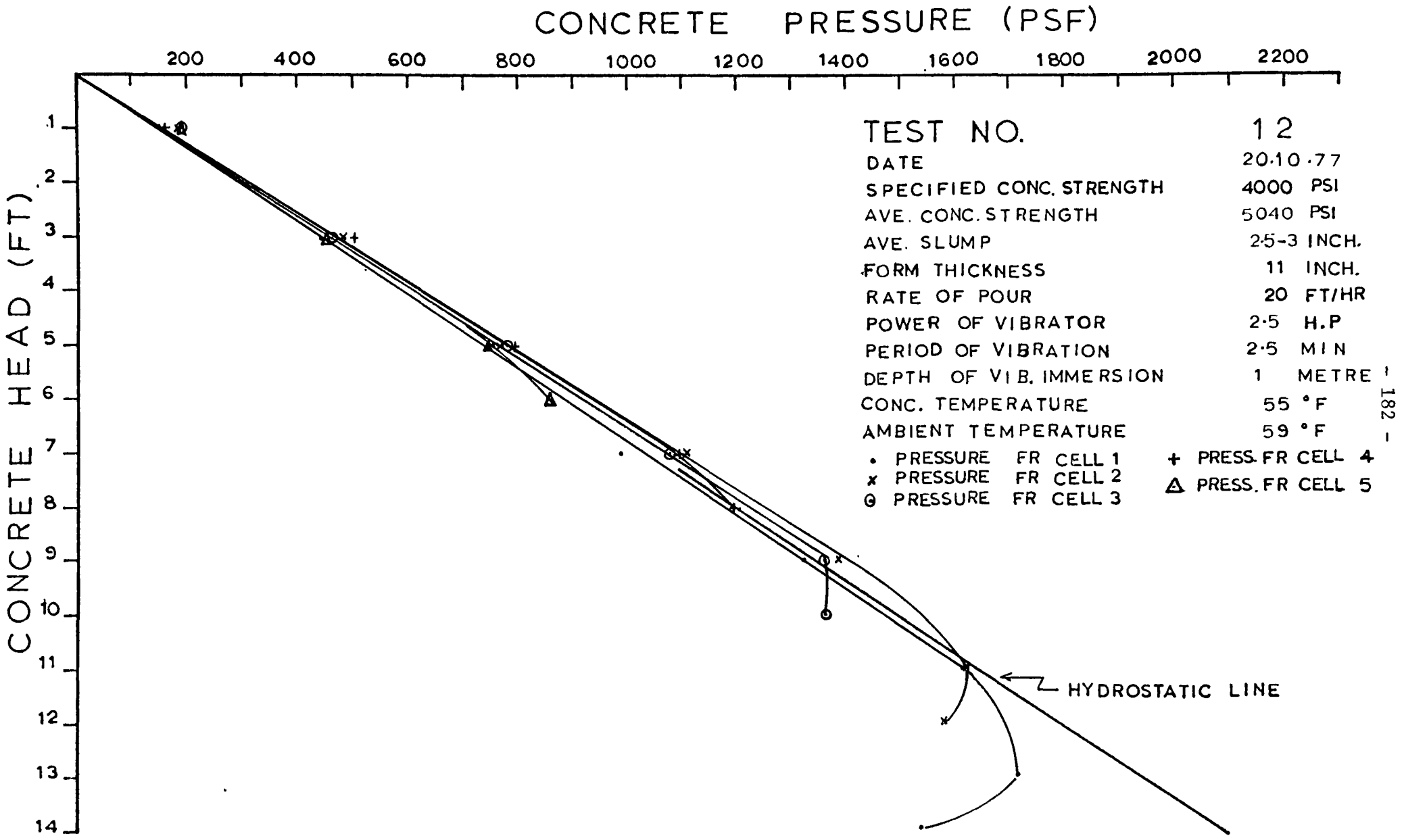

FIG. 6·12 b RELATION BETWEEN PRESSURE & CONC. HEAD

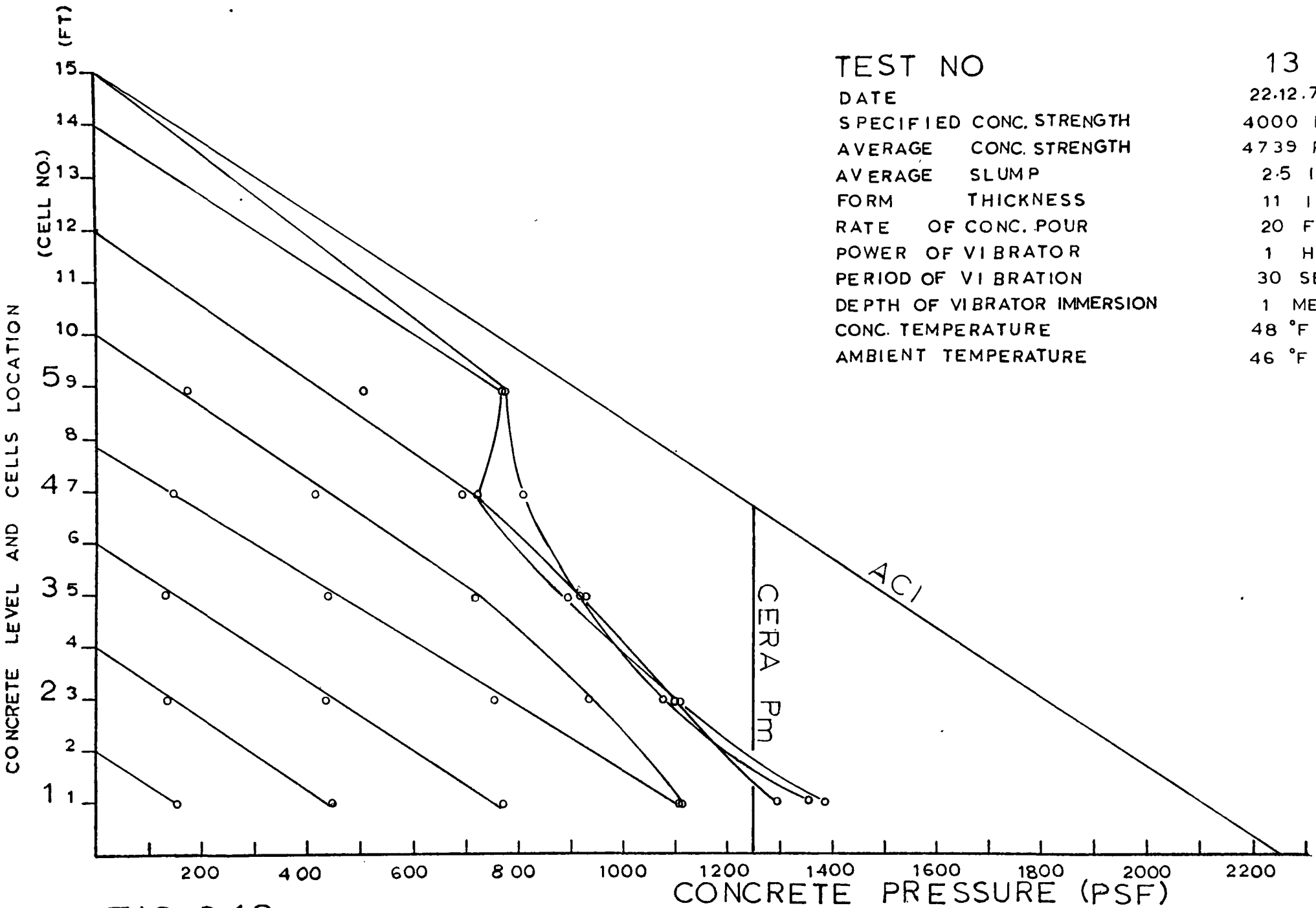

FIG. 6·13 a PRESSURE DEVELOPED AT VARIOUS CONC. LEVELS IN FORM

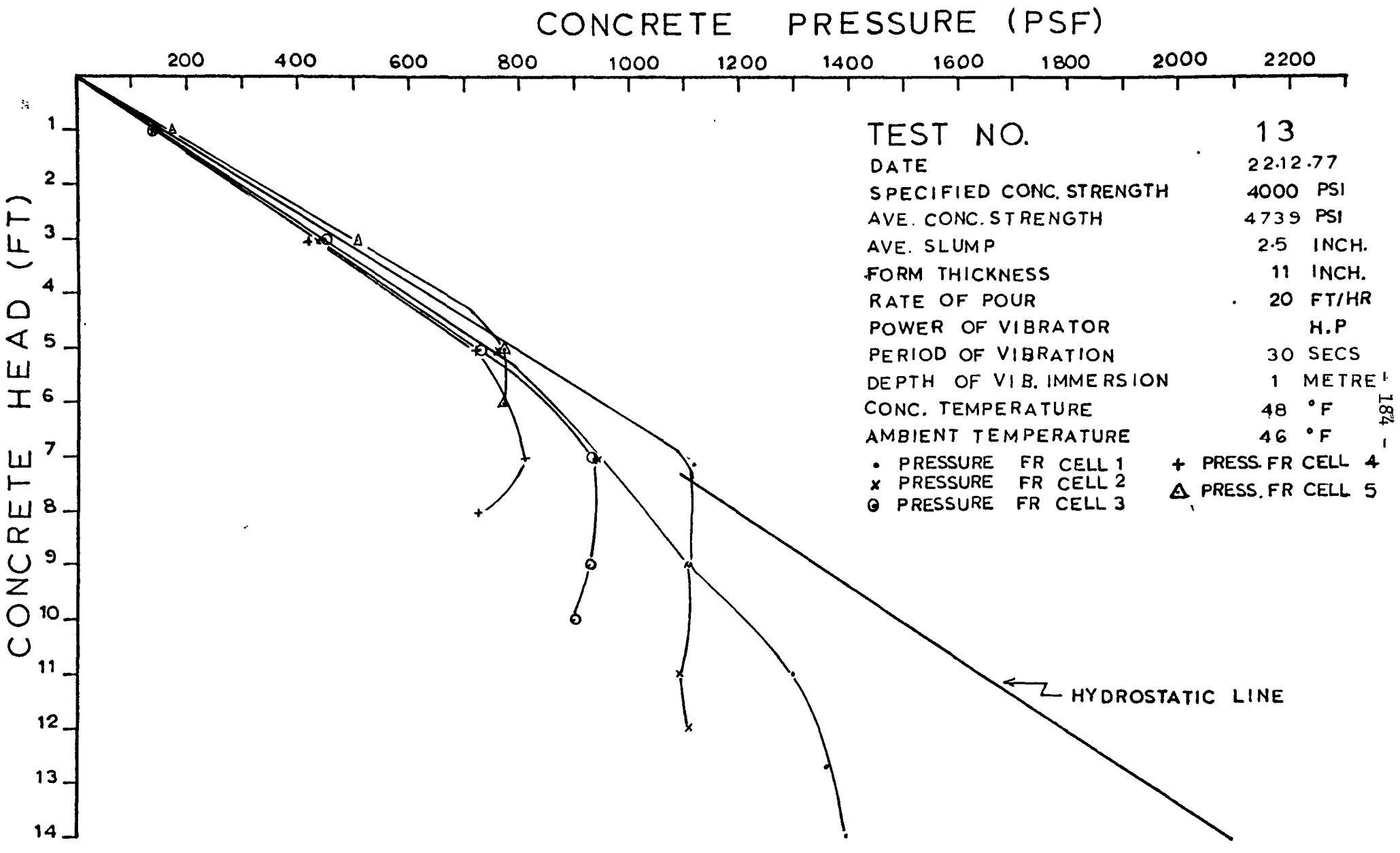

FIG. 6·13 b RELATION BETWEEN PRESSURE & CONC. HEAD

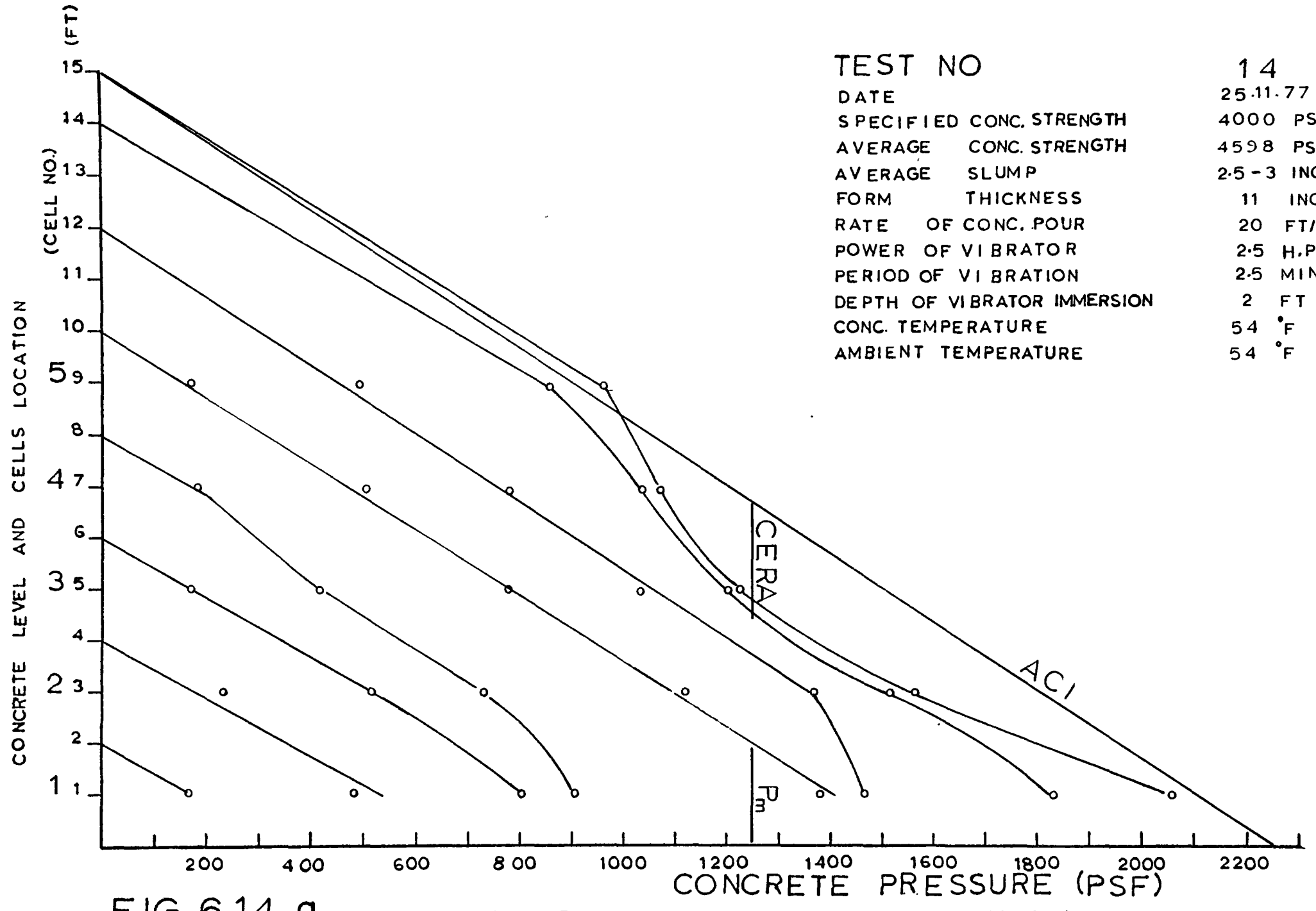

FIG. 6·14 a PRESSURE DEVELOPED AT VARIOUS CONC. LEVELS IN FORM

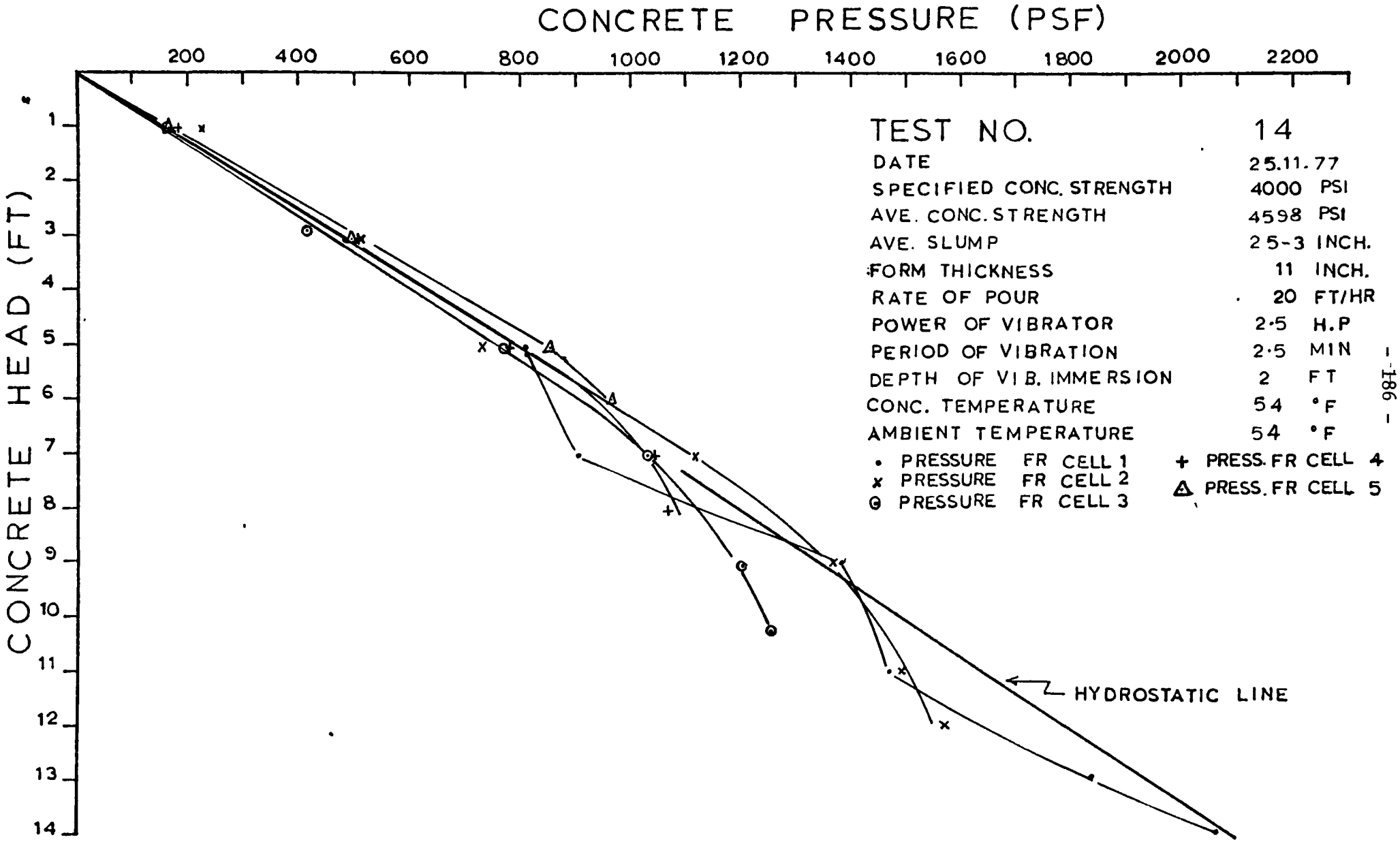

FIG. 6·14 b RELATION BETWEEN PRESSURE & CONC. HEAD

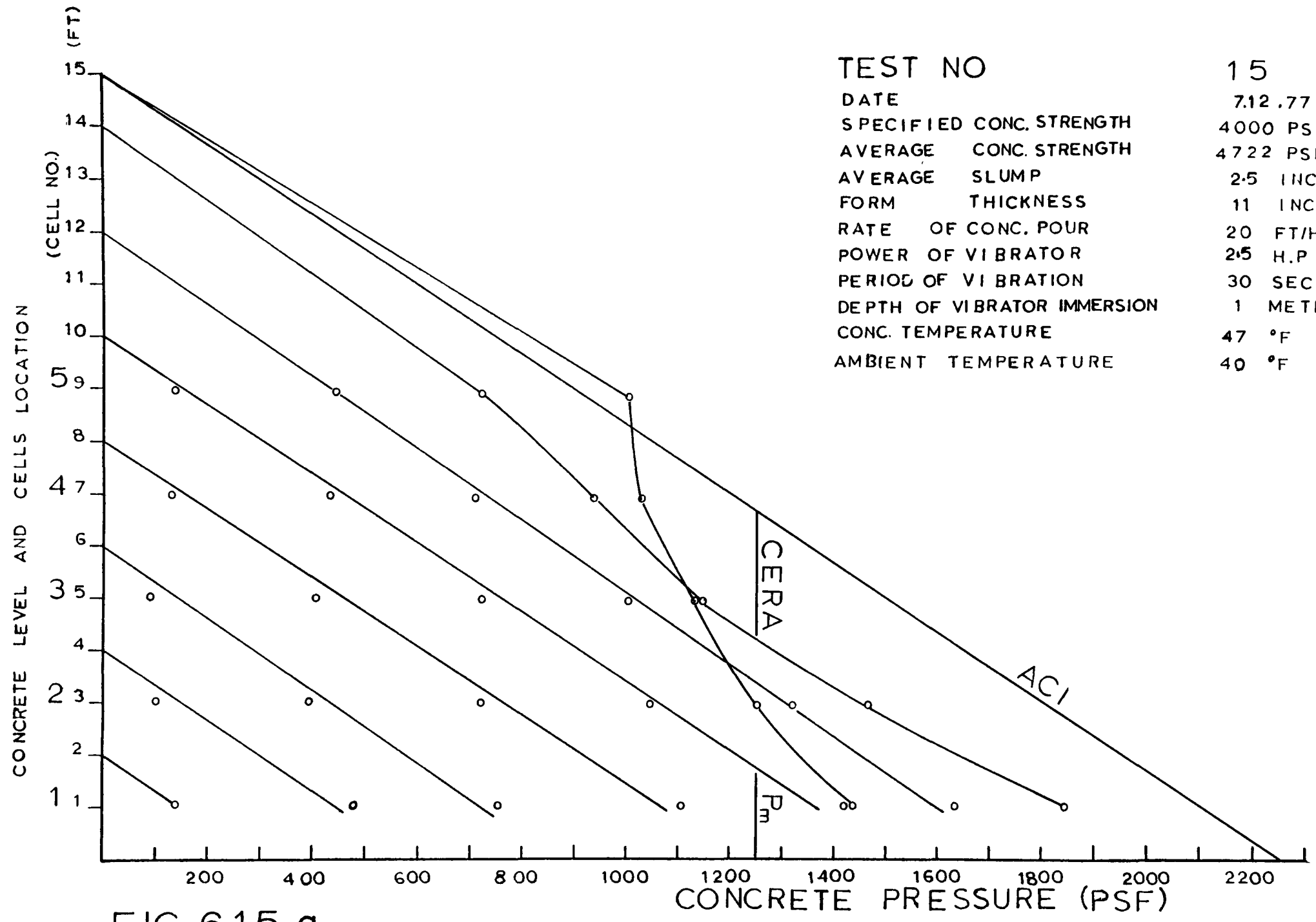

FIG. 6·15 a PRESSURE DEVELOPED AT VARIOUS CONC. LEVELS IN FORM

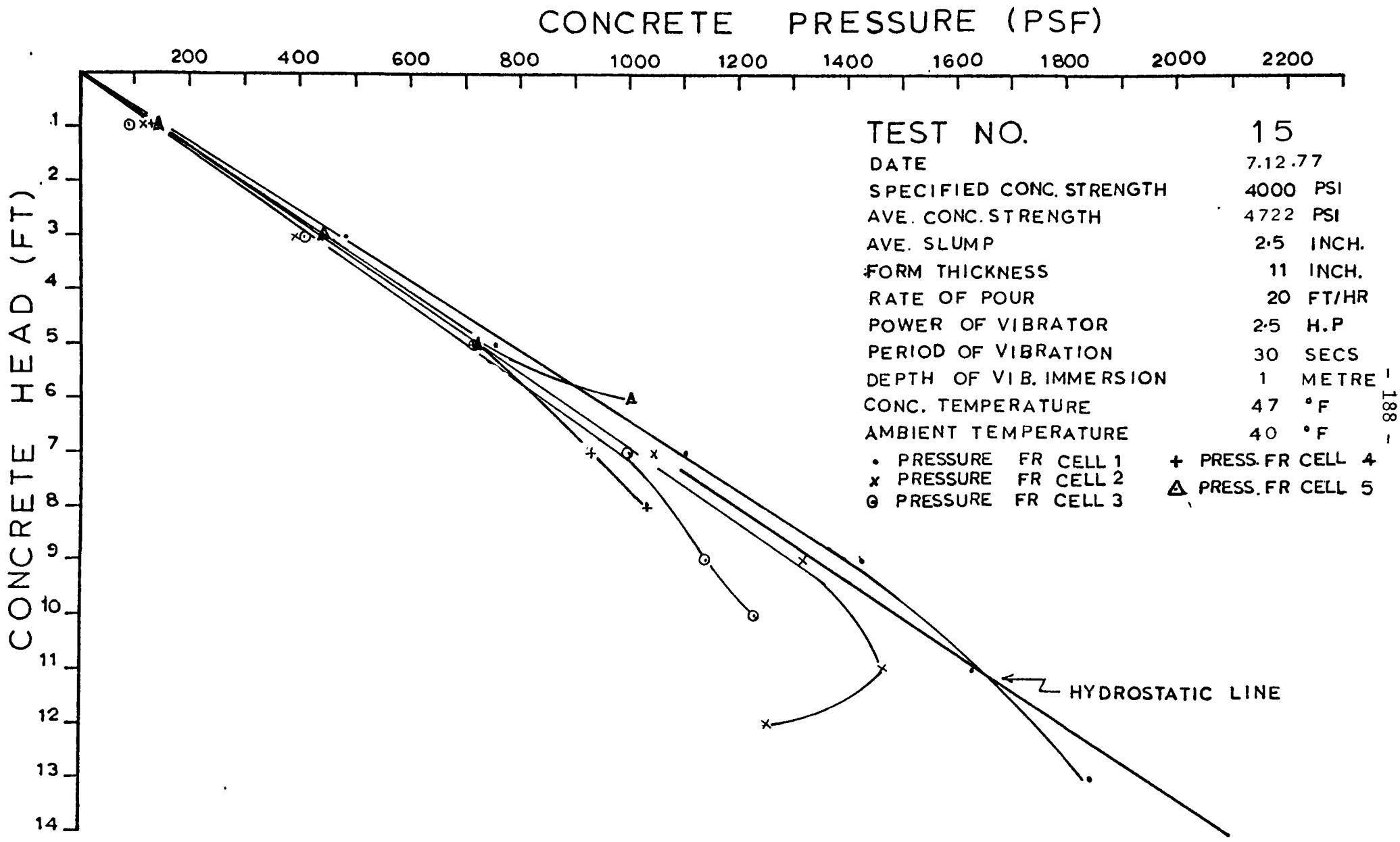

FIG. 6·15b RELATION BETWEEN PRESSURE & CONC. HEAD

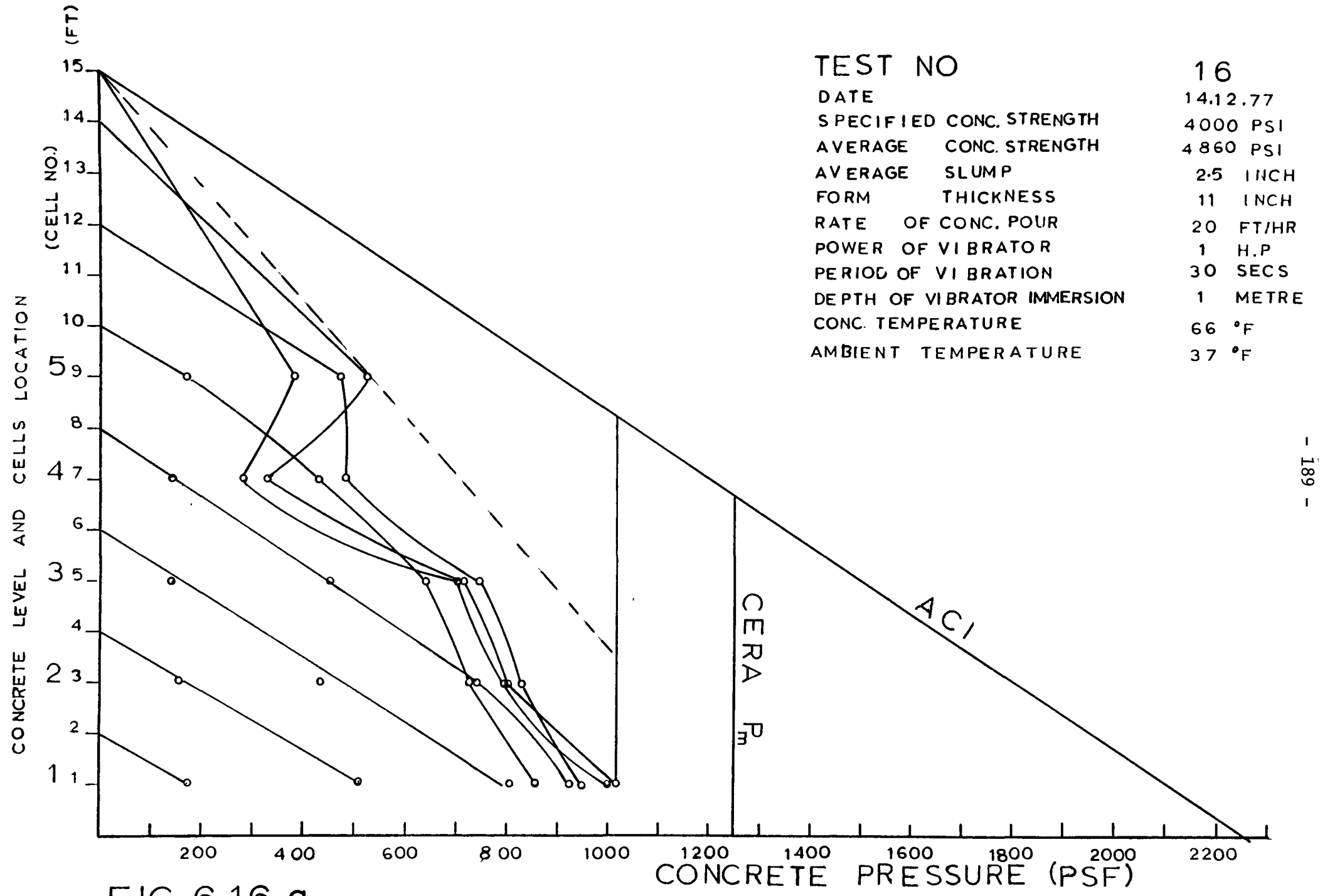

FIG. 6·16 a PRESSURE DEVELOPED AT VARIOUS CONC. LEVELS IN FORM

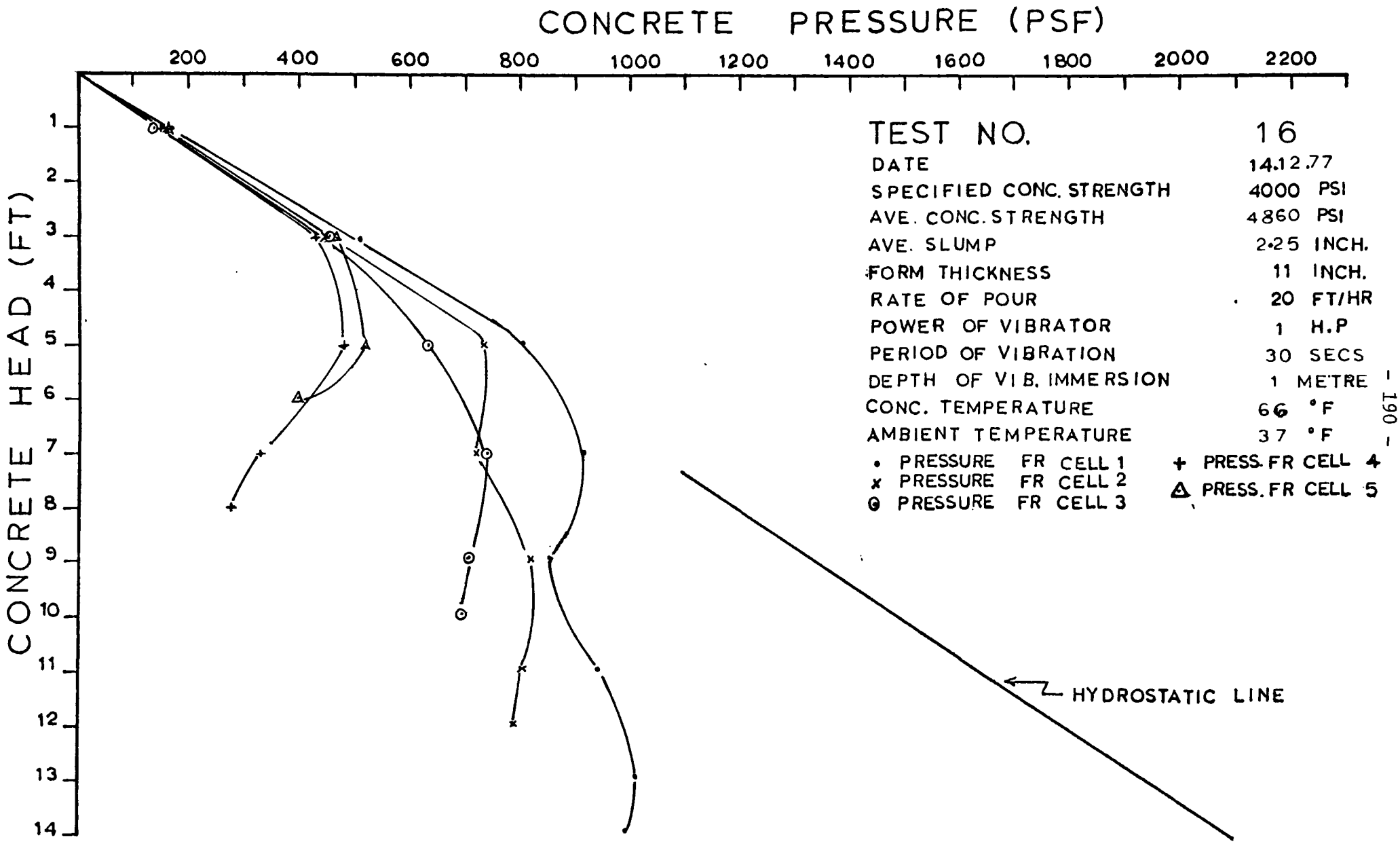

FIG. 6·16 b RELATION BETWEEN PRESSURE & CONC. HEAD

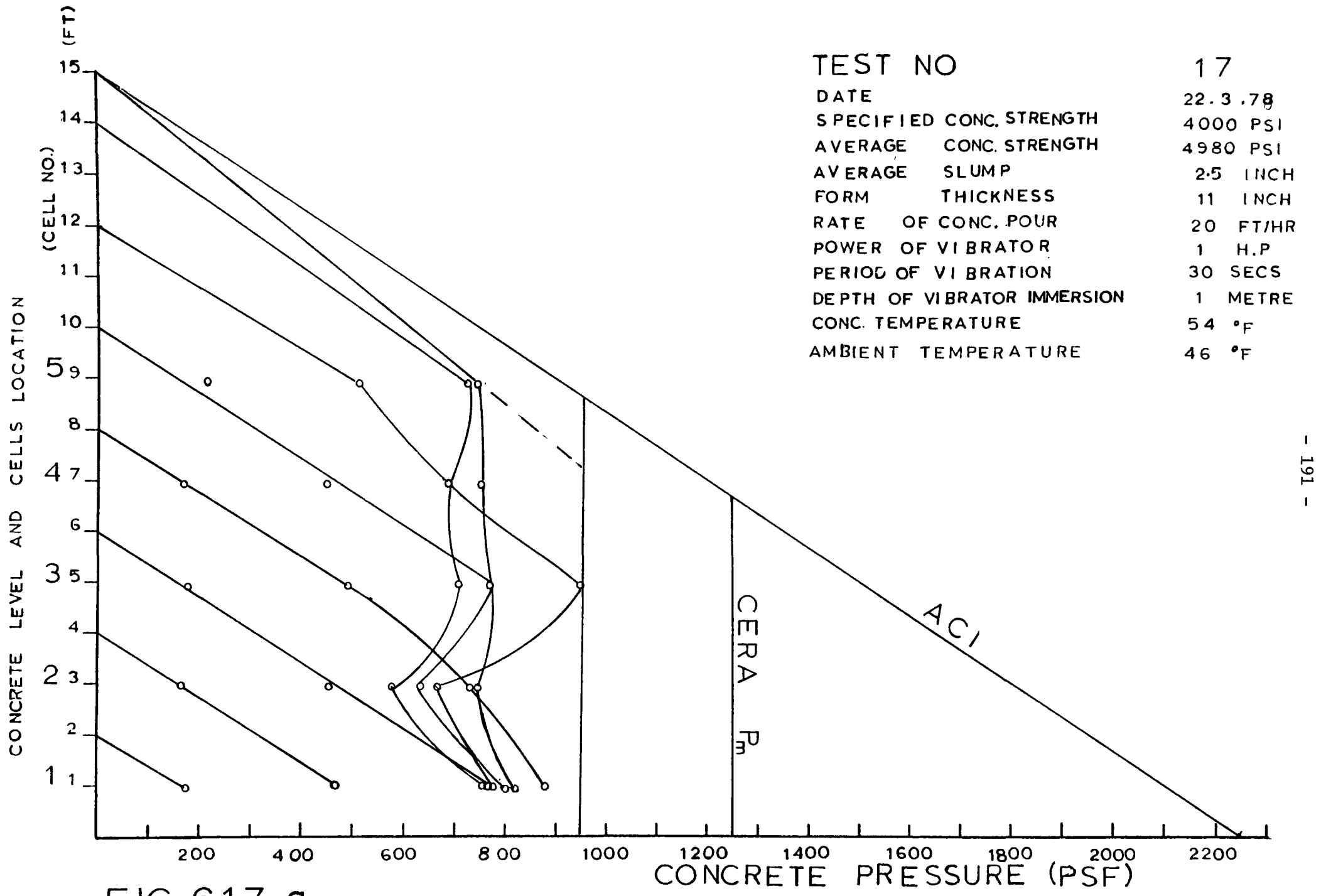

FIG. 6.17 a PRESSURE DEVELOPED AT VARIOUS CONC. LEVELS IN FORM

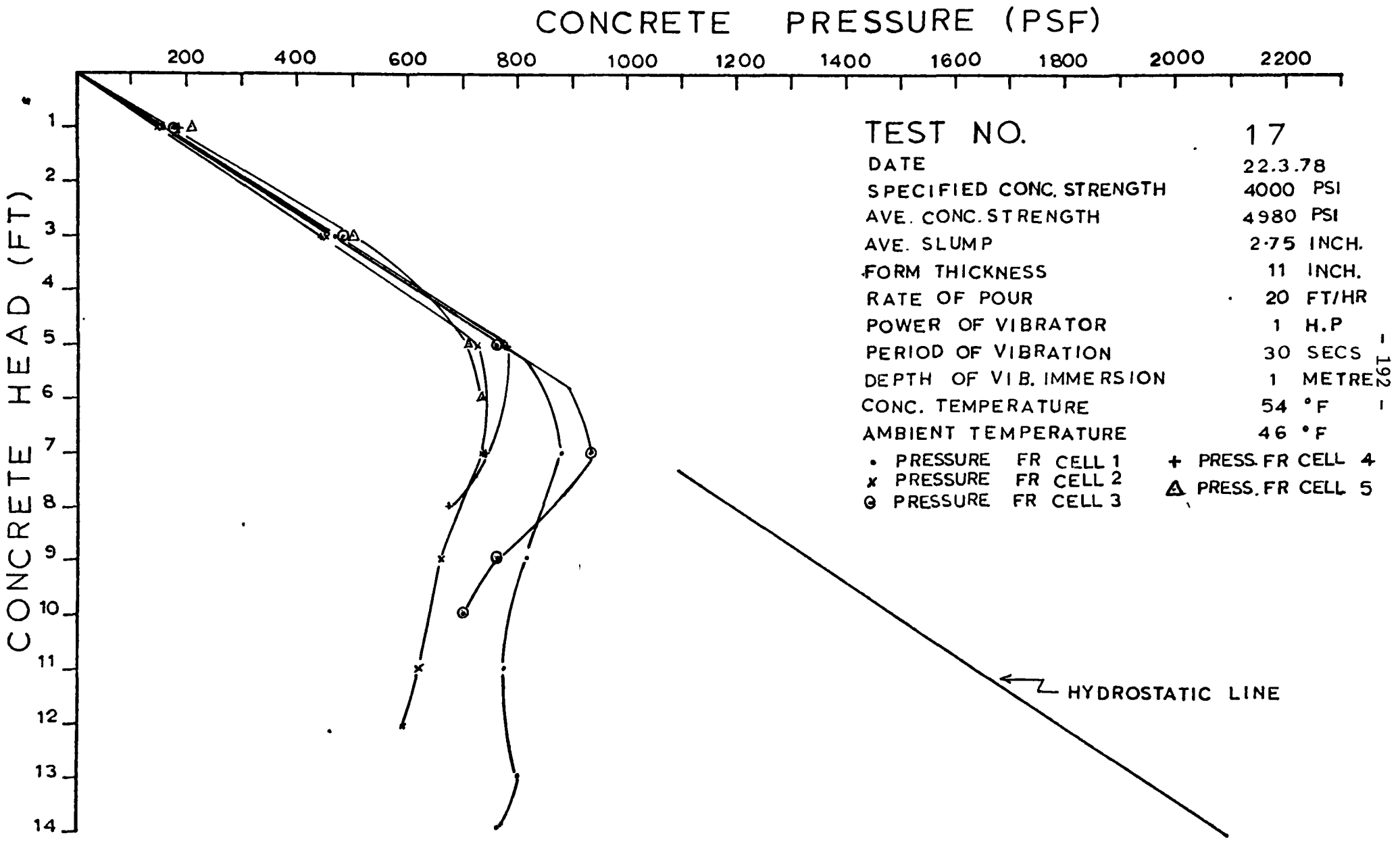

FIG. 6·17b RELATION BETWEEN PRESSURE & CONC. HEAD

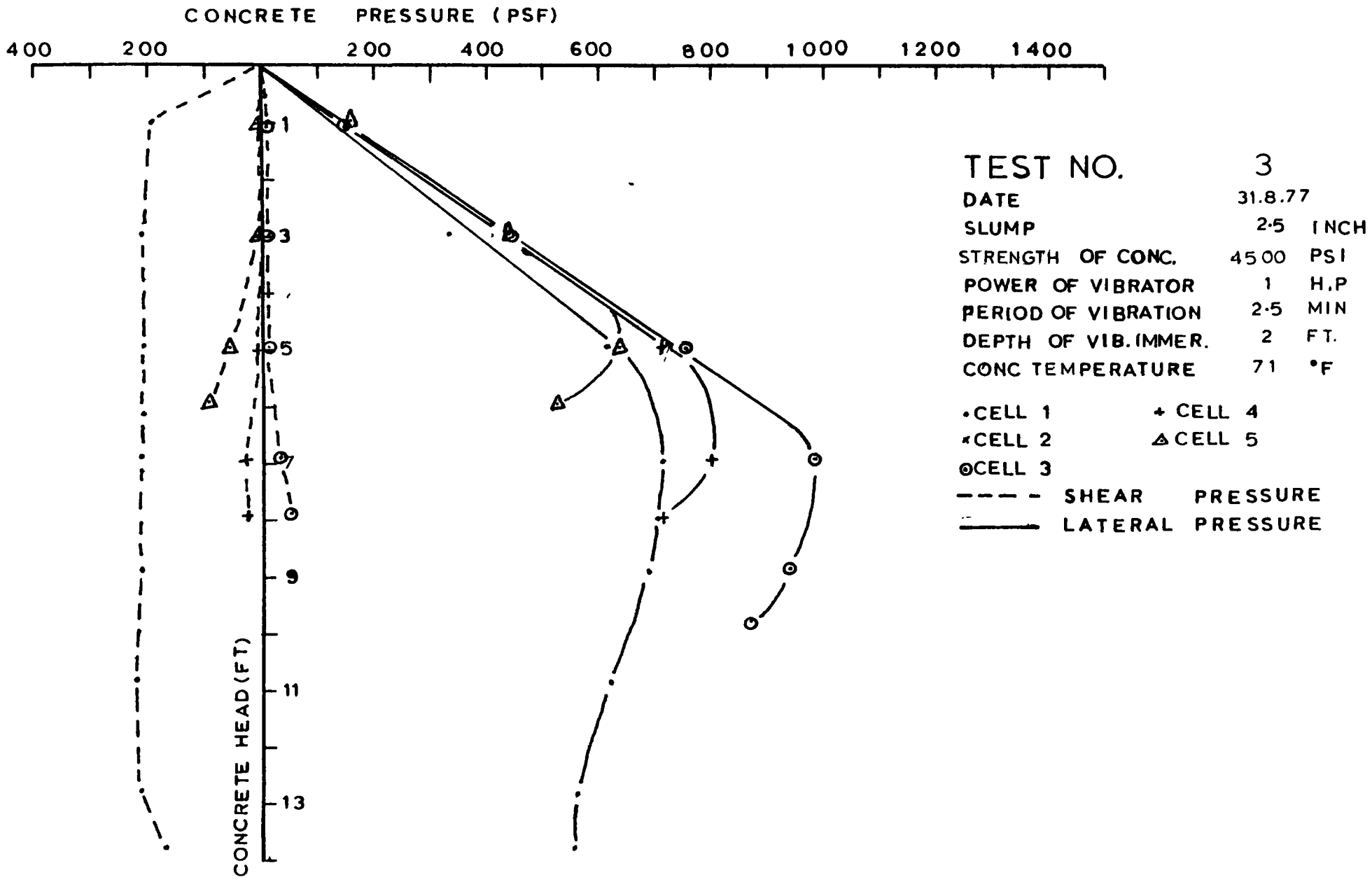

FIG. 6·18 VARIATION OF SHEAR AND LATERAL CONCRETE PRESSURES WITH CONC. HEAD

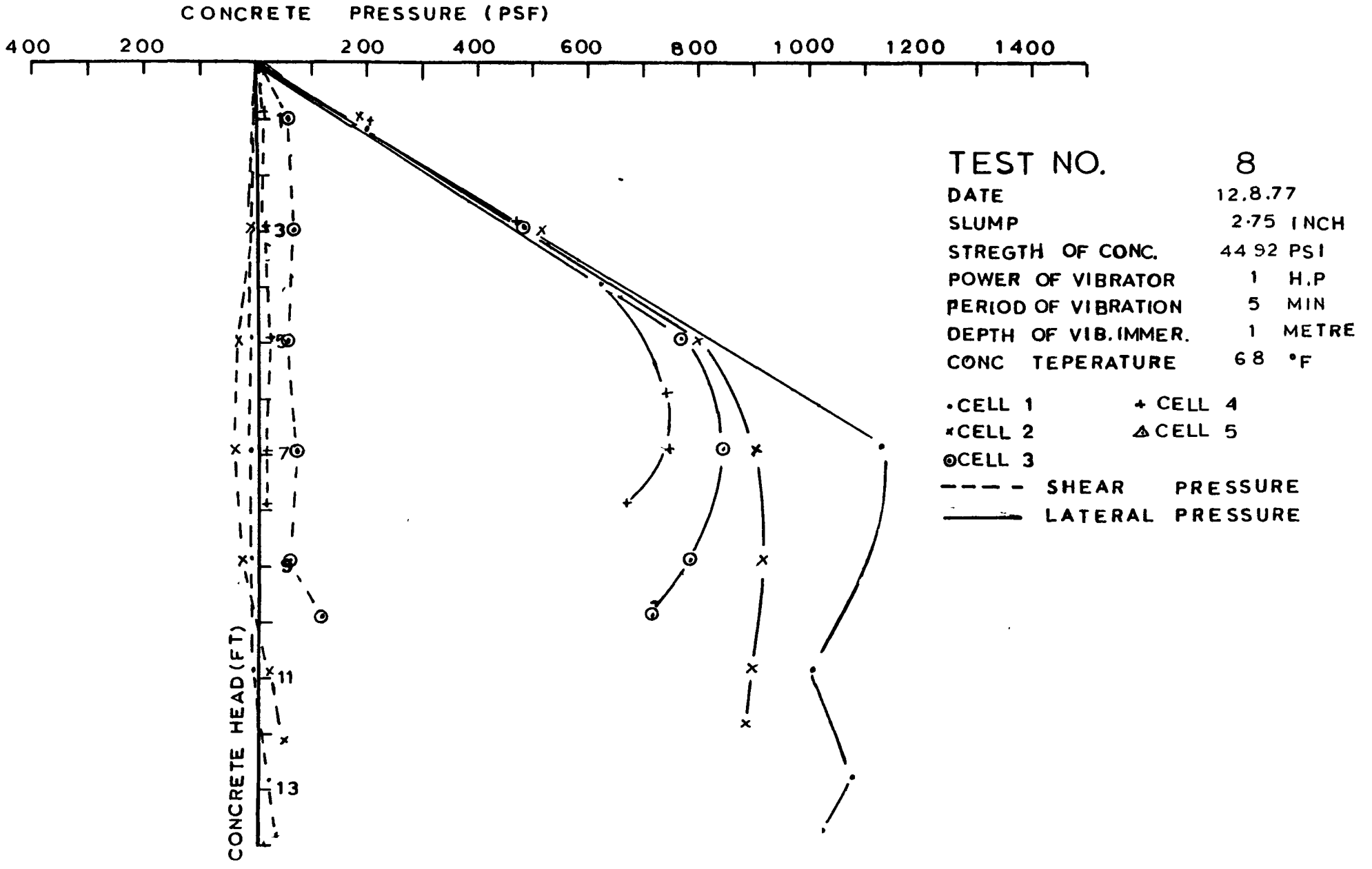

FIG. 6·19 VARIATION OF SHEAR AND LATERAL CONCRETE PRESSURES WITH CONC. HEAD

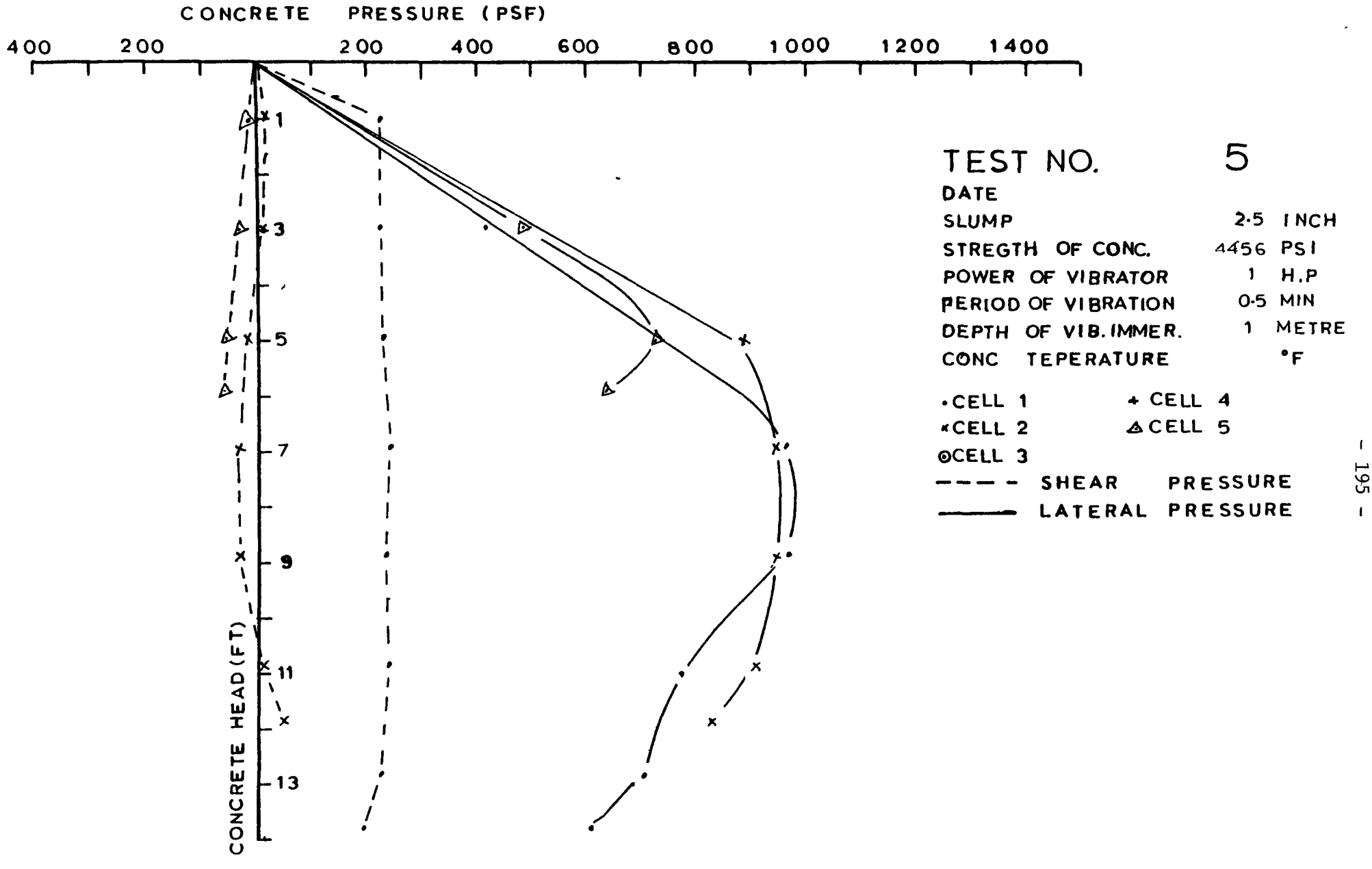

FIG. 6·20 VARIATION OF SHEAR AND LATERAL CONCRETE PRESSURES WITH CONC. HEAD

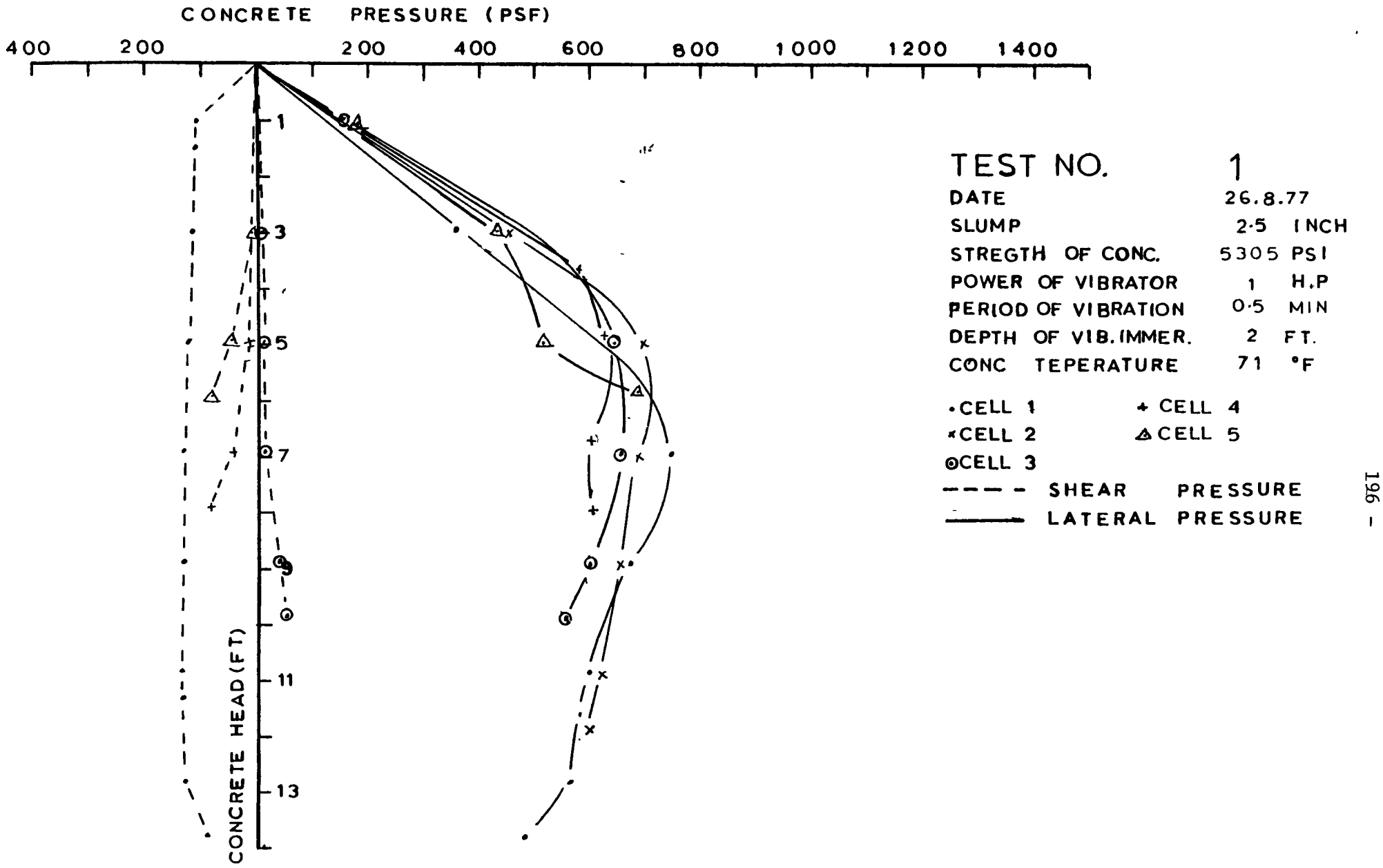

FIG. 6·21 VARIATION OF SHEAR AND LATERAL CONCRETE PRESSURES WITH CONC. HEAD

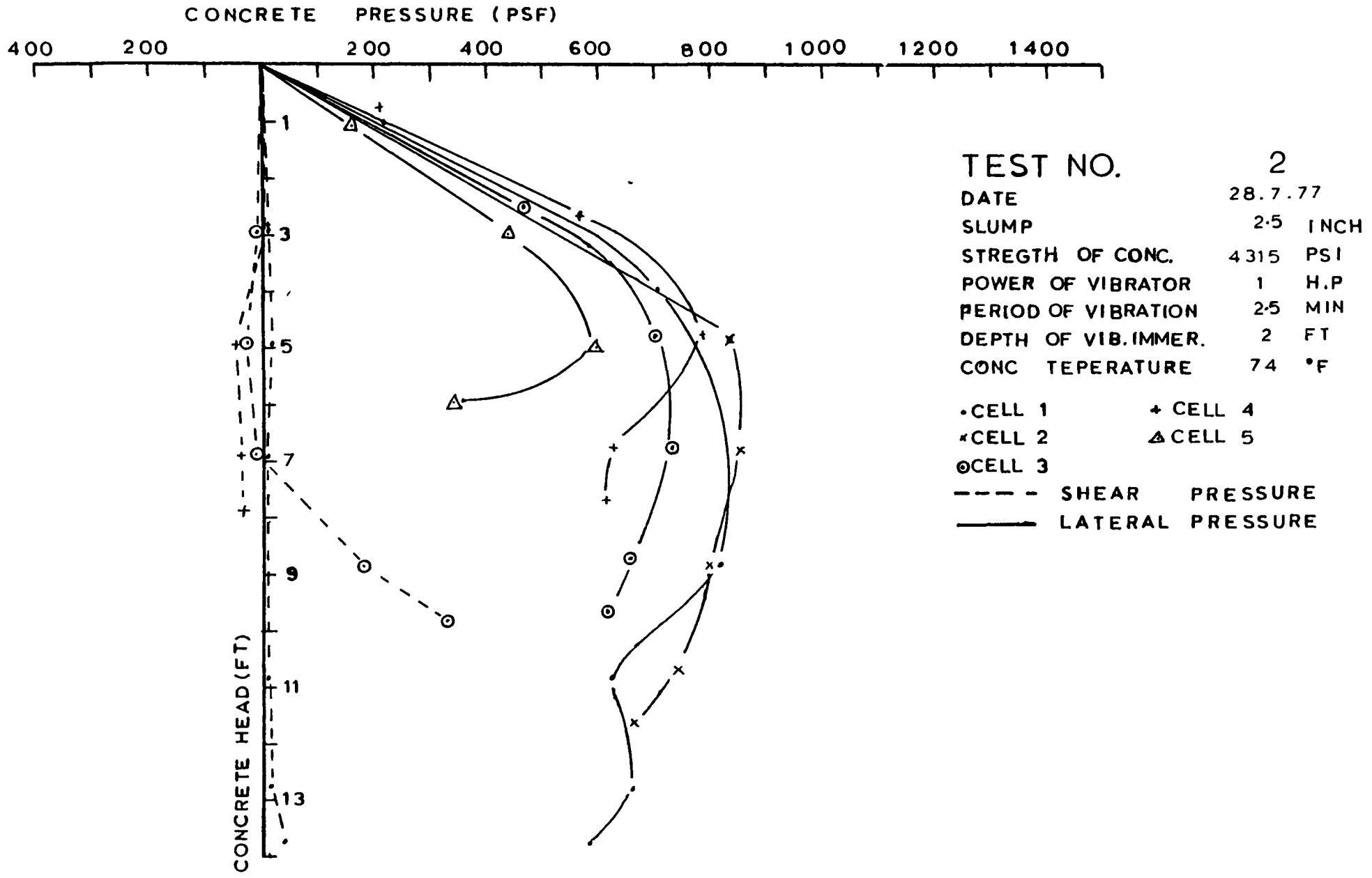

FIG. 6·22 VARIATION OF SHEAR AND LATERAL CONCRETE PRESSURES WITH CONC. HEAD

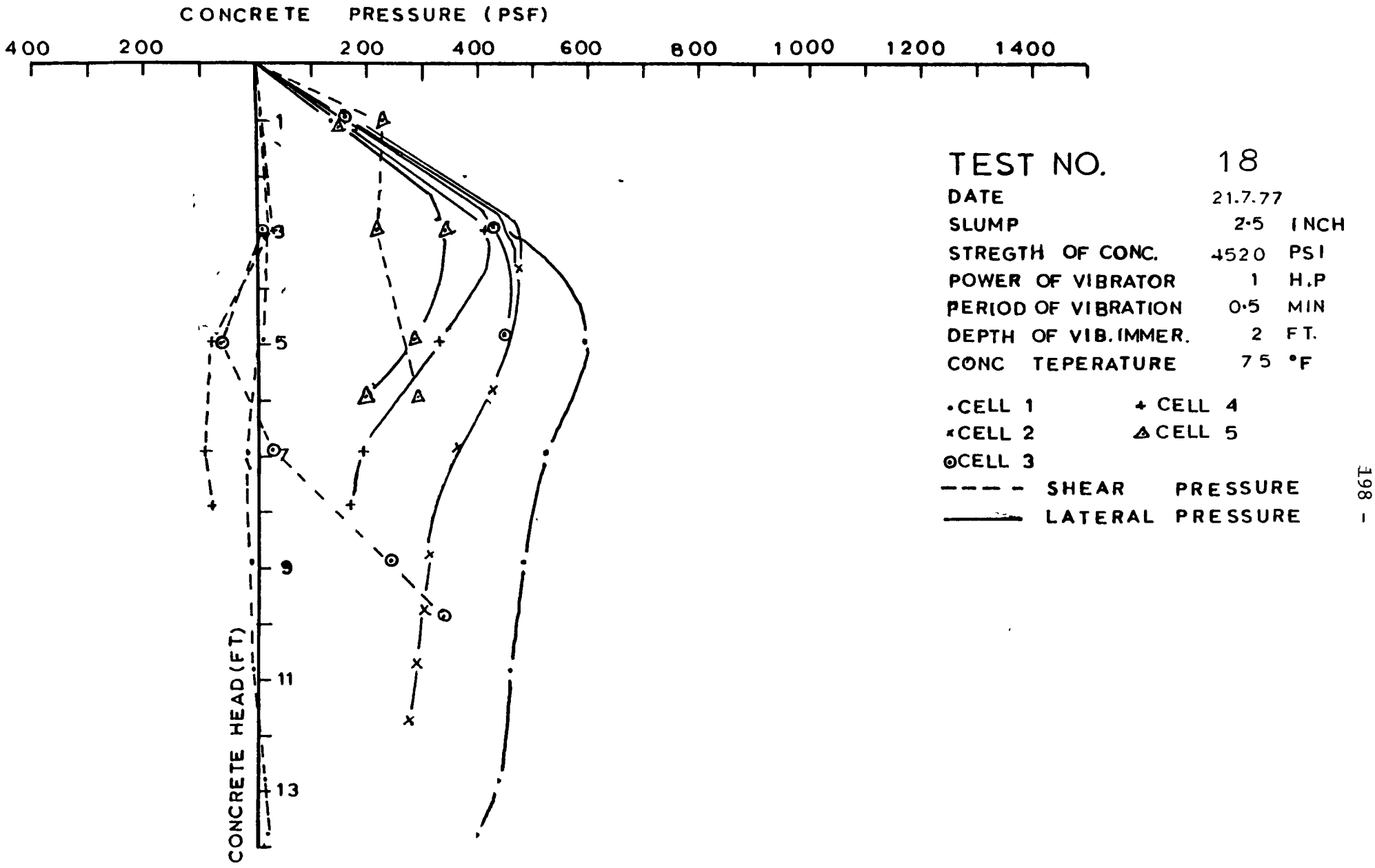

FIG. 6·23 VARIATION OF SHEAR AND LATERAL CONCRETE PRESSURES WITH CONC. HEAD

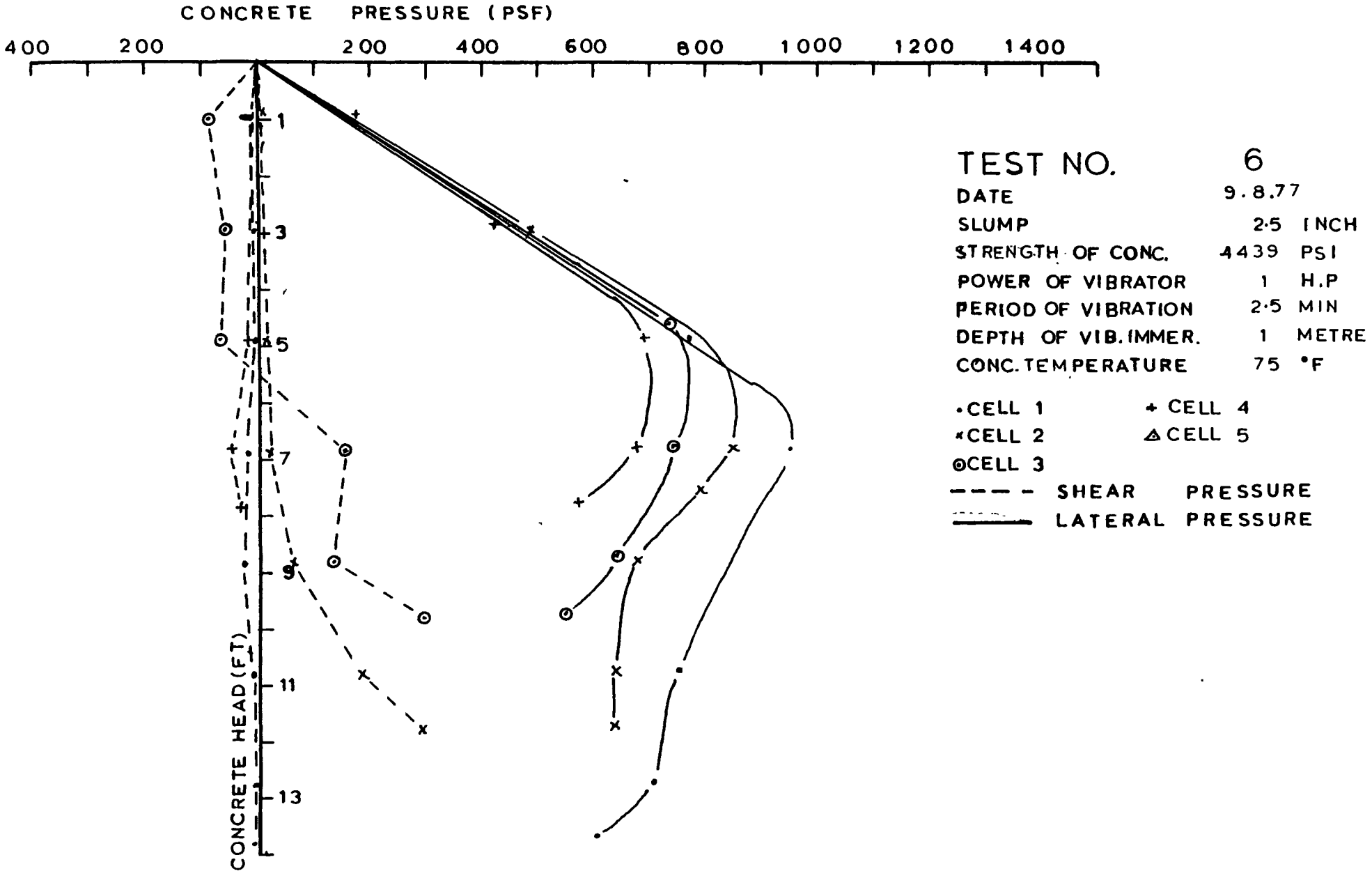

FIG. 6·24 VARIATION OF SHEAR AND LATERAL CONCRETE PRESSURES WITH CONC. HEAD

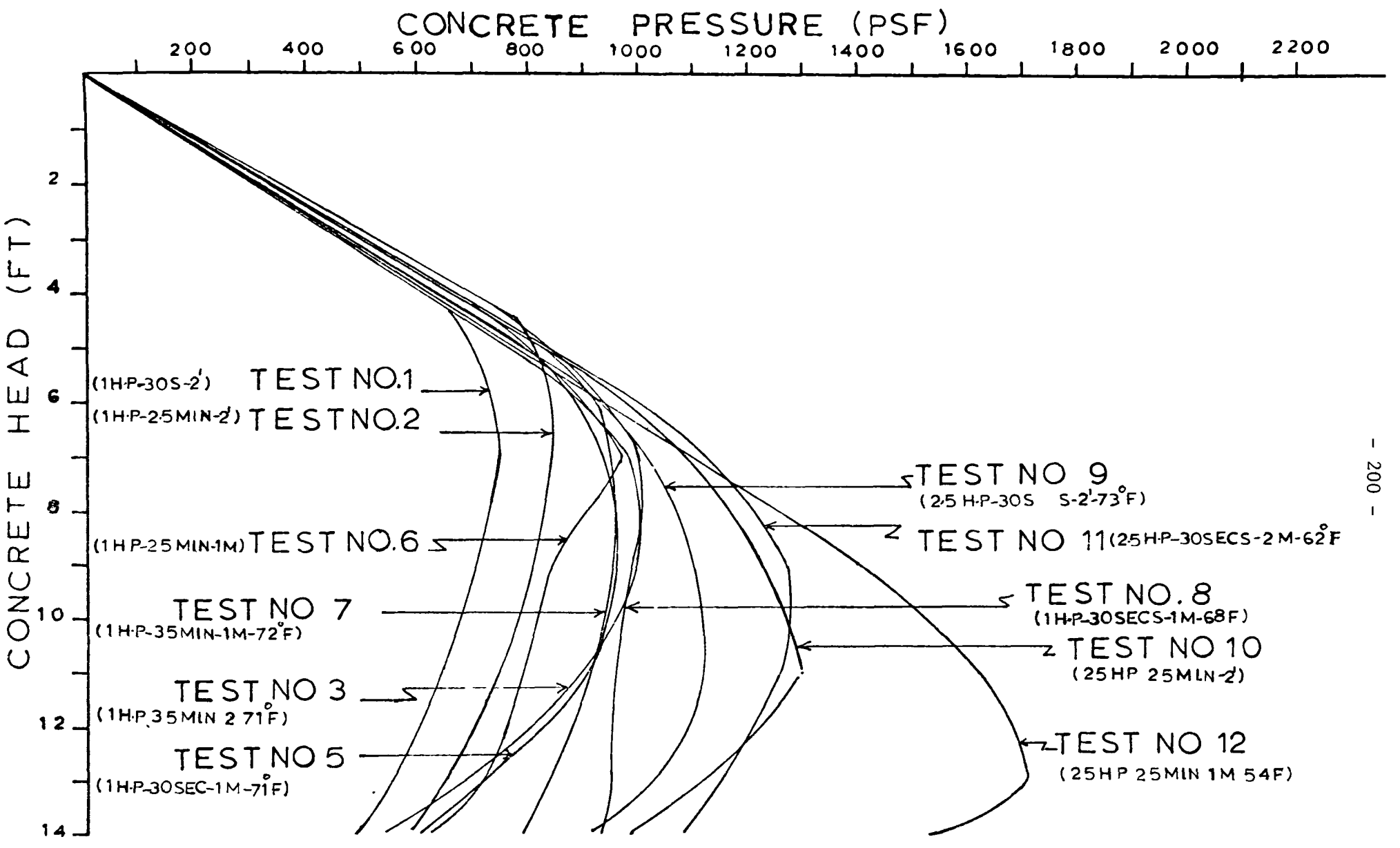

FIG. 6·25 COMPARISON OF PRESSURE ENVELOPES AT 1FT. ELEVATION OF THE FORM (54 to 71°F)

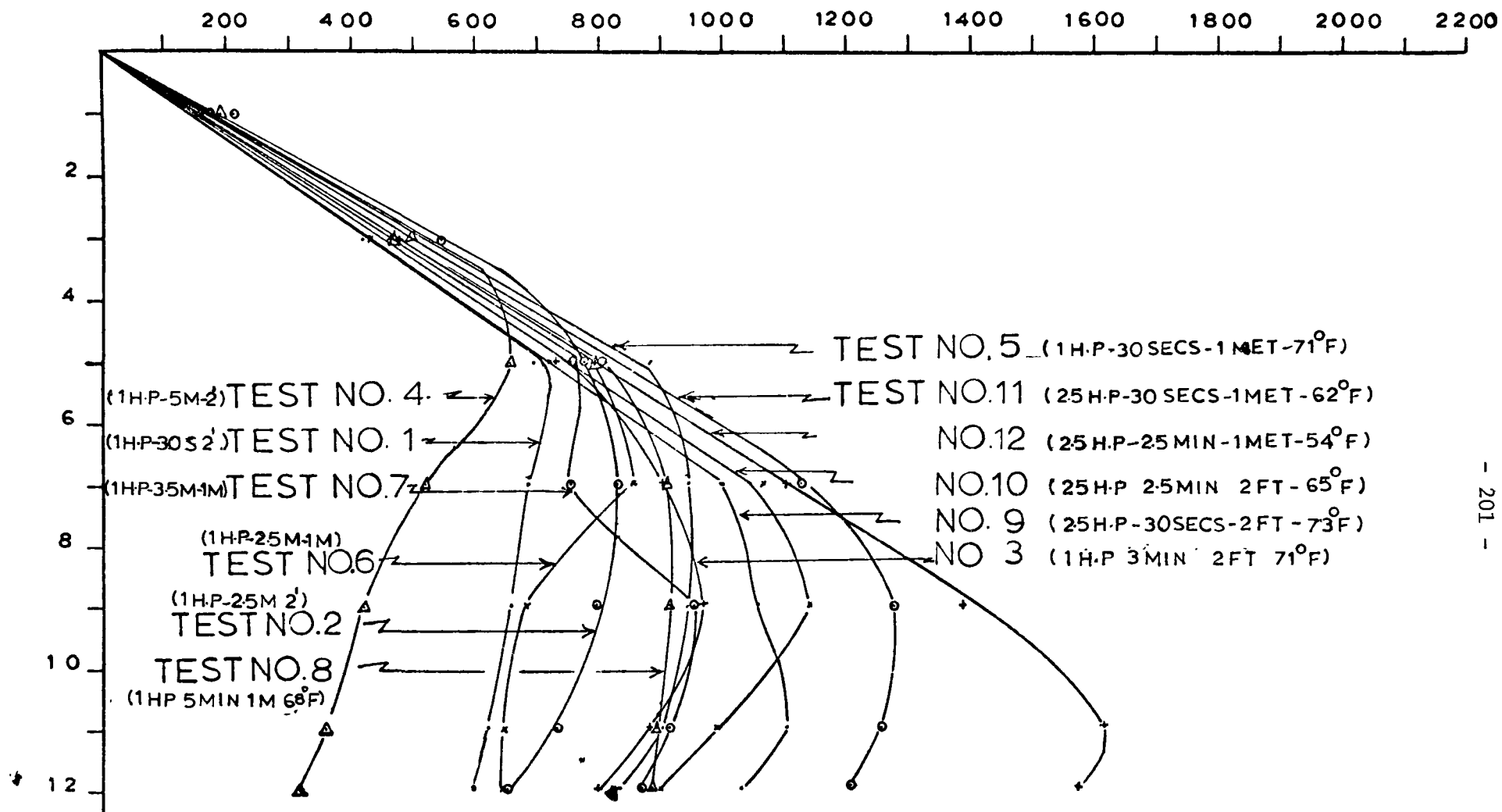

FIG. 6·26 COMPARISON OF PRESSURE ENVELOPE AT 3 FT. ELEVATION OF FORM

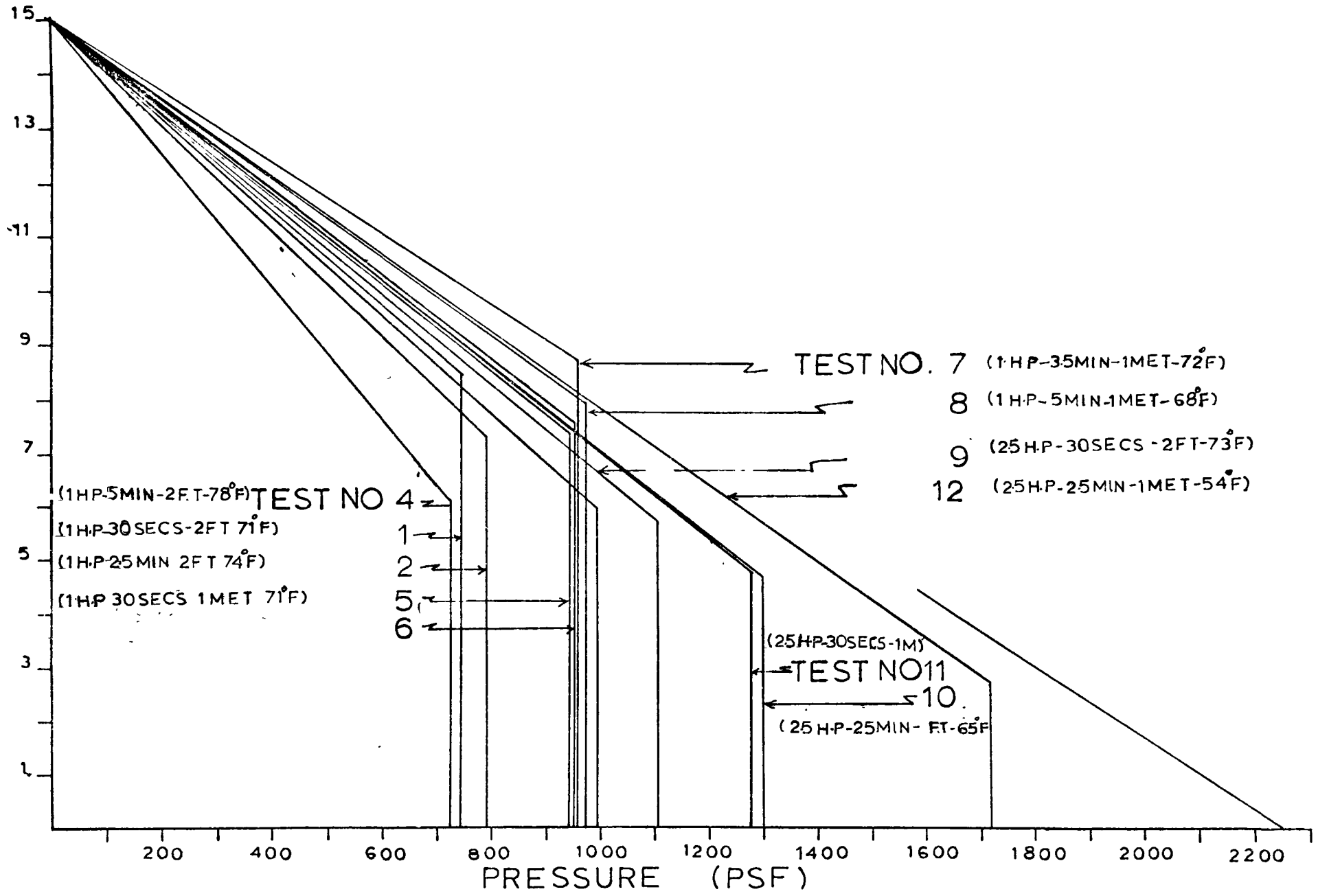

FIG.6·27 COMPARISON OF PRESSURES AT DIFF. VIBRATION PARAMETERS.

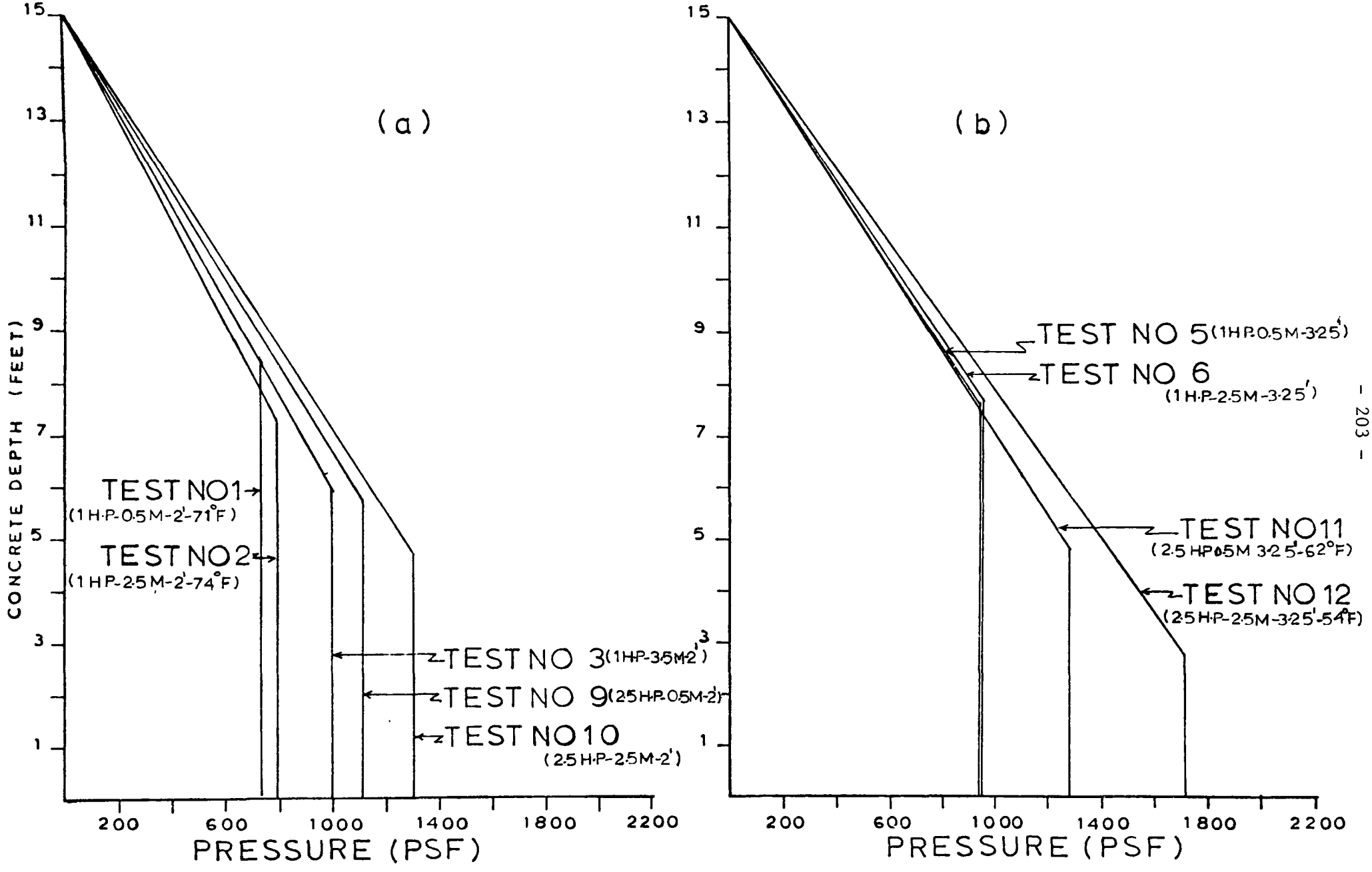

FIG.6·28 EFFECT OF POWER OF VIBRATOR ON CONC. PRESSURE

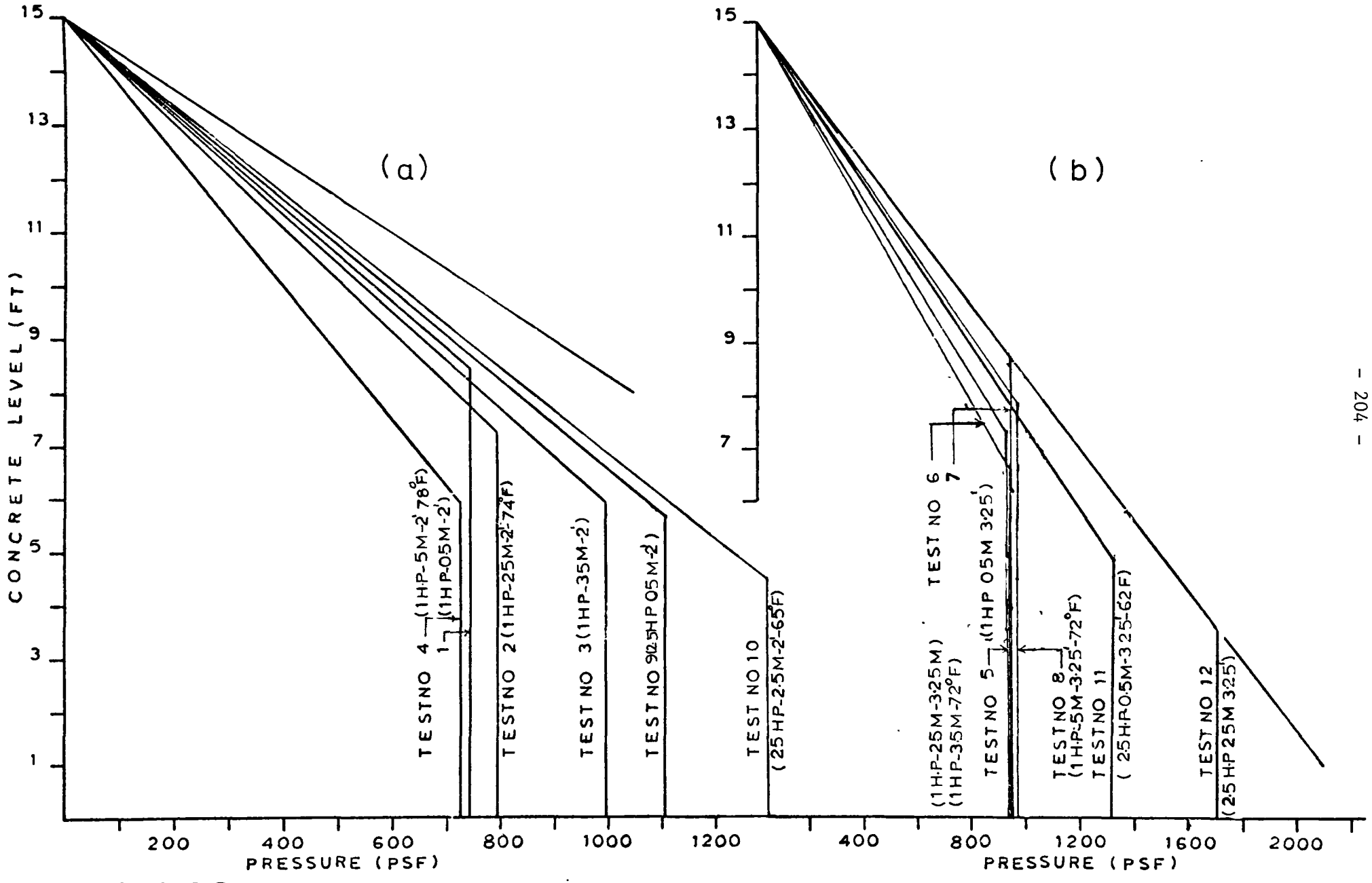

FIG.6.29 EFFECT OF DURATION OF VIBRATION ON CONCRETE PRESSURE

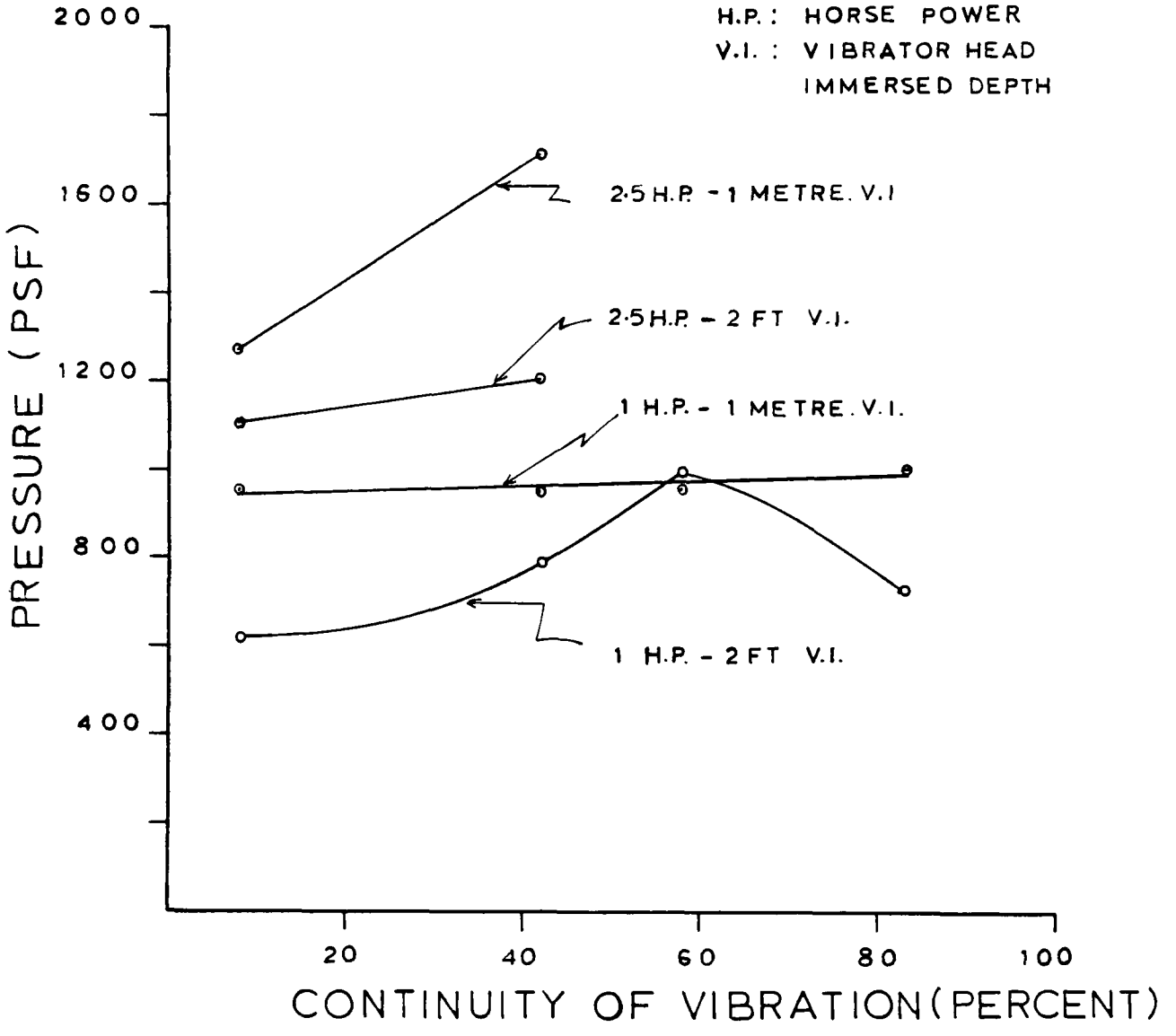

FIG. 6·30 RELATION BETWEEN CONC. PRESSURE & DURATION OF VIBRATION

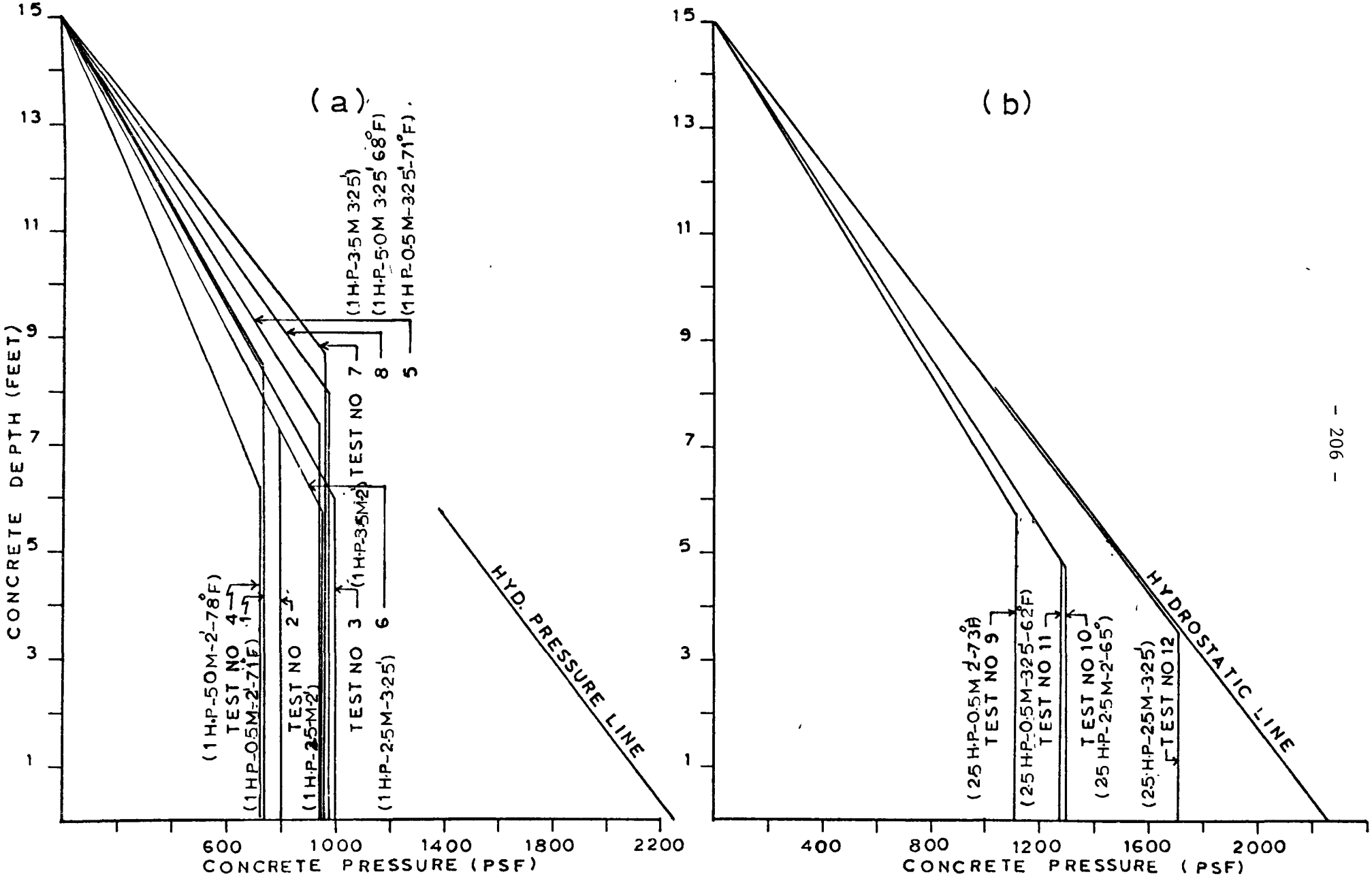

FIG.6.31 EFFECT OF DEPTH OF VIBRATOR IMMERSION ON CONCRETE PRESSURE

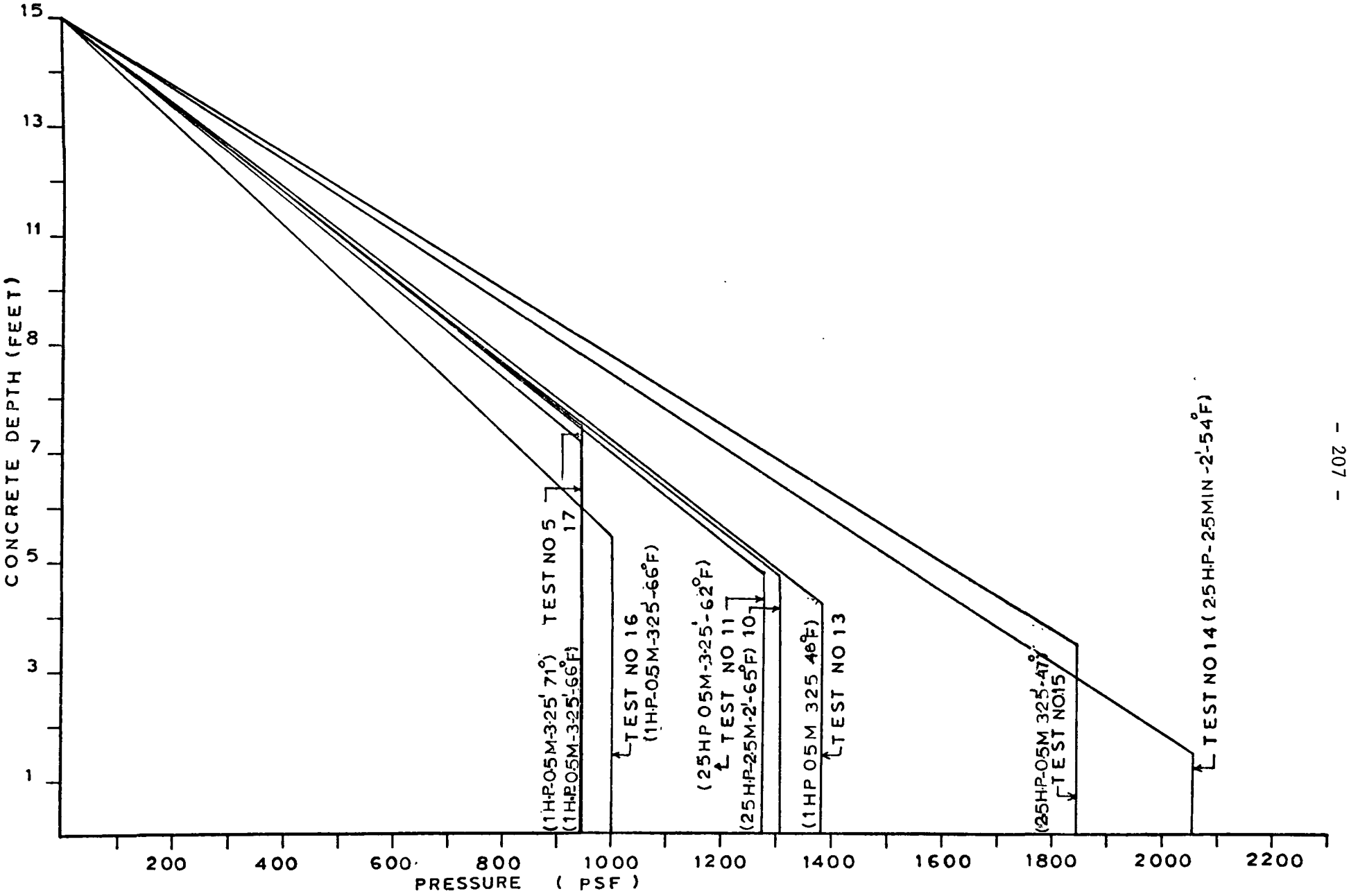

FIG.6-32 EFFECT OF TEMPERATURE ON LATERAL PRESSURE OF CONCRETE

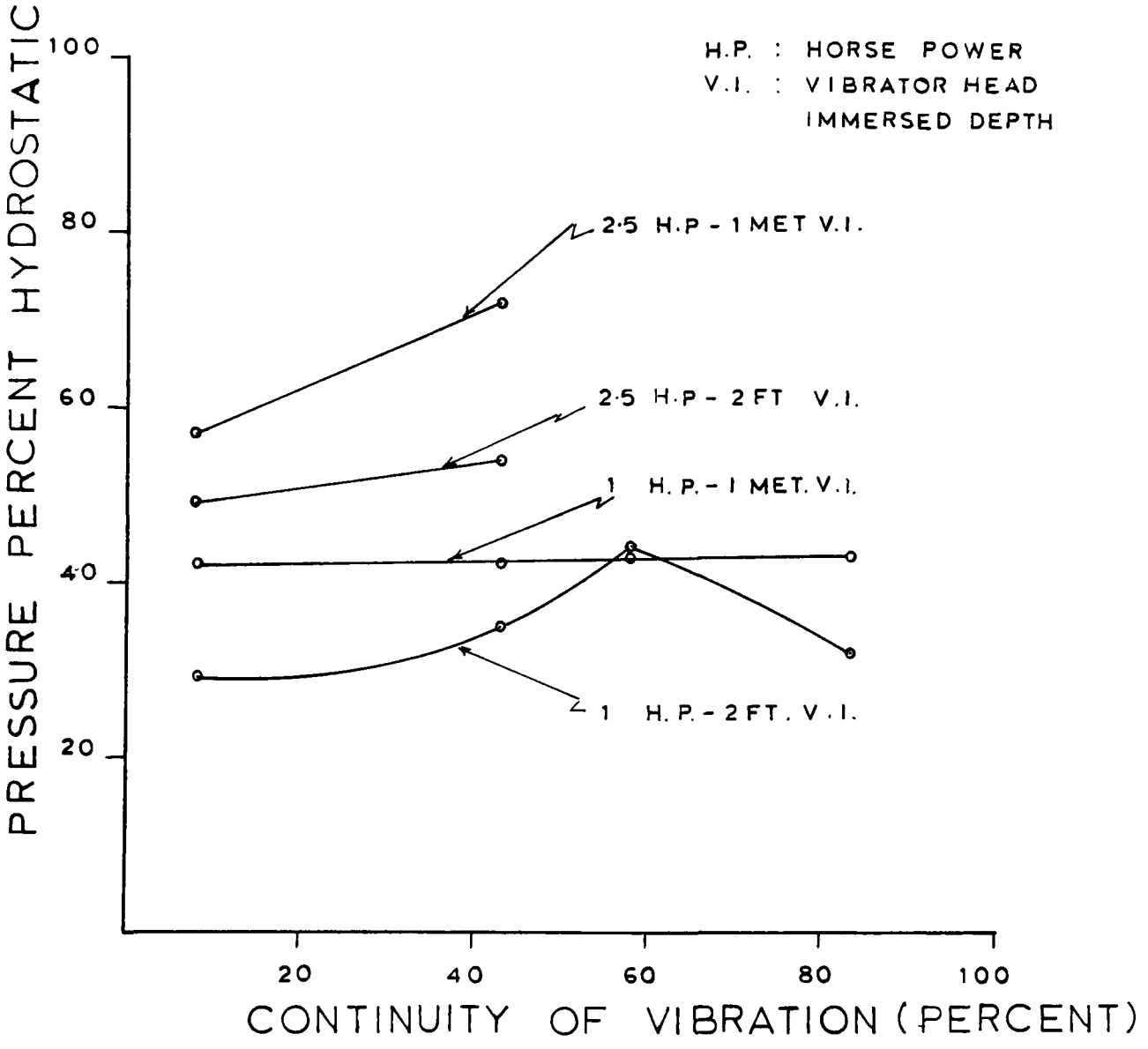

FIG 6·33 RELATION BETWEEN PERCENT HYDROSTATIC PRESSURE & CONTINUITY OF VIBRATION

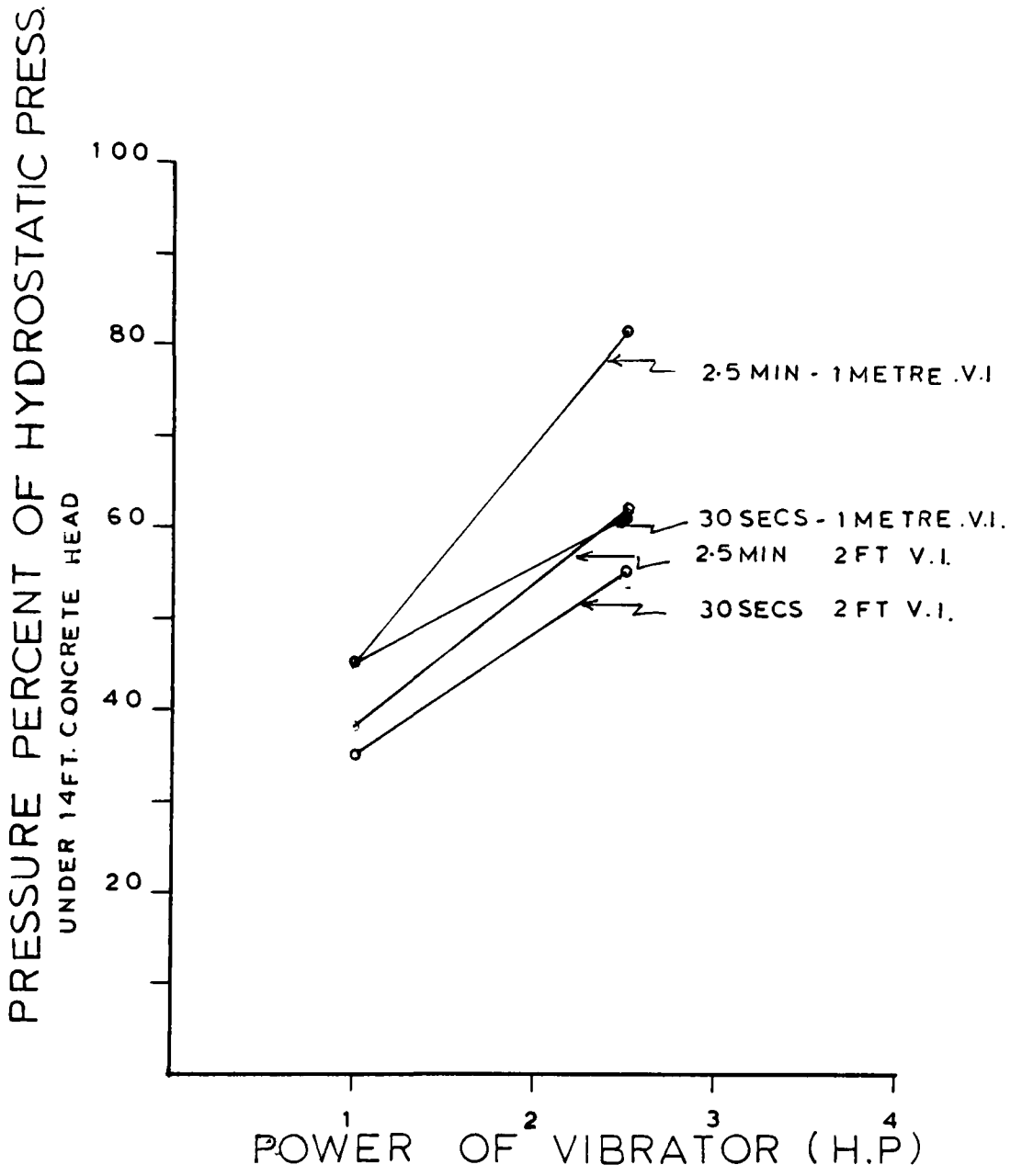

FIG 6.34 RELATION BETWEEN CONC. PRESSURE (% HYDROSTATIC) AND POWER OF VIBRATOR

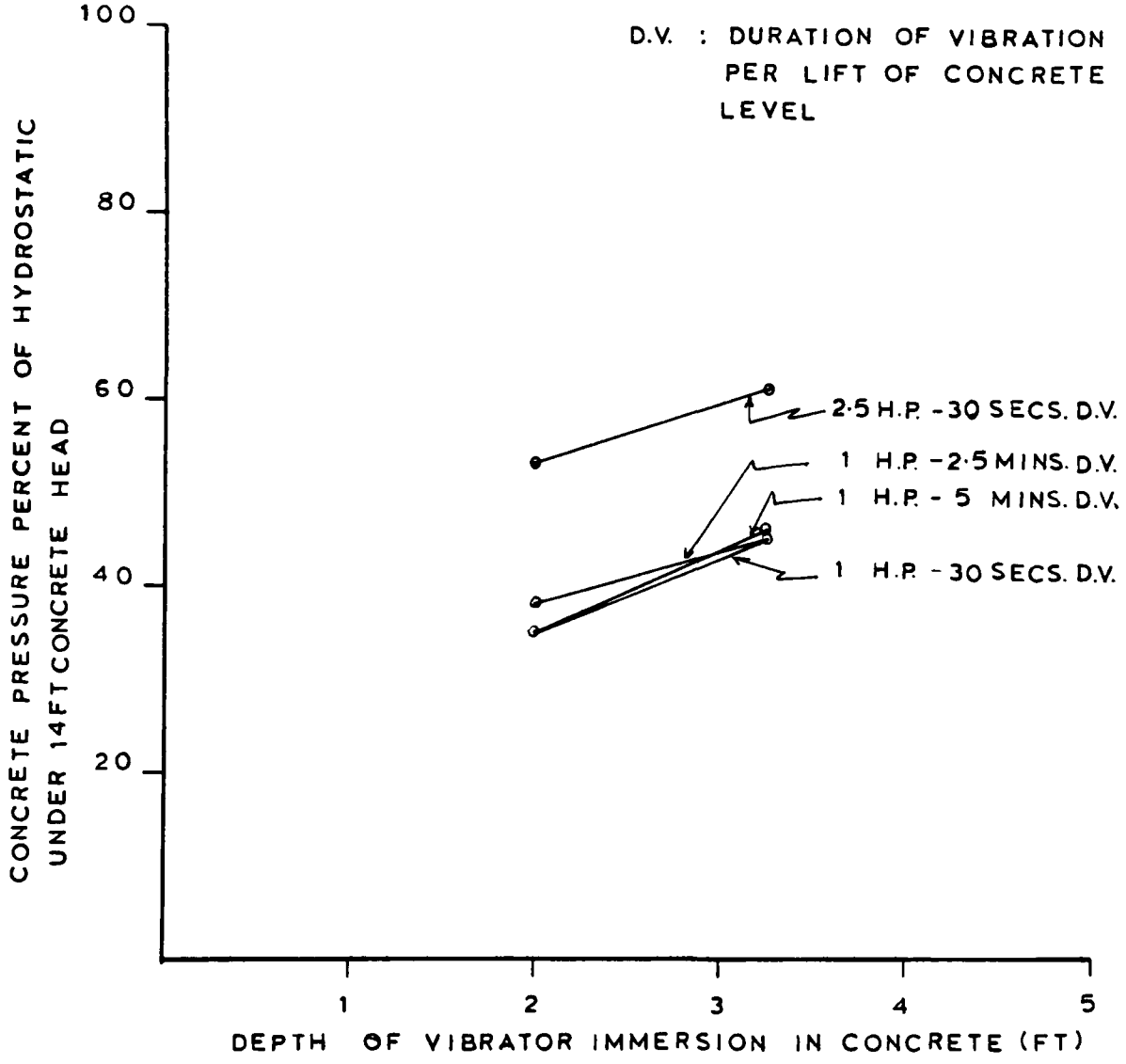

FIG.6·35 VARIATION OF CONCRETE PRESSURE (% HYDROSTATIC) WITH DEPTH OF VIBRATOR IMMERSION.

VITA

NAME Amjid Rauf QURESHI

BORN Peshawar, North West Frontier Province, Pakistan

EDUCATED

Primary

Presentation Convent School, Peshawar, 1953-58

Secondary

St. Mary's Cambridge School, Peshawar, Pakistan, 1958-1965

Pre-Engineering

Edward's College, Peshawar, Pakistan, 1965-1967

University

University of Peshawar, Pakistan, 1967-1971

Course

Civil Engineering
B.A.Sc., September 1971

University

University of Ottawa, Ottawa, Canada, 1977-1978

Course

M.A.Sc., 1978

EXPERIENCE

Senior Field and Planning Engineer
Cementation Intrafor Ltd
Tarbela Dam Project, Pakistan
September 1971 - February 1974

Assistant Engineer
Buildings and Roads
Public Works Department
N.W.F.P., Pakistan
February 1974 - May 1976